2-27-2013

Towards the Development of Tropolone Natural Product Derivatives as Novel, Potent Anticancer Therapeutics that Selectively Target Histone Deacetylase (HDAC) Enzymes

Sophia Nnenna Ononye
University of Connecticut - Storrs, sophia.ononye@uconn.edu

Towards the Development of Tropolone Natural Product Derivatives as Novel, Potent

Anticancer Therapeutics that Selectively Target Histone Deacetylase (HDAC) Enzymes

Sophia Nnenna Ononye, Ph.D.

University of Connecticut 2013

Cancer is the second leading cause of death in the United States. Inhibitors that target key enzymes involved in epigenetic alterations, particularly histone deacetylases (HDACs), are garnering interest in cancer research because of their unique ability to reversibly induce terminal differentiation of transformed cells by influencing chromatin structure. Through an in-house collaborative effort, derivatives of hinokitiol, a troplone-related non-benzenoid aromatic compound, are being synthesized and characterized by the Wright and Anderson laboratories as HDAC inhibitors (HDACi). Given the novelty of these tropolones as antineoplastic agents, a number of biochemical and functional studies were conducted in order to develop tropolones as isoform-selective HDACi with potent antitumor properties. These studies include: (1) Elucidation of HDAC enzymatic activity and inhibition, (2) Comparative analyses of antiproliferative effects in a panel of normal dermal fibroblasts, solid tumor and hematological cell lines, (3) Evaluation of induction and mechanisms of cell death by apoptosis, (4) Assessment of histone and tubulin modulation, and (5) Investigation of specific gene expression. Ultimately, the knowledge garnered from these studies will be used to develop a new library of isoform-selective HDAC inhibitors with a wider therapeutic index for the treatment of both solid tumors and hematological malignancies.

Towards the Development of Tropolone Natural Product Derivatives as Novel, Potent Anticancer Therapeutics that Selectively Target Histone Deacetylase (HDAC) Enzymes

Sophia Nnenna Ononye

B.S. Honors, Bowling Green State University, 2006

M.P.H., Bowling Green State University & University of Toledo, 2007

A Dissertation

Submitted in Partial Fulfillment of the

Requirements for the Degree of

Doctor of Philosophy

at the University of Connecticut

2013

Copyright by
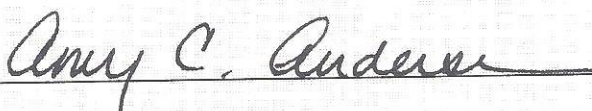
Sophia Nnenna Ononye

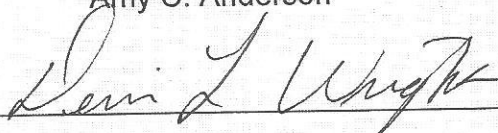2013

i

APPROVAL PAGE

Doctor of Philosophy Dissertation

Towards the Development of Tropolone Natural Product Derivatives as Novel, Potent

Anticancer Therapeutics that Selectively Target Histone Deacetylase (HDAC) Enzymes

Presented by

Sophia Nnenna Ononye, B.S. Honors, M.P.H.

Major Advisor _____
Amy C. Anderson

Associate Advisor _____
Dennis L. Wright

Associate Advisor _____
Charles A. Giardina

University of Connecticut

2013

ii

This dissertation signifies the fulfillment of my American dream of liberty and the pursuit of excellence. I dedicate this degree to the Ononye family, the legacy of my future family, and the friends in Nigeria and worldwide who have supported me over the years.

Table of Contents

iv

List of Common Abbreviations

ACS	American Cancer Society
BSA	Bovine Serum Albumin
CDC	Centers for Disease Control and Prevention
CDK	Cyclin-dependent Kinase
CDKI	Cyclin-dependent Kinase Inhibitor
CTCL	Cutaneous T-cell Lymphoma
CTL	Cytolytic T Lymphocyte
FACS	Fluorescence Activated Cell Sorting
FBS	Fetal Bovine Serum
FCCM	Flow Cytometry and Confocal Microscopy
FDA	Food and Drug Administration
FITC	Fluorescein Isothiocyanate
GI_{50}	Growth inhibition at 50%
GMFI	Geometric Mean Fluorescence Intensities
HAT	Histone Acetyltransferase
HDAC	Histone Deacetylase
HDACi	Histone Deacetylase Inhibitor
hDF	Human Dermal Fibroblast
IARC	International Agency for Research on Cancer
IC_{50}	Inhibitory concentration at 50%
K_i	Inhibition constant

K_M	Michaelis-Menten constant
MOA	Mechanism of Action
NCI	National Cancer Institute
NK	Natural Killer
PBS	Phosphate-buffered Saline
PDB	Protein Data Bank
PI	Propidium Iodide
PI3K	Phosphoinositide 3-Kinase
SAHA	Suberoylanilide bishydroxamide
SAR	Structure-activity relationship
TSA	Trichostatin A
V_{max}	Maximum enzyme velocity
WHO	World Health Organization

Chapter 1

Cancer: A Global Disease Burden

A. Introduction

Cancer, alternatively known as malignant tumors or malignant neoplasms, is a generic term that refers to a large group of more than 100 diseases that are generally characterized by uncontrolled growth and spread of abnormal cells (1-5). Colloquially, cancer is used to describe malignant tumors that are typically invasive and metastatic but tumors can also be benign in which the abnormal cell growth is localized and noninvasive (1). Globally, cancer accounted for 7.6 million deaths (approximately 13% of all deaths) in 2008 with 70% of these cancer deaths occurring in low- and middle-income countries (4). The World Health Organization (WHO) projects a continuous increase in cancer deaths worldwide with an estimated 13.1 million deaths in 2030 primarily due to late detection and treatment of most cancers in developing countries (3, 4).

There are six important factors, known as the hallmarks of cancer that are required for cancer development and tumor progression: limitless replicative potential, blocking of apoptosis and differentiation as well as the stimulation of angiogenesis, proliferation, and metastasis (1, 6, 7). These cancer hallmarks are regulated by epigenetic mechanisms including histone acetylation which will be discussed in detail in subsequent chapters.

1

However, it should be noted that the primary cause of cancer deaths is the process of metastasis by which abnormal cells in malignant tumors rapidly invade and spread to other organs (1, 7).

B. Classification of cancers

Most tumors can be classified according to their origin into four major groups: epithelial, mesenchymal, neuroectodermal and mesenchymal (1). However, it should be noted that not all tumors fall neatly into these four categories. Examples include melanomas which are derived from pigmented skin cells known as melanocytes and small-cell lung carcinomas (SCLCs). Yet, more than 80% of all cancers are carcinomas that arise from the epithelial cell layers of the skin, lungs, gastrointestinal (GI) tract, mammary glands, and other organs (1). Most carcinomas fall into two major groups, squamous cell carcinomas and adenocarcinomas. Squamous cell carcinomas refer to tumors that arise from epithelial cells forming the protective cell layers such as in the skin and the esophagus. Conversely, many epithelia that contain specialized cells that secrete substances into the cavities they line such as the lung, stomach & colon generate adenocarcinomas. The remainders of malignant tumors arise from nonepithelial tissues throughout the body and are divided into 3 major groups: sarcomas, neuroectodermal tumors, and hematopoietic cancers. Sarcomas, including osteosarcomas and liposarcomas, are derived from mesenchymal cells and constitute only about

2

1% of all tumors (1). Tumors that arise from the central & peripheral nervous systems are known as neuroectodermal tumors and include gliomas, glioblastomas and neuroblastomas. While comprising only about 1% of cancers, they make up 2.5% of cancer-related deaths (1).

Cancers that make up the hematopoietic or blood-forming tissues include leukemias and lymphomas, a focal point of this dissertation. Leukemias refer to malignant derivatives of hematopoietic cell lineages that move freely through the circulation and unlike red blood cells are nonpigmented. Alternatively, lymphomas refer to tumors of the lymphoid lineages which yield B and T lymphocytes that aggregate to form solid masses instead of the dispersed, single-cell populations of tumor cells typically associated with leukemias. In 2008, the International Agency for Research on Cancer (IARC), a part of the WHO, developed a new classification of tumors of hematopoietic and lymphoid tissues into five broad categories (8, 9): mature B-cell neoplasms, mature T-cell and NK-cell (natural killer) neoplasms, Hodgkin lymphoma, histiocytic and dendritic cell neoplasms, and posttransplantation lymphoproliferative disorders (PTLDs). Mycosis fungoides (MF) is the most common form of about 15 sub-types of skin tumors collectively known as cutaneous T-cell lymphoma (CTCL), a mature T-cell neoplasm that will be discussed at length in this dissertation (10).

Each cancer type is further described by a numerical staging system that describes the severity of a patient's cancer based on the extent of the primary tumor (11). The TNM system, arguably the most widely used staging system for cancer combines a numerical staging system (0-IV) to describe the extent of a tumor (T), the extent of spread to the lymph nodes (N), and the presence of distant metastasis (M). A number is added to each letter to indicate the size or extent of the primary tumor and the extent of cancer spread. Stage 0 [Carcinoma *in situ* (CIS)], stage I-III (higher numbers indicate more extensive disease) and stage IV (the cancer has spread to another organ(s)). It should be noted that CIS are considered precursors of cancer that may, if left untreated for a long duration, transform into a malignant neoplasm. Alternatively, many cancer registries, such as the NCI's-National Cancer Institute-Surveillance, Epidemiology, and End Results Program (SEER), use summary staging for all types of cancer into five main categories (11):

1. In situ: Abnormal cells are present only in the layer of cells in which they developed.
2. Localized: Cancer is limited to the organ in which it began, without evidence of spread.
3. Regional: Cancer has spread beyond the primary site to nearby lymph nodes or organs and tissues.
4. Distant: Cancer has spread from the primary site to distant organs or lymph nodes.
5. Unknown: Insufficient information for accurate stage determination.

4

C. Epidemiology of cancer

Cancer is the second leading cause of death in the United States and a major cause of death worldwide (2-5). According to IARC reports (3), 5.6 million (44%) of the 12.7 million new cases of cancer worldwide in 2008 occurred in economically developed countries whereas 7.1 million (56%) occurred in economically developed countries; however, of the 7.6 million cancer deaths in 2008, 2.8 million (37%) were in developed countries whereas 4.8 million (63%) were in developing countries. Globally, the three leading causes of cancer deaths in men are lung, liver and stomach cancers and concurrently breast, lung and colorectal cancers for women. In developing countries, the three leading causes of cancer-related deaths in men are lung, liver and stomach cancers whereas the three leading causes of cancer-related deaths in women are breast, cervical and lung cancers. Alternatively, in developed countries, the three leading causes of cancer-related deaths in men are lung, colorectal and prostate cancers whereas the three leading causes of cancer-related deaths in women are breast, lung and colorectal cancers.

Cancer mortality rates for the US mirrors that of other developed countries. In 2012, the estimated US cancer deaths in men were attributed to lung cancer (29%), prostate cancer (9%) and colorectal cancers (9%) whereas in women, lung cancer (26%), breast cancer (14%) and colorectal (9%) were the top three causes of cancer deaths. Moreover, the American

Cancer Society (ACS) predicts that there will be a total of 1,660,290 new cancer cases almost evenly divided among men (51%) and women (49%) in 2013. Furthermore, a total of 580,350 deaths from cancer, 53% in men and 47% in women, are projected to occur in the US in 2013.

The ACS further reports that cancer deaths in the US have reduced between 1991 and 2009 by 20% overall, 24% in men and 16% in women (12). This reduction is most likely as a result of lower smoking rates for lung cancers, and earlier detection and treatment for prostate, colon and breast cancers (12). While the etiology of most cancers is unknown, it is generally agreed that heredity and environmental exposures play key roles in the onset and progression of many cancers. For example, many Japanese immigrants are typically at a lower risk of developing stomach cancers caused by the bacteria, *H. pylori*, when compared to indigenous populations (1). Lifestyle cancers account for almost 80% of total cancers in the US (1, 12); these lifestyle cancers are primarily linked to tobacco consumption (example, lung cancer) and high fat diets (example, pancreatic cancer). Furthermore, the National Institutes of Health (NIH) estimates that the overall costs of cancer in 2007 were over $226.8 billion (2): $103.8 billion for direct medical costs (total of all health expenditures) and $123.0 billion for indirect mortality costs (cost of lost productivity due to premature death).

D. Clinical manifestations and prevention of cancer

Researchers at Keele University in the United Kingdom have shown eight clinical features that have a higher predictive value for cancer onset and progression particularly in older adults (13): rectal bleeding, iron deficiency anemia, rectal examination that gives cause for concern, hematuria (blood in the urine), hemoptysis (coughing up blood), a breast lump, postmenopausal bleeding, and dysphagia (difficulty in swallowing). Early screening and detection of cancers in addition to lifestyle choices such as reduction in tobacco consumption and high fat diets are regarded as preventive measures for cancer onset and progression. However, the risk of cancer incidence also increases with age as a result of prolonged damage to the body's immune system and DNA repair systems.

E. Current trends in cancer treatment

Invasion and metastasis of malignant cells can result in death if the spread is not controlled; however treatment methods are dependent on the stage and type of cancer and include radiation, surgery, chemotherapy, hormone therapy, biological therapy, targeted therapy and complementary and alternative medicine (CAM) (14). Depending on the stage, many non-hematological cancers can be terminated by surgical exclusion whereas radiation therapy can be used to treat virtually any type of cancer. CAM refers

7

to non-standard medical practices used in the treatment of cancer including acupuncture and yoga.

There are three broad categories of drugs for treatment of cancers and these are cytotoxic chemotherapy, hormone therapies and targeted therapies (14). Cytotoxic chemotherapy refer to drugs that kill rapidly diving cells in general and constitutes the most conventional class of drugs for cancer treatment. Cytotoxic chemotherapy drugs are subdivided into six major classes. The first are alkylating agents that directly damage DNA by cross-linking DNA strands via the addition of alkyl groups directly to guanine bases in DNA thus preventing DNA replication and concurrently RNA transcription. Alkylating agents, particularly the nitrogen mustards, were the first reported chemotherapy drug but are no longer widely used due to toxicity issues. However, the FDA approved Treanda (generically known as bendamustine) a nitrogen mustard, for the treatment of chronic lymphocytic leukemias and lymphomas in 2008 (15). It should be noted that alkylating agents do not selectively damage malignant cells and as such are associated with a broad range of local and systemic toxic effects; long term use is associated with damage to the bone marrow and onset of second cancers particularly bladder cancer and acute leukemia. Platinum-containing drugs, particularly cisplatin used in the treatment of testicular cancer, are often grouped with alkylating agents because they exert a similar mechanism of action but are less likely to cause leukemias (16).

8

Antimetabolites are a second class of antineoplastic drugs that function as cytostatics because they interfere with DNA and RNA production and concurrently cell division and tumor growth. For example, Efudex (generically known as 5-Fluorouracil or 5-FU) is a pyrimidine analog that is classified as a suicide inhibitor because it works through an irreversible inhibition of thymidylate synthase, an enzyme that plays a key role in DNA synthesis and repair (17). 5-FU is an established form of treatment for colorectal and pancreatic cancer; But 5-FU is also associated with toxicity and a range of side effects including myelosuppression and diarrhea.

Anti-tumor antibiotics are a third class of cancer chemotherapy drugs that consist of five major drug groups: anthracyclines, dactinomycin, plicamycin, mitomycin, and bleomycin. The anthracyclines are by far the most popular anti-tumor antibiotics and have been shown to be effective against more types of cancer than any other class of chemotherapeutic agents (18, 19). The prototypical anthracyclines, Daunomycin cerebudine (daunorubicin)—the first reported anthracycline—and Adriamycin (doxorubicin), are both isolated from the bacterium, *Streptomyces peucetius* but there are currently over 2,000 known analogs of doxorubicin (18). Anthracyclines work by intercalating DNA thus interfering with enzymes involved in DNA replication. Anthracyclines are used in the treatment of a wide variety of cancers including leukemias, lymphomas, breast, uterine and

lung cancers. However, the biggest limitation to their use is cardiotoxicity (19).

Topoisomerase (ToP) inhibitors constitute the fourth class of antineoplastic drugs; as the same suggests, these inhibitors interfere with the action of topoisomerases, which are ubiquitous enzymes that control DNA supercoiling and entanglements structure by catalyzing the breaking and rejoining of DNA strands (20). The mechanism of action (MOA) of ToP inhibitors also classifies them as pharmacological inhibitors of poly (ADP-ribose) polymerase (PARP) used for the therapy of many diseases including cancer (20, 21). There are two major classes of topoisomerases (I and II) and ToP inhibitors are typically classified based on the class of topoisomerase that is inhibited (20). For example, Camptosar (irinotecan) is a topoisomerase I inhibitor that is typically combined with 5 F-U for the treatment of colon cancers. Alternatively, Etopophos (Etoposide, etoposide phosphate or VP-16) is a topoisomerase II inhibitor that is often used in combination with other chemotherapy drugs to treat many cancers including lung cancer and testicular cancer. However, it should be noted that treatment with topoisomerase II inhibitors is associated with an increased risk of a second cancer — acute myelogenous leukemia (AML) (14).

Mitotic inhibitors are a fifth class of cancer chemotherapeutic drugs that are typically plant alkaloids and other natural product derivatives. Mitotic

10

inhibitors prevent the process of mitosis through microtubule polymerization thus preventing cancerous growth. Mitotic inhibitors are used in the treatment of many cancers including breast, lung and myelomas. For example, the taxanes, Taxol (paclitaxel) and Taxotere (docetaxel) are commonly used for the treatment of breast and lung cancers (22). However, these mitotic inhibitors are known for their potential to induce peripheral nerve damage which can be a dose-limiting side effect (14).

Corticosteroids constitute the sixth class of cancer chemotherapy drugs and refer to natural steroidal hormones and steroidal-like drugs that are used to destroy malignant neoplasms, particularly lymphomas, leukemias and lymphomas. Corticosteroids are also widely used for their anti-emetic properties to prevent nausea and vomiting caused by chemotherapy. Corticosteroids such as prednisone can also be used to prevent hypersensitivity prior to administering chemotherapy (14).

There are many other drugs, such as differentiating agents, used in the treatment of cancer that are not classically cytotoxic chemotherapeutic drugs. Differentiating agents are based on the concept that cancer cells are immature and as a result less differentiated than normal cells thus these differentiating agents are therapies that induce cancer cell to resume the process of maturation. Even though differentiation therapies do not destroy cancerous cells, they restrain cell growth thus allowing for the use of more

11

conventional chemotherapy drugs. For example, retinoids have been successfully used in the treatment of acute promyelocytic leukemia (23, 24).

Hormonal therapies constitute the second broad classification of drugs used in the treatment of cancer. Hormone therapy include sex hormones or hormone-like drugs that change the action or production of specific hormones, particularly steroid hormones, or drugs that inhibit the production or activity of such hormones known as hormone antagonists. Hormone therapies are used to slow the growth of breast, prostate, and endometrial (uterine) cancers because these sex hormones are powerful drivers of gene expression in these cancers; therefore the drugs work by preventing cancerous cells from using the hormones needed for growth or by preventing the body from making the hormones (14). Hormonal therapies are largely subdivided into inhibitors of hormone synthesis, hormone receptor antagonists and hormone supplements. Aromatase inhibitors and Gonadotropin-releasing hormone (GnRH) analogs are considered inhibitors of hormone synthesis (25-27). Aromatase inhibitors are used primarily in the treatment of breast cancer in post-menopausal women and include Arimidex (anastrozole) (25). Analogs or agonists of GnRH, also known as luteinizing hormone-releasing hormone (LHRH), induce a chemical castration that involves complete suppression of testosterone production from the male testes or complete suppression of the production of estrogen and progesterone from the female ovaries (26, 27). For example, Lupron

12

(leuprolide) and Zoladex (goserelin) are used in the treatment of hormone-responsive cancers: breast, prostate, and estrogen-dependent conditions such as endometriosis and uterine fibroids (27).

Hormone receptor antagonists include antiandrogens and selective estrogen receptor modulators (SERMs). Antiandrogens like Eulexin (flutamide) work by blocking the androgen receptor (28) whereas SERMs work by blocking the estrogen receptor (29, 30). However, some SERMs like tamoxifen are only partial agonists that can actually increase estrogen receptor signaling in some tissues, such as the endometrium (29, 30). Tamoxifen is currently first-line treatment for nearly all pre-menopausal women with hormone receptor-positive breast cancer (29, 30). Hormone supplementations include androgens like Halotestin (fluoxymesterone) that is used in the treatment of breast cancers (31).

Targeted therapies are becoming increasingly more popular in cancer treatment as a result of a better understanding of proteins through major discoveries in the field of molecular oncology (1, 14). Targeted therapies can be used as part of the main treatment, or they may be used after treatment to maintain remission or decrease the chance of recurrence. Targeted therapies work by blocking the growth of cancer cells by interfering with specific protein targets that are needed for carcinogenesis and tumor growth. For example, Gleevec (Imatinib Mesylate) is a tyrosine kinase inhibitor that was rapidly

13

approved by the FDA in 2001 for the treatment of a specific abnormality associated with chronic myelogenous leukemia (CML) known as the Philadelphia chromosome-positive CML (32, 33). Gleevec has also been approved for the treatment of gastrointestinal stromal tumors (GIST) and for use in children with acute lymphoblastic leukemia (ALL) (34, 35).

Targeted therapies can either be small molecule inhibitors like Gleevec or imunotherapies such as vaccines and monoclonal antibodies. Cancer immunotherapies employ the use of the immune system to reject cancer by stimulating a patient's immune system to attack the malignant tumor cells. Compared to other types of cancer treatments, immunotherapies are relatively new and are typically classified as either active or passive (14). Active immunotherapies stimulate the body's own immune system to fight cancers. Active immunotherapies are usually administered via immunization, such as the prostate cancer vaccine, Provenge (generically known as sipuleucel-T) that was the first FDA therapeutic cancer vaccine that was approved in 2010 (36). Alternatively, passive immunotherapies utilize therapeutic antibodies as drugs, in which case the patient's immune system is recruited to destroy tumor cells by the therapeutic antibodies For example, Herceptin (trastuzumab) is a monoclonal antibody that selectively binds with high affinity to the extracellular domain of the human epidermal growth factor receptor 2 protein (HER2) that is implicated in many breast cancers (14).

14

F. Conclusions

Cancers are complex diseases that present significant financial and emotional burden due to high prevalence worldwide and concomitantly high mortality rates particularly in developing countries. While efforts are currently in place for more effective prevention and treatment of cancer, there are many limitations that have reduced cancer survival including late stage screening, expensive treatment costs, toxicity and debilitating side effects. Reductions in cancer mortality rates in the US are attributed to lower smoking rates and earlier screening and treatments. Targeted therapies are becoming more popular because of improved efficacy particularly when compared to cytotoxic chemotherapeutic agents that show poor selectivity between proliferating cells in cancerous and normal tissues.

G. References

1. Weinberg, R. The Biology of Cancer. New York, NY: Garland Science, Taylor & Francis Group, LLC., 2007.
2. The American Cancer Society. Cancer Facts and Figures 2013. Retrieved from http://www.cancer.org/acs/groups/content/@epidemiologysurveilance/documents/document/acspc-036845.pdf
3. The American Cancer Society. Global Cancer Facts and Figures, 2nd Edition. Retrieved from http://www.cancer.org/acs/groups/content/@epidemiologysurveilance/documents/document/acspc-027766.pdf
4. World Health Organization. Cancer Key Facts. Retrieved from http://www.who.int/mediacentre/factsheets/fs297/en/index.html
5. National Institutes of Health, Cancer. Retrieved from http://www.ncbi.nlm.nih.gov/pubmedhealth/PMH0002267/

6. Hagelkruys, A., Sawicka, A., Rennmayr, M., et.al. The biology of HDAC in cancer: the nuclear and epigenetic components. Handb Exp. Pharmacol. 2011; 206: 13-37.

7. Hanahan, D., & Weinberg, R.A. The hallmarks of cancer. Cell. 2000; 100(1):57-70.

8. Jaffe, E.S. The 2008 WHO classification of lymphomas: implications for clinical practice and translational research. Hematology Am Soc Hematol Educ Program. 2009; 523-31.

9. Campo, E., Swerdlow, S.H., Harris, N.L., et. al. The 2008 WHO classification of lymphoid neoplasms and beyond: evolving concepts and practical applications. Blood. 2011; 117(19):5019-32.

10. Asadullah, K., Friedrich, M., & Döcke, W.D., et. al. Enhanced expression of T-cell activation and natural killer cell antigens indicates systemic anti-tumor response in early primary cutaneous T-cell lymphoma. J Invest Dermatol. 1997; 108 (5):743-7.

11. National Cancer Institute. Cancer Staging. Retrieved from http://www.cancer.gov/cancertopics/factsheet/detection/staging

12. Simon, Stacy. Facts and Figures Reports: Decline in Cancer Rates Reach Milestone. Retrieved from http://www.cancer.org/cancer/news/news/facts-and-figures-report-declines-in-cancer-deaths-reach-milestone

13. Shapley, M., Mansell, G., Jordan, J.L., et.al. Positive predictive value of ≥5% in primary care for cancer: systematic review. Br J Gen Pract. 2010; 60 (578): e366-77.

14. American Cancer Society. Chemotherapy Principles: An In-depth Discussion. Retrieved from http://www.cancer.org/treatment/treatmentsandsideeffects/treatmenttypes/chemotherapy/chemotherapyprinciplesanin-depthdiscussionofthetechniquesanditsroleintreatment/chemotherapy-principles-types-of-chemo-drugs

15. National Cancer Institute. FDA Approval for Bendamustine Hydrochloride. Retrieved from http://www.cancer.gov/cancertopics/druginfo/fda-bendamustine-hydrochloride

16. Wheate, N.J., Walker, S., Craig, G.E., et. al. The status of platinum anticancer drugs in the clinic and in clinical trials. Dalton Trans. 2010; 39(35):8113-27.

17. Longley, D.B., Harkin, D.P., & Johnston, P.G. 5-fluorouracil: mechanisms of action and clinical strategies. Nat. Rev. Cancer 2003; 3 (5): 330–8.

18. Weiss, R.B. The anthracyclines: will we ever find a better doxorubicin? Semin. Oncol. 1992; 19 (6): 670–86.

19. Minotti, G., Menna, P., Salvatorelli, E., et. al. Anthracyclines: molecular advances and pharmacologic developments in antitumor activity and cardiotoxicity. Pharmacol. Rev. 2004; 56 (2): 185–229.

20. Pommier, Y. Drugging topoisomerases: lessons and challenges. ACS Chem Biol. 2013; 18; 8 (1):82-95.
21. Curtin, N., & Szabo, C. Therapeutic applications of PARP inhibitors: Anticancer therapy and beyond. Mol Aspects Med. 2013 Jan 29. pii: S0098-2997(13)00007-1. doi: 10.1016/j.mam.2013.01.006. [Epub ahead of print]
22. Sparano, J,A. Taxanes for Breast Cancer: An Evidence-based review of randomized phase II and phase III trials. Clin Breast Cancer. 2000; 1(1):32-40.
23. Garattini, E., Gianni, M., & Terao, M. Retinoids as differentiating agents in oncology: a network of interactions with intracellular pathways as the basis for rational therapeutic combinations. Curr Pharm Des. 2007; 13 (13):1375-400.
24. Garattini, E., Gianni, M., & Terao, M. Cytodifferentiation by retinoids, a novel therapeutic option in oncology: rational combinations with other therapeutic agents. Vitam Horm. 2007; 75: 301-54.
25. Haque, R., Ahmed, S.A., Fisher, A., et.al. Effectiveness of aromatase inhibitors and tamoxifen in reducing subsequent breast cancer. Cancer Med. 2012;1 (3):318-27.
26. Limonta, P., & Manea, M. Gonadotropin-releasing hormone receptors as molecular therapeutic targets in prostate cancer: Current options and emerging strategies. Cancer Treat Rev. 2013 Jan 3. pii: S0305-7372(12)00242-3. doi: 10.1016/j.ctrv.2012.12.003. [Epub ahead of print]
27. Aydiner, A., Kilic, L., Yildiz, I., et. al. Two different formulations with equivalent effect? Comparison of serum estradiol suppression with monthly goserelin and trimonthly leuprolide in breast cancer patients. Med Oncol. 2013; 30 (1):354.
28. Simard, J., Luthy, I., Guay, J., et. al. Characteristics of interaction of the antiandrogen flutamide with the androgen receptor in various target tissues. Mol Cell Endocrinol. 1986; 44 (3):261-70.
29. Cirillo, F., Nassa, G., Tarallo, R., et. al. Molecular Mechanisms of Selective Estrogen Receptor Modulator Activity in Human Breast Cancer Cells: Identification of Novel Nuclear Cofactors of Antiestrogen-ERα Complexes by Interaction Proteomics. J Proteome Res. 2013;12 (1):421-31.
30. Lin, S-L., Yan, L-Y., Zhang, X-T., et. al. ER-α36, a Variant of ER-α, Promotes Tamoxifen Agonist Action in Endometrial Cancer Cells via the MAPK/ERK and PI3K/Akt Pathways. PLoS One. 2010; 5(2): e9013
31. Cleve, A., Fritzemeier, K.H., Haendler, B., et. al. Pharmacology and clinical use of sex steroid hormone receptor modulators. Handb Exp Pharmacol. 2012; (214):543-87.
32. U.S. Food and Drug Administration. Gleevec (Imatinib Mesylate). Retrieved from

http://www.fda.gov/drugs/drugsafety/postmarketdrugsafetyinformationforpatientsandproviders/ucm110502.htm

33. National Cancer Institute. FDA Approves Important New Leukemia Drug. Retrieved from http://www.cancer.gov/newscenter/newsfromnci/2001/gleevecpressrelease

34. U.S. Food and Drug Administration. FDA approves Gleevec for expanded use in patients with rare gastrointestinal cancer. Retrieved from http://www.fda.gov/NewsEvents/Newsroom/PressAnnouncements/ucm289760.htm

35. U.S. Food and Drug Administration. FDA approves Gleevec for children with acute lymphoblastic leukemia. Retrieved from http://www.fda.gov/NewsEvents/Newsroom/PressAnnouncements/ucm336868.htm

36. U.S. Food and Drug Administration. FDA Approves a Cellular Immunotherapy for Men with Advanced Prostate Cancer. Retrieved from http://www.fda.gov/NewsEvents/Newsroom/PressAnnouncements/ucm210174.htm

Chapter 2

Biological and clinical significance of histone deacetylases (HDACs)

A. Introduction

Epigenetic alterations of chromatin structure are implicated in carcinogenesis and malignant transformations and refer to heritable changes in gene expression that are not accompanied by changes in DNA sequence (1, 2). The fact that histone acetylation is a key component in the regulation of gene expression has inspired the study of enzymes known as histone deacetylases (HDAC) because of their role in changing the accessibility of DNA to regulatory proteins (3-11). HDACs possess complex, multifunctional roles including transcriptional regulation, regulation of tubulin and cytoskeletal function, control of cardiac growth, regulation of thymocyte development and facilitation of DNA repair (12-16). In this chapter, we will discuss the biological and clinical relevance of HDACs as targets for the treatment of cancer and other key therapeutic areas.

B. HDACs are key players in the regulation of gene expression

The precise organization of chromatin is essential for many cellular processes, including transcription, replication, repair, recombination and chromosome segregation (3, 10, 16-19). Dynamic changes in chromatin structure are directly modulated by post-translational modifications of the amino-terminal tails (3); these covalent modifications typically alter the

interaction of the highly basic histone tails with the negatively charged DNA backbone or with other chromatin-associated proteins that may be required for different downstream cellular processes (3). Post-translational modifications of histones include phosphorylation, methylation, ubiquitylation, sumoylation, and acetylation (3, 6, 17-21).

Histone acetylation is considered to be the most studied post-translational modulation of nucleosomes (21, 22). Histone acetylation is regulated by histone acetyltransferases (HATs) and results in an open chromatin configuration and gene transcription whereas histone deacetylation is regulated by HDACs and results in gene silencing (3, 20, 23). Hypo-acetylated histones increase the positive charge of histone and condense the chromatin while hyperacetylated histones neutralize the electrostatic charge thus resulting in chromatin relaxation (20, 23). Moreover, many transcription activators such as the p300/CBP complex and transcription repressors like the retinoblastoma protein (pRb) have been associated with HATs and HDACs respectively (20,25). Furthermore, the balance between acetylated and nonacetylated proteins is controlled by the activity of HDACs and HATs (3, 17, 20, 21, 23-25).

Many recent studies have shown that inhibition of HDACs elicits anticancer effects in several tumor cells by inhibition of cell growth and inducing cell differentiation (6, 10, 19, 22, 23, 24, 26-29). HDAC inhibition is

20

also associated with neuroprotective effects in both *in vivo* and *in vitro* models of brain disorders (11, 25, 27-29). Furthermore, HDACs are also garnering interest in stem cell research since HDAC inhibition results in a two- to fivefold increase in the efficiency of reprogramming of somatic cells to a pluripotent state (12, 27-29). Inhibition of HDAC enzymes also results in the alteration of the response to ischemic injury in the heart and reduces infarct size which suggests novel therapeutic approaches for acute coronary syndromes (13, 27). HDAC inhibitors (HDACi) have also found applications as anti-inflammatory agents (27-29) and in the treatment of autoimmune disorders including colitis (27, 30).

C. Classification and distribution of HDACs

HDACs, also known as lysine deacetylases (KDACs) that more aptly describes their function instead of their targets, are a family of enzymes that catalyze the reversible removal of acetyl groups on lysine residues of proteins, including the core nucleosomal histones H2A, H2B, H3, and H4 (6, 24). There are 18 known HDAC isozymes classified into four groups on the basis of phylogenetic and functional analysis (4, 15, 17-20, 22, 24,26, 31-40). The most studied HDACs are the classical HDACs (Table 1) that are zinc-dependent amidohydrolases and consist of 11 enzymes sub-divided into class I (HDAC-1,-2,-3, &-8), IIa (HDAC-4,-5, -7 & -9), IIb (HDAC-6 & -10) and IV (HDAC11). The Class III HDACs require nicotinamide adenine

21

dinucleotide (NAD$^+$) as a co-substrate and consist of the silent information

regulator 2 (SIR2)-related-proteins (Sirtuins; SIRT) SIRT 1-7 (7, 15, 16, 26,

31, 32).

Class I HDACs are approximately 400-500 residues long, and consist of

HDAC1, -2, -3, and -8; class II HDACs are approximately 1,000 residues long

and are subdivided into class IIa and IIb HDAC enzymes.

Table 1: Biological functions of class I and class II HDACs(1,8).		
HDAC Class	**Isoform**	**Biological Functions**
Class I	HDAC1	Proliferation; gene regulation; apoptosis
	HDAC2	Proliferation; cardiac morphogenesis
	HDAC3	Proliferation; regulation of Interferon expression
	HDAC8	Proliferation; regulation of contractile capacity; telomerase activity
Class IIa	HDAC4	Skeletogenesis; chondrocyte hypertrophy; mediator of neuronal death; repression of retinoid signaling; stabilization of Hypoxia-inducible factor-1 (HIF-1)
	HDAC5	Suppression of cardiac stress; cardiac development
	HDAC7	Regulation of apoptosis in developing thymocytes
	HDAC9	Cardiac development
Class IIb	HDAC6	Proliferation; regulation of tubulin acetylation; heat shock protein (Hsp90) acetylation

Class IIa HDACs consists of HDAC4, -5, -7, and -9; HDAC6 and

HDAC10 constitute the class IIb HDACs and are the only HDACs that have

two catalytic sites that are believed to work independently (33). HDAC11, the

lone member of class IV, is made up of 347 amino acids and shares

22

conserved residues in its catalytic site with class I and II HDACs (7, 15, 16, 28, 19, 26).

HDACs as well as HATs are recruited to transcription factor protein complexes without directly binding to DNA (3, 7). In fact, with the exception of HDAC8, HDACs exist as multiprotein complexes that include co-repressors such as Sin3, nuclear receptor co-repressor (N-CoR), silencing mediator for retinoic acid and thyroid hormone receptor (SMRT), activators, chromatin-remodelling proteins and HATs (7, 26, 38, 40-42). For example, the enzymatic activity of HDAC3 is greatly enhanced through interaction with the SMRT/N-CoR repressor complex (38, 42) whereas HDAC1 and HDAC2 are recruited together into three main transcriptional complexes: Sin3A, NuRD and CoREST (40, 41).

With the exception of HDAC8, class I HDACs are ubiquitously expressed in various human tissues, located in the nucleus, and function as transcription corepressors (6, 7, 19, 20, 39). However, HDAC8 expression is restricted to primary cells that show smooth muscle differentiation and possibly shifts between the nucleus and cytoplasm potentially implying a different biological function for HDAC8 (19, 26, 32, 35, 36). Class II HDACs are selectively distributed in human tissues; class IIa enzymes shuttle between the cytoplasm and the nucleus whereas class IIb HDACs are primarily located in the cytoplasm. Three of the class III sirtuins (SIRT1,

23

SIRT6-7) are localized in the nucleus, SIRT3-5 are localized in the

mitochondria and SIRT2 is a cytoplasmic protein (14). HDAC11, the unique

member of class IV, resides in the nucleus and is found primarily in the brain,

heart, skeletal muscle and kidney (7).

D. HDAC8 as a model for the elucidation of target-ligand interactions

HDAC8 is a 377 residue class I enzyme that lies close to the

phylogenetic boundary between class I and class II HDACs, and maps to the

X chromosome (16, 18, 19, 26, 35). The three dimensional crystal structure of

human HDAC8 (Figure 1) complexed with structurally diverse hydroxamic

acid HDAC inhibitors was first solved in 2004 by two independent groups

(PDB ID: 1W22 and 1T64; 16, 19). Since then, the HDAC2 foot pocket and

catalytic domains of HDAC4 and HDAC7 have been solved (26).

Furthermore, the crystal structure of the tetrameric oligomerization domain of

HDAC3 complexed with transducin (beta)-like 1-linked protein (TBL1), SMRT,

and G protein pathway suppressor 2 (GPS2) was recently solved (38, 42).

However, with the exception of HDAC8, functional HDACs are not found as

single polypeptides, but as high-molecular weight multiprotein complexes (6,

7, 19, 20, 39); therefore, from a structural biology perspective, HDAC8 is the

best model for the study of catalysis and inhibition of HDAC enzymes (19,

26).
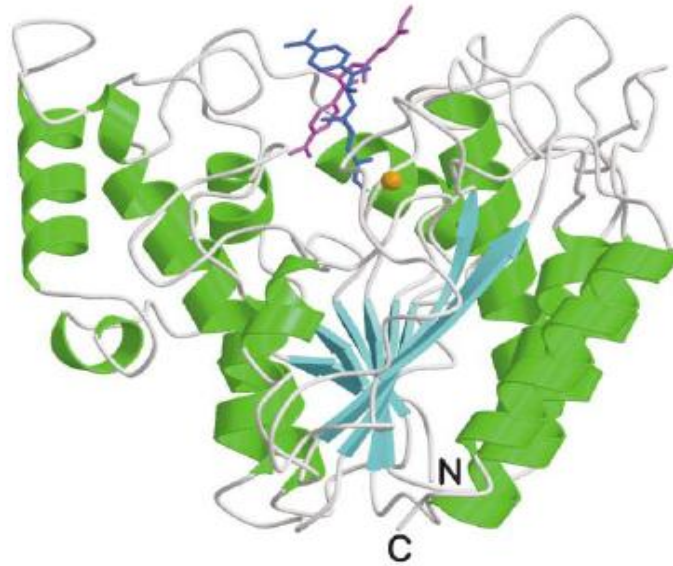
Figure 1: Ribbon diagram of the HDAC8:TSA complex showing the HDAC8 fold, the TSA molecules (blue and pink) and the zinc ion (orange) (PDB ID 1T64; 16).

X-ray crystallographic studies of HDAC8 have revealed that the architecture of the HDAC8 active site, likely to be common to all zinc-dependent HDACs, shares a 30% sequence identity (Figure 2) with the archeobacterial homolog of eukaryotic deacetylases (HDLP) (16,19, 37). HDAC8 also has a distinct inhibition pattern that differs from that of HDAC1 and -3, which both share 43% sequence identity with HDAC8 (19). Evaluation of HDAC inhibition by a diverse class of HDACi including TSA shows greater than a 300-fold difference between inhibition of either HDAC1 or HDAC3 when compared to HDAC8 inhibition (19). Furthermore, sequence alignments of HDAC8 with other class I HDACs

25

suggest that the other isozymes possess longer L1 loops that may result in more conformationally static active sites for HDAC-1, -2, and -3 when compared to HDAC8 (16). The structure of HDAC8 consists of a compact α/β-domain composed of a central eight-stranded parallel β-sheet (Figure 1) flanked by 13 α-helices (19, 26).
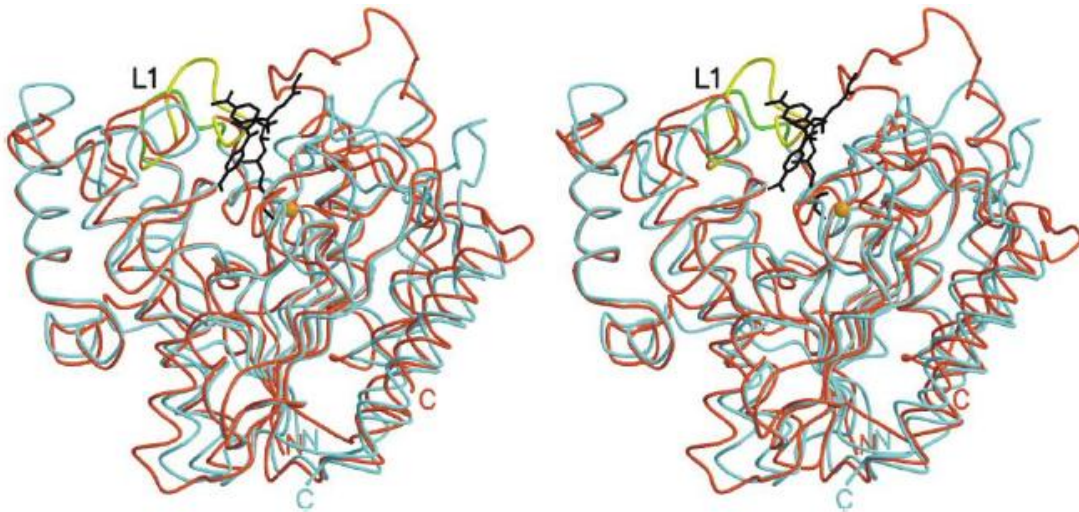
Figure 2: Stereo diagram (16) depicting superposition of the HDAC8:TSA structure (cyan) and the L1 loops of HDAC8 (green) and HDLP (yellow).

The asymmetric unit of HDAC8 (Figure 1) consists of two molecules packed as a head-to-head dimer (19). Each molecule binds one Zn^{2+} ion and two K^+ ions and the presence of K^+ ion is hypothesized to stabilize the oxyanion formed in the transition state of the deacetylation reaction (19, 26). The dimeric arrangement in the HDAC8 crystal is mediated by the two capping groups (pyridine and thiophene) of each hydroxamic acid inhibitor

26

molecule stacking against each other (19). This phenomenon explains why initial attempts to crystallize the enzyme without a bound ligand, otherwise known as the apoprotein, was unsuccessful (16, 18-19); this is because each capping group interacts with protein residues, Pro-273 and Tyr-306, of the opposite molecule, forming an extensive hydrophobic sandwich and giving rise to the twofold axis relating the two molecules in the asymmetric unit (19).

The HDAC8 active site displays characteristics of both serine and zinc proteases, and contains two histidine-to-aspartate (His–Asp) dyads with both histidine residues apparently acting as a general acid–base catalytic pair (Figure 3; 18, 19, 26, 35, 37). It is hypothesized that the catalytic metal ion (zinc) and a general base (Histidine142; H142) activates the water molecule in the HDAC active site (Figure 3) for a nucleophilic attack on the carbonyl group of the susbstrate (17, 26). The tetrahedral intermediate is stabilized by the formation of a hydrogen bond with Y306 (Phenylalanine306), and a general acid (H143) protonates the lysine leaving group and catalyzes the formation of the products from the tetrahedral intermediate (17).

27
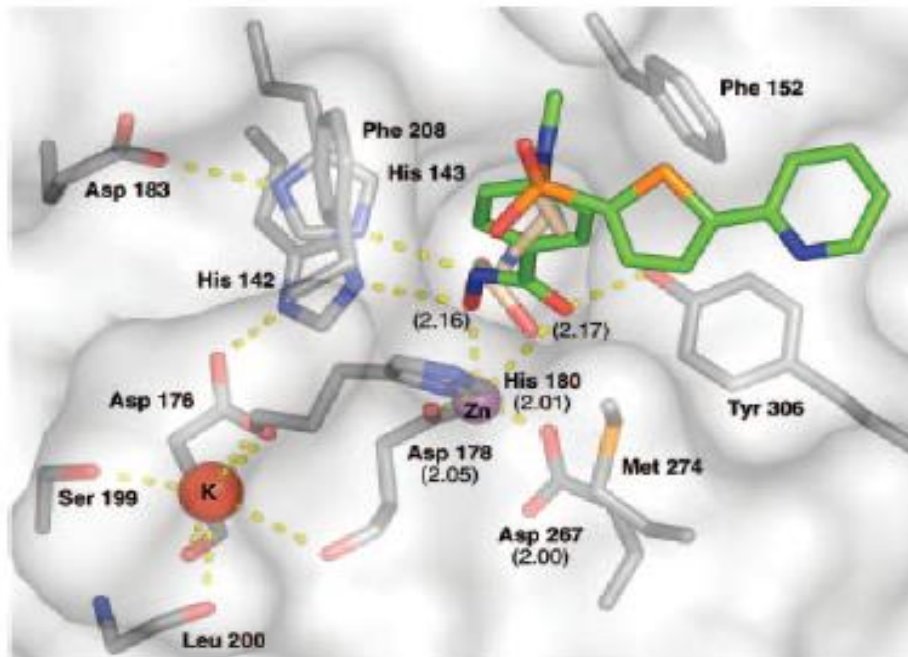
Figure 3: Molecular surface representation and architecture of the HDAC8 active site (19). Stick representations are used to depict residues important in catalysis and inhibitor binding as well as the inhibitor and the modeled acetyllysine substrate. Oxygen (red); nitrogen (blue); sulfur (orange); and carbon (gray).

The crystal structure of HDAC8 has led to a firmer understanding of how catalysis occurs within the HDAC family of enzymes but also revealed unique features of HDAC8, including conformational flexibility proximal to the binding site pocket mediated by the L1 active site loop (Figure 2) and the absence of a 50-111 amino acid C-terminal domain that extends from catalytic domain (16, 18, 19).

E. Diverse application of HDACi in several therapeutic areas

In recent years, many HDAC inhibitors (HDACi) have either been approved by the FDA or are in clinical development for cancer treatment particularly due to the fact that these HDACi exert minimally drastic side effects when compared to conventional chemotherapy (5-9, 14, 23, 27-29, 31, 34, 39, 43-45). However, an increasing number of structurally diverse HDACi have also been identified for the treatment of many other diseases, including, neurodegeneration, metabolic, inflammatory and autoimmune disorders, infectious diseases, and cardiovascular diseases (25, 27-29). Yet, the mechanisms of action of these HDACi for the treatment of most diseases remain poorly understood thus limiting advancement in clinical development and therapeutic administration (6, 28, 46, 47)
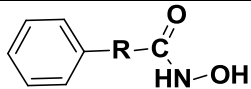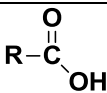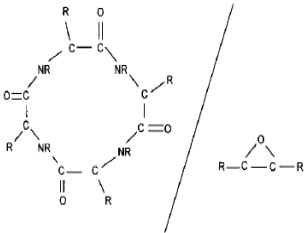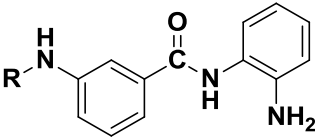
There are four major classes of HDAC inhibitors (Table 2) currently in clinical development: hydroxamic acids, short chain fatty acids, cyclic tetrapeptides and benzamides (4, 15). They all share a common pharmacophore pattern consisting of: a metal binding domain that complexes zinc; a linker domain that mimics the substrate and occupies the active site channel; a connecting unit, and a surface domain that makes contact with the rim of the catalytic pocket (15). All HDAC inhibitors (HDACi) inhibit HDAC enzymes in a reversible fashion, except for the epoxides (trapoxin and depudesin), which inhibit HDACs irreversibly via covalent binding to the epoxyketone group (4). Most HDACi, including the FDA-approved vorinostat,

are relatively nonselective inhibitors of all or most HDAC enzymes but are permeable to the blood-brain barrier (BBB) (25); this permeability to the BBB is an attractive feature particularly for the treatment of neurodegenerative diseases (25).

The largest class of HDAC inhibitors with the most promising therapeutic potential is the hydroxamic acids (4, 6, 7). In fact, seven of the twelve HDACi including currently undergoing clinical trials for the treatment of cancer, including panobinostat and belinostat are hydroxamic acids (6, 9, 23). Zolinza, (generically known as vorinostat and suberoylanilide bishydroxamide (SAHA); Table 3), a hydroxamic acid HDACi was approved by the U.S. Food and Drug Administration (FDA) in 2006 for the treatment of cutaneous T-cell lymphoma (6-9, 23, 48). Vorinostat is currently in clinical trials as monotherapy or in combination therapy for the treatment of both solid and hematological cancers (6, 48).

The use of the potent, antifungal hydroxamic acid HDACi, Trichostatin A (TSA) and its analog, vorinostat, in the treatment of colitis in mice results in an increase in the expression of thymic-derived $Foxp3^+$ T regulatory cells (Tregs) presumably as a result of HDAC9 inhibition (44). Administration of TSA in a middle cerebral artery occlusion model of brain ischemia resulted in a forty eight percent (48%) reduction in injury volume in treated animals when compared to non-treated models (13).

Table 2: Classification, potency and clinical application of key HDACi				
Group	**Structure**	**HDAC Inhibition**	*In vitro* IC$_{50}$ range	**Clinical Application**
Hydroxamic acids	R–C with O (double bond) and HN–OH, attached to phenyl ring	**Class I & II:** TSA, SAHA **HDAC6 only** (class IIb**):** Tubacin	nM	▪ Neurodegenerative ▪ Neurological ▪ Gastroentereology (colitis) ▪ Cardiovascular ▪ HIV ▪ **Cancer**
Short-chain fatty acids	R–C with O (double bond) and OH	**Class I & IIa:** Butyrate, VPA	mM	▪ Neurodegenerative ▪ Neurological ▪ Anti-epileptic ▪ Bipolar disorders ▪ HIV ▪ Stem cell research (lupus) ▪ **Cancer**
Cyclic tetrapeptides/ epoxides[4]	cyclic tetrapeptide structure and epoxide structure R–C–C–R	**HDAC-1 &-2** (class I): Romidepsin **HDAC-2& -3** (class I): Apicidin	nM	▪ **Cancer**
Benzamides	R–NH attached to benzene ring with C=O, NH, and benzene ring with NH$_2$	**HDAC1**: MS-275	µM	▪ **Cancer**
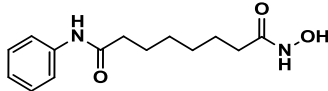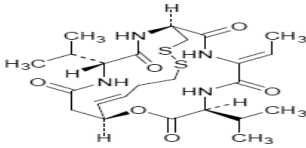
Treatment of wild-type mice as well as of mouse models of neurodegenerative diseases show that the inhibition of HDAC2 by vorinostat restored learning ability and promoted the retrieval of long-term memory more potently than the fatty acid HDACi, sodium butyrate (11). However, studies have shown that TSA, like many HDACi, have basal toxicity and prolonged treatment at high doses often leads to neuronal death thus limiting their neuroprotective effects (25, 49, 50).

Sodium phenylbutyrate (PB), a fatty acid HDACi, has also been shown to promote cytostasis and differentiation in myelodysplastic syndrome and acute myeloid leukemia (AML; 44). These effects may possibly be as a result of HDAC8 inhibition since HDAC8 has been shown to associate specifically with the inv(16) fusion protein found in AML(19, 51); besides, TSA has already been shown to impair inv(16)-mediated repression (19, 51). The fatty acid HDACi, valproic acid (VPA), is a pan-HDACi used in the treatment of epilepsy and bipolar disorders and shows promise in the treatment of both solid tumors and hematological malignancies (7, 25, 45, 48). VPA has also been shown to possess neuroprotective effects, presumably as a result of reducing excitotoxicity, in cultured primary neurons that are induced by exposure to glutamate (25, 48-50); glutamate-induced excitotoxicity is implicated in the pathophysiology of many neurodegenerative diseases such as Parkinson's disease suggesting a promising therapeutic application for VPA (11, 25, 48-50).

Moreover, HDAC2 inhibition has been shown to facilitate learning and memory in wild-type mice as well as in mouse models of neurodegeneration (11). Thus, the neuroprotective effects of VPA may be attributed to HDAC2 inhibition. VPA is also currently in clinical studies for the treatment of HIV and retinitis pigmentosa (45, 48, 52, 53). VPA has been shown to be more potent than the hydroxamates, TSA and vorinostat, in the reprogramming of somatic cells to a pleuripotent state possibly by the collective effects of upregulation of embryonic stem (ES)-specific genes and the downregulation of mouse embryonic fibroblasts (MEF) as a result of HDAC inhibition (12).

The bicyclic peptide, Istodax (generically known as Romidepsin; Table 3) was the second HDACi to be approved by the FDA in 2009 for the treatment of CTCL (6, 47). MS-275, a benzamide derivative, is in Phase I clinical trials in the treatment of several forms of cancer but no full report has been published to date (7). Entinostat, a synthetic benzamide derivative, has been shown to selectively inhibit two class I HDAC enzymes, HDAC1 and HDAC3 (6). Entinostat and mocetinostat are isoform-selective, synthetic benzamide derivatives that are currently in clinical trials for the treatment of both solid and hematological cancers (2, 6, 48). Entinostat is also in clinical trials for the treatment of relapsed or refractory Hodgkin lymphoma (6).

33

Table 3: Comparative analysis of the two FDA-approved HDACi		
Category	**HDACi**	
Brand name	Zolinza (Merck & Co., Inc.)	Istodax (Gloucester Pharma)
Generic names (s)	Vorinostat; SAHA	Romidepsin
Approval Date:	October 2006	November 2009
Structural Class	Hydroxamic acid	Cyclic tetrapeptide
Structure[4]		
HDAC inhibition	Broad-spectrum	Class I-specific
Source	Trichostatin A (TSA) Analog **Note:** TSA isolated from the bacterium *Streptomyces hygroscopius*	Isolated from the bacterium *Chromobacterium violaceum*
Clinical Indication	CTCL (progressive or recurrent or following 2 systemic therapies; based on 2 clinical trials with 107 patients total)	CTCL (in patients who have received at least 1 prior systemic therapy; based on 2 clinical trials with 167 patients total)
Mode of Action	Not fully characterized but shown to: 1. Cause accumulation of acetylated histones *in vitro*. 2. Induce cell cycle arrest and/or apoptosis of some transformed cells.	Not fully characterized but shown to: 1. Induce cell differentiation, cell-cycle arrest and apoptosis. 2. Inhibit hypoxia-induced angiogenesis and depletes several oncoproteins.
Adverse effects	1. Gastrointestinal symptoms: diarrhea, nausea, anorexia, weight decrease, vomiting, constipation. 2. Constitutional symptoms: fatigue, chills. 3. Hematologic abnormalities: thrombocytopenia (low platelet count), anemia. 4. Taste disorders: dysgeusia, dry mouth.	1. Gastrointestinal symptoms: nausea, vomiting, anorexia. 2. Constitutional symptoms: fatigue. 3. Hematologic abnormalities: anemia, thrombocytopenia, neutropenia (low white blood cells), and lymphopenia. 4. Other adverse effects: electrocardiogram (ECG) changes.

34

F. HDACs are validated targets for the treatment of cancer

The increased focus on HDAC inhibitors (HDACi) for cancer treatment stems from their ability to alter several cellular functions known to be important in cancer cells (4, 6, 8, 14, 15, 19, 26). HDACi have demonstrated anticancer efficacy across a range of malignancies, especially in the hematological cancers resulting in the approval of two HDACi for CTCL treatment (16). The mechanisms of the antiproliferative effects of HDACi is not fully elucidated but generally involves the accumulation of acetylated histones and non-histone protein substrates that are involved in the regulation of gene expression, cell proliferation and cell death (7).

HDACs have been shown to play a significant role in transcriptional regulation and regulation of tubulin and cytoskeletal function (54-56). HDAC1, HDAC2, HDAC3, and HDAC9 have been shown to coimmunoprecipitate with the ATP-dependent heat shock protein-70 (Hsp-70) resulting in inhibition of the chaperone activity of the protein (9, 30). HDAC6 has been shown to deacetylate the structural protein, α-tubulin, resulting in a modulation of cell motility (9, 56). HDACs are known to associate with a number of well characterized cellular oncogenes and tumor-suppressor genes such as the retinoblastoma protein, leading to an aberrant recruitment of HDAC activity, which in turn results in changes in gene expression (4). Overexpression of HDACs has also been observed in different tumor types including gastric,

35

colorectal, breast and prostate cancers as well as hematological cancers like leukemias and lymphomas (9, 19, 31, 35, 39, 57-60).

Gene knockout experiments have shown that class 1 HDACs are important in cell survival and proliferation whereas class II HDACs have tissue-specific roles (15, 19, 36). Class I enzymes, especially HDACS -1, -2 and -3, are the most frequently expressed in cancers including lymphoid cell lines and primary tumors (4, 7, 14, 26, 32, 56). Evidence for increased expression of the class I HDACs, HDAC-1, -2 and -3, have also been reported in colon cancer (58, 59). Overexpression of HDAC1 has been reported in approximately 70% of all prostate cancer lesions (57, 60); whereas, overexpression of HDAC8 has been observed in a common form of acute myeloid leukemia (16, 19). Overexpression of the class II enzyme, HDAC10 has also been reported in gastric cancer (56).

G. Therapeutic limitations of broad-spectrum HDACi

It has been demonstrated that broad-spectrum inhibition of several HDAC isoforms disrupt multiple cellular processes that depend on protein acetylation (55); however, some of these processes may not be involved in the maintenance of tumor progression thus broad-spectrum HDAC inhibition increases the potential for toxicity (23, 55). A recent high-throughput profiling of the potency of a panel of structurally diverse small HDACi against all class I and II HDAC enzymes showed an apparent redundancy of these HDACi

36

such as vorinostat towards inhibition of toward HDAC-1, -2, and -3 but the class IIa enzymes are not targeted by most HDACi tested (6).

Furthermore, most HDACi, especially the hydroxamic acids, bind the zinc ion in the HDAC active site and show limited isoform selectivity within or between class I, II and IV HDACs (19). The two FDA-approved HDACi, vorinostat and romidepsin, like most HDACi currently in clinical development, are nonselective inhibitors of all or most of class 1 and class II HDACs resulting in significant adverse side-effects that become dose-limiting in clinical trials (6, 9, 19).

H. Current trends in pre-clinical and clinical development of HDACi: Isoform-selective HDACi and combination therapies

We have recently reported increased development of isoform-selective HDACi presumably as a result of superiority in the reduction of toxic effects as well as improved efficacy (48). However, seven of the twelve HDAC inhibitors currently in clinical development are hydroxamic acids (15); this hydroxamic acid functionality binds to a zinc ion in the active site displaying little isoform selectivity between class I, II and IV HDACs (16). Furthermore, the presence of the strong metal chelating group in hydroxamic acids can result in inhibition of other metalloenzymes or sequestration of metal ions (16).

37

Isoform-selective HDAC inhibitors (HDACi) offer the ability to alter distinct pathways, which are more specifically involved in the tumor phenotype and could therefore provide a wider therapeutic index compared with the broad spectrum HDACi currently in clinical development (4, 23, 37). There are several factors that have hindered the development of potent isoform-selective HDAC inhibitors (HDACi); these factors include similarity between the catalytic sites of HDAC enzymes, and until recently, lack of X-ray crystal structures (7, 19). A ranking of the substrate selectivity of HDACs using a library of fluorogenic tetrapeptide substrates suggests that HDAC8 has the highest substrate selectivity followed by HDAC-1, -3 and -6 (37, 61). Differences in catalytic activity and even substrate selectivity can be exploited in developing isoform-selective class I and possibly class II HDACi with a wider therapeutic index against more aggressive and more common forms of cancer (10, 37, 61).

Three-dimensional models for four class I histone deacetylases (HDAC-1, -2, -3, and -8), built using homology modeling and docked to three widely studied hydroxamic acid HDACi (TSA, CG-1521, and SK683) shows small differences in the shape and charge distribution around the opening of the active site of the enzymes (10). These observations indicate that it is possible to develop HDAC8-selective inhibitors, whereas development of isoform-selective inhibitors between HDACs that show more sequence homology, such as HDAC1 and -3, may be more challenging (10). However,

Arqule Inc. has reported a series of aliphatic hydroxamic acids that show selectivity towards HDAC1 (48). Furthermore, screens of large compound libraries have yielded selective inhibitors of HDACs 1, 4, 6, and 8 but structural determinants of selective HDAC inhibition remain unknown (7, 9, 45, 48).

It is generally agreed that combination of chemotherapy or chemoradiotherapy is preferable over single-agent therapy in order to maximize treatment efficacy and concurrently reducing toxicity (6, 7, 9). Various preclinical and clinical studies have shown that HDACi can improve the efficacy of several chemotherapeutic and radiotherapeutic treatments including targeted anticancer drugs, cytotoxic agents, antiangiogenesis drugs, or radiation therapy (6). This improvement in efficacy may be attributed to synergistic or additive effects particularly given that these HDACi exert relatively minor side effects when compared to conventional chemotherapy (6, 28). Furthermore, combination therapies may also help to overcome potential mechanisms of drug resistance to HDACi possibly by inducing caspase-independent cell death rather than autophagic cell death as has been reported for combination of the FDA-approved anti-estrogen drug, tamoxifen, with vorinostat in tamoxifen-resistant MCF-7 (TAMR-MCF-7) cells xenograft model (6, 62). Combination of vorinostat with tamoxifen has been shown to reverse hormone resistance in a phase II study of patients with hormone therapy-resistant breast cancer (63). Combination of tamoxifen with

vorinostat, MS-275 and valproic acid has also been shown to improve apoptosis in breast cell lines (64).

Several preclinical studies of vorinostat in combination with other anticancer agents have shown remarkable synergistic or additive effects in multiple solid tumor cell lines as well as hematological malignancies such as multiple myeloma, non-Hodgkin lymphoma and leukemia (6). Mocetinostat has been evaluated in single-agent and combination therapies in several phase I and phase II clinical trials in both solid and hematological malignancies. Various panobinostat-based combination studies are currently being conducted, including a phase I/II trial of panobinostat with the FDA-approved kinase inhibitor, immunosuppressant and anti-cancer agent, everolimus, in patients with relapsed Hodgkin lymphoma and non-Hodgkin lymphoma (6).

I. Conclusions

HDACs are a family of 18 enzymes that play key roles in regulation of gene expression. X-ray crystallographic structures of HDAC8 have led to a better understanding of catalysis and inhibition of HDAC enzymes. Structures of the foot pocket of HDAC2, catalytic domains of HDAC4 and HDAC7, and the crystal structure of the tetrameric domain of HDAC3 complexed with TBL1, SMRT, and GPS2 have been solved. These structural studies have also been pivotal in understanding target-ligand interactions. HDAC inhibitors

show promise in the treatment of cancer, neurodegenerative diseases and

other key therapeutic areas. Two pan-HDACi, vorinostat and romidepsin,

have been approved by the FDA for CTCL treatment but broad spectrum

HDAC inhibition has been associated with increased toxicity. Therefore,

current trends favor the development of isoform-selective inhibitors that could

provide better pharmacokinetic profiles while maintaining efficacy as a result

of selective targeting of HDAC enzymes.

J. References

1. Hagelkruys, A., Sawicka, A., Rennmayr, M., et.al. The biology of HDAC in cancer: the nuclear and epigenetic components. Handb Exp. Pharmacol. 2011; 206: 13-37.
2. Boumber, Y., Younes, A., & Garcia-Manero, G. Mocetinostat (MGCD0103): a review of an isotype-specific histone deacetylase inhibitor. Expert Opin. Investig. Drugs 2011; 20 (6): 823-829.
3. Rice, J.C., & Allis, C.D. Histone methylation versus histone acetylation: new insights into epigenetic regulation. Curr Opin Cell Biol. 2001; 13(3):263-73.
4. de Ruijter, A.J., van Gennip, A.H., Caron, H.N. et al. Histone deacetylases (HDACs): characterization of the classical HDAC family. Biochem J, 2003. 370: 737-49.
5. Seidel, C., Schnekenburger, M., Dicato, M., et.al. Histone deacetylases modulators provided by Mother Nature. Genes Nutr 2012; 7:357-367.
6. Lemoine, M. & Younes, A. Histone deacetylase inhibitors in the treatment of lymphoma. Discov Med. 2010; 10 (54): 462-70.
7. Marks, P.A. & Dokmanovic, M. Histone deacetylase inhibitors: discovery and development as anticancer agents. Expert Opin Investig Drugs 2005; 14(12): 1497-511.
8. Paris, M., Porcelloni, M., Binaschi, M., et al. Histone deacetylase inhibitors: from bench to clinic. J Med Chem 2008; 51(6): 1505-29.
9. Dokmanovic, M., C. Clarke, & Marks, P.A. Histone deacetylase inhibitors: overview and perspectives. Mol Cancer Res 2007; 5(10): 981-9.
10. Wang, D-F., Helquist, P., Wiech, N.L., et. al. Toward selective histone deacetylase inhibitor design: homology modeling, docking studies, and

molecular dynamics simulations of human class I histone deacetylases, J Med Chem. 2005; 48(22):6936-47.

11. Guan, J.S., Haggarty, S.J., Giacometti, E., et. al. HDAC2 negatively regulates memory formation and synaptic plasticity. Nature. 2009; 459 (7243):55-60.

12. Huangfu, D., Maehr, R., Guo, W., et.al. Induction of pluripotent stem cells by defined factors is greatly improved by small-molecule compounds. Nat Biotechnol. 2008; 26 (7):795-7.

13. Granger, A., Abdullah, I., Huebner, F., et.al. Histone deacetylase inhibition reduces myocardial ischemia-reperfusion injury in mice, FASEB J. 2008; 22(10):3549-60.

14. Ouaissi, M., Giger, U., Sielezneff, I., et al. Rationale for possible targeting of histone signaling in cancer diseases with a special reference to pancreatic cancer. J Biomed Biotechnol. 2011: 315939.

15. Estiu, G., West, N., Mazitschek, R., et al. On the inhibition of histone deacetylase 8. Bioorg Med Chem. 2010; 18 (11): 4103-10.

16. Somoza, J.R., Skene, R.J., Katz, B.A., et al. Structural snapshots of human HDAC8 provides insights into the class I histone deacetylases. Structure, 2004; 12 (7): 1325-34.

17. Gantt, S. L., Gattis, S. G., & Fierke, C. A. Catalytic activity and inhibition of human histone deacetylase 8 is dependent on the identity of the active site metal ion. Biochem J 2006; 45(19): 6170-6178.

18. Dowling, D.P., Gantt, S.L., Fierke, C.A., et al. Structural studies of human histone deacetylase 8 and its site-specific variants complexed with substrate and inhibitors. Biochem J 2008; 47(51): 13554-63.

19. Vannini, A., Volpari, C., Filocamo, G., et al. Crystal structure of a eukaryotic zinc-dependent histone deacetylase, human HDAC8, complexed with a hydroxamic acid inhibitor. Proc Natl Acad Sci U S A 2004; 101(42): 15064-9.

20. Hu, E., Zunxuan, C., Fredrickson, T., et.al. Cloning and characterization of a novel human class I histone deacetylase that functions as a transcription repressor. J. Biol Chem. 2000; 275(20):15254-64.

21. Galdieri, L., Moon, J., & Vancura, A. Determination of histone acetylation status by chromatin immunoprecipitation. Methods Mol Biol. 2012; 809:255-65.

22. Khan O., & La Thangue, N.B. HDAC inhibitors in cancer biology: emerging mechanisms and clinical applications. Immunol Cell Biol. 2012; 90 (1):85-94.

23. Noureen, N., H. Rashid, & Kalsoom, S. Identification of type-specific anticancer histone deacetylase inhibitors: road to success. Cancer Chemother Pharmacol. 2010; 66(4):625-33.

24. Bradner, J.E., West, N., Grachan, M.L., et.al. Chemical phylogenetics of histone deacetylases. Nat Chem Biol. 2010; 6(3):238-243.

25. Chuang, D., Leng, Y., Marinova, Z., et. al. Multiple roles of HDAC inhibition in neurodegenerative conditions. Trends Neurosci. 2009; 32(11):591-601.
26. Vannini, A., Volpari, C., Gallinari, P., et al. Substrate binding to histone deacetylases as shown by the crystal structure of the HDAC8-substrate complex. EMBO Rep 2007; 8(9): 879-84.
27. Carafa, V., Miceli, M., Altucci, L., et. al. Histone deacetylase inhibitors: a patent review (2009 - 2011). Expert Opin Ther Pat. 2013; 23(1):1-17.
28. Elaut, G., Rogiers, V., & Vanhaecke, T. The pharmaceutical potential of histone deacetylase inhibitors. Curr Pharm Des. 2007; 13(25):2584-620.
29. Dinarello, C.A., Fossati. G., & Mascagni, P. Histone deacetylase inhibitors for treating a spectrum of diseases not related to cancer. Mol Med. 2011; 17(5-6):333-52.
30. de Zoeten, E.F., Wang, L., Dillmann, S.H., et.al. Inhibition of HDAC9 increases T regulatory cell function and prevents colitis in mice, Gastroenterology. 2010; 138(2):583-94
31. Hu, E., Chen, Z., Fredrickson, T., et al. Identification of novel isoform-selective inhibitors within class I histone deacetylases. J Pharmacol Exp Ther 2003; 307 (2): 720-8.
32. Waltregny, D., de Leval, L., Glenisson, W., et al. Expression of histone deacetylase 8, a class I histone deacetylase, is restricted to cells showing smooth muscle differentiation in normal human tissues. Am J Pathol, 2004; 165 (2): 553-64.
33. Liu, Y., Peng, L., Seto, E., et.al. Modulation of histone deacetylase 6 (HDAC6) nuclear import and tubulin deacetylase activity through acetylation. J Biol Chem. 2012; 287(34): 29168-74.
34. Ontoria, J.M., Altamura, S., Di Marco, A., et al. Identification of novel, selective, and stable inhibitors of class II histone deacetylases. Validation studies of the inhibition of the enzymatic activity of HDAC4 by small molecules as a novel approach for cancer therapy. J Med Chem 2009; 52(21): 6782-9.
35. Van den Wyngaert, I., de Vries, W., Kremer, A., et al. Cloning and characterization of human histone deacetylase 8. FEBS Lett, 2000; 478 (1-2): 77-83.
36. Krennhrubec, K., Marshall, B.L., Hedglin, M., et al. Design and evaluation of 'Linkerless' hydroxamic acids as selective HDAC8 inhibitors. Bioorg Med Chem Lett 2007; 17(10): 2874-8.
37. Finnin, M. S., Donigian, J.R., Cohen, A., et. al. Structures of a histone deacetylase homologue bound to TSA and SAHA inhibitors. Nature 1999; 401(6749):188-93.
38. Arrar, M., Turnham, R., Pierce, L., et. al. Structural insight into the separate roles of inositol tetraphosphate and deacetylase-activating

domain in activation of histone deacetylase 3. Protein Sci. 2013; 22(1):83-92.

39. Balasubramanian, S., Ramos, J., Luo, W., et al. A novel histone deacetylase 8 (HDAC8)-specific inhibitor PCI-34051 induces apoptosis in T-cell lymphomas. Leukemia 2008; 22(5): 1026-34.

40. Dovey, O.M., Foster, C.T., Conte, N., et. al. Histone deacetylases (HDAC) 1 and 2 are essential for normal T cell development and genomic stability in mice. Blood, 2013; Epub ahead of print.

41. Zhang, Y., Ng, H.H., Erdjument-Bromage, H., et. al. Analysis of the NuRD subunits reveals a histone deacetylase core complex and a connection with DNA methylation. Genes Dev. 1999; 13 (15):1924-35.

42. Oberoi, J., Fairall, L., Watson, P.J., et. al. Structural basis for the assembly of the SMRT/NCoR core transcriptional repression machinery. Nat Struct Mol Biol. 2011; 18(2):177-84.

43. Ouaissi, M., Cabral, S., Tavares, J., et al. Histone deacetylase (HDAC) encoding gene expression in pancreatic cancer cell lines and cell sensitivity to HDAC inhibitors. Cancer Biol Ther. 2008; 7(4): 523-531.

44. Gore, S.D., Weng, L.J., Figg, W.D., et.al. Impact of prolonged infusions of the putative differentiating agent sodium phenylbutyrate on myelodysplastic syndromes and acute myeloid leukemia, Clin Cancer Res. 2002; 8(4):963-70.

45. Hrebackova, J., Hrabeta, J., Eckschlager, T., et.al. Valproic acid in the complex therapy of malignant tumors. Curr Drug Targets. 2010; 11(30): 361-379.

46. Prescribing information for Zolinza (Vorinostat) Capsules. Retrieved from http://www.merck.com/product/usa/pi_circulars/z/zolinza/zolinza_pi.pdf

47. Prescribing information for Istodax (Romidepsin). Retrieved from http://www.istodax.com/pdfs/ISTODAX_PackageInsert.pdf

48. Ononye, S.N., van Heyst, M., Falcone, E., et.al. Toward isozyme selective histone deacetylase inhibitors as therapeutic agents for the treatment of cancer. Pharm. Patent Analyst 2012; 1 (2), 207-221.

49. Ryu, H., Lee, J, Olofsson, B.A., et al. Histone deacetylase inhibitors prevent oxidative neuronal death independent of expanded polyglutamine repeats via an Sp1-dependent pathway. Proc Natl Acad Sci U S A 2003; 100:4281–4286.

50. Jeong, M.R., Hashimoto, R., Senatorov, V.V., et al. Valproic acid, a mood stabilizer and anticonvulsant, protects rat cerebral cortical neurons from spontaneous cell death: a role of histone deacetylase inhibition. FEBS Lett 2003; 542:74–78.

51. Durst K.L., Lutterbach, B., Kummalue, T., et. al. The inv(16) fusion protein associates with corepressors via a smooth muscle myosin heavy-chain domain. Mol Cell Biol. 2003; 23(2):607-19.

52. The Effects of Valproic Acid on Zidovudine Glucuronidation and Pharmacokinetics in HIV-Infected Patients. Retrieved from: http://clinicaltrials.gov/ct2/show/NCT00000629?term=valproic+acid&rank=48.

53. A Phase II Multiple Site, Randomized, Placebo-Controlled Trial of Oral Valproic Acid for Retinitis Pigmentosa. Available from: http://clinicaltrials.gov/ct2/show/NCT01233609

54. Warrener, R., Chia, K., Warren, W.D., et.al. Inhibition of histone deacetylase 3 produces mitotic defects independent of alterations in histone H3 lysine 9 acetylation and methylation. Mol. Pharmacol. 2010; 78(3): 384-393.

55. Kim, N.H., Kim, S.N., & Kim, Y.K. Involvement of HDAC1 in E-cadherin expression in prostate cancer cells; its implication for cell motility and invasion. Biochem Biophys Res Commun. 2011; 404(4):915-21.

56. Lee, J-H., Jeong, E-G., Choi, M-C., et.al. Inhibition of Histone Deacetylase 10 Induces Thioredoxin-Interaction Protein and Causes Accumulation of Reactive Oxygen Species in SNU-620 Human Gastric Cancer Cells, 2010; Mol. Cells 30: 107-112.

57. Butler, L.M., Agus, D.B., Scher, H.I., et al. Suberoylanilide hydroxamic acid, an inhibitor of histone deacetylase, suppresses the growth of prostate cancer cells in vitro and in vivo. Cancer Res, 2000; 60(18): 5165-70.

58. Spurling, C.C., Godman, C.A., Noonan, E.J., et. al. HDAC3 Overexpression and Colon Cancer Cell Proliferation and Differentiation, Mol. Carc. 2008; 43: 137-147.

59. Godman, C.A., Joshi, R., Tierney, B.R., et.al. HDAC3 impacts multiple oncogenic pathways in colon cancer cells with effects on Wnt and vitamin D signaling. Cancer Biol. & Ther. 2008; 7 (10): 1570-1580.

60. Noonan, E.J., Place, R.F., Pookot, D., et al. miR-449a targets HDAC-1 and induces growth arrest in prostate cancer. Oncogene, 2009; 28(14): 1714-24.

61. Riester, D., Hildmann, C., Grunewald, S., et.al. Factors affecting the substrate selectivity of histone deacetylases, Biochemical and biophysical research communications 2007; 357: 439–445.

62. Lee, Y.J., Won, A.J., Lee, J., et. al. Molecular mechanisms of SAHA on regulation of autophagic cell death in tamoxifen-resistant MCF-7 breast cancer cells. Intl J Med Sci 2012; 9 (10): 881-93.

63. Munster, P.N., Thurn, K.T., Thomas, S., et.al. A phase II study of the histone deacetylases inhibitor vorinostat combined with tamoxifen for the treatment of patients with hormone therapy-resistance breast cancer. Br J Cancer 2011; 104: 1828-1835.

64. Bicaku, E., Marchion, D.C., Schmitt, M.L., et.al. Selective inhibition of histone deacetylase 2 silences progesterone receptor-mediated signaling. Cancer Res 2008; 68: 1513-1519.

Chapter 3

Discovery and Development of Tropolone natural product derivatives as HDAC inhibitors

A. Introduction

Natural products have found diverse applications as antimicrobial, antifungal, and anticancer agents as well as in the treatment of neurological disorders (1-6). Several HDACi are either natural products or derivatives of natural products (Figure 1; 7-14); examples include the hydroxamate, TSA, that is isolated from the actinomycete *Streptomyces hygroscopius;* SAHA, a synthetic derivative of TSA, that was approved by the FDA in 2006 for CTCL treatment; the bicyclic depsipeptide antibiotic, romidepsin, that is isolated from *Chromobacterium violaceum* and approved by the FDA in 2009 for CTCL treatment. However, preclinical development of natural products is often limited by structural complexity and high molecular weight.

β-thujaplicin, otherwise known as hinokitiol, is a tropolone-related compound and natural product that is isolated from the woods of *Thujopsis dolabrata* and *Chamaecyparis obtusa* (6,15-19); hinokitiol is associated with a range of biochemical and pharmacological activities including antifungal and antimicrobial activities as well as antiproliferative activities in multiple cell lines including malignant melanomas, stomach and prostate cancers. Tropolones are non-benzenoid aromatic compounds characterized by a seven-membered

47

ring and an alpha-hydroxyl ketone (Figure 1). The presence of the alpha-hydroxyl ketone on the tropolone ring in hinokitiol has been shown to chelate metal ions and to inhibit metalloenzymes (6). However, to the best of our knowledge, this is the first comprehensive study dedicated to the development of tropolone natural product derivatives as isoform-selective histone deacetylases inhibitors (HDACi). Therefore, in this chapter we will discuss the history of the development of tropolones as (HDACi) and our efforts to elucidate target-ligand interactions via *in silico* docking studies and biochemical assays.

a)

b)

c)

d)

e)
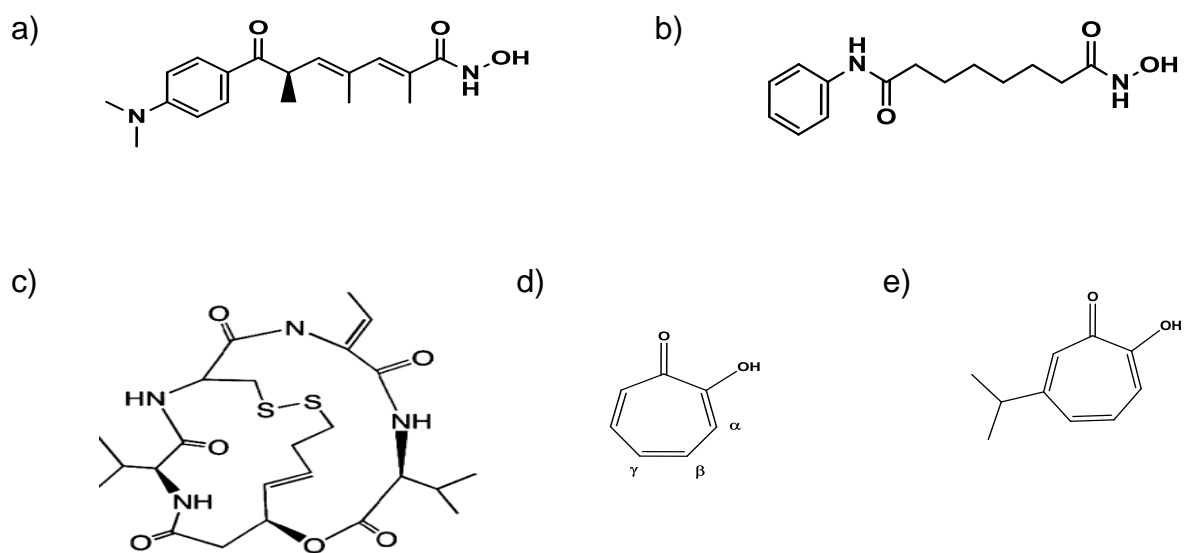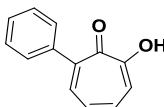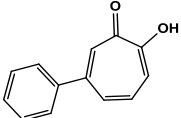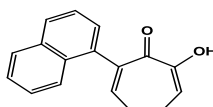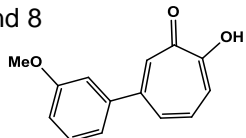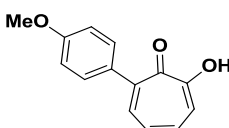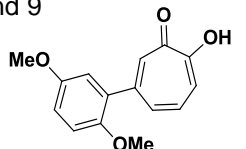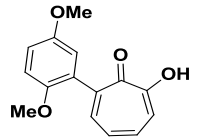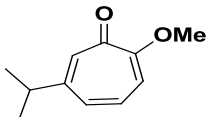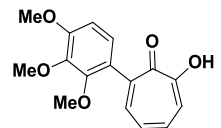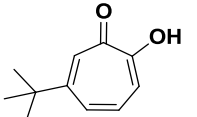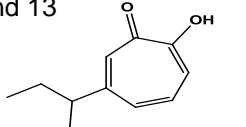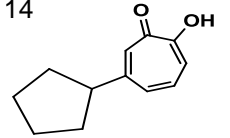
Figure 1: Structures of (a) TSA; b) SAHA; c) Romidepsin (10); d) tropolone scaffold; e) β-thujaplicin.

B. Development of the tropolone library

We hypothesize that the lead-like nature of the simple tropolone scaffold will allow for zinc metal binding, a lipophillic seven-membered ring to interact with the hydrophobic pocket surrounding the zinc ion and three unique positions (α, β, γ) available for substitution to reach essential pockets in HDAC isozymes. Therefore, a library of tropolone natural product derivatives are currently being synthesized and characterized in-house by the Wright and Anderson laboratories with the goal of evaluating structure-activity relationships (SAR) via the addition of structurally-diverse substituents at the alpha, beta, and possibly gamma positions of the tropolone ring.

These structurally-diverse substituents involve the addition of alkyl and aryl groups to the tropolone ring in order to evaluate SAR via biochemical and functional studies. We expect that structure-guided substitutions to the tropolone scaffold will be used to elucidate potency and selectivity, not only for HDAC enzymes relative to other metalloenzymes, but within individual HDAC isozymes. There are currently fourteen compounds in the tropolone library (Table 1). The structures of compound 1, an unsubstituted tropolone, and compound 10—β-thujaplicin—are shown in Figure 1.

Table 1: Tropolone library		
Structure		**Structure**
Alpha-substituted tropolones		**Beta-substituted tropolones**
Compound 2		Compound 7
Compound 3		Compound 8
Compound 4		Compound 9
Compound 5		Compound 11
Compound 6		Compound 12
		Compound 13
		Compound 14

50

C. Prospective *in silico* docking studies

As previously discussed in Chapter 2, HDAC8 is the best model for the study of HDAC catalysis and inhibition because it is the only isozyme that does not exist as a multiprotein complex (20-24). The HDAC8 active site consists of a long, 12-Å-deep, narrow tunnel with a zinc ion positioned near the bottom of the enzyme active site (Figure 2) that accommodates the acetylated lysine during the catalytic reaction (20-24).
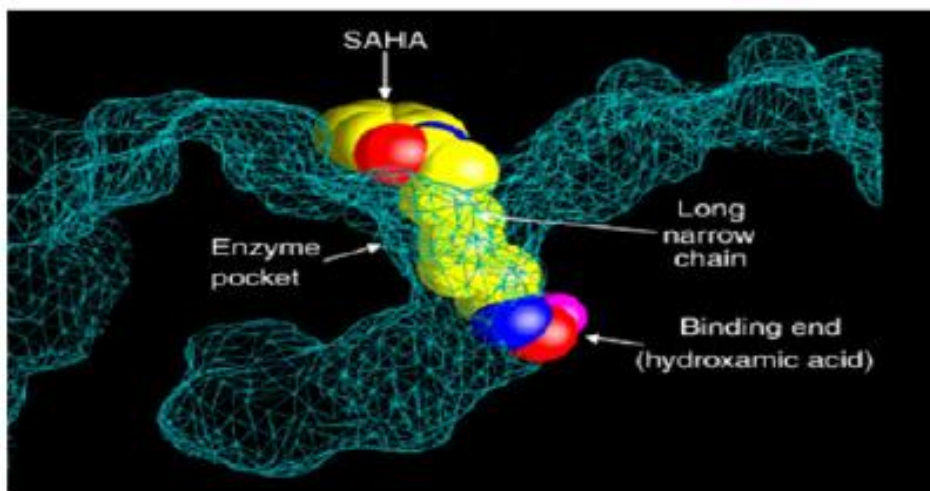
Figure 2: Mesh diagram depicting the binding of the hydroxamate moiety of SAHA to the zinc atom (pink) in the cavity of HDAC8 (20, 21).

Computational studies of a tropolone docked in the HDAC8 crystal structure (PDB ID1T64; 22) show that the tropolone ring sits in a hydrophobic pocket that consists of Phe208, Tyr306, Met274 and Phe152 (Figure 3). Mutational studies have shown that the catalytic tyrosine residue (Tyr306) is essential for enzymatic activity (24). Tyr306 is also

51

conserved in all HDACs except for class IIa enzymes where it is replaced

by a histidine (25). Hence, this position will be very important in

determining isoform selectivity among HDAC enzymes. The tropolone ring

is also within van der Waals distance of Phe208, His143 and Gly151

which should provide stabilizing interactions for the ligand-target complex.
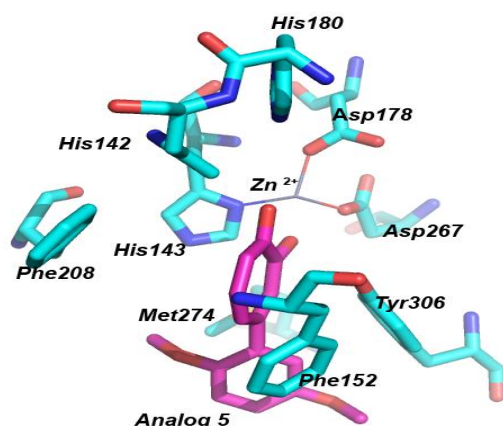
Figure 3: A tropolone, analog 5 (compound 10 in table 1) modeled in the active site of HDAC8

To date, nine crystal structures of human HDAC8 complexed with

various inhibitors have been solved (26). All crystal structures contain a

Zn^{2+} ion in the HDAC8 active site, two K^+ ions bound to structural sites,

and conformational variability in the L1 and L2 loop segments (Figure 4a)

that may be responsible for the polymorphism observed for HDAC8-

inhibitor complexes (22, 26). In fact, a comparison of the crystal structure

52

of HDAC8 (22) complexed with four structurally diverse hydroxamates (TSA, SAHA, MS-344 and CRA-A) also reveals remarkable malleability and structural differences in the protein surface in the vicinity of the opening of the active site (Figure 4b). Our docking studies of a tropolone modeled in the active site of HDAC8 (Figure 4c) also revealed similar trends in the flexibility of the HDAC8 active site. Therefore, from a physiological perspective, this flexibility shows that HDAC8 might be able to bind acetylated lysines that are presented in a variety of structural contexts. These observations indicate that is possible to develop HDAC8-selective inhibitors (22, 27-29). Indeed, several hydroxamate HDAC8-selective inhibitors have been reported to be in preclinical development today particularly for cancer treatment by Pharmacyclics Inc., Gladstone Institutes and Ithaca College (29).

53

Figure 4: a) Simplified illustration with the aid of of C_α traces show movement of the L1 loop between the HDAC8:MS-344 and HDAC8:TSA complexes (11); b) Solvent accessible surfaces (11) of the active site regions of the HDAC8:TSA, HDAC8:MS-344, HDAC8:SAHA, and HDAC8:CRA-A complexes; c) Space-filled structure of a tropolone (Compound 9) superimposed with TSA docked into the active site of HDAC8 (PDB ID: 1T64; 22).

a)

b)

54
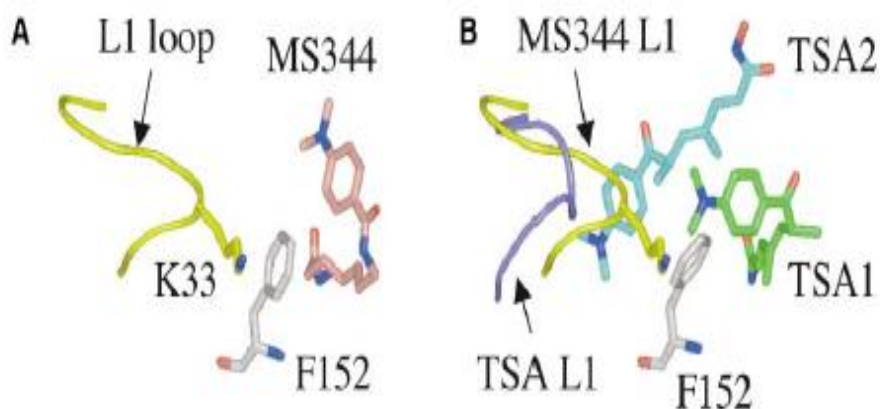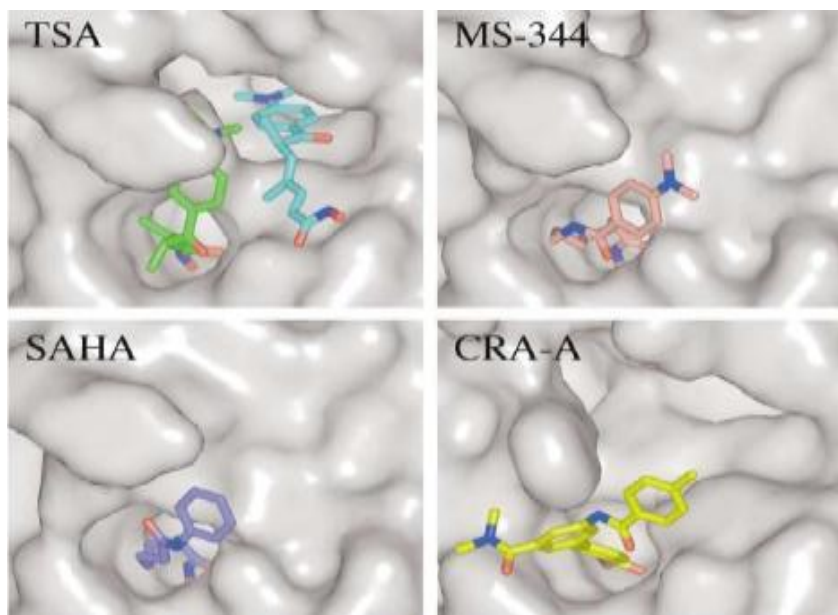
c)
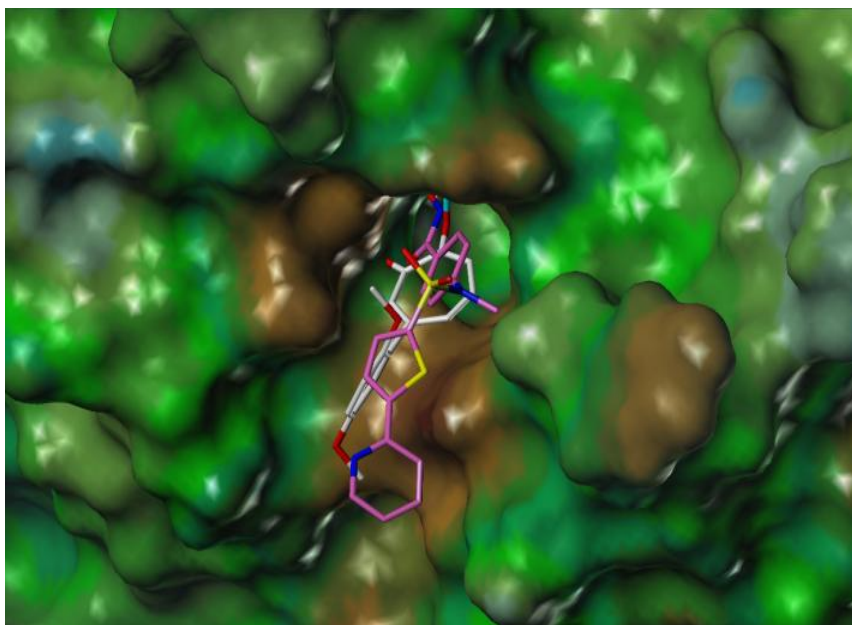
D. Cloning, expression and purification of HDAC8

The strength of structure-based drug design (SBDD) as a tool in medicinal chemistry relies primarily on high-resolution three-dimensional X-ray crystal structures of a target-ligand complex (30, 31). Our *in silico* docking studies suggest that tropolones are promising HDACi and have prompted interest towards the co-crystallization of an HDAC8:tropolone complex with the goal of generating a focused library, evaluating structure activity relationships (SAR) and designing new compounds that show selectivity and potency towards HDAC isozymes. We herein describe our efforts to clone, express and purify HDAC8.

55

We cloned HDAC8 based on modifications of previously reported conditions (22, 23, 26, 32). HDAC8 (Open Biosystems: clone ID LIFESEQ257457) was expressed in *Escherichia coli* using a T7 Lac promoter-driven vector, pET41b (EMD4 Biosciences, USA). The HDAC8 coding sequence was PCR-amplified using the following primer sequences (forward , 5'- GTGTC TCTAGA TGGAGGA GCCGGAGGAA CCG – 3'; reverse, 5'- GTGTC CTCGAG GAC CACATGCTTC AGATTCCCTT TGATGTAGTT G 3') with XhoI and XbaI restriction endonuclease sites, respectively. The PCR product was digested with XhoI and XbaI and subcloned into the multiple cloning region of pET41b. The inserted gene sequence was confirmed on both strands by automated dideoxynucleotide sequencing using the T7 promoter primers (UCONN DNA Biotechnology Facility). The resultant HDAC8 expression plasmid was then transferred to the lysogenic BL21 DE3 *E. coli* strain containing a chromosomal copy of T7 RNA polymerase under lacUV5 promoter control.

Subsequent expression and purification was performed essentially as described by the Vannini group in reference 23 and is described in Section A of the Materials and Methods chapter. Efforts are currently in place by the Anderson laboratory to solve the crystal structure of our HDAC8 protein (ACA-HDAC8) bound to a tropolone. The use of structure-based drug design (SBDD) will allow for modifications at the unique positions (α, β and γ) of the seven-membered tropolone ring, provide a more distinct appraisal of the

structure-activity relationships (SAR), and produce leads for the development
of tropolones as isoform-selective HDAC inhibitors.

E. Evaluation of HDAC enzyme kinetic parameters

We evaluated key enzyme kinetic parameters for three class I HDACs
(HDAC1, HDAC2 and HDAC8), two class IIa HDACs (HDAC4 and HDAC5),
and one class IIb HDAC (HDAC6) using fluorogenic assays that correlate
HDAC activity to fluorescence (Table 2). Experimental methods are
highlighted in Section B of the Materials and Methods chapter (33). With the
aid of non-linear regression analysis (GraphPad Prism Software, Inc., CA),
we were able to determine best fit values for the Michaelis-Menten (K_M)
constant and maximum enzyme velocity (V_{max}) and concurrently determine
values for the enzyme turnover number (k_{cat}) as well as the catalytic efficiency
(k_{cat} /K_M). We compared our results to published data for HDAC enzyme
kinetics (34, 35). Standard error values are reported in Section 1 of the
Appendix. Corresponding histograms are in the Appendix, Section 2.

There were some notable differences within and between HDAC
isozymes (Table 2). For example, the K_M for HDAC4 was 43 µM whereas the
K_M for HDAC5 was 116.6 µM but k_{cat} /K_M values for HDAC4 and HDAC5 were
52,308 M^{-1} s^{-1} and 947 M^{-1} s^{-1} respectively. These values indicate that HDAC4
has a better catalytic efficiency than HDAC5. Conversely, HDAC8 had a K_M
value of 56.82 µM and k_{cat} /K_M value of 29,224 M^{-1} s^{-1} whereas HDAC6, the

57

only assayed isozyme with two catalytic active sites, had a K_M value of 23.42 µM and k_{cat}/K_M value of 123,641 M^{-1} s^{-1}, the highest value for any isozyme. But this observation is not surprising particularly given that the two catalytic domains in HDAC6 contribute independently to the overall activity of the enzyme (36, 37). These observations are promising and validate the use of the fluorogenic assays for evaluation of HDAC enzyme inhibition by our tropolone library.

Table 2: Kinetics and comparative reactivity analysis						
	Class I HDAC			**Class IIa HDAC**		**Class IIb HDAC**
Kinetic Parameter	**HDAC1**	**HDAC2**	**HDAC8**	**HDAC4**	**HDAC5**	**HDAC6**
K_M (µM)	29.09	39.05	56.82	43.00	116.6	23.42
V_{max} (µM)	437.40	599.50	5,661.00	5803.00	772.5	4,069
k_{cat} (s^{-1})	0.25	0.26	1.70	2.25	0.10	2.90
k_{cat}/K_M (M^{-1} s^{-1})	8,615	6,552	29,224	52,308	947	123,641

58

F. Elucidation of HDAC inhibition

Our initial assessment of HDAC inhibition was evaluated using the natural product (compound 10), a commercially available human recombinant HDAC2 enzyme (BPS Bioscience, San Diego, CA), and a fluorogenic HDAC assay kit (Active Motif, Carlsbad, CA). Experimental methods are highlighted in Section C of the Materials and Methods chapter. We compared our results to reported data for HDAC enzyme inhibition (34, 35, 38). Standard error values are reported in Section 3 of the Appendix. Assay data are highlighted in Figure 5a and Figure 5b. Our data show that the fluorogenic assay is highly reproducible and allowed us to subsequently conduct a comprehensive analysis of the tropolone library in a panel of HDAC enzymes.

Figure 5: a) Single time-point analysis of HDAC2 inhibition by compound 10; b) Histogram summarizing comprehensive analysis of HDAC2 inhibition by compound 10. Note that graph and histogram represent non-linear regression analysis (GraphPad Prism) of HDAC2 inhibition by compound 10 (Log C = Log Concentration).

a)

$IC_{50} = 106$ nM

b)

$IC_{50} = 90.87$ nM
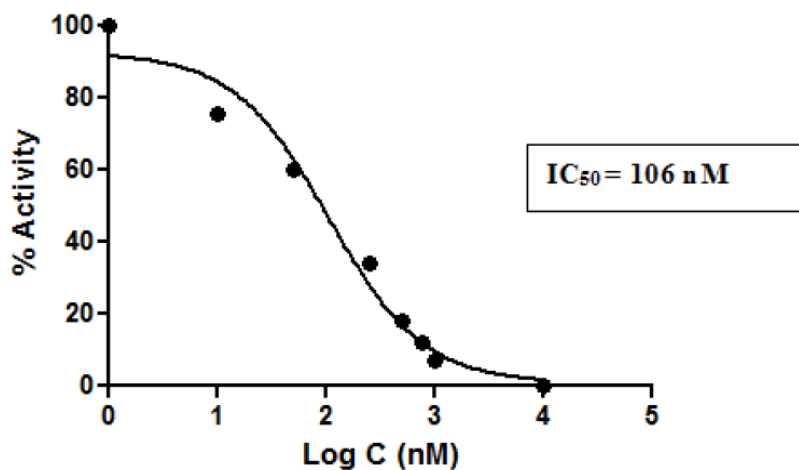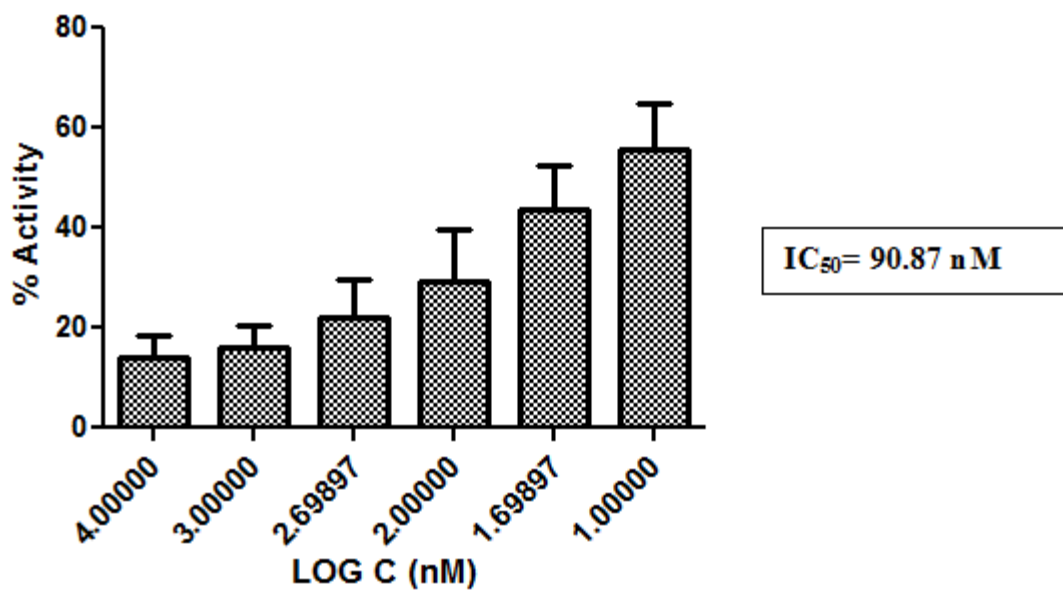
We evaluated inhibition constant (K_i) values for our tropolone library for three class I HDACs (HDAC1, HDAC2 and HDAC8), two class IIa HDACs (HDAC4 and HDAC5), and one class IIb HDAC (HDAC6) using fluorogenic assays that correlate HDAC activity to fluorescence. Detailed assay methods are highlighted in Section C of the Materials and Methods Chapter. We compared our data to reported values for HDAC inhibition (28, 34, 35, 38). Assay data indicated that our compounds showed high potency and selectivity towards HDAC2 and HDAC8 relative to the other evaluated HDAC isozymes. Standard error values for IC_{50} analysis of HDAC2 and HDAC8 are reported in the Appendix, Section 4. With the aid of non-linear regression analysis (GraphPad Prism), we were able to determine IC_{50} values and convert them to K_i values using methods described by Cheng and Prusoff (39).

There were significant differences in inhibition within and between HDAC isozymes; between TSA and the tropolones; as well as between the alpha-substituted and beta-substituted tropolones (Table 3). The tropolones showed preferential inhibition of the class I HDACs when compared to either class IIa or class IIb HDACs. For example, the tropolones were not active in HDAC5 at the tested concentrations (0.0002-20 µM) whereas TSA had a K_i value of 5 µM. With the exception of compound 2 (K_i =527 nM), the tropolones were not active in HDAC6 whereas TSA had a K_i value of 3.02 nM. However, in a similar manner as TSA, the tropolones inhibited HDAC4 relatively poorly with K_i values greater than 8 µM. Yet this discovery is not surprising since most HDACi show poor

61

selectivity towards inhibition of class IIa HDACs possibly due to difficulty in establishing accurate methods for evaluation of HDAC activity and inhibition (35, 40). HDAC2 and HDAC8 share 43% sequence identity (22) and inhibition of these two isozymes by the tropolones were by far more promising than any of the other HDAC isozymes.

With the exception of the natural product, (compound 10; K_i = 15. 44 nM) and the methylated tropolone (compound 11) that was inactive even at 2500 nM, the tropolones exhibited notable potency in the inhibition of HDAC2 with values that were even more potent than that of TSA (K_i =1.06 nM). Inhibition of HDAC2 by both the alpha-substituted and beta-substituted tropolones was similar; for example, compounds 5 and 9 with dimethoxyphenyl groups at the alpha and beta positions respectively had corresponding K_i values of 0.42 nM and 0.51 nM for HDAC2.

62

Table 3: Inhibition constants for class I and class II HDACs

Note: For all HDAC isozymes except HDAC4 & HDAC5; Not Active (N.A.) refers to K_i values >2500 nM, the upper limit of assayed inhibitor concentrations; for HDAC4 & HDAC5, N.A. refers to K_i values >20,000 nM, the upper limit of the assay.

Compound	K_i (nM)					
	Class I HDAC			Class II HDAC		
	HDAC1	HDAC2	HDAC8	HDAC4	HDAC5	HDAC6
TSA	0.87	1.06	69.65	14,547.00	5,000	3.02
1	N.A.	0.04	N.A.	N.A.	N.A.	N.A.
2	N.A.	0.26	1.09	N.A.	N.A.	527.00
3	N.A.	0.25	186.30	N.A.	N.A.	N.A.
4	N.A.	0.81	83.80	N.A.	N.A.	N.A.
5	N.A.	0.42	811.50	N.A.	N.A.	N.A.
6	N.A.	0.23	123.65	N.A.	N.A.	N.A.
7	N.A.	0.06	1.47	10,860.00	N.A.	N.A.
8	N.A.	0.12	2.38	8,361.00	N.A.	N.A.
9	N.A.	0.51	266.30	11,204.00	N.A.	N.A.
10	N.A.	15.44	177.95	N.A.	N.A.	N.A.
11	N.A.	N.A.	7.87	11,641.00	N.A.	N.A.
12	N.A.	0.13	12.81	806.13	N.A.	N.A.
13	N.A.	0.22	2.27	6115.00	N.A.	N.A.
14	N.A.	0.04	122.70	990.23	N.A.	N.A.

63

With the exception of the unsubstituted tropolone (compound 1) that was inactive even at 2500 nM, the tropolones had submicromolar K_i values for HDAC8 that were comparable to TSA (K_i =69.65 nM). However, the beta-substituted tropolones seemed to be more potent than the alpha-substituted tropolones. For example, compound 5 had a K_i value of 811.50 nM whereas compound 9 had a K_i value of 266.30 nM. Furthermore, the tropolones show some selectivity towards HDAC2 when compared to HDAC8. For example, compound 9 exhibits greater than 500-fold selectivity towards HDAC2 relative to HDAC8. This observation is highly promising and shows that it is possible to develop these tropolones as HDAC2-selective inhibitors. This discovery is groundbreaking particularly given the fact that there are no reported HDAC2-selective inhibitors in pre-clinical and clinical development presumably due to the high degree of similarity in the catalytic sites of HDAC1, HDAC2 and -HDAC3 (29, 41).

Furthermore, hinokitiol (compound 10) has also been shown to possess neuroprotective activity in HT22 mouse hippocampal cells (42). Published reports have shown that treatment with HDACi such as TSA, sodium butyrate, or vorinostat protected against glutathione depletion-induced oxidative stress, a mechanism that is implicated in many neurodegenerative diseases including strokes and Alzheimer's disease (43, 44). Concurrently, HDAC2 inhibition has been shown to facilitate learning and memory in wild-type mice as well as in mouse models of neurodegeneration (46). Our studies

may have shown that the neuroprotective effects of hinokitiol may be as a result of HDAC2 inhibition. However, we cannot rule out the possibility that other protein substrates and HDAC isoforms might be implicated by the tropolones (42). Yet, our data suggests that it is indeed possible to explore the use of tropolones in the treatment of neurodegenerative diseases.

Interestingly, the tropolones did not inhibit HDAC1 whereas TSA had a K_i value of 0.87 nM. This observation is quite significant particularly given that HDAC1 and HDAC2 share 80% sequence identity, exhibit functional redundancy in many cell types, and are recruited together into three main transcriptional complexes: Sin3A, NuRD and CoREST (46). However, our studies may be limited by difficulty in standardizing data obtained from different HDAC fluorogenic substrates particularly given high batch to batch variability in substrate properties (47). Yet, as previously stated, our data indicates that it may be possible to develop these tropolones as HDAC2-selective inhibitors, and explore potential therapeutic uses for the treatment of cancers and possibly neurodegenerative diseases.

G. Investigation of the mechanism of action of tropolones in HDAC8

Based on enzyme inhibition data, compound 2 was chosen to evaluate the mechanism of action of tropolones in HDAC8. Experimental methods are described in section D of the Materials and Methods chapter. Assay data (Figure 6) were analyzed via non-linear regression analysis (GraphPad

65

Prism). Standard error values for K_i and alpha are reported in section 5 of the Appendix.

The parameter, alpha, ($K_i^{'}/K_i$) is used to determine the degree to which binding of an inhibitor changes the affinity of the enzyme for the substrate (48). The alpha value obtained for Compound 2 in HDAC8 was 4.5 indicating competitive binding since alpha is statistically greater than 1 (48, 49). Furthermore, the measured K_i for compound 2 is 0.53 nM, which correlates well with the calculated Cheng and Prusoff K_i of 1.09 nM. Therefore, the competitive mode of inhibition as well as relatively poor binding by the methylated tropolone (compound 11) highly suggests that the tropolones inhibit HDAC activity by targeting the bound Zn^{2+} metal at the active site.
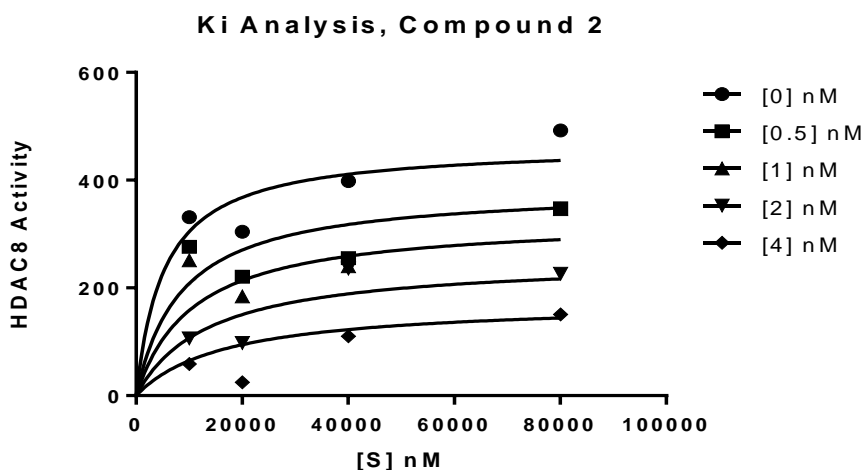
Figure 6: Analysis of mode of binding of compound 2 against HDAC8

66

H. Optimizing the tropolone scaffold to explore the HDAC hydrophobic pocket

We are currently working on the development of a second generation library of tropolones that will potentially maintain isoform selectivity in HDAC inhibition while exerting a more robust therapeutic application particularly for the treatment of solid tumors and hematological malignancies. The proposed scaffold for second-generation tropolones (Figure 7) will now include a linker domain (the alkyl chain) that is presumed to mimic the natural HDAC substrate and occupy the active site channel thus allowing for exploration for isozyme selectivity (41, 50). R groups will either be hydrogen atoms, alkyl groups, or aryl groups. The same substitutions will also be evaluated in the alpha and possibly the gamma positions in order to elucidate structure-activity relationships (SAR).
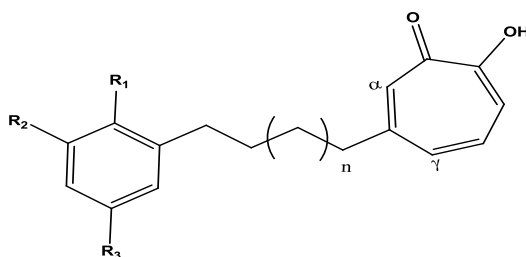
Figure 7: Proposed scaffold for 2nd generation tropolones

Moreover, virtually all HDACi currently in clinical development for the treatment of cancer share this common pharmacophore pattern (28-30, 41, 50) consisting of: a metal binding domain which complexes zinc; a linker domain and a surface domain or cap group that makes contact with the rim of the catalytic pocket. In our case, the tropolone ring with the alpha-hydroxyl ketone serves as the metal-binding domain, the alkyl chain will serve as the linker domain and the secondary aryl moiety will serve as the cap group. It is expected that modification of the tropolone scaffold may also lead to improvements in pharmacokinetic properties that may improve *in vitro* potency & possibly *in vivo* efficacy (51, 52). Knowledge garnered from the work presented in this dissertation as well as the proposed studies is crucial towards further development of tropolones as isoform-selective HDAC inhibitors with enhanced antitumor properties.

I. Conclusions

Many HDACi, including the two FDA-approved HDACi, are natural products or derivatives of natural products. Our tropolone natural product derivatives are highly promising competitive HDACi that show preferential inhibition of class I HDACs, particularly HDAC2 and HDAC8. *In silico* docking studies have provided visual insights on HDAC8 binding by the tropolones; efforts are currently in place to co-crystallize a tropolone with our purified HDAC8 protein (ACA-HDAC8) in order to more aptly evaluate target-ligand

68

interactions and use this knowledge to guide substitutions to the tropolone scaffold. Furthermore, our biochemical analyses indicate that it is possible to develop tropolones as HDAC2-selective inhibitors and exploit their therapeutic potential particularly for the treatment of neurodegenerative diseases; this observation is groundbreaking since there are no reported HDAC2-selective inhibitors either in preclinical or clinical development. We are also developing new compounds potentially for the treatment of cancer that is based on a modified scaffold that will allow us to further probe the HDAC hydrophobic pocket and explore isozyme selectivity.

J. Acknowledgments

K. References

1. Harvey, A.L. Natural products in drug discovery. Drug Discov Today. 2008 : 13(19-20):894-901.
2. Cutler, S.J., & Cutler, H. G. Biologically active natural products: pharmaceuticals. CRC Press L.L.C., 2000.
3. Newman, D.J., & Cragg, G.M. Natural products as sources of new drugs over the last 25 years. J Nat Prod 2007; 70 (3): 461-477.
4. Russo, P., Frustaci, A., Fini, M., et. al. Multitarget drugs of plants origin acting on Alzheimer's disease. Curr Med Chem. 2013 Feb 14. [Epub ahead of print]

5. Baker, D.D., Chu, M., Oza, U., et. al. The value of natural products to future pharmaceutical discovery. Nat Prod Rep. 2007; 24(6):1225-44.

6. Liu, S., & Yamauchi, H. Hinokitiol, a metal chelator derived from natural plants, suppresses cell growth and disrupts androgen receptor signaling in prostate carcinoma cell lines. Biochem Biophys Res Commun, 2006; 351(1): 26-32.

7. Licciardi, P.V., Kwa, F.A., Ververis, K., et. al. Influence of natural and synthetic histone deacetylase inhibitors on chromatin. Antioxid Redox Signal. 2012; 17(2):340-54.

8. Seidel, C., Schnekenburger, M., Dicato, M., et.al. Histone deacetylases modulators provided by Mother Nature. Genes Nutr 2012; 7:357-367.

9. Lemoine, M. & Younes, A. Histone deacetylase inhibitors in the treatment of lymphoma. Discov Med. 2010; 10 (54): 462-70.

10. Furumai, R., Matsuyama, A., Kobashi, N., et al. FK228 (depsipeptide) as a natural prodrug that inhibits class I histone deacetylases. Cancer Res, 2002; 62(17): 4916-21.

11. Carafa, V., Miceli, M., Altucci, L., et. al. Histone deacetylase inhibitors: a patent review (2009 - 2011). Expert Opin Ther Pat. 2013; 23(1):1-17.

12. Elaut, G., Rogiers, V., & Vanhaecke, T. The pharmaceutical potential of histone deacetylase inhibitors. Curr Pharm Des. 2007; 13(25):2584-620.

13. Dinarello, C.A., Fossati. G., & Mascagni, P. Histone deacetylase inhibitors for treating a spectrum of diseases not related to cancer. Mol Med. 2011; 17(5-6):333-52.

14. Nakajima, H., Kim, Y.B., Terano, H., et. al. FR901228, a potent antitumor antibiotic, is a novel histone deacetylase inhibitor. Exp Cell Res. 1998 May 25;241(1):126-33.

15. Koufaki, M., Theodorou, E., Alexi, X., et. al. Synthesis of tropolone derivatives and evaluation of their in vitro neuroprotective activity. Eur J Med Chem. 2010; 45(3):1107-12.

16. Murakami, K., Ohara, Y., Haneda, M., et. al. Prooxidant action of hinokitiol: hinokitiol-iron dependent generation of reactive oxygen species. Basic Clin Pharmacol Toxicol. 2005; 97(6):392-4.

17. Liu, S., & Yamauchi, H. p27-Associated G1 arrest induced by hinokitiol in human malignant melanoma cells is mediated via down-regulation of pRb, Skp2 ubiquitin ligase, and impairment of Cdk2 function. Cancer Lett, 2009; 286(2): 240-9.

18. Matsumura, E., Morita, Y., Date, T., et al., Cytotoxicity of the hinokitiol-related compounds, gamma-thujaplicin and beta-dolabrin. Biol Pharm Bull, 2001; 24 (3): 299-302.

19. Morita, Y., Matsumura, E., Okabe, T., et al. Biological activity of alpha-thujaplicin, the minor component of Thujopsis dolabrata SIEB. et ZUCC. var. hondai MAKINO. Biol Pharm Bull, 2001; 24(6): 607-11.

20. Noureen, N., H. Rashid, & Kalsoom, S. Identification of type-specific anticancer histone deacetylase inhibitors: road to success. Cancer Chemother Pharmacol. 2010 Sep; 66(4):625-33.
21. Marks, P., Rifkind, R.A., Richon, V.M., et. al. Histone deacetylases and cancer: causes and therapies. Nat Rev Cancer. 2001; 1 (3):194-202.
22. Somoza, J.R., Skene, R.J., Katz, B.A., et al. Structural snapshots of human HDAC8 provides insights into the class I histone deacetylases. Structure, 2004; 12 (7): 1325-34.
23. Vannini, A., Volpari, C., Filocamo, G., et al. Crystal structure of a eukaryotic zinc-dependent histone deacetylase, human HDAC8, complexed with a hydroxamic acid inhibitor. Proc Natl Acad Sci U S A 2004; 101(42): 15064-9.
24. Vannini, A., Volpari, C., Gallinari, P., et al. Substrate binding to histone deacetylases as shown by the crystal structure of the HDAC8-substrate complex. EMBO Rep 2007; 8(9): 879-84.
25. Lahm, A. Unraveling the hidden catalytic activity of vertebrate class IIa histone deacetylases. Proc Natl Acad Sci U S A. 2007; 104 (44):17335-40.
26. Dowling, D.P., Gantt, S.L., Fierke, C.A., et al. Structural studies of human histone deacetylase 8 and its site-specific variants complexed with substrate and inhibitors. Biochem J 2008; 47(51): 13554-63.
27. Ontoria, J.M., Altamura, S., Di Marco, A., et al. Identification of novel, selective, and stable inhibitors of class II histone deacetylases. Validation studies of the inhibition of the enzymatic activity of HDAC4 by small molecules as a novel approach for cancer therapy. J Med Chem 2009; 52(21): 6782-9.
28. Estiu, G., West, N., Mazitschek, R., et al. On the inhibition of histone deacetylase 8. Bioorg Med Chem. 2010; 18 (11): 4103-10.
29. Ononye, S.N., van Heyst, M, Falcone, E., et.al. Toward isozyme selective histone deacetylase inhibitors as therapeutic agents for the treatment of cancer. Pharm. Patent Analyst 2012; 1 (2), 207-221.
30. Damm, K.L., & Carlson, H.A. Exploring Experimental Sources of Multiple protein Conformations in Structure-Based Drug Design, J. Am. Chem. Soc. 2007; 129 (26): 8225-35.
31. Anderson, A.C. Structure-based functional design of drugs: from target to lead compound. Methods Mol Biol. 2012;823:359-66
32. Hu, E., Zunxuan, C., Fredrickson, T., et.al. Cloning and characterization of a novel human class I histone deacetylase that functions as a transcription repressor. J. Biol Chem. 2000; 275(20):15254-64.
33. Williams, J. W., & Morrison, J. F. The kinetics of reversible tight-binding inhibition. Methods Enzymol. 1979; 63, 437-467.

34. Schultz, B.E., Misialek, S., Wu, J., et. al. Kinetics and comparative reactivity of human class I and class IIb histone deacetylases. Biochemistry 2004; 43(34):11083-91.

35. Bradner, J.E., West, N., Grachan, M.L., et.al. Chemical phylogenetics of histone deacetylases. Nat Chem Biol. 2010; 6(3):238-243.

36. Jose, B., Okamura, S., Kato, T., et.al. Toward an HDAC6 inhibitor: synthesis and conformational analysis of cyclic hexapeptide hydroxamic acid designed from α-tubulin sequence. Bioorg Med Chem. 2004; 12(6):1351-6.

37. Liu, Y., Peng, L., Seto, E., et.al. Modulation of histone deacetylase 6 (HDAC6) nuclear import and tubulin deacetylase activity through acetylation. J Biol Chem. 2012; 287(34): 29168-74.

38. BPS Bioscience HDAC screening and profiling. Retrieved from http://bpsbioscience.com/images/pdf/HDAC_profiling_Sheet.pdf

39. Cheng, Y., & Prusoff, W.H. Relationship between the inhibition constant (Ki) and the concentration of inhibitor which causes 50 per cent inhibition (IC_{50}) of an enzymatic reaction. Biochem Pharmacol. 1973; 22(23): 3099-108.

40. Jones, P., Altamura, S., De Francesco, R., et al. Probing the elusive catalytic activity of vertebrate class IIa histone deacetylases. Bioorg Med Chem Lett 2008;18:1814–1819.

41. Noureen, N., H. Rashid, & Kalsoom, S. Identification of type-specific anticancer histone deacetylase inhibitors: road to success. Cancer Chemother Pharmacol. 2010; 66(4):625-33.

42. Koufaki, M., Theodorou, E., Alexi, X., et. al. Synthesis of tropolone derivatives and evaluation of their in vitro neuroprotective activity. Eur J Med Chem. 2010 Mar;45 (3):1107-12.

43. Chuang, D., Leng, Y., Marinova, Z., et. al. Multiple roles of HDAC inhibition in neurodegenerative conditions. Trends Neurosci. 2009; 32(11):591-601.

44. Ryu, H., Lee, J., Olofsson, B.A., et al. Histone deacetylase inhibitors prevent oxidative neuronal death independent of expanded polyglutamine repeats via an Sp1-dependent pathway. Proc Natl Acad Sci U S A 2003; 100:4281–4286.

45. Guan, J.S., Haggarty, S.J., Giacometti, E., et. al. HDAC2 negatively regulates memory formation and synaptic plasticity. Nature. 2009; 459 (7243):55-60.

46. Dovey, O.M., Foster, C.T., Conte, N., et. al. Histone deacetylases (HDAC) 1 and 2 are essential for normal T cell development and genomic stability in mice. Blood, 2013; Epub ahead of print.

47. Heltweg, B., Trapp, J., & Jung, M. et. al. In vitro assays for the determination of histone deacetylase activity. Methods 2005; 36(4):332-7

48. Copeland, R.A. Enzymes: A Practical Introduction to Structure, Mechanism and Data Analysis. New York, NY: Wiley-VCH Inc., 2000.
49. Strelow, J., Dewe, W., Iversen, P.W., et.al. Mechanism of Action assays for Enzymes. Retrieved from http://www.ncbi.nlm.nih.gov/books/NBK92001/
50. Krennhrubec, K., Marshall, B.L., Hedglin, M., et al., Design and evaluation of 'Linkerless' hydroxamic acids as selective HDAC8 inhibitors. Bioorg Med Chem Lett, 2007; 17(10): 2874-8.
51. Elaut, G., Rogiers, V., & Vanhaecke, T. The pharmaceutical potential of histone deacetylase inhibitors. Curr Pharm Des. 2007; 13(25):2584-620.
52. Kerns, E., & Di, L. Drug-like Properties: Concepts, Structure Design and Methods from ADME to Toxicity Optimization. UK: Academic Press, 2008.

Chapter 4

Analysis of cancer cell line selective cytotoxicity

A. Introduction

The ability of established HDACi to induce cell death alone and/or in combination with other anticancer agents has been previously reported for both solid tumors and hematological malignancies (1-49). Evidence for the antiproliferative properties of β-thujaplicin has been previously reported in multiple cell lines including malignant melanoma, stomach cancer, and prostate cancer at micromolar levels (50-55). The cellular reduction of the yellow tetrazolium compound, MTS, into soluble purple formazan is accomplished by dehydrogenase enzymes found only in metabolically active cells (56, 57). Thus, we employed this MTS assay to evaluate cancer cell line selective cytotoxicity in ten human cell lines: HT29 and HCT116 colon cancer cell lines; BXPC3 pancreatic cell line; MCF-7 and MCF-10A breast cell lines; Jurkat acute T-cell leukemia cell line; HuT-78 cutaneous T-cell lymphocytes (CTCL); U87 glioblastoma cell line; A549 lung cancer cell line; and normal adult human dermal fibroblasts (hdF).

The focus of this chapter is to comprehensively evaluate cytotoxicity in multiple cell lines and determine the cell lines that are the most sensitive to inhibition by the tropolones. Assays were performed in triplicate and assay data werecompared to published data for the experimental control, SAHA,

when possible (1-5). Detailed experimental methods for cell culturing and cell viability assays are in sections E and F respectively of the Materials and Methods Chapter. Standard errors values are reported in Sections 6 and 7 of the Appendix.

B. Evaluation of cancer cell line selective cytotoxicity in solid tumors

It is well established that HDACi are able to inhibit a diverse panel of solid tumor cell lines as well as hematological cell lines (1-49). Inhibition of solid tumors by SAHA and TSA has been reported for the primary breast adenocarcinoma cell line, MCF-7 (1, 14-17), and two primary colon adenocarcinoma cell lines, HCT-116 (3, 18-25), and HT-3, 22, 24). Overexpression of HDAC1, -2, and -3 has been reported in colorectal carcinomas (56-58). Increased expression of class IIa HDACs has been correlated with reduced survival in estrogen receptor-positive (ER$^+$) breast cancer patients (26). Aberrant expression of HDAC1, HDAC2, and HDAC7 has been observed in pancreatic cancer cells (27). TSA has been shown to inhibit the BXPC3 pancreatic cancer cell line in the submicromolar levels (28). Glioblastomas are the most common, most aggressive, and most chemoresistant type of brain tumors (31). TSA has also been shown to inhibit the growth of U87 cells presumably by altering the HDAC1 levels (31). MCF-10A cells are spontaneously immortalized 'normal' breast epithelial cell lines that have been shown to exhibit no signs of terminal differentiation or

75

senescence (59). The antiproliferative effects of SAHA on the MCF-10A cell line have been reported (1, 16). Structurally diverse HDACi, including SAHA, have been shown to inhibit the growth of the A549 lung cancer cell line (32, 34-36).

We performed cytotoxicity studies in these seven human solid tumor cell lines: HT29, HCT116, BXPC3, MCF-7, MCF-10A, U87, and A549. The cancer cell growth inhibitory results was proportional to HDAC inhibition data particularly given that the unsubstituted tropolone, compound 1, and the methylated tropolone, compound 11, exhibited poor inhibition of all solid tumor cell lines (Table 1). The alpha-substituted tropolones were generally more potent than the beta-substituted tropolones in all seven solid tumor cell lines. Surprisingly, the tropolones and SAHA were more active in the MCF-10A cell line than the more differentiated MCF-7 breast cell line; perhaps indicating a better prognosis for early onset treatment of breast cancer versus treatment at a more advanced stage (60). However, given recent trends in cell line contamination and cell-specific genomic alterations associated with breast cell lines, we cannot rule out the possibility that the integrity of the MCF-10A cells may be compromised (61-63).

Table 1: Evaluation of cancer cell line selective cytotoxicity in solid tumors							
Compound	GI_{50} (µM), 72h						
	Solid Tumors						
	HCT116	HT-29	BXPC-3	A549	U87	MCF-7	MCF-10A
SAHA	2.50	5.17	5.56	43.66	39.12	29.45	2.70
1	63.73	>100	>100	>100	>100	85.28	3.31
2	15.24	>100	29.39	>100	>100	91.48	33.17
3	32.06	75.40	17.13	>100	>100	>100	17.50
4	56.99	56.99	35.93	85.53	>100	>100	26.50
5	46.65	46.70	14.06	57.60	>100	>100	21.70
6	34.98	35.00	21.16	75.00	>100	>100	34.00
7	53.44	>100	18.49	69.20	>100	>100	2.90
8	43.67	43.70	91.57	52.40	>100	>100	13.30
9	>100	>100	34.79	53.44	>100	>100	38.81
10	6.92	92.00	18.50	52.00	>100	>100	1.90
11	>100	>100	>100	>100	>100	>100	85.38
12	62.61	>100	43.02	38.00	>100	>100	4.44
13	26.86	>100	>100	25.68	>100	84.62	5.07
14	>100	>100	>100	36.00	>100	>100	21.00

Alternatively, the tropolones showed relatively poor inhibition of the A549 cells and had half maximal growth inhibition (GI_{50}) values in U87 cells that were greater than 100 micromolar. The gastrointestinal cancer cell lines, BXPC3, HCT116 and HT-29, seemed to be the most sensitive to inhibition by the tropolones. The tropolones were particularly cytotoxic in the BXPC3 and HCT116 cell lines with mean GI_{50} values of 32 µM and 40 µM respectively. These observations have prompted further investigation on the antiproliferative effects on cell cycle progression in BXPC3 and HCT116 cell lines by the tropolones which will be discussed in subsequent chapters.

Figure 1: Evaluation of cancer cell line selective cytotoxicity in solid tumors

HT29

BXPC3

U87

MCF-10A

MCF-7

A549
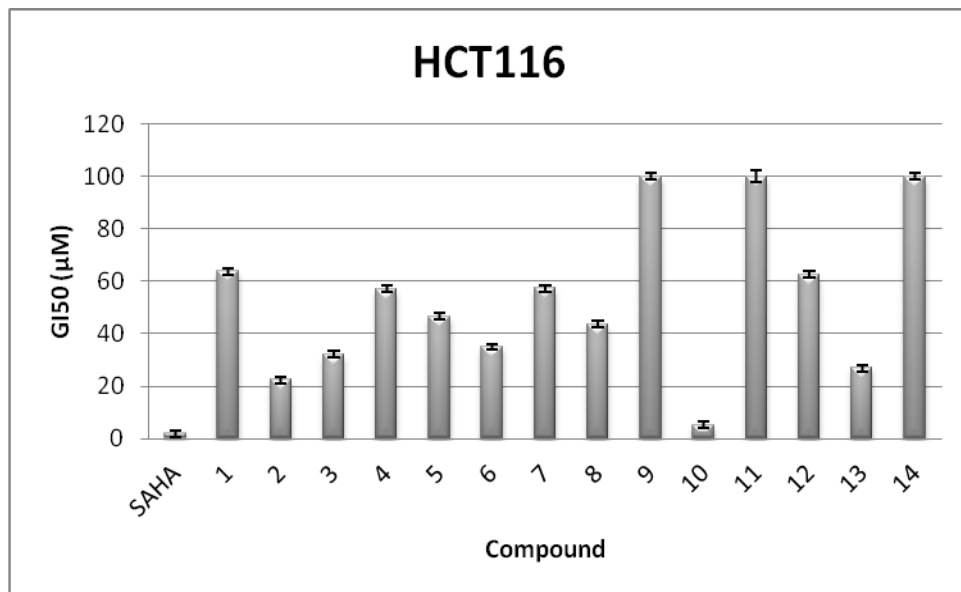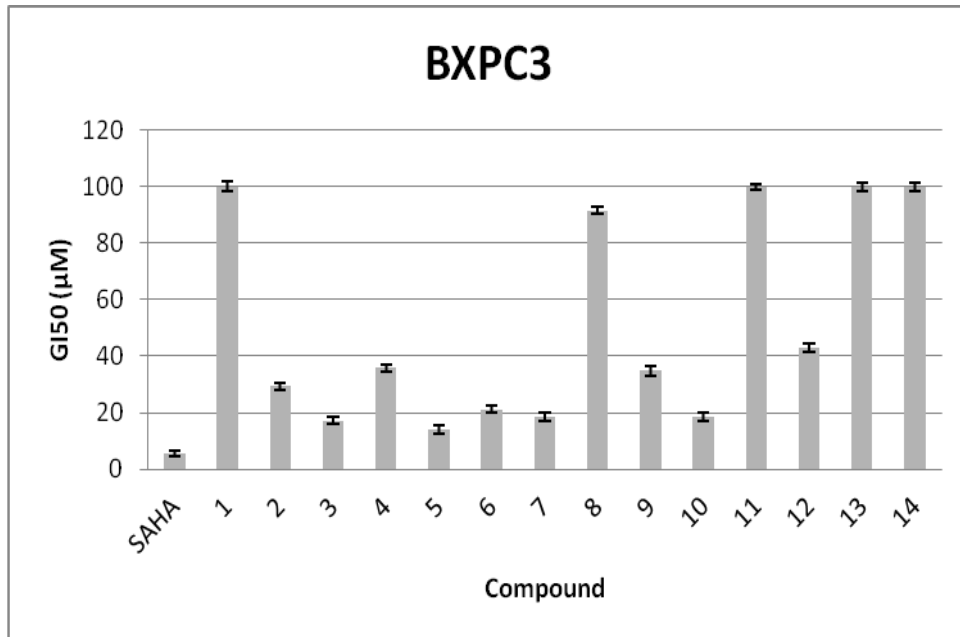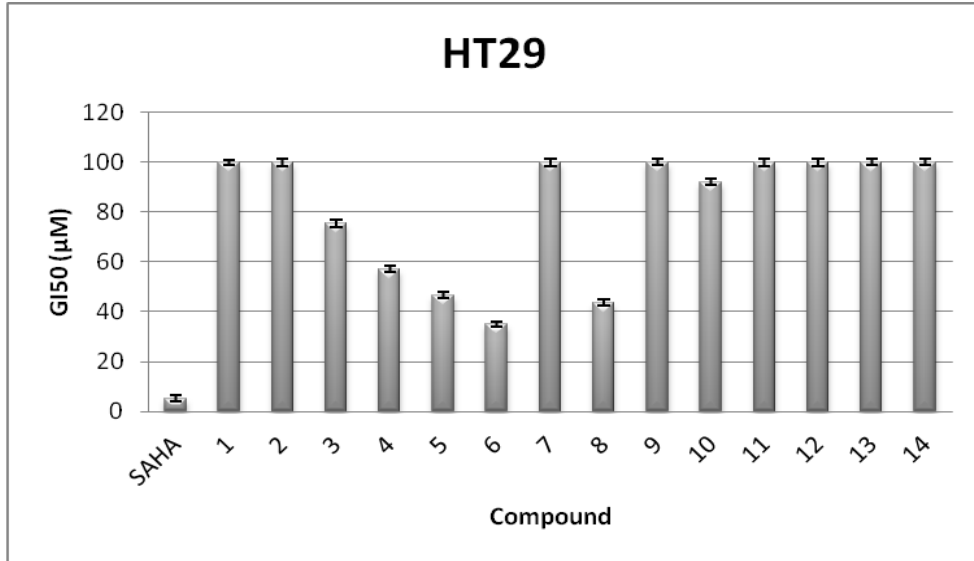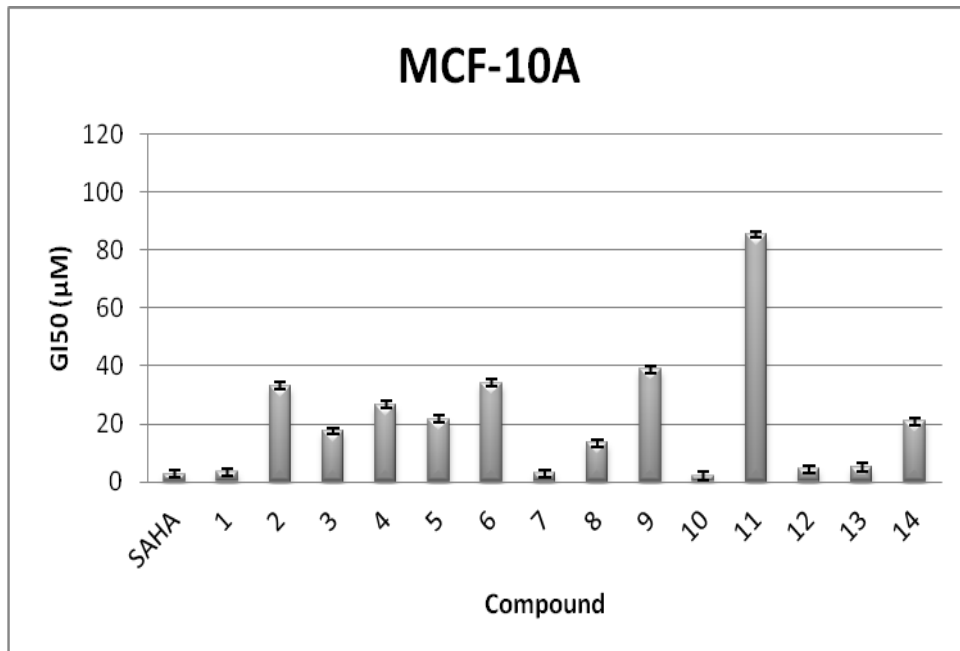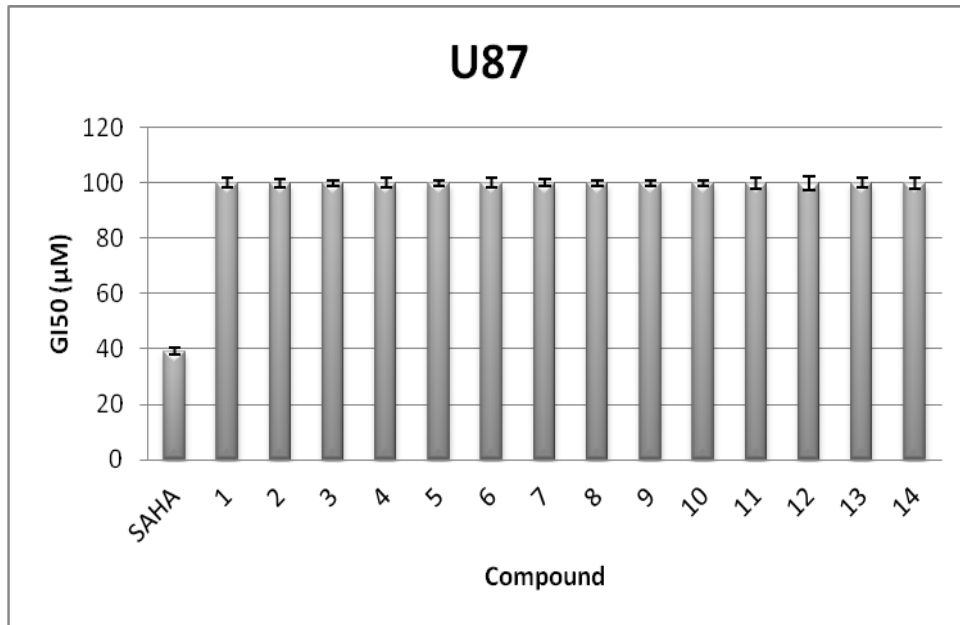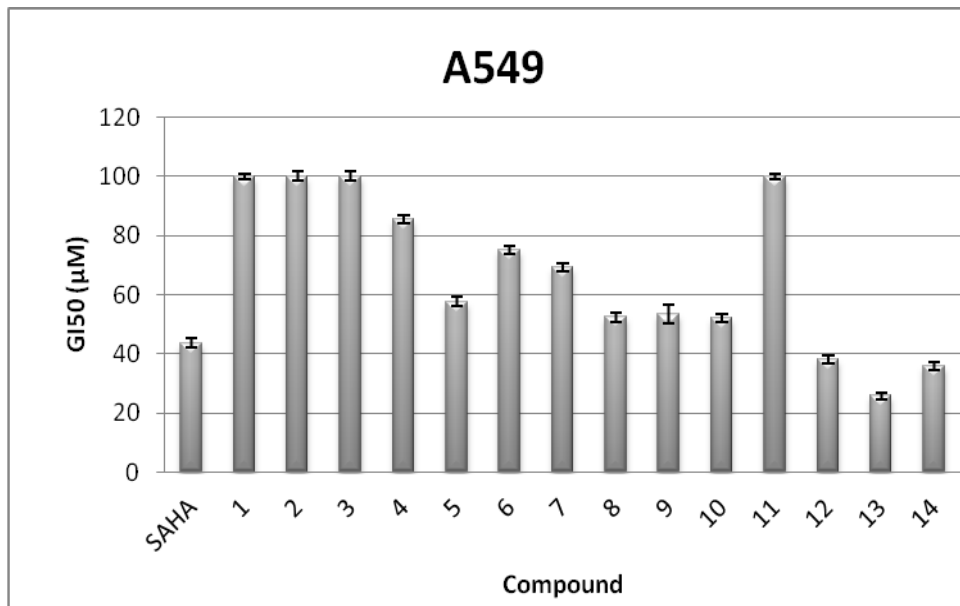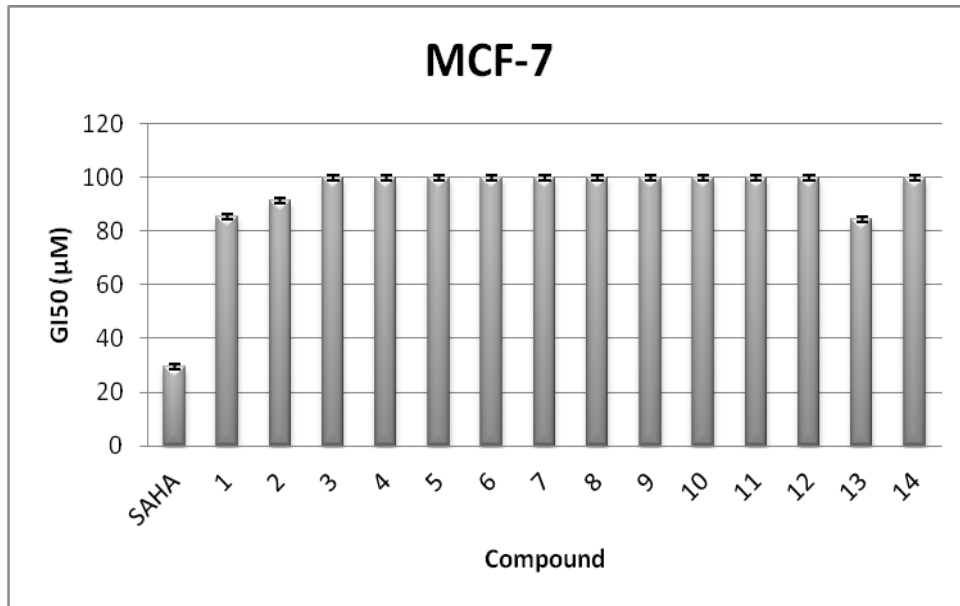
C. Evaluation of cancer cell line selective cytotoxicity in hematological cell lines and normal dermal fibroblasts

The benefits of HDAC inhibitors (HDACi) in the treatment of hematological malignancies are supported by the fact that both SAHA and Romidepsin were approved by the FDA for the treatment of cutaneous T-cell lymphoma (CTCL) (2, 4, 8-10, 33, 39, 42, 45-47). Overexpression of HDAC-1, -2 and -6 has also been reported in CTCL (33). Inhibition of the growth of Jurkat T-leukemia and HuT-78 cells by SAHA and other HDACi has been reported (2, 4, 5, 28). We have previously reported that the beta-substituted tropolones show selective inhibition of proliferating cells in cancerous tissues versus normal adult human dermal fibroblasts (hDF) (50). Therefore, we further explored the cytotoxicity of the tropolone library in the normal fibroblasts, hDF, and the two hematological cell lines, Jurkat and HuT-78. The cell growth inhibitory results was proportional to HDAC inhibition data particularly given that the methylated tropolone, compound 11, exhibited poor inhibition of both the Jurkat and HuT-78 cell lines (Table 2).

Compound	GI$_{50}$ (µM), 72h			
	Hematological			Normal
	Jurkat	HuT-78		hDF
SAHA	0.90	2.10		18.95
1	12.21	43.02		>100
2	3.33	7.83		96.46
3	1.15	4.11		93.07
4	0.62	2.87		>100
5	0.76	3.05		>100
6	1.86	4.74		>100
7	0.67	4.14		12.40
8	4.62	8.95		>100
9	5.89	17.09		>100
10	1.10	4.99		>100
11	>100	>100		>100
12	4.45	13.11		>100
13	0.59	3.25		>100
14	6.30	11.36		>100

Table 2: Evaluation of cancer cell line selective cytotoxicity in hematological cell lines and normal fibroblasts.

83

Tropolones, like many HDACi, show preferential inhibition of the hematological malignancies, as evidenced by the fact that most of the tropolones had GI_{50} values in the very low micromolar range (Figure 2).

Figure 2: Tropolones show preferential selectivity to hematological malignancies
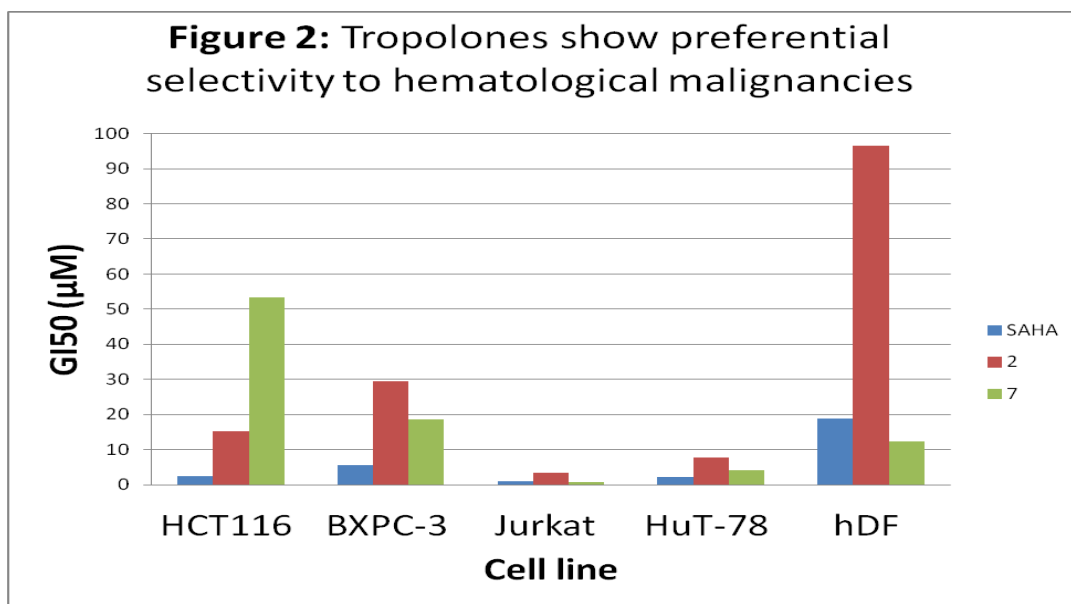
Growth inhibition was more pronounced in the Jurkat cells but the GI_{50} values were still relatively potent in the HuT-78 cells particularly when compared to the solid tumor cell lines or the dermal fibroblasts (Figure 3). For example, compound 2 showed a 12-fold selectivity towards HuT-78 cells and a 30-fold selectivity towards Jurkat cells when compared to hDF cells. The alpha-substituted tropolones were slightly more potent than the beta-substituted compounds in both hematological cell lines. For example, compounds 5 and 9 have a dimethoxyl phenyl functional group substituted at the alpha and beta

positions respectively; but compound 5 had lower GI_{50} values of 0.76 µM and 3.05 µM in Jurkat and HuT-78 cells respectively whereas compound 9 had GI_{50} values of 5.89 µM and 17.09 µM respectively in the two hematological cell lines.

Interestingly, SAHA and compound 7 were the only compounds to significantly inhibit growth of the hDF cells with GI_{50} values of 18.95 µM and 12.40 µM respectively. This observation is promising in the pre-clinical development of tropolones since many anticancer drugs currently in clinical development are cytotoxic agents with low therapeutic index acting non-selectively against proliferative cells of both cancerous and normal tissues (37). Furthermore, it may be inferred that SAHA and other broad-spectrum HDACi can modulate the acetylation status of a wide range of protein targets leading to undesired toxic effects (8-10, 39, 44-47). Therefore, the development of more selective isoform-selective HDACi, like the tropolones, could result in improved therapeutic efficacy in cancer treatment as well as improved pharmacokinetic profiles.

Figure 3: Evaluation of cancer cell line selective cytotoxicity in hematological cell lines and normal human adult dermal fibroblasts

HuT-78
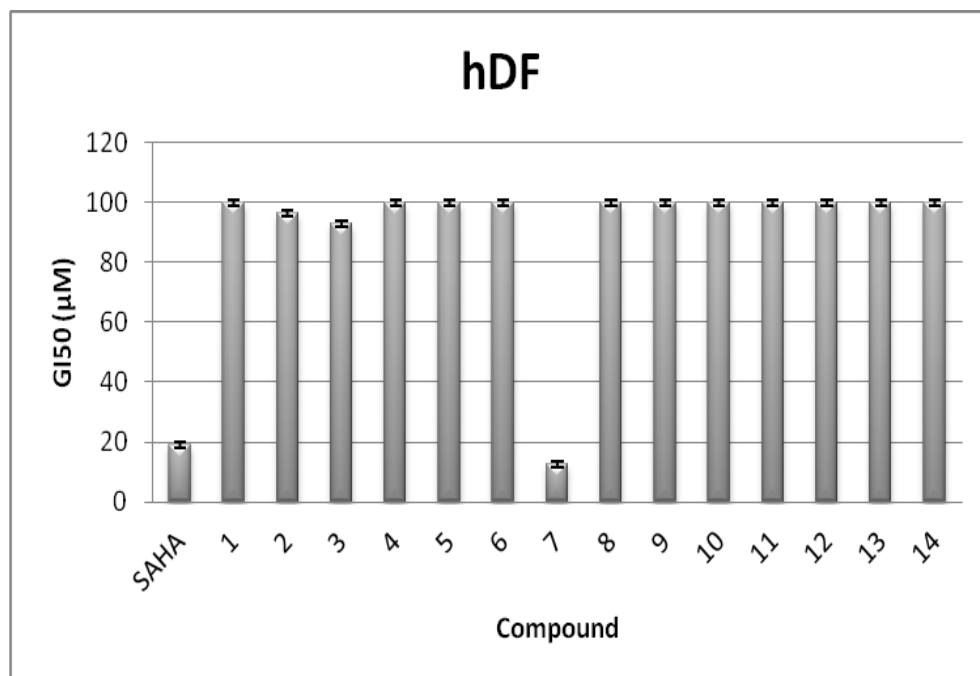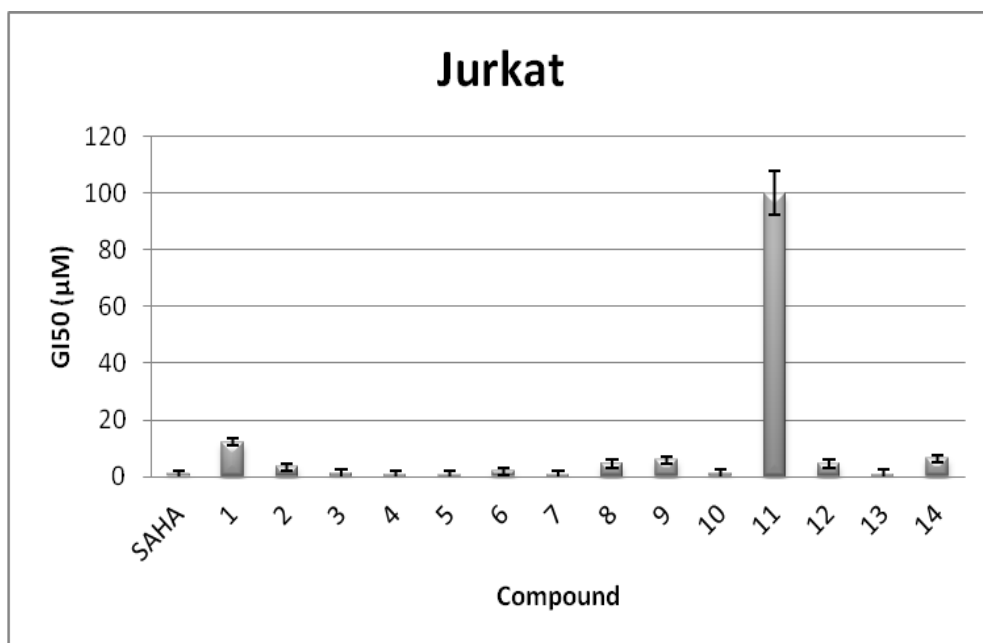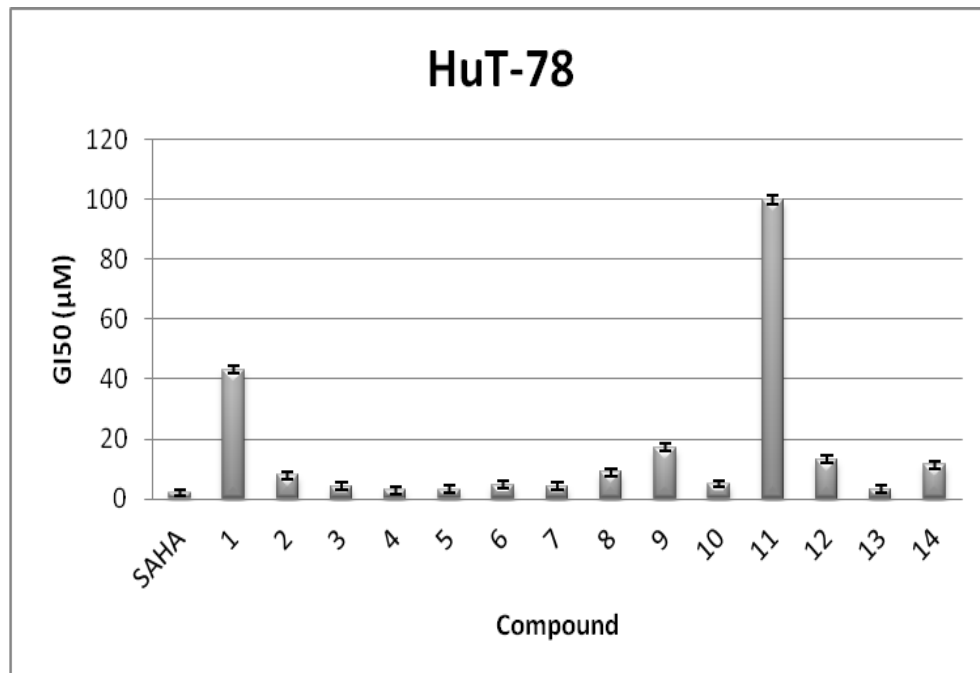
D. Conclusions

The benefits of HDACi as anticancer agents have been widely explored resulting in FDA approval of vorinostat and romidepsin for the treatment of CTCL. Many HDACi are currently in preclinical and clinical development for the treatment of cancer. Given these developments, we explored cell line selective cytotoxicity of tropolones presumably as a result of HDAC inhibition. We observed a correlation between HDAC inhibition and cancer cell line growth inhibition particularly given that the methylated tropolone, compound 11 inhibited all of the cell lines relatively poorly when compared to the rest of the library. Tropolones also display cancer cell line selective cytotoxicity as evidenced by

87

preferential inhibition of the two hematological cell lines, Jurkat and HuT-78. The nature and position of substituents on the tropolone ring seems to be critical in inducing growth inhibition since the unsubstituted tropolone, compound 1, inhibited all of the cell lines relatively poorly when compared to the rest of the library. There was also a correlation between increased hydrophobicity and more potent cytotoxicity; furthermore, the alpha-substituted tropolones seemed to be slightly more potent than the beta-substituted compounds in all cell lines. Additionally, it seems that selective HDAC inhibition may result in reduced toxicity profiles as evidenced by the fact that with the exception of compound 7, none of the tropolones showed significant inhibition of the normal dermal fibroblasts unlike the pan HDAC inhibitor, SAHA (GI_{50} = 18.95 µM). It may be deduced that SAHA and other broad-spectrum HDACi can modulate the acetylation status of a wide range of protein targets leading to undesired toxic effects. Thus, the development of more selective isoform-selective HDACi, like the tropolones, could result in improved therapeutic efficacy while reducing toxic effects.

E. Acknowledgments

88

www.manaraa.com

the MCF-7 cell line; and Dr. Edward Mena from LifePharms for the MCF-10A

cell line.

F. References

1. Huang, L., & Pardee, A. Suberoylanilide Hydroxamic Acid as a Potential Therapeutic Agent for Human Breast Cancer Treatment. Mol Med. 2000; 6 (10): 849-866.
2. Zhang, Q-L, Wang, L., Zhang, J.W., et.al. The proteasome inhibitor bortezomib interacts synergistically with the histone deacetylase inhibitor suberoylanilide hydroxamic acid to induce T-leukemia/lymphoma cells apoptosis. Leukemia 2009; 23 (8): 1507–1514.
3. LaBonte, M.J., Wilson, P.M., Fazzone, W., et.al. DNA microarray profiling of genes differentially regulated by the histone deacetylase inhibitors vorinostat and LBH589 in colon cancer cell lines. BMC Med Genomics 2009; 2:67
4. Ulrike, H., Rademacher, J., Lamottke, B., et.al. Synergistic interaction of the histone deacetylase inhibitor SAHA with the proteasome inhibitor bortezomib in cutaneous T cell lymphoma. Eur J Haematol 2009; 82 (6): 440–449.
5. Wozniak, M.B., Villuendas, R., Bischoff, J.R., et.al. Vorinostat interferes with the signaling transduction pathway of T-cell receptor and synergizes with phosphoinositide-3 kinase inhibitors in cutaneous T-cell lymphoma.
6. Schrump, D.S. Cytotoxicity Mediated by Histone Deacetylase Inhibitors in Cancer Cells: Mechanisms and Potential Clinical Implications. Clin. Cancer. Res 2009; 15: 3947-3957.
7. Ruefli, A.A., Ausserlechner, M.J., Bernhard, D., et. al. The histone deacetylase inhibitor and chemotherapeutic agent suberoylanilide hydroxamic acid (SAHA) induces a cell-death pathway characterized by cleavage of Bid and production of reactive oxygen species. Proc Natl Acad Sci U S A. 2001; 98(19):10833-8.
8. Ononye, S.N., van Heyst, M., Falcone, E., et.al. Toward isozyme selective histone deacetylase inhibitors as therapeutic agents for the treatment of cancer. Pharm. Patent Analyst 2012; 1 (2), 207-221.
9. Lemoine, M., & Younes, A. Histone deacetylase inhibitors in the treatment of lymphoma. Discov Med. 2010; 10(54): 462-70.
10. Marks, P.A., & Dokmanovic, M. Histone deacetylase inhibitors: discovery and development as anticancer agents. Expert Opin Investig Drugs 2005; 14(12):1497-511.

11. Kong, Y., Jung, M., Wang, K., et. al. Histone deacetylase cytoplasmic trapping by a novel fluorescent HDAC inhibitor. Mol Cancer Ther. 2011;10 (9):1591-9.

12. Bolden, J.E., Peart, M.J., & Johnstone, R.W. Anticancer activities of histone deacetylase inhibitors. Nat Rev Drug Discov. 2006; 5(9):769-84.

13. Frew, A.J., Johnstone, R.W, & Bolden, J.E. Enhancing the apoptotic and therapeutic effects of HDAC inhibitors. Cancer Lett. 2009; 280(2):125-33.

14. Knutson, A.K., Welsh, J., Taylor, T., et.al. Comparative effects of histone deacetylase inhibitors on p53 target gene expression, cell cycle and apoptosis in MCF-7 breast cancer cells. Oncol Rep. 2012; 27(3):849-53.

15. Vigushin, D.M., Ali, S., Pace, P.E., et al. Trichostatin A is a histone deacetylase inhibitor with potent antitumor activity against breast cancer in vivo. Clin Cancer Res, 2001; 7(4): 971-6.

16. Huang, L., & Pardee, A.B. Suberoylanilide hydroxamic acid as a potential therapeutic agent for human breast cancer treatment. Mol Med. 2000; 6(10):849-66.

17. Walker, G.E., Wilson, E.M., Powell, D., et al., Butyrate, a histone deacetylase inhibitor, activates the human IGF binding protein-3 promoter in breast cancer cells: molecular mechanism involves an Sp1/Sp3 multiprotein complex. Endocrinology, 2001; 142(9): 3817-27.

18. Cao, Z.A., Bass, K.E., Balasubramanian, S., et al. CRA-026440: a potent, broad-spectrum, hydroxamic histone deacetylase inhibitor with antiproliferative and antiangiogenic activity in vitro and in vivo. Mol Cancer Ther, 2006; 5(7): 1693-701.

19. Thaler, F., Colombo, A., Mai, A., et al., Synthesis and biological evaluation of N-hydroxyphenylacrylamides and N-hydroxypyridin-2-ylacrylamides as novel histone deacetylase inhibitors. J Med Chem. 2010; 53(2): 822-39.

20. Vannini, A., Volpari, C., Filocamo, G., et al. Crystal structure of a eukaryotic zinc-dependent histone deacetylase, human HDAC8, complexed with a hydroxamic acid inhibitor. Proc Natl Acad Sci U S A 2004; 101(42): 15064-9.

21. Ontoria, J.M., Altamura, S., Di Marco, A., et al. Identification of novel, selective, and stable inhibitors of class II histone deacetylases. Validation studies of the inhibition of the enzymatic activity of HDAC4 by small molecules as a novel approach for cancer therapy. J Med Chem 2009; 52(21): 6782-9.

22. Na, Y.S., Jung, K.A., Kim, S.M., et. al. The histone deacetylase inhibitor PXD101 increases the efficacy of irinotecan in in vitro and in vivo colon cancer models. Cancer Chemother Pharmacol. 2011; 68 (2):389-98.

23. Attenni, B., Ontoria, B., Cruz, J.C., et al., Histone deacetylase inhibitors with a primary amide zinc binding group display antitumor activity in xenograft model. Bioorg Med Chem Lett, 2009; 19(11): 3081-4.

24. Portanova, P., Russo, T., Pellerito, O., et.al. The role of oxidative stress in apoptosis induced by the histone deacetylase inhibitor suberoylanilide hydroxamic acid in human colon adenocarcinoma HT-29 cells. Intl J Oncol. 2008; 33(2): 325-31.

25. Blagosklonny, M., Robey, R., Bates, S., et.al. Pretreatment with DNA-damaging agents permits selective killing of checkpoint-deficient cells by microtubule-active drugs. J. Clin. Invest. 2000; 105: 533–553

26. Clocchiatti A., Di Giorgio, E., Ingrao, S., et.al. Class IIa HDACs repressive activities on MEF2-depedent transcription are associated with poor prognosis of ER+ breast tumors. FASEB J. 2012 Nov 16. [Epub ahead of print]

27. Zafar, S.F., Nagaraju, G.P., & El-Raves, B. Developing histone deacetylase inhibitors in the therapeutic armamentarium of pancreatic adenocarcinoma. Expert Opin Ther Targets. 2012; 16(7):707-18.

28. Ouaissi, M., Cabral, S., Tavares, J., et al. Histone deacetylase (HDAC) encoding gene expression in pancreatic cancer cell lines and cell sensitivity to HDAC inhibitors. Cancer Biol Ther. 2008; 7(4): 523-531.

29. Ouaissi, M., Giger, U., Sielezneff, I., et al. Rationale for possible targeting of histone deacetylase signaling in cancer diseases with a special reference to pancreatic cancer. J Biomed Biotechnol. 2011: 315939.

30. Ouaissi, M., & Ouaissi, A. Histone deacetylase enzymes as potential drug targets in cancer and parasitic diseases. J Biomed Biotechnol 2006; 2006 (2): 13474.

31. Bajbouj, K., Mawrin, C., Hartig, R., et.al. P53-dependent antiproliferative and pro-apoptotic effects of trichostatin A (TSA) in glioblastoma cells. J Neurooncol. 2012; 107(3):503-16.

32. Vinodhkumar, R., Song, Y-S., & Devaki, T. Romidepsin (depsipeptide) induced cell cycle arrest, apoptosis and histone hyperacetylation in lung carcinoma cells (A549) are associated with increase in p21 and hypophosphorylated retinoblastoma proteins expression. Biomed Pharmacother. 2008; 62(2):85-93.

33. Weichert, W. HDAC expression and clinical prognosis in human malignancies. Cancer Letters. 2009; 280: 168-176.

34. Leoni, F., Zaliani, A., Bertolini, G., et.al. The antitumor histone deacetylase inhibitor suberoylanilide hydroxamic acid exhibits anitinflammatory properties via suppression of cytokines. Proc Natl Acad Sci U S A 2012; 99 (5):2995-3000

35. Lai, M.J., Huang, H.L., Pan, S.L., et. al. Synthesis and biological evaluation of 1-arylsulfonyl-5-(N-hydroxyacrylamide)indoles as potent histone deacetylase inhibitors with antitumor activity in vivo. J Med Chem. 2012 26; 55(8):3777-91.

36. Tang, Y.A., Wen, W.L., Chang, J.W., et. al. A novel histone deacetylase inhibitor exhibits antitumor activity via apoptosis induction, F-actin

disruption and gene acetylation in lung cancer. PLoS One. 2010; 5(9):e12417.

37. Krennhrubec, K., Marshall, B.L., Hedglin, M., et al., Design and evaluation of 'Linkerless' hydroxamic acids as selective HDAC8 inhibitors. Bioorg Med Chem Lett, 2007; 17(10): 2874-8.

38. Butler, L.M., Agus, D. B., Scher, H.I., et al. Suberoylanilide hydroxamic acid, an inhibitor of histone deacetylase, suppresses the growth of prostate cancer cells in vitro and in vivo. Cancer Res 2000; 60(18): 5165-70.

39. Dokmanovic, M., C. Clarke, & Marks, P.A. Histone deacetylase inhibitors: overview and perspectives. Mol Cancer Res 2007; 5(10): 981-9.

40. Estiu, G., West, N., Mazitschek, R., et al. On the inhibition of histone deacetylase 8. Bioorg Med Chem. 2010; 18 (11): 4103-10.

41. Furumai, R., Komatsu, Y., Nishino, N., et al., Potent histone deacetylase inhibitors built from trichostatin A and cyclic tetrapeptide antibiotics including trapoxin. Proc Natl Acad Sci U S A, 2001; 98(1): 87-92.

42. Garber, K. HDAC inhibitors overcome first hurdle. Nat Biotechnol 2007; 25(1): 17-9.

43. Hrzenjak, A., Moinfar, F., Kremser, M.L., et al. Histone deacetylase inhibitor vorinostat suppresses the growth of uterine sarcomas in vitro and in vivo. Mol Cancer. 2010; 9: 49.

44. Lobjois, V., Frongia, C., Jozan, S., et.al. Cell cycle and apoptotic effects of SAHA are regulated by the cellular microenvironment in HCT116 multicellular tumour spheroids. Eur J Cancer. 2009; 45(13):2402-11.

45. Marks, P., Rifkind, R.A., Richon, V.M., et. al. Histone deacetylases and cancer: causes and therapies. Nat Rev Cancer. 2001;1(3):194-202.

46. Noureen, N., H. Rashid, & Kalsoom, S. Identification of type-specific anticancer histone deacetylase inhibitors: road to success. Cancer Chemother Pharmacol. 2010; 66(4):625-33.

47. Paris, M., Porcelloni, M., Binaschi, M., et al. Histone deacetylase inhibitors: from bench to clinic. J Med Chem 2008; 51(6): 1505-29.

48. Zhou, Q., Dalgard, C.L., Wynder, C., et. al. Histone deacetylase inhibitors SAHA and sodium butyrate block G1-to-S cell cycle progression in neurosphere formation by adult subventricular cells. BMC Neurosci. 2011;12:50.

49. Dickinson, M., Johnstone, R.W., & Prince, H.M. Histone deacetylase inhibitors: potential targets responsible for their anti-cancer effect. Invest New Drugs. 2010; 28 Suppl 1:S3-20.

50. Oblak, E.Z., Bolstad, E.S., Ononye, S.N., et.al. The Furan Route to Tropolones: Probing the anti-proliferative effects of β-thujaplicin analogs. J. Org. Biomol. Chem. 2012; 10(43):8597-604.

51. Wakabayashi, H., Yokoyama, K., Hashiba, K., et al. Cytotoxic activity of tropolones against human oral tumor cell lines. Anticancer Res, 2003; 23(6C): 4757-63.

52. Liu, S., & Yamauchi, H. Hinokitiol, a metal chelator derived from natural plants, suppresses cell growth and disrupts androgen receptor signaling in prostate carcinoma cell lines. Biochem Biophys Res Commun, 2006; 351(1): 26-32.

53. Liu, S., & Yamauchi, H. p27-Associated G1 arrest induced by hinokitiol in human malignant melanoma cells is mediated via down-regulation of pRb, Skp2 ubiquitin ligase, and impairment of Cdk2 function. Cancer Lett 2009; 286(2): 240-9.

54. Matsumura, E., Morita, Y., Date, T., et al., Cytotoxicity of the hinokitiol-related compounds, gamma-thujaplicin and beta-dolabrin. Biol Pharm Bull, 2001; 24 (3): 299-302.

55. Murakami, K., Ohara, Y., Haneda, M., et. al. Prooxidant action of hinokitiol: hinokitiol-iron dependent generation of reactive oxygen species. Basic Clin Pharmacol Toxicol. 2005; 97(6):392-4.

56. Spurling, C.C.,Godman, C.A., Noonan, E.J., et. al. HDAC3 Overexpression and Colon Cancer Cell Proliferation and Differentiation, Mol. Carc. 2008; 43: 137-147.

57. Godman, C.A., Joshi, R., Tierney, B.R., et.al. HDAC3 impacts multiple oncogenic pathways in colon cancer cells with effects on Wnt and vitamin D signaling. Cancer Biol. & Ther. 2008; 7 (10): 1570-1580.

58. Noonan, E.J., Place, R.F., Pookot, D., et al. miR-449a targets HDAC-1 and induces growth arrest in prostate cancer. Oncogene, 2009; 28(14): 1714-24.

59. Soule, H.D., Maloney, T.M., Wolman, S.R., et.al. Isolation and characterization of a spontaneously immortalized human breast epithelial cell line, MCF-10. Cancer Res. 1990; 50(18): 6075-86.

60. American Cancer Society. Breast Cancer. Retrieved from http://www.cancer.org/cancer/breastcancer/detailedguide/breast-cancer-new-research

61. Rojas, A., Gonzalez, I., & Figueroa, H. Cell line cross-contamination in biomedical research: a call to prevent unawareness. Acta Pharmacol Sin. 2008; 29(7):877-80.

62. Lacroix, M. Persistent use of "false" cell lines. Int J Cancer. 2008; 122(1):1-4.

63. Tsuji, K., Kawauchi, S., Saito S, et. al. Breast cancer cell lines carry cell line-specific genomic alterations that are distinct from aberrations in breast cancer tissues: comparison of the CGH profiles between cancer cell lines and primary cancer tissues. BMC Cancer. 2010; 10:15.

Chapter *5*

Assessment of histone and tubulin modulation

A. Introduction

Modulation of chromatin structure is critical in the regulation of transcription (1-21). The amino terminal tails of the core histones (H2A, H2B, H3 and H4) undergo various post-transcriptional modifications, including methylation, acetylation and phosphorylation (3-4; 8-14). Histone acetylation is considered to be the most studied posttranslation modification of nucleosomes (2, 3). In fact, a recent global proteomic analysis has revealed more than 1700 protein substrates of HDACs including histones and structural proteins like tubulin (Figure 1; 13-14). Furthermore, accumulation of acetylated histones has been demonstrated as one of the molecular mechanisms for HDAC inhibition (3, 14-18). Therefore in this chapter, we will explore the modulation of histones and tubulins as a result of HDAC inhibition by the tropolones.
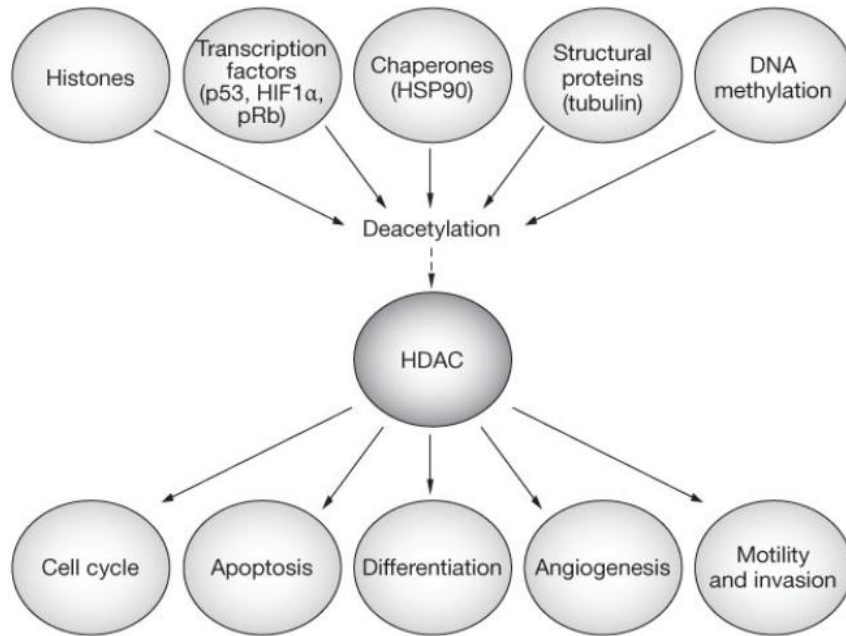
Figure 1: Illustration of the multiple roles of HDACs in cells (14).

B. Initial assessment of histone hyperacetylation in HT-29 colon cancer cells

In collaboration with Dr. Cassandra Godman, a former member of the Giardina laboratory here at the University of Connecticut, our preliminary assessment of histone hyperacetylation was conducted in HT-20 colon cancer cells after a 24h treatment with 40 μM compound 9 (DWI) via Western blot analysis. Four millimolar of the broad spectrum fatty acid HDACi, butyric acid (BA), served as experimental control. Following treatment, a 3-part protein extraction was performed and the nucleolar fraction was run on a

95

12.5% SDS gel, transferred overnight, and probed for acetyl-specific histones.
Compound 9 showed some specificity to certain acetyl marks since no
differences were observed in either the acetylated Histone H4 Lysine 12
(H4K12Ac) or H3K18Ac but the results showed hyperacetylation of H3K9 and
H3K23 (Figure 2). Moreover, it has been demonstrated that the deacetylation
of H3K9 is required for proper chromosome condensation and H3K9 levels
are reduced in mitotic cells (4, 16-18). These results show that the tropolones
display selectivity towards acetyl-specific histones and may not be pan
HDACi like many HDACi including BA and SAHA.
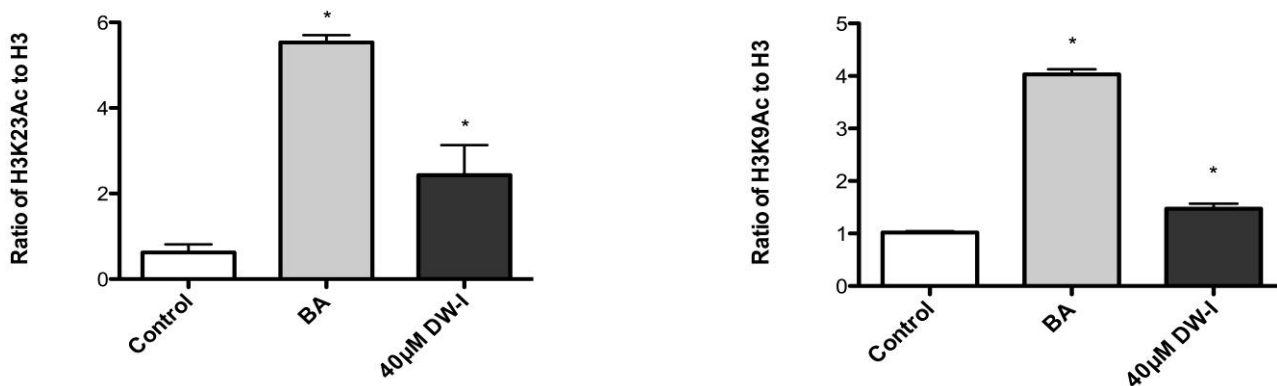
Figure 2: Western blot analysis of Compound 9 (DW-I) and butyric acid (BA).
The graphs represent the quantification of the triplicate gel using ImageJ
software.

96

C. Investigation of histone modulation in Jurkat cells

Based on the fact that Jurkat and HuT-78 cells were the most sensitive to treatment by tropolones, we investigated hyperacetylation of key lysine residues on histones in these two hematological cell lines. Acetylation of histone H3 at lysine9 (K9) has been shown to be essential for histone deposition and chromatin assembly (4, 18). Hyperacetylation of H3K9 is also associated with an increase in the expression of the cyclin-dependent kinase inhibitors (CDK), p21 & p27 that play important roles in cell cycle progression (20). Acetylation of histone H4 particularly at lysine12 (K12) has been correlated with HDAC2 inhibition in CTCL and regulation of telomeric hereochromatin plasticity in yeast cells (3, 21). Furthermore, it has been reported that *in vivo* HDAC8 inhibition leads to hyperacetylation of histones H3 and H4 (19). Given these observations and our biochemical data that shows that tropolones selectively target HDAC2 and HDAC8, we decided to conduct a comprehensive analysis of the hyperacetylation of specific lysine residues on histones H3 and H4.

Our initial assessment of histone hyperacetylation in the hematological cell lines was conducted in Jurkat cells after a 12h treatment via flow cytometric analyses by sequentially incubating treated cells with primary antibodies for histone H4 and H4K12Ac followed by treatment with secondary antibodies conjugated with a fluorescein isothiocyanate (FITC). Flow cytometry has been shown to be a convenient method for evaluating

epigenetic alterations (22-25). We determined geometric mean fluorescence intensities (GMFI), equivalent to the median cell population, for each treatment with the aid of the FlowJo Workstation (26-28). Epigenetic alterations were measured at multiple time points and/or multiple concentrations when possible. We also compared our data for our experimental control, SAHA, to published values for histone hyperacetylation when possible (3, 20). Detailed methods for flow cytometric analyses are in Section G of the Materials and Methods chapter. We compared global hyperacetylation of histone H4 to specific hyperacetylation of histone H4 lysine12 (K12) for a more quantitative analysis of the modulation of specific histone hyperacetylation (Table 1). Histograms for the modification of H4 and additional histograms for H4K12Ac evaluation are in the Appendix, Section 8.

Modulation of histone H4 by the tropolones and SAHA were within the same range as the untreated control (Table 1). However, modulation of the specific lysine residue on histone H4K12, varied between the untreated control and the HDACi (Table 1; Figure 2). In fact, SAHA exerted more than 10-fold increase in the modulation of H4K12Ac. The tropolones exhibited at least a 2-fold increase in hyperacetylation of H4K12 with the alpha dimethoxyphenyl tropolone (compound 5) and the natural product (compound 10) inducing a corresponding 6-fold increase in H4K12 hyperacetylation, the highest among the tropolones.

Table 1: Evaluation of histone hyperacetylation in Jurkat and HuT-78 cells after a 12h treatment with 10 µM HDACi			
Treatment	**Jurkat, GMFI**		
	H4	**H4K12Ac**	**H4K12/H4 ratio**
Control	1.50	7.13	4.8
SAHA	2.04	100.00	49.0
Compound 2	1.88	33.50	17.8
Compound 5	1.75	42.20	24.1
Compound 7	2.17	13.10	6.0
Compound 9	1.88	25.70	13.7
Compound 10	2.04	45.40	22.3
Compound 11	1.87	25.20	13.5
Compound 13	2.08	34.00	16.4
Compound 14	1.86	34.90	18.8

Furthermore, we investigated global (H4 acetylation) and specific (H4K12Ac) hyperacetylation for more quantitative comparative analysis. Similar to our observations on H4K12Ac modulation alone, we found that the H4K12Ac/H4 ratio was the highest in cells treated with SAHA followed by compound 5 and compound 10. Interestingly, the beta-phenyl (compound 7) and the methylated tropolone (compound 11) exhibited the lowest H4K12Ac/H4 ratio indicating that the tropolones show selectivity towards

99

acetyl marks depending on the nature and position of the substituents on the

tropolone ring.

Figure 2: Evaluation of the modulation of H4K12Ac in Jurkat cells. Note that histograms represent the untreated control (red) superimposed with the HDACi treatment (blue) for comparative analysis.

a)   SAHA   b)   Compound 2
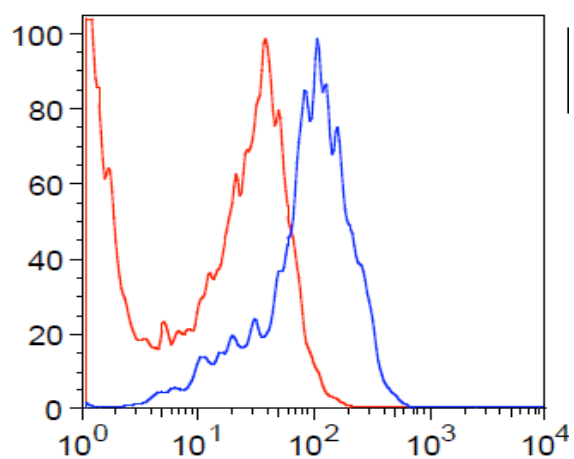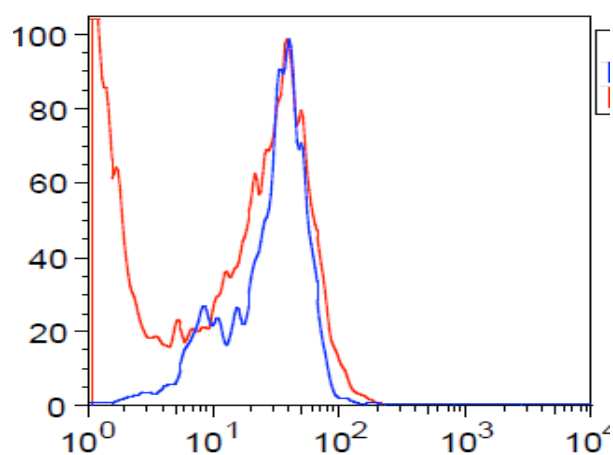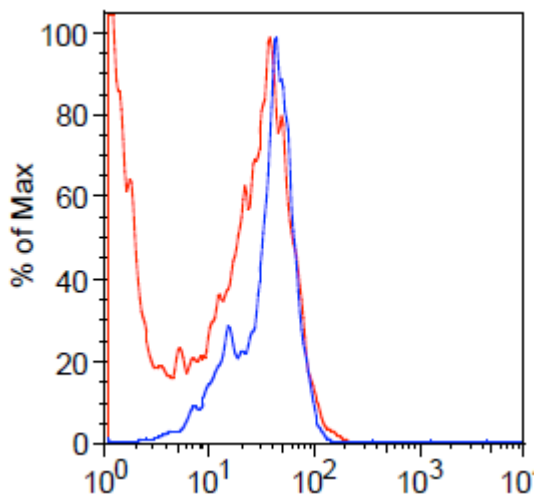
c) Compound 5
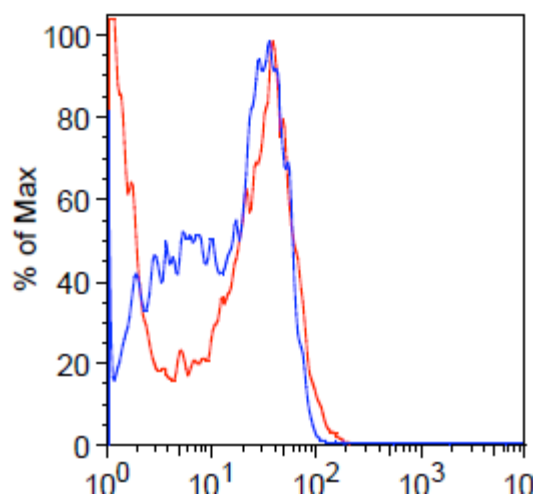
d) Compound 7
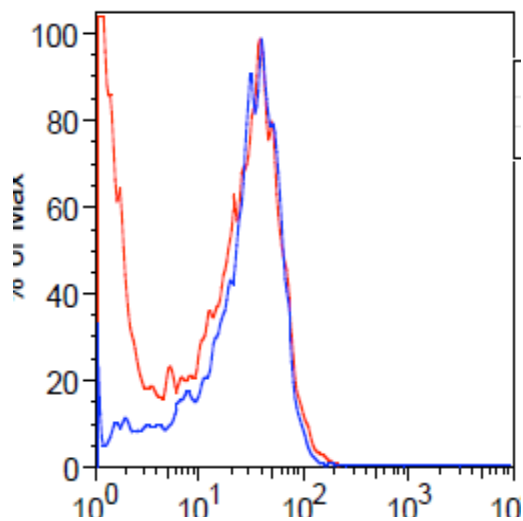
e) Compound 9
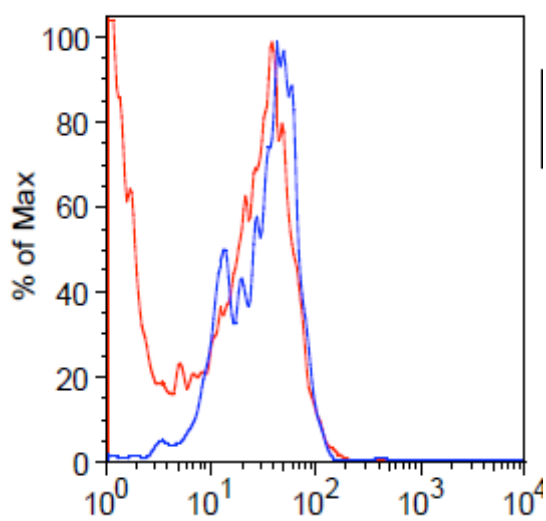
f) Compound 10
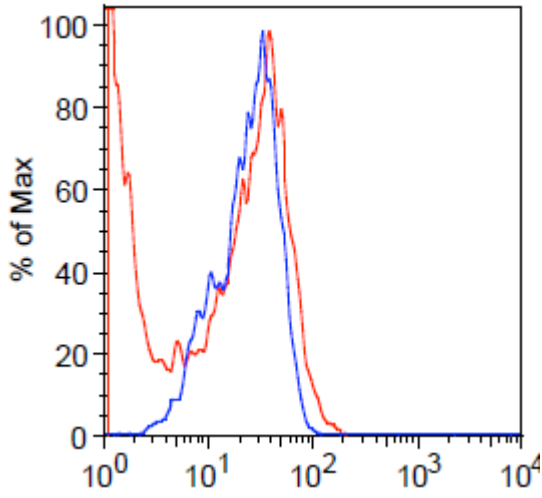
g)   Compound 11   h)   Compound 13
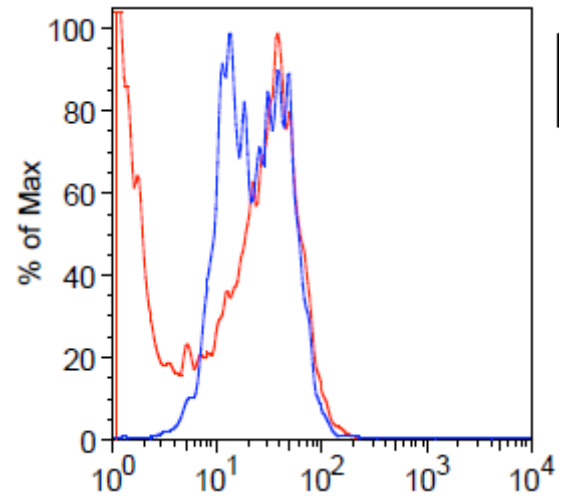
i)   Compound 14
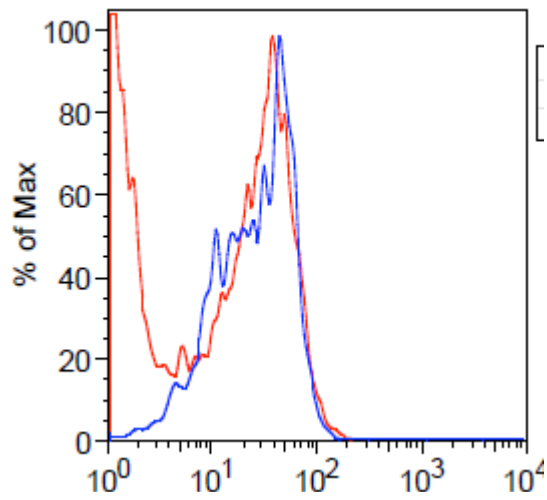
Given our promising results at a 10 µM concentration, we decided to evaluate time effects as well as the effects of a higher concentration of the tropolones on the modulation of H4K12Ac in Jurkat cells. We followed up our 12h analysis with a 4h treatment using a higher inhibitor concentration, 25 µM tropolones, in Jurkat cells (Table 2); histograms for this analysis are in the Appendix, Section 9. It should be noted that we did not evaluate SAHA at 25 µM due to excessive cell death. However, we did not observe any significant hyperacetylation by any of the tropolones; for example, compounds 2 and 7 had GMFI values of 5.56 and 5.02 which were less than the untreated control (5.87). Compound 13 was the only tropolone to have a slightly higher value (7.78) than the untreated control prompting further investigation after a longer treatment period. Moreover, SAHA had a GMFI of 4.11 which was within the same threshold as the untreated control suggesting that a 4h period may not be sufficient for the accumulation of histones.

Table 2: Modulation of H4K12Ac in Jurkat cells after **4h** treatment with HDACi. **Note:** All HDACi at 25 µM except for SAHA which is at 10 µM.

Treatment	GMFI in Jurkat cells									
	Control	SAHA	2	5	7	9	10	11	13	14
(H4K12Ac, 4h)	5.87	4.11	5.56	5.18	5.02	3.84	4.56	4.05	7.78	3.69

We also evaluated the effects of a 25 μM concentration of the tropolones on H4K12Ac modulation after a 12h treatment period (Table 3); histograms for this analysis are in the Appendix, Section 10. Assay data strongly suggest that evaluation of the tropolones at a 25 μM concentration did not result in more significant hyperacetylation of H4K12 after a 12h treatment in Jurkat cells; for example, compounds 5, 10 and 13 had GMFI values of 18.3, 18.6 and 18.8 respectively compared to 18.0 in the untreated control. We hypothesize that the higher concentration of the tropolones may result in an arrest of the S-phase (DNA synthesis) in Jurkat cells but we will further explore this observation via cell cycle analysis in Chapter 6. Furthermore, a higher concentration of the tropolones may have resulted in increased cell death thus reducing the percentage of intact cells available for response to treatment by H4K12Ac antibodies in Jurkat cells. Interestingly, the methylated tropolone, compound 11, that typically exerts the lowest activity among the tropolones, exerted the highest propotion of histone hyperacetylation. Based on our growth inhibition data (Chapter 4), it may be possible that compound 11 was the least cytotoxic in Jurkat cells thus resulting in a higher percentage of intact cells to respond to treatment by H4K12Ac antibodies.

Table 3: Modulation of H4K12Ac in Jurkat cells after **12h** treatment with **25 μM** tropolones									
Treatment (H4K12Ac, 12h)	**GMFI in Jurkat cells**								
	Control	2	5	7	9	10	11	13	14
	18.0	21.0	18.3	17.8	24.3	18.6	46.0	18.8	17.2

Based on our promising results with a 10 μM treatment, we investigated the ability of 10 μM treatments of the tropolones and SAHA to hyperacetylate H3K9Ac levels after a 12h incubation period in Jurkat cells via FACS analysis (Table 4). Corresponding histograms are in Section 11 of the Appendix. 10 μM SAHA induced a 10-fold increase in the modulation of H3K9Ac antibodies when compared to the untreated control. Alternatively, compounds 2, 5, 9, and 13 were the only tropolones that activated a two-fold increase; the rest of the tropolones were within the same threshold as the untreated control. These observations suggest that tropolones could be isoform-selective HDACi since they show selectivity towards promoter-specific histone residues unlike the pan-HDACi SAHA that exerted a 10-fold increase in hyperacetylation of both H3K9Ac and H4K12Ac antibodies.

Table 4: Modulation of H3K9Ac in Jurkat cells after **12h** treatment with 10 µM.HDACi										
	GMFI in Jurkat cells									
Treatment	Control	SAHA	2	5	7	9	10	11	13	14
(H3K9Ac, 12h)	5.91	61.70	13.70	14.20	2.12	15.50	8.19	3.23	14.70	7.91

We followed up our assessment of the hyperacetylation of H3K9 levels in Jurkat cells with an evaluation of the modulation of H3K23Ac in Jurkat cells after a 12h treatment with 10 µM HDACi (Table 5). Corresponding histograms are in the Appendix, Section 12. With the exception of SAHA, compounds 2, 7, and 14, the rest of the compounds had GMFI values lower than the untreated control. SAHA exerted almost a two-fold increase in hyperacetylation (36.90 vs. 20.20) whereas compounds 2, 7 and 14 had slightly higher values than the untreated controls (24.6, 24.0 and 27.2 respectively). Once again, we can deduce that the tropolones show selectivity towards acetyl-specific histones in Jurkat cells.

106

Table 5: Modulation of H3K23Ac in Jurkat cells after **12h** treatment with 10 µM HDACi										
	GMFI in Jurkat cells									
Treatment	Control	SAHA	2	5	7	9	10	11	13	14
(H3K23Ac, 12h)	20.20	36.90	24.60	18.30	24.00	17.20	17.50	17.80	17.80	27.20

D. Investigation of histone modulation in HuT-78 cells

Given our promising results in Jurkat cells, we also evaluated the

modulation of H3K9Ac and H4K12Ac antibodies in HuT-78 cells following a

12h treatment with 10 µM HDACi via FACS analysis (Table 6). Corresponding

histograms are in the Appendix, sections 13 and 14. Similar to our data in

Jurkat cells, the tropolones were more sensitive to H4K12Ac treatment than

H3K9Ac. Compound 9 exerted almost a 2-fold increase in H4K12 (84.40 vs.

51.00 in the untreated control). Alternatively, compound 9 had a lower GMFI

value for H3K9Ac modulation than the untreated control (20.90 vs. 29.20).

SAHA treatment resulted in slightly more than a 2-fold increase in HuT-78

cells that is notably less than the 10-fold increase we observed in Jurkat cells

indicating cell line selectivity towards both H3K9 and H4K12 hyperacetylation.

Concurrently, the tropolones seem to also be more sensitive to both H3K9Ac

and H4K12Ac treatment in Jurkat cells than in HuT-78 cells; this observation

107

also matches the cellular data that we have previously obtained on growth

inhibition (Chapter 4).

Table 6: Comparative analysis of histone modulation in HuT-78 cells treated with 10 µM HDACi after a 12h treatment		
Treatment	**GMFI in HuT-78 cells**	
	H3K9Ac	**H4K12Ac**
Control	29.20	51.00
SAHA	72.40	111.00
Compound 2	17.40	58.20
Compound 5	16.40	56.00
Compound 7	18.80	56.10
Compound 9	21.00	84.40
Compound 10	18.60	61.20
Compound 11	18.10	47.00
Compound 13	21.50	63.40
Compound 14	20.90	61.90

We also investigated H3K23Ac modulation in HuT-78 cells after a

24h treatment period in order to evaluate if a longer treatment period may

lead to a higher accumulation of histones by the tropolones.

Corresponding histograms are in the Appendix, Section 15. Compound 14

exerted the most significant hyperacetylation of H3K23 antibodies with approximately a 1.6 fold increase compared to the untreated control. While the rest of the tropolones were within close range to the untreated control, SAHA exerted more than a 5-fold increase in H3K23 hyperacetylation. These results suggest once again that tropolones show selectivity towards acetyl-specific histone acetylation whereas SAHA is a broad-spectrum HDACi.

Table 7: Modulation of H3K23Ac in HuT-78 cells after 24h treatment with 10 µM HDACi										
	GMFI in Jurkat cells									
Treatment	Control	SAHA	2	5	7	9	10	11	13	14
(H3K23Ac, 24h)	24.0	133.0	22.1	28.3	28.2	22.4	25.5	25.1	34.7	37.4

E. Investigation of tubulin modulation in Jurkat and HuT-78 cells

HDAC6, a class IIb isozyme, is a unique HDAC with two catalytic subunits and a C-terminal zinc finger domain (29-32). HDAC6 resides mainly in the cytoplasm and regulates many important biological processes, including cell migration and degradation of misfolded proteins (29-32).Many cell movements are mediated by the microtubule, which is made up of globular tubulin subunits (α, β, and γ), with the α/β-tubulin heterodimers forming the tubulin subunit common to all eukaryotic cells (29, 30-32).

109

HDAC6, has been shown to deacetylate the structural protein, α-tubulin at lysine40 (K40), resulting in a modulation of cell motility (16, 29, 32).

Evaluation of inhibition constants (K_i) obtained for HDAC6 (Chapter 3) indicate that the tropolones exhibited poor inhibition of this isozyme (Table 8). In fact, with the exception of compound 2 (K_i = 527 nM), the inhibition constants for the tropolones were greater than 2500 nM. Hence, we predicted that the tropolones will weakly modulate the acetyl-specific tubulin, Ac-α-tub-K40, in Jurkat and HuT-78 cells and tested our hypothesis after a 12h treatment with 10 µM HDACi via FACS analysis. We used 10 µM concentrations because it resulted in significantly low cell death compared to higher concentrations thus allowing for a more precise evaluation of cellular effects. We compared our results to published data for tubulin modulation by our experimental control, SAHA (33). Detailed experimental methods are in Section G of the Materials and Methods chapter. Corresponding histograms are in sections 16 and 17 of the Appendix.

We found that SAHA activated about a 10-fold increase in tubulin hyperacetylation in both Jurkat and HuT-78 cells when compared to the untreated control (Table 8; Figure 3). On the other hand, our compounds modulated tubulin within the threshold of the untreated control. In fact, many of the tropolones, such as compounds 2 and 7, had lower GMFI values for Ac-α-Tub-K40 modulation than the untreated control. However, selective

110

inhibition of class I HDAC enzymes, particularly HDAC8, is also associated with weak tubulin modulation (34); conversely, pan-HDACi and HDAC6-selective HDACi show significant tubulin modulation as a result of HDAC6 hyperacetylation (30, 33, 34). Therefore, these observations support our biochemical data that shows very poor inhibition of HDAC6 by the tropolones and lends support to our claim on the isoform-selective nature of HDAC inhibition by the tropolones.

Table 8: Comparative analysis of tubulin modulation and HDAC6 inhibition. Note: Not applicable (N.A.); Not determined (N.D.)

Treatment	Tubulin modulation (10 µM HDACi)		HDAC6 enzyme Inhibition (K_i, nM)
	Jurkat, GMFI	HuT-78, GMFI	
Control	5.38	18.20	N.A.
SAHA	54.20	177.00	3.02
Compound 2	2.89	13.40	527
Compound 5	2.75	N.D.	>2500
Compound 7	1.89	13.20	>2500
Compound 9	6.71	17.30	>2500
Compound 10	2.14	9.21	>2500
Compound 11	3.74	12.80	>2500
Compound 13	6.57	2.52	>2500
Compound 14	6.2	11.60	>2500

111
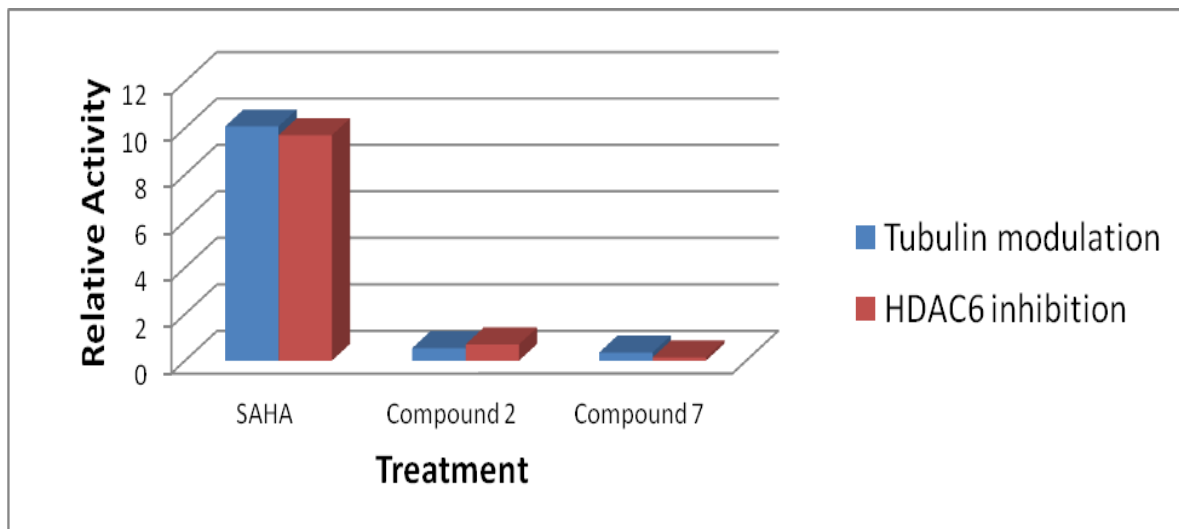
Figure 3: Comparative analysis of tubulin modulation and HDAC6 inhibition

F. Conclusions

Accumulation of histones and non-histone proteins such as tubulin are validated mechanisms of HDAC inhibition. Therefore, we conducted a comprehensive investigation of the hyperacetylation of a panel of acetyl-specific histones and tubulins in HT29, Jurkat and HuT-78 cells. Our compounds were the most sensitive to treatment in Jurkat cells and activated hyperacetylation of H4K12Ac; some of our compounds responded to H3K9Ac and H3K23Ac whereas SAHA responded with at least a 2-fold increase in hyperacetylation for all the promoter-specific histones. BA, an experimental control for our HT29 data, showed the same trend indicating that both HDACi

112

are pan-HDACi unlike the tropolones which showed selectivity to promoter-specific histones. Furthermore, we conducted a comparative analysis of tubulin modulation and HDAC6 inhibition and we found that our compounds did not significantly induce hyperacetylation of Ac-α-tub-K40 unlike SAHA that activated a ten-fold increase in tubulin hyperacetylation in both HuT-78 and Jurkat cells. Our cellular data on tubulin hyperacetylation correlates with our biochemical data that showed weak inhibition of HDAC6. Overall, our comprehensive analysis of tubulin and histone modulation lends support to our claim on the isoform nature of HDAC inhibition by the tropolone library.

G. Acknowledgments

H. References

1. Hagelkruys, A., Sawicka, A., Rennmayr, M., et.al. The biology of HDAC in cancer: the nuclear and epigenetic components. Handb Exp. Pharmacol. 2011; 206: 13-37.
2. Galdieri, L., Moon, J., & Vancura, A. Determination of histone acetylation status by chromatin immunoprecipitation. Methods Mol Biol. 2012; 809:255-65.
3. Khan O., & La Thangue, N.B. HDAC inhibitors in cancer biology: emerging mechanisms and clinical applications. Immunol Cell Biol. 2012; 90 (1):85-94.
4. Strahl, B.D., & Allis, C.D. The language of covalent histone modifications. Nature. 2000; 403(6765):41-5.

5. de Ruijter, A.J., van Gennip, A.H., Caron, H.N. et al. Histone deacetylases (HDACs): characterization of the classical HDAC family. Biochem J, 2003. 370: 737-49.
6. Wang, D-F., Helquist, P., Wiech, N.L., et. al. Toward selective histone deacetylase inhibitor design: homology modeling, docking studies, and molecular dynamics simulations of human class I histone deacetylases, J Med Chem. 2005; 48(22):6936-47.
7. Vannini, A., Volpari, C., Gallinari, P., et al. Substrate binding to histone deacetylases as shown by the crystal structure of the HDAC8-substrate complex. EMBO Rep 2007; 8(9): 879-84.
8. de Zoeten, E.F., Wang, L., Dillmann, S.H., et.al. Inhibition of HDAC9 increases T regulatory cell function and prevents colitis in mice, Gastroenterology. 2010; 138(2):583-94.
9. Hu, E., Chen, Z., Fredrickson, T., et al. Identification of novel isoform-selective inhibitors within class I histone deacetylases. J Pharmacol Exp Ther 2003; 307 (2): 720-8.
10. Gantt, S. L., Gattis, S. G., & Fierke, C. A. Catalytic activity and inhibition of human histone deacetylase 8 is dependent on the identity of the active site metal ion. Biochem J 2006; 45(19): 6170-6178.
11. Dowling, D.P., Gantt, S.L., Fierke, C.A., et al. Structural studies of human histone deacetylase 8 and its site-specific variants complexed with substrate and inhibitors. Biochem J 2008; 47(51): 13554-63.
12. Lemoine, M. & Younes, A. Histone deacetylase inhibitors in the treatment of lymphoma. Discov Med. 2010; 10 (54): 462-70.
13. Bradner, J.E., West, N., Grachan, M.L., et.al. Chemical phylogenetics of histone deacetylases. Nat Chem Biol. 2010; 6(3):238-243.
14. Khan, O., & La Thangue, N.B. Drug Insight: histone deactylase inhibitor-based therapies for cutaneous T-cell lymphomas. Nat Clin Pract Oncol. 2008; 5 (12):714-26.
15. Dokmanovic, M., C. Clarke, & Marks, P.A. Histone deacetylase inhibitors: overview and perspectives. Mol Cancer Res 2007; 5(10): 981-9.
16. Warrener, R., Chia, K., Warren, W.D., et.al. Inhibition of histone deacetylase 3 produces mitotic defects independent of alterations in histone H3 lysine 9 acetylation and methylation. Mol. Pharmacol. 2010; 78(3): 384-393.
17. Park, J.A., Kim, A.J., Kang, Y., et. al. Deacetylation and methylation at histone H3 lysine 9 (H3K9) coordinate chromosome condensation during cell cycle progression. Mol Cells. 2011; 31(4):343-9.
18. Tse, C., Georgieva, E.I., Ruiz-García, A.B.., et. al. Gcn5p, a transcription-related histone acetyltransferase, acetylates nucleosomes and folded nucleosomal arrays in the absence of other protein subunits. J Biol Chem. 1998; 273(49):32388-92.

19. Vannini, A., Volpari, C., Filocamo, G., et al. Crystal structure of a eukaryotic zinc-dependent histone deacetylase, human HDAC8, complexed with a hydroxamic acid inhibitor. Proc Natl Acad Sci U S A 2004; 101(42): 15064-9.
20. Zhou, Q., Dalgard, C.L., Wynder, C., et. al. Histone deacetylase inhibitors SAHA and sodium butyrate block G1-to-S cell cycle progression in neurosphere formation by adult subventricular cells. BMC Neurosci. 2011;12:50.
21. Zhou, B.O., Wang, S.S., Zhang, Y., et. al. Histone H4 lysine 12 acetylation regulates telomeric heterochromatin plasticity in Saccharomyces cerevisiae. PLoS Genet. 2011; 13; 7(1):e1001272.
22. Obier, N., & Muller, A.M. Chromatin flow cytometry identifies changes in epigenetic cell states. Cells Tissues Organs. 2010; 191(3):167-74.
23. Ronzoni S, Faretta M, Ballarini M, et. al. New method to detect histone acetylation levels by flow cytometry. Cytometry A. 2005; 66(1):52-61.
24. Morales, J.C., Ruiz-Magana, M.J., Carranza, D., et. al. HDAC inhibitors with different gene regulation activities depend on the mitochondrial pathway for the sensitization of leukemic T cells to TRAIL-induced apoptosis. Cancer Lett. 2010 ;297(1):91-100.
25. Verma, R., Rigatti, M.J., Belinsky, G.S., et. al. DNA damage response to the Mdm2 inhibitor nutlin-3. Biochem Pharmacol. 2010 ;79(4):565-74.
26. Yale School of Medicine. Introduction to Flow Cytometry: A Learning Guide. Retrieved from: http://medicine.yale.edu/labmed/cellsorter/start/411_66019_Introduction.pdf
27. Herzenberg, L.A., Tung, J., Moore, W.A., et. al. Interpreting flow cytometry data: a guide for the perplexed. Nat Immunol. 2006; 7(7):681-5.
28. Qu, C.X., Wang, J.Z., Wan, W.H., et.al. Establishment of a flow cytometric assay for determination of human platelet glycoprotein VI based on a mouse polyclonal antibody.J Clin Lab Anal. 2006; 20(6):250-4.
29. Liu, Y., Peng, L., Seto, E., et.al. Modulation of histone deacetylase 6 (HDAC6) nuclear import and tubulin deacetylase activity through acetylation. J Biol Chem. 2012; 287 (34):29168-74.
30. Jose, B., Okamura, S., Kato, T., et.al. Toward an HDAC6 inhibitor: synthesis and conformational analysis of cyclic hexapeptide hydroxamic acid designed from α-tubulin sequence. Bioorg Med Chem. 2004; 12(6):1351-6.
31. Yang, X.J., & Gregoire, S. Class II histone deacetylases: from sequence to function, regulation, and clinical implication. Mol Cell Biol 2005; 25(8): 2873-84.
32. Westermann, S., & Weber, K. Post-translational modifications regulate microtubule function. Nat Rev Mol Cell Biol. 2003; 4(12):938-47.

33. Kaliszczak, M., Trousil, S., Aberg, O., et. al. A novel small molecule hydroxamate preferentially inhibits HDAC6 activity and tumour growth. Br J Cancer. 2013; 108 (2):342-50.
34. Balasubramanian, S., Ramos, J., Luo, W., et al. A novel histone deacetylase 8 (HDAC8)-specific inhibitor PCI-34051 induces apoptosis in T-cell lymphomas. Leukemia 2008; 22(5): 1026-34.

Chapter 6

Elucidating the antiproliferative effects of tropolones on cell cycle progression

A. Introduction

The cell cycle is a precisely programmed series of events that enables a cell to duplicate its contents and generate two daughter cells (1). The machinery that constitutes the cell cycle clock (2; Figure 1) operates on a similar level in all cell types throughout the body (1, 2). The cell cycle clock uses a subfamily of serine/threonine protein kinases, known as the cyclin-dependent kinases (CDK), to execute the various steps of the cell cycle.
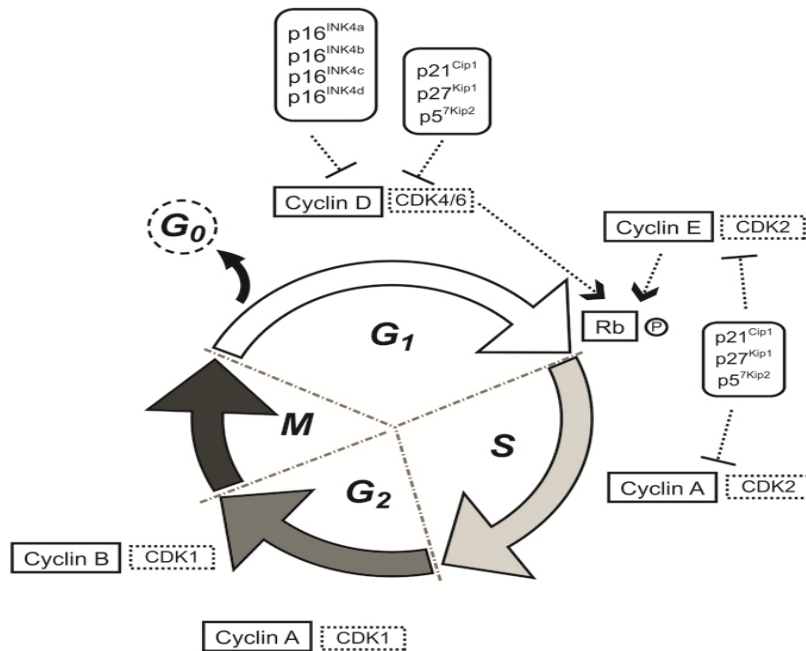
Figure 1: Depiction of cell cycle machinery (2).

A newly formed cell either retreats to a quiescent stage, G0, or initiates a new round of active growth and division, collectively termed proliferation. Unlike the accumulation of RNA and proteins which is initiated immediately, DNA synthesis is deferred for 12-15 hours resulting in the 1st gap of the cell cycle known as G1. Following G1, DNA synthesis (the S phase), typically takes 6-8 hours to reach completion. Before cells can proceed to the M phase (mitosis), there is a second gap, termed G2, typically lasting 3-5 hours, in which cells further prepare for entry into mitosis into the M phase (mitosis).

Cell cycle deregulation is recognized as the hallmark of cancer progression in most malignant tumors (3). HDAC inhibitors (HDACi) of various structural classes have been shown to induce G1, S phase and/or G2/M arrest and concurrently disrupt mitotic progression in proliferating cells in normal and malignant tissues (4-25). The natural product, hinokitiol (compound 10), has been reported to induce arrest of the G1 phase of the cell cycle in malignant melanomas presumably as a result of association with the CDK inhibitor, p27 (26). Therefore, the focus of this chapter is to evaluate the antiproliferative effects of our tropolone library on cell cycle progression in the four cell lines that were the most sensitive to treatment by tropolones via flow cytometric analyses.

The use of fluorescent activated cell sorting (FACS) in flow cytometry allows for fast, objective and quantitative measurements on apoptotic cells when compared to the classic methods of morphological examination by electron

118

microscopy or DNA ladder formation by gel electrophoresis (27). The amount of bound fluorescent dye, typically propidium iodide, in a given cell is correlated with the DNA content in the cell (27-30); thus, percentages of cell populations in each cell cycle phase were calculated based on DNA content histograms with the aid of the FlowJo Analysis Workstation (Tree Star, Inc.). Furthermore, when represented on frequency histograms, DNA fragmentation in apoptotic cells is characterized by a distinctive sub-G1 peak which represents oligonucleosomal DNA fragments and exhibits a fluorescent intensity lower than that of G_1 cells (27-30). Cell cycle analysis was performed at multiple time points and/or multiple concentrations when possible. We compared our data with published reports of cell cycle analysis for the experimental control, SAHA, when possible (22-24). With the exception of the 12h time-point for the Jurkat cells, corresponding histograms for cell cycle analyses are in sections 18-22 of the Appendix.

B. Elucidation of antiproliferative effects in HCT116 colon cancer cells

Initial assessment of the antiproliferative effects of tropolones on cell cycle progression was conducted in HCT116 colon cancer cells at two different concentrations (10 µM and 50 µM) after a 24h incubation period via flow cytometric analyses. 10 µM SAHA served as experimental control. It should be noted that a higher concentration of SAHA could not be evaluated since it resulted in excessive cell death that significantly altered the cell cycle profiles and reduced data accuracy. Based on cytotoxicity data, four compounds (2, 7, 12

119

and 13) were chosen for FACS analysis (Table 1). An increase in the sub-diploid peak (<G0/G1) that is indicative of apoptosis was observed for both the 10 µM and 50 µM treatments for the tropolones. However, the antiproliferative effects of tropolones on cell cycle progression seem to be concentration-dependent since a higher percentage of cells in both the sub-G0/G1 phase and the G1 phase were observed at a concentration of 50 µM compared to a 10 µM concentration. In fact, treatment with 50 µM of compound 13 resulted in the most significant G1 arrest since 77.3% of cells were observed in the G1 stage compared to 48.3% in the untreated control, 47.5% in the 10 µM treatment of compound 13, and 51.2% in the 10 µM SAHA treatment.

G1 arrest is typically associated with increased growth inhibition and concurrently decreased DNA synthesis (31). G1 arrest is also associated with increased expression of the cyclin-dependent kinase inhibitor (CDKI), p21, indicating that the anti-proliferative effects of SAHA and compound 13, may be arbitrated by changes in the expression of CDKI (23. 24). Correspondingly, a decrease in the S and G2-M phases was also observed for the treatment with 50 µM compound 13 and SAHA. Conversely, 50 µM of compound 12 was the only compound that activated an increase in the population of cells in the G2-M phase since 27.1% of cells were observed in the G2-M phase compared to 21% in the untreated control, 19.1% in the 10 µM treatment of compound 12, and 17.3% in the 10 µM SAHA treatment. Increased G2-M arrest is associated with enhanced apoptosis (31).

120

Table 1: Cell-cycle distribution as measured via FACS analysis after a 24h treatment in HCT116 cells.				
Treatment	**24h**			
	<G0/G1	**%G1**	**%S**	**%G2-M**
Control	2.06	48.30	24.60	21.00
10 µM SAHA	13.60	51.20	9.90	17.30
10 µM Compound 2	5.15	50.00	23.30	11.40
50 µM Compound 2	6.99	51.50	28.10	6.04
10 µM Compound 3	6.40	51.80	30.50	5.11
50 µM Compound 3	9.64	43.60	32.10	1.43
10 µM Compound 7	3.98	51.00	19.50	18.80
50 µM Compound 7	6.58	55.00	21.10	2.22
10 µM Compound 12	2.80	44.30	15.40	27.10
50 µM Compound 12	2.97	50.30	19.10	19.10
10 µM Compound 13	3.06	47.50	22.70	18.50
50 µM Compound 13	5.72	77.30	9.10	3.99

Compound 2 at a 10 µM concentration and compound 3 at both concentrations were the only compounds to activate an S-phase arrest. However, at a 10 µM concentration in HCT116 cells, the tropolones did not exhibit any notable cellular effects indicating that further modifications to the

121

current tropolone scaffold may be needed in order to exert more potent cellular effects at lower concentrations in these solid tumor cells.

C. Elucidation of cell cycle progression in BXPC3 cells

SAHA induced a more significant cell cycle arrest in BXPC3 pancreatic cells than the tropolones after a 12h incubation period. Specifically, SAHA treatment resulted in an increase in the population of cells in the sub-G0/G1 phase and G2/M phase; concurrently, SAHA treatment also decreased the percentage of cells in the G1 phase and the S phase. Conversely, the distribution of DNA content by ten tropolones (Compounds 2, 3, 5,7, 9-14) essentially resembled that of the untreated control; although on average, there was a lower percentage of cells in the G1 phase and more cells in the S phase and G2-M phase.

Furthermore, there was no significant arrest of the sub-G0/G1 phase of the cell cycle by either SAHA or the tropolones. Given that arrest of the sub-G0/G1 phase of the cell cycle is usually seen as an index for apoptosis (27-30), it may be deduced that these HDACi may not significantly induce apoptosis in BXPC-3 cells after a 12h incubation period. However, these observations correlate with data from the cancer cell line selective cytotoxicity assays (Chapter 5) in which the HDACi showed the most pronounced antiproliferative effects in the hematological cell lines. In a similar manner to the HCT116 colon cancer

122

cells, it may be possible that a higher concentration and/or a longer treatment period may result in more pronounced effects in the BXPC3 cell line.

Table 2: Elucidation of the antiproliferative effects of tropolones on cell cycle progression as measured via FACS analysis after a 12h treatment in BXPC3 cells.

Treatment	12h			
	%<G0/G1	%G1	%S	%G2-M
Control	1.21	67.20	7.44	11.30
10 µM SAHA	3.55	59.60	2.92	15.90
10 µM Compound 2	1.44	58.10	11.00	10.70
10 µM Compound 3	0.81	69.10	7.60	10.50
10 µM Compound 5	0.59	59.70	9.44	12.10
10 µM Compound 7	0.96	60.50	9.89	10.90
10 µM Compound 9	0.99	63.40	8.01	11.70
10 µM Compound 10	1.67	63.20	8.45	11.00
10 µM Compound 11	1.90	60.50	10.30	10.90
10 µM Compound 12	0.59	57.90	11.10	10.70
10 µM Compound 13	0.62	66.80	7.49	11.50
10 µM Compound 14	0.95	65.70	8.55	11.40

123

D. Time-dependent analysis of cell cycle progression in Jurkat cells

Given that our compounds, like most HDACi in clinical development today, showed preferential inhibition to hematological malignances, we decided to conduct cell cycle analyses at multiple time points in both Jurkat and HuT-78 cells (5-7, 9, 10, 15, 16, 19-21, 25). We observed a distinct arrest of the sub-diploid phase (<G0/G1) of the cell cycle by 10 µM treatments of the tropolones over multiple time points (Table 3). As previously indicated, an increase in the subdiploid peak is often seen as an index for apoptosis; thus this observation will be further evaluated in subsequent chapters where we will explore the induction as well as mechanisms of apoptosis of tropolones in Jurkat cells.

There was also a subtle arrest of the G1 phase of the cell cycle followed by correspondent decreases in both the S-phase and G2-M phase of the cell cycle following tropolone treatment at all three time-points. On the other hand, SAHA was able to induce an increase in the population of cells in the sub-G0/G1, S and G2-M phases of the cell cycle at 12h (Figure 2) but at 24h and 36h, the percentage of apoptotic cells (<G0/G1) was 48.90% and 60.80% respectively resulting in concurrent decreases in the population of cells in other phases of the cell cycle. Furthermore, our internal negative control, compound 11 with a methylated tropolone as the key moiety, essentially resembled the untreated control. This observation lends support to our hypothesis on the availability of the alpha-hydroxyl ketone on the tropolone

124

ring being essential for metal chelation at the HDAC active site. However, as previously stated in previous chapters, efforts are currently in place by the Anderson laboratory to further explore this hypothesis via structural studies of a tropolone bound to HDAC8.

Table 3: Time-dependent analysis of the antiproliferative effects of tropolones on cell cycle progression as measured via FACS analysis in Jurkat cells after a 12h treatment.

Treatment	12h			
	%<G0/G1	%G1	%S	%G2-M
Control	4.16	65.0	19.5	10.0
10 µM SAHA	20.4	25.9	31.6	19.7
10 µM Compound 2	22.3	64.3	11.1	1.39
10 µM Compound 7	16.3	71.5	10.2	1.25
10 µM Compound 11	3.14	68.4	17.5	9.52
10 µM Compound 13	13.3	67.4	15.2	2.67

Table 4: Time-dependent analysis of the antiproliferative effects of tropolones on cell cycle progression as measured via FACS analysis in Jurkat cells after a 24h treatment.

Treatment	24h			
	%<G0/G1	%G1	%S	%G2-M
Control	2.39	60.90	20.90	14.30
10 µM SAHA	48.90	7.46	19.90	12.30
10 µM Compound 2	13.90	70.20	13.30	1.81
10 µM Compound 7	13.90	66.50	15.80	2.58
10 µM Compound 11	1.62	63.00	20.60	13.50
10 µM Compound 13	13.00	69.40	14.20	2.32

Table 5: Time-dependent analysis of the antiproliferative effects of tropolones on cell cycle progression as measured via FACS analysis in Jurkat cells after a 36h treatment.

Treatment	36h			
	%<G0/G1	%G1	%S	%G2-M
Control	1.80	59.10	23.00	14.20
10 µM SAHA	60.80	6.90	15.60	14.90
10 µM Compound 2	18.50	64.20	13.30	2.97
10 µM Compound 7	13.40	65.90	14.60	4.35
10 µM Compound 11	1.22	60.70	21.80	14.60
10 µM Compound 13	17.70	64.70	13.10	3.21

126

Figure 2: Evaluation of the antiproliferative effects of tropolones on cell cycle proliferation after a 12h treatment in Jurkat cells.

a.   Control

b.   10 µM SAHA
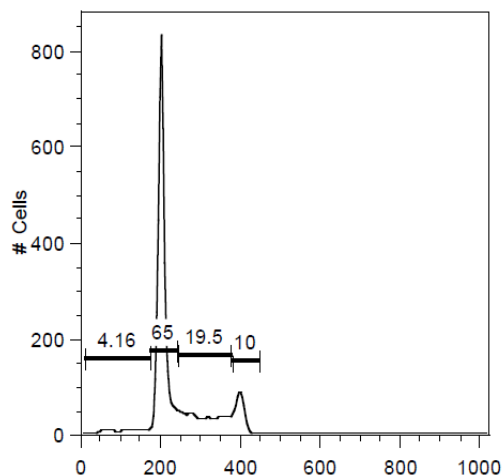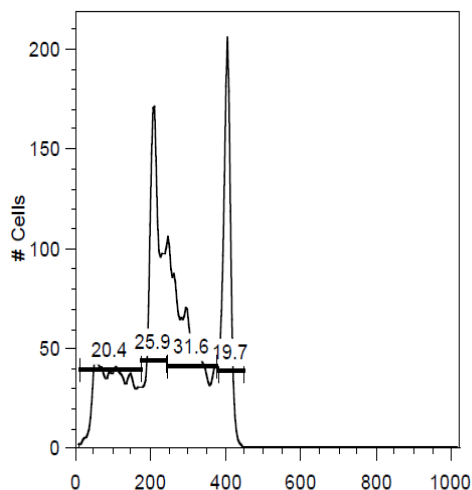
c.   10 µM Compound 2
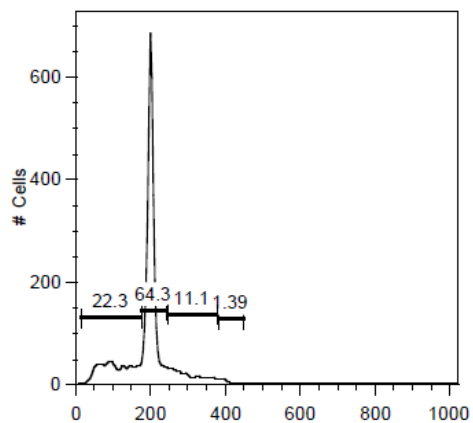
d.   10 µM Compound 7
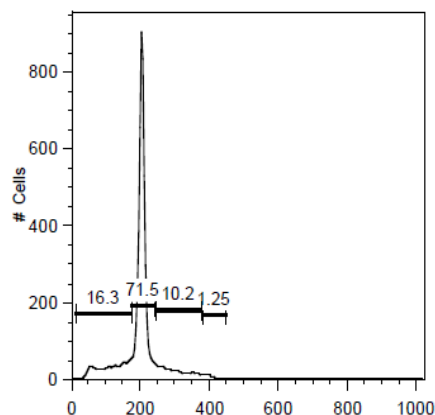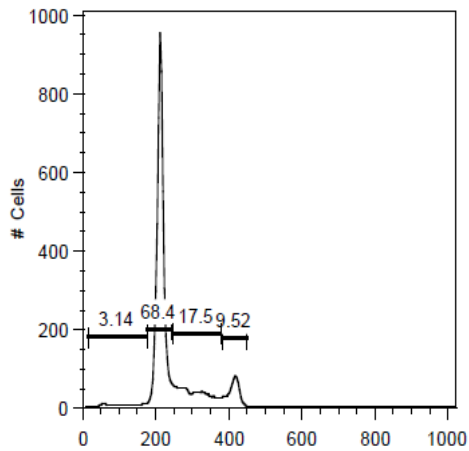
e.   10 µM Compound 11   f.   10 µM Compound 13
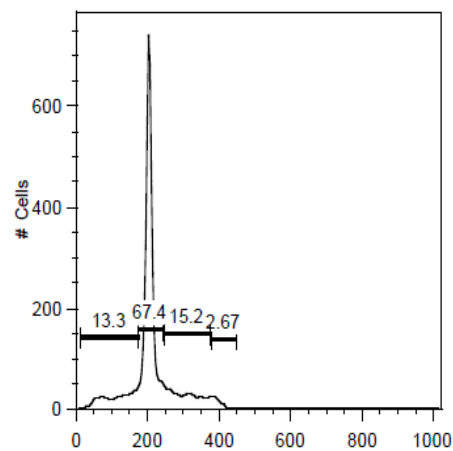
Given our promising results with 10 µM treatments, we also evaluated the antiproliferative effects of eight tropolones (Compounds 2, 5, 7, 9-11, 13 and 14) at a higher concentration of 25 µM after a 12h incubation period in Jurkat cells (Table 4). The tropolones were able to induce a subtle subdiploid phase arrest but activated a more pronounced increase in the population of cells in the S phase particularly when compared to the 10 µM treatment. However, it seems that a 10 µM concentration is sufficient to activate an increase in the subdiploid phase without excessive cell death which alters cell cycle profiles thus reducing data accuracy; Therefore, future assays on apoptosis and mechanisms of gene expression will utilize this 10 µM concentration.

Table 6: Elucidation of the antiproliferative effects of 25 µM tropolones on cell cycle progression as measured via FACS analysis after a 12h treatment in Jurkat cells.

Treatment	12h			
	%<G0/G1	%G1	%S	%G2-M
Control	3.78	64.20	17.50	13.20
25 µM Compound 2	4.25	59.40	27.10	7.09
25 µM Compound 5	5.20	60.90	27.60	4.94
25 µM Compound 7	3.47	61.10	25.30	7.66
25 µM Compound 9	3.93	60.10	27.90	6.22
25 µM Compound 10	5.17	53.90	33.30	6.00
25 µM Compound 11	3.34	63.10	18.70	13.00
25 µM Compound 13	4.94	57.00	29.10	6.37
10 µM Compound 14	4.06	58.50	27.60	7.27

E. Elucidation of antiproliferative effects of tropolones on HuT-78 cells

In a similar manner to Jurkat cells, 10 µM treatments of tropolones were used to evaluate antiproliferative effects on cell cycle progression in HuT-78 cells. 5 µM SAHA served as experimental control to allow for more accurate observation of cell cycle profiles with reduced cell death. After a 12h treatment, there was no significant increase in the subdiploid population, G1 or S phases by either SAHA or the tropolones. However, all the compounds were able to activate a G2-M arrest with the most significant effect being exhibited by compound 7. After a 24h treatment, there was a significant

129

increase in the subdiploid phase of the cell cycle and a subtle G1 arrest

followed by a corresponding decrease in the S phase and G2-M phases for all

the compounds except for compound 11 that basically resembled the

untreated control. After 36h, the most significant observation that we saw for

all the treatments was an increase in the subdiploid peak; thus prompting for

future investigations into the induction and execution of apoptosis.

Table 7: Time-dependent analysis of cell cycle progression in HuT-78 cells as measured via FACS analysis in HuT-78 cells after a 12h treatment.

Treatment	12h			
	%<G0/G1	%G1	%S	%G2-M
Control	11.20	54.70	16.50	13.80
5 µM SAHA	7.73	46.90	17.10	23.80
10 µM Compound 2	4.78	56.30	15.10	22.40
10 µM Compound 7	5.96	46.70	16.40	29.20
10 µM Compound 11	7.12	51.70	17.70	21.90
10 µM Compound 13	7.44	55.50	16.20	20.40

130

Table 8: Time-dependent analysis of cell cycle progression in HuT-78 cells as measured via FACS analysis in HuT-78 cells after a 24h treatment.

Treatment	24h			
	%<G0/G1	%G1	%S	%G2-M
Control	4.71	43.40	31.80	15.90
5 µM SAHA	42.80	29.40	12.70	11.50
10 µM Compound 2	19.10	41.60	22.40	14.70
10 µM Compound 7	11.70	46.40	17.50	23.00
10 µM Compound 11	5.33	49.70	25.50	14.90
10 µM Compound 13	10.50	48.00	19.10	21.60

Table 9: Time-dependent analysis of cell cycle progression in HuT-78 cells as measured via FACS analysis in HuT-78 cells after a 36h treatment.

Treatment	36h			
	%<G0/G1	%G1	%S	%G2-M
Control	8.98	41.60	24.50	22.70
5 µM SAHA	43.20	34.30	14.00	6.24
10 µM Compound 2	8.24	53.10	21.60	14.70
10 µM Compound 7	16.70	40.40	21.80	18.00
10 µM Compound 11	39.40	20.00	26.50	13.90
10 µM Compound 13	18.00	42.70	20.00	17.00

131

F. Conclusions

Cell cycle arrest is well established as a major mechanism of HDAC inhibition. Analyses of cell cycle distribution in multiple cell lines treated with tropolones indicate that the tropolones exert antiproliferative effects on cell cycle progression in a time-dependent manner particularly in the two hematological cell lines, Jurkat and HuT-78. An increase in the sub-diploid population of cells treated with tropolones, an index for apoptosis, was the most evident in Jurkat cells followed by the HuT-78 cells. These observations prompted further investigation on the induction and mechanisms of apoptosis that will be discussed in future chapters. The antiproliferative effects of tropolones on cell cycle progression in hematological cell lines seem to be time-dependent since more notable events were observed after longer incubation periods. On the other hand, a high concentration of 50 µM was required in order to induce significant changes in cell cycle distribution in HCT116 cells. 10µM concentrations of the tropolones did not result in significant cellular changes in HCT116 and BXPC3 cells lending support to earlier observations that we observed in the cytotoxicity assays. Finally, compound 11, typically exhibited changes in cell cycle distribution that were essentially the same as the untreated control thus lending support to our claim on the availability of the alpha-hydroxyl ketone being essential for metal chelation at the HDAC active site.

132

G. References

1. Weinberg, R. The Biology of Cancer. New York, NY: Garland Science, Taylor & Francis Group, LLC., 2007.
2. Currais, A., Hortobágyi, T., & Salvador, S. The neuronal cell cycle as a mechanism of pathogenesis in Alzheimer's disease. Aging (Albany NY) 2009; 1(4): 363–371.
3. Hagelkruys, A., Sawicka, A., Rennmayr, M., et.al. The biology of HDAC in cancer: the nuclear and epigenetic components. Handb Exp. Pharmacol. 2011; 206: 13-37.
4. Schrump, D.S. Cytotoxicity Mediated by Histone Deacetylase Inhibitors in Cancer Cells: Mechanisms and Potential Clinical Implications. Clin. Cancer. Res 2009; 15: 3947-3957.
5. Ononye, S.N., van Heyst, M., Falcone, E., et.al. Toward isozyme selective histone deacetylase inhibitors as therapeutic agents for the treatment of cancer. Pharm. Patent Analyst 2012; 1 (2): 207-221.
6. Noureen, N., H. Rashid, & Kalsoom, S. Identification of type-specific anticancer histone deacetylase inhibitors: road to success. Cancer Chemother Pharmacol. 2010; 66(4):625-33.
7. Dickinson, M., Johnstone, R.W., & Prince, H.M. Histone deacetylase inhibitors: potential targets responsible for their anti-cancer effect. Invest New Drugs. 2010; 28 Suppl 1:S3-20.
8. Zafar, S.F., Nagaraju, G.P., & El-Raves, B. Developing histone deacetylase inhibitors in the therapeutic armamentarium of pancreatic adenocarcinoma. Expert Opin Ther Targets. 2012; 16(7):707-18.
9. Marks, P.A., & Dokmanovic, M. Histone deacetylase inhibitors: discovery and development as anticancer agents. Expert Opin Investig Drugs 2005; 14(12):1497-511.
10. Lemoine, M., & Younes, A. Histone deacetylase inhibitors in the treatment of lymphoma. Discov Med. 2010; 10(54): 462-70.
11. Blagosklonny, M., Robey, R., Bates, S., et.al. Pretreatment with DNA-damaging agents permits selective killing of checkpoint-deficient cells by microtubule-active drugs. J. Clin. Invest. 2000; 105: 533–553
12. Ouaissi, M., Cabral, S., Tavares, J., et al. Histone deacetylase (HDAC) encoding gene expression in pancreatic cancer cell lines and cell sensitivity to HDAC inhibitors. Cancer Biol Ther. 2008; 7(4): 523-531.
13. Ouaissi, M., Giger, U., Sielezneff, I., et al. Rationale for possible targeting of histone deacetylase signaling in cancer diseases with a special reference to pancreatic cancer. J Biomed Biotechnol. 2011: 315939.
14. Weichert, W. HDAC expression and clinical prognosis in human malignancies. Cancer Letters. 2009; 280: 168-176.
15. Dokmanovic, M., C. Clarke, & Marks, P.A. Histone deacetylase inhibitors: overview and perspectives. Mol Cancer Res 2007; 5(10): 981-9.

16. Ouaissi, M., & Ouaissi, A. Histone deacetylase enzymes as potential drug targets in cancer and parasitic diseases. J Biomed Biotechnol 2006; 2006 (2): 13474.
17. Bajbouj, K., Mawrin, C., Hartig, R., et.al. P53-dependent antiproliferative and pro-apoptotic effects of trichostatin A (TSA) in glioblastoma cells. J Neurooncol. 2012; 107(3):503-16.
18. Vinodhkumar, R., Song, Y-S., & Devaki, T. Romidepsin (depsipeptide) induced cell cycle arrest, apoptosis and histone hyperacetylation in lung carcinoma cells (A549) are associated with increase in p21 and hypophosphorylated
19. Bolden, J.E., Peart, M.J., & Johnstone, R.W. Anticancer activities of histone deacetylase inhibitors. Nat Rev Drug Discov. 2006; 5(9):769-84.
20. Frew, A.J., Johnstone, R.W, & Bolden, J.E. Enhancing the apoptotic and therapeutic effects of HDAC inhibitors. Cancer Lett. 2009; 280(2):125-33.
21. Knutson, A.K., Welsh, J., Taylor, T., et.al. Comparative effects of histone deacetylase inhibitors on p53 target gene expression, cell cycle and apoptosis in MCF-7 breast cancer cells. Oncol Rep. 2012; 27(3):849-53.
22. Zhu, P., Huber, E., Kiefer, F., et. al. Specific and redundant functions of histone deacetylases in regulation of cell cycle and apoptosis. Cell Cycle. 2004; 3(10):1240–1242
23. Zhou, Q., Dalgard, C.L., Wynder, C., et.al., Histone deacetylase inhibitors SAHA and sodium butyrate block G1-to-S cell cycle progression in neurosphere formation by adult subventricular cells. BMC Neurosci. 2011; 12:50.
24. Lobjois, V., Frongia, C., Jozan, S., et.al. Cell cycle and apoptotic effects of SAHA are regulated by the cellular microenvironment in HCT116 multicellular tumour spheroids. Eur J Cancer. 2009; 45(13):2402-11.
25. Paris, M., Porcelloni, M., Binaschi, M., et al. Histone deacetylase inhibitors: from bench to clinic. J Med Chem 2008; 51(6): 1505-29.
26. Liu, S., & Yamauchi, H. p27-Associated G1 arrest induced by hinokitiol in human malignant melanoma cells is mediated via down-regulation of pRb, Skp2 ubiquitin ligase, and impairment of Cdk2 function. Cancer Lett 2009; 286(2): 240-9.
27. Wlodkowic, D., Skommer, J., Darzynkiewicz, Z., et.al. Flow cytometry-based apoptosis detection. Methods Mol Biol. 2009; 559:19-32.
28. Semenov D.V., Aronov, P.A., Kuligina, E.V., et.al. Oligonucleosome DNA fragmentation of caspase 3 deficient MCF-7 cells in palmitate-induced apoptosis. Nucleosides Nucleotides Nucleic Acids. 2004; 23(6-7):831-6.
29. Gong, J., Traganos, F., & Darzynkiewicz, Z. A Selective Procedure for DNA extraction from Apoptotic Cells Applicable for Gel Electrophoresis and Flow Cytometry. Anal Biochem. 1994; 218: 314-319.

30. Nicoletti I., Migliorati, G., Pagliacci, M.C., et.al. A rapid and simple method for measuring thymocyte apoptosis by propidium iodide staining and flow cytometry. J. Immunol Methods 1991; 139:271-279.
31. DiPaola, R.S. To Arrest or Not to G2-M Cell Cycle Arrest. Clin Cancer Res 2002; 8: 3311-3314.

Chapter 7

Investigation of specific gene expression

A. Introduction

Alterations of various cell signaling pathways can result in dysregulation of apoptosis and lead to cancer and neurodegenerative diseases (1-5). The p53 tumor suppressor gene is a transcription factor that regulates the cell cycle and is the most widely mutated gene in human tumorigenesis (4-13). The critical role of p53 is evident by the fact that it is mutated in over 50% of all human cancers (4-13). In fact, the selective binding of HDACs may involve pathways where p53 mediate repression of transcription (Figure 1; 6, 12, 13). For example, the levels of cell death by apoptosis that is induced by the fatty acid HDACi, sodium butyrate, is greatly reduced in the absence of p53 (6); whereas the hydroxamates, TSA and SAHA, can induce cell death by apoptosis in either a p53-dependent or a p53-independent manner (5-7, 9). Thus, it will be enlightening to evaluate if tropolone-mediated growth inhibition involves a p53-dependent pathway.

Cyclin-dependent kinases (CDKs) are a family of serine/threonine kinases that rely on associated cyclin proteins to execute the various steps of the cell cycle (1, 2, 14). CDK activity is regulated through posttranslational modifications

136

and subcellular translocations of specific CDK inhibitors (CDKIs), which are
organized in two families, INK4 and Cip/Kip (1, 2).
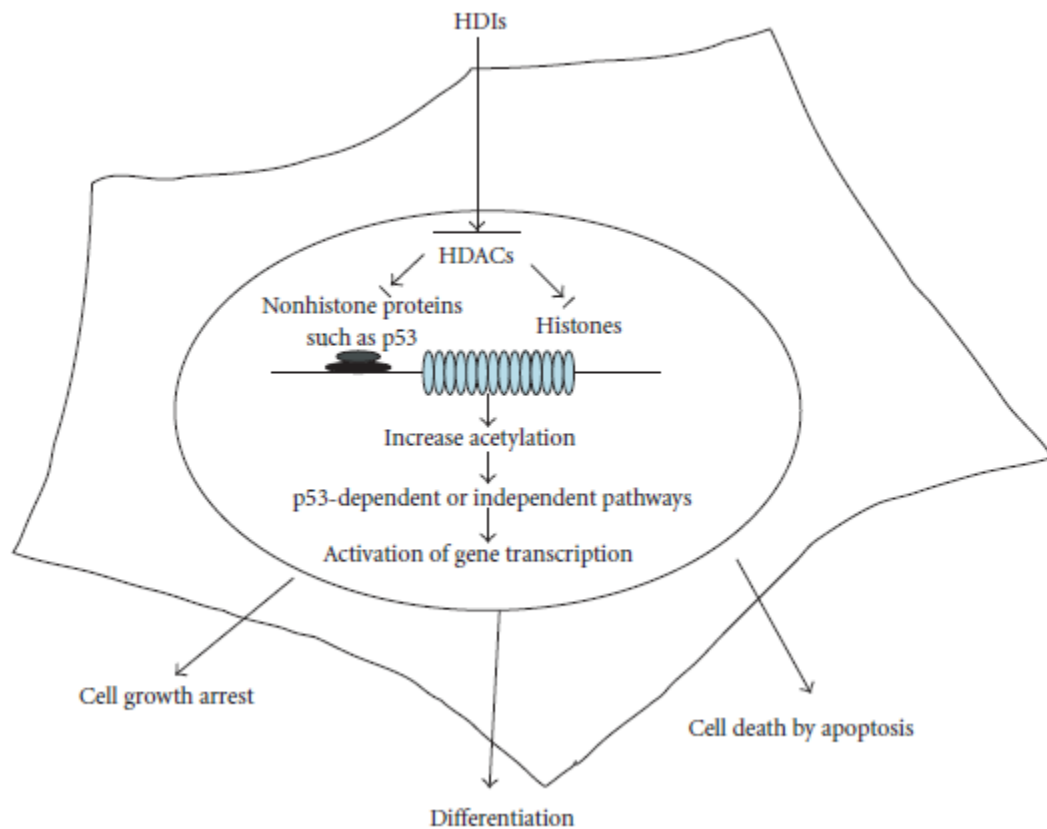
Figure 1: Schematic representation of the mechanism of action of HDAC inhibitors (HDI, HDACi; 6)

The INK4 family (inhibitors of cyclin D-dependent kinases) consists of four members: $p16^{INK4A}$, $p15^{INK4B}$, $p18^{INK4C}$ and $p19^{INK4D}$, and the Cip/Kip family (inhibitors of cyclin D-, cyclin E-, and cyclin A-dependent kinases) comprises $p21^{Cip1}$ (also known as $p21^{Waf1}$), $p27^{Kip1}$ and $p57^{Kip2}$ (1, 2). The overexpression of

137

CDKI such as p21$^{CIP1/WAF1}$ through histone hyperacetylation is well demonstrated as one of the molecular mechanisms for anti-cancer effect of HDACi (6, 8, 11-33). The natural product, hinokitiol (compound 10), has been reported to arrest the G1 phase of the cell cycle in malignant melanoma cells presumably as a result of p27 activation (34). Furthermore, p15 and other INK4 proteins are implicated in early to mid-stage G1 whereas p21 and p27 act broadly on all stages of the cell cycle (2). Therefore, we will explore the ability of tropolones to suppress tumor growth via specific gene expression of p15^{INK4B}, p21$^{CIP1/WAF1}$ and p27^{KIP1} in Jurkat and HuT-78 cells, the two cell lines that are the most sensitive to tropolone-mediated growth inhibition. Results garnered from evaluation of specific gene expression will lend support to cell cycle analysis data (Chapter 6) and further illuminate the mechanisms of action of tropolones as HDACi.

We evaluated specific gene expression via FACS analysis by sequentially incubating treated cells with primary antibodies for p53, p21, or p27 followed by treatment with secondary antibodies conjugated with a fluorescein isothiocyanate (34-38). We determined values for geometric mean fluorescence intensities (GMFI), equivalent to the median cell population response, for each cell treatment with the aid of the FlowJo Workstation (36-38). Assays were performed at multiple time points and/or multiple concentrations when possible. We compared our data with published reports for specific gene expression for the experimental control, SAHA, when possible (6, 15, 20, 21, 33). Detailed experimental methods are in Section I of the Materials and Methods chapter.

With the exception of the 24h time-point for the Jurkat cells, corresponding histograms for evaluation of specific gene expression are in sections 23-36 of the Appendix.

B. Elucidation of p53 expression in Jurkat cells

The tumor suppressor p53 belongs to a family of structurally and functionally related transcription factors, including p73 and p63 (10). Diverse cellular stresses, genotoxic stresses, and many anticancer agents can activate p53 activity that consequently stimulates the transcription of many genes that are involved in cell cycle regulation and apoptosis (2, 10). The mechanisms of action of many HDACi may either be p53-dependent or p53-independent (6, 12). Hence, we evaluated activation of p53 in Jurkat cells after a 12h treatment with 10 µM HDACi via flow cytometric analysis (Table 1). We observed that the values for geometric mean fluorescence intensities (GMFI) for the tropolones and SAHA were within the same threshold of the untreated control. Given that there was no significant overexpression of p53 protein levels following treatment, our results suggest that tropolones may mediate growth inhibition in Jurkat cells in a p53-independent manner. However, further investigation at multiple time points and in multiple cell lines may be needed to validate our data since HDACi have been reported to act uniquely in different cell lines (6, 7, 11, 12, 15, 23-25, 27-30).

139

Table 1: Elucidation of p53 expression in Jurkat cells after a 12h treatment with 10 µM HDACi										
Treatment (p53, 12h)	**GMFI in HuT-78 cells**									
	Control	SAHA	2	5	7	9	10	11	13	14
	4.22	3.92	4.39	4.34	3.34	3.37	3.48	5.13	3.65	3.92

C. Comparative analysis of p15 expression in Jurkat and HuT-78 cells

The INK4 family of CDKIs consists of four members, $p16^{INK4A}$, $p15^{INK4B}$, $p18^{INK4C}$ and $p19^{INK4D}$ (2); these CDKI are targeted specifically to the CDK4 and CDK6 complexes and as a result are active in the early and mid-G1 phase of the cell cycle (2). Based on our cell cycle analyses data (Chapter 6), we investigated the activation of $p15^{INK4b}$ primary antibodies in Jurkat and HuT-78 cells following a 24h treatment with 10 µM and 50 µM tropolones correspondingly via FACS analysis (Table 2). 10 µM SAHA served as experimental control and we did not evaluate 50 µM SAHA due to excessive cell death. We observed that activation of p15 antibodies were within the same range for the tropolones and the untreated control for both the 10 µM and 50 µM treatments in Jurkat cells. For example, 10 µM and 50 µM treatments of compound 2 resulted in GMFI values of 2.27 and 2.38 respectively whereas the untreated control had a GMFI value of 2.21. Concurrently, SAHA treatment

140

resulted in a slightly higher increase in p15 activation in Jurkat cells (GMFI=3.43).

We also observed similar trends in HuT-78 cells; SAHA treatment resulted in a slightly higher increase in p15 activation (GMFI of 28.00 vs. 17.00 in the untreated control). Compound 12 was the only tropolone that showed a notable increase in p15 activation at a higher concentration resulting in more than two-fold increase in p15 activation at 50 μM when compared to the 10 μM treatment that was essentially the same as the untreated control (GMFI = 17.90). These results suggest that activation of p15^{INK4B} may not be a mechanism for tropolone-mediated growth inhibition for Jurkat and HuT-78 cells but it is possible that other INK4 proteins may be implicated by the tropolones.

Treatment	Jurkat			HuT-78	
	p15^{INK4B}, GMFI (24h)				
	10 µM	50 µM		10 µM	50 µM
Control	2.21			17.00	
SAHA	3.43	N.D.		28.00	N.D.
Compound 2	2.27	2.38		19.40	18.20
Compound 3	2.25	2.82		17.50	19.40
Compound 5	2.65	N.D.		15.30	N.D.
Compound 7	2.28	2.68		17.30	20.60
Compound 9	2.65	N.D.		17.30	N.D.
Compound 10	1.90	2.62		17.70	18.60
Compound 11	2.23	2.35		15.60	17.10
Compound 12	2.51	2.46		17.90	38.10
Compound 13	2.34	2.43		14.70	17.10
Compound 14	2.39	2.35		14.30	18.00

Table 2: Comparative analysis of p15 activation in Jurkat and HuT-78 cells. **Note:** N.D. = Not determined.

D. Elucidation of p27 activation in Jurkat and HuT-78 cells

The three broad-spectrum CDKI, p21$^{CIP1/WAF1}$, p27^{KIP1} and p57^{KIP2} are known to act at all stages of the cell cycle and inhibit all of the cyclin-CDK complexes that form at later stages of the cell cycle (2). While relatively little is known about p57, p21 and p27 function similarly but p27 expression is unique in

its own way and has been shown to be implicated in HDAC inhibition (20, 34, 40); moreover, p27 is reported to be available in high concentrations in the G0 quiescent stage (2). Given these observations and our cell cycle analyses data, we conducted an initial assessment of p27 activation in HuT-78 cells after a 12h treatment with 10 µM HDACi via FACS analysis.

With the exception of compounds 2 and 8, the HDACi activated p27 levels within the same threshold as the untreated control; compound 2 had a notably lower GMFI (8.25 vs. 24.40 in the untreated control) whereas compound 9 had the highest GMFI of all the compounds (31.80). These results suggest that p27 activation may not be implicated in tropolone-mediated cell cycle arrest after a 12h treatment with 10 µM in HuT-78 cells.

Table 3: Initial assessment of p27 activation in HuT-78 cells after a **12h** treatment with 10 µM HDACi										
	GMFI in HuT-78 cells									
Treatment	Control	SAHA	2	5	7	9	10	11	13	14
(p27, 12h)	24.40	20.30	8.25	20.60	20.20	31.80	20.10	25.00	22.90	20.80

Alternatively, we evaluated p27 activation in Jurkat cells after 12h and 24h treatments with the tropolones in Jurkat cells (Table 4). 10 µM treatments of SAHA, compound 2 and compound 7 did not exert any overexpression of p27

143

when compared to the untreated control after a 12h treatment. However, after a 24h treatment period, 10 µM treatments of SAHA, compound 2 and compound 7 resulted in slightly higher expression levels of p27 but still resulting in less than a two-fold difference when compared to the untreated control.

Treatment	Jurkat	
	p27^{KiP1}, GMFI	
	12h	24h
Control	10.10	7.76
10 µM SAHA	5.57	8.64
10 µM Compound 2	6.14	9.18
50 µM Compound 2	ND	12.10
10 µM Compound 7	8.87	9.47
50 µM Compound 7	ND	8.58

Table 4: Time-dependent analysis of p27 activation in Jurkat cells treated with HDACi. **Note:** ND=Not determined.

Interestingly, treatment with 50 µM of compound 2 resulted in the most significant overexpression of all treatments (12.10 vs. 7.76 in the untreated control) whereas 50 µM of compound 7 actually resulted in a lower activation of p27 when compared to the corresponding 10 µM treatment (8.58 vs. 9.47). This observation may be due to the fact that compound 7 is more cytotoxic in Jurkat cells than compound 2 (GI_{50} of 0.67 µM vs. 3.33 µM) thus the 50 µM treatment

144

with compound 7 may have resulted in more cell death leading to a lower number of intact cells to respond to the p27 treatment.

Given that there was no significant overexpresssion of p27 at either 12h or 24h treatment periods or with either 10 µM or 50 µM treatments of the tropolones, it may be deduced that p27 may not be implicated in tropolone-mediated growth inhibition and cell cycle arrest in Jurkat and HuT-78 cells. However, studies in human malignant melanoma cells have shown that 80 µM of the natural product, hinokitiol (compound 10), activated p27 expression after a 24h treatment (34). Therefore, it is possible that a higher concentration of the tropolones may result in increased p27 expression in Jurkat and HuT-78 cells; but given the high potency of the tropolones in both cell lines, a higer concentration may also result in excessive cell death that will result in a decreased amount of intact cells that respond to antibody treatments.

E. Investigation of p21 overexpression in Jurkat and HuT-78 cells

The p21 gene is a repressor complex, tightly controlled by the tumor suppressor protein p53, which inhibits cell cycle progression by blocking CDK activity and arresting the cell cycle in G1 phase (2, 4-6, 8, 11-13, 29). Expression profiling studies have shown that treatment of HDACi alters the expression of approximately 2% to 10% of cellular genes including the up-regulation of histones, tubulins, and the CDKI, p21$^{CIP1/WAF1}$ (6, 8, 11-13, 15, 21, 23, 28-30, 41-43). In fact, p21 is one of the most commonly induced genes by

145

HDACi and HDACi-mediated expression of p21 is correlated with an increase in the acetylation of histones associated with the p21 promoter region (15, 20, 28). For example, the p21 gene promoter has been shown to be a direct target for SAHA in ARP-1 human multiple myeloma cells but SAHA treatment did not concurrently alter p27 expression levels once again indicating that both pan-CDKI have unique functions within cells (15, 20, 28). Therefore, we conducted comprehensive analyses of p21 overexpression in Jurkat and HuT-78 cells via FACS studies.

Our initial assessment of p21 activation in Jurkat cells was conducted after a 12h treatment with 10 μM HDACi (Table 5). We found that SAHA and the tropolones exerted p21 expression within the same threshold as the untreated control. For example, the natural product (compound 10) exerted the most significant expression among all HDACi (GMFI = 5.30 vs. 4.62 in the untreated control and 5.18 in SAHA). The results of the preliminary assessment warranted further investigation of p21 activation by the tropolones in Jurkat cells.

Table 5: Initial assessment of p21 activation in Jurkat cells after a **12h** treatment with 10 μM HDACi

	GMFI in Jurkat cells									
Treatment	Control	SAHA	2	5	7	9	10	11	13	14
(p21, 12h)	4.62	5.18	4.75	4.06	4.91	4.09	5.30	2.47	4.72	3.03

146

Based on our initial 12h assessment, we hypothesized that a longer treatment period and/or a higher concentration of the tropolones may be required in order to induce notable effects in p21 expression in the two hematological cell lines. Therefore, we conducted an investigation of p21 overexpression at after a 24h treatment with 10 µM and 50 µM concentrations of the tropolones in Jurkat and HuT-78 cell lines (Table 6; Figure 2). After a 24h period, SAHA treatment resulted in a three-fold increase in expression levels of p21 whereas the tropolones were either slightly higher or lower than the untreated controls at both 10 µM and 50 µM treatments in Jurkat cells. Once again, compound 10 exerted the most significant effect (2.52 vs. 1.35 in the untreated control) at a 10 µM concentration whereas compound 2 exerted the most significant effect (2.53 vs. 1.57 in the untreated control) at a 50 µM concentration in Jurkat cells.

On the other hand, SAHA treatment resulted in more than a two-fold increase in p21 expression levels whereas the tropolones were around the same range as the untreated control in HuT-78 cells. For example, compound 13 induced the most significant effect (32.30 vs. 21.80 in the untreated control) at a 10 µM concentration whereas compound 2 induced the most significant effect (2.53 vs.1.57 in the untreated control) at a 50 µM concentration in Jurkat cells.

Treatment	Jurkat		HuT-78	
	Table 6: Comparative analysis of p21 activation in Jurkat and HuT-78 cells. **Note**: ND = Not determined.			

Treatment	Jurkat		HuT-78	
	$p21^{Cip1/WAF1}$ GMFI (24h)			
	10 µM	**50 µM**	**10 µM**	**50 µM**
Control	1.35	1.57	21.8	
SAHA	4.03	ND	53.20	ND
Compound 2	2.26	2.53	21.50	39.50
Compound 3	2.42	2.42	ND	34.30
Compound 5	2.41	ND	26.70	ND
Compound 7	1.67	1.87	21.80	26.20
Compound 9	1.44	ND	23.90	ND
Compound 10	2.52	2.03	21.70	29.10
Compound 11	1.16	1.52	22.40	20.40
Compound 12	ND	1.84	ND	26.70
Compound 13	2.01	1.85	32.30	29.60
Compound 14	1.39	1.86	23.20	23.90

Figure 2: Evaluation of p21 expression in Jurkat cells after a **24h** treatment with **10** µM HDACi. **Note:** Untreated control for pertinent HDACi treatments represented in red and HDACi represented in blue on the corresponding histograms.

a)   SAHA
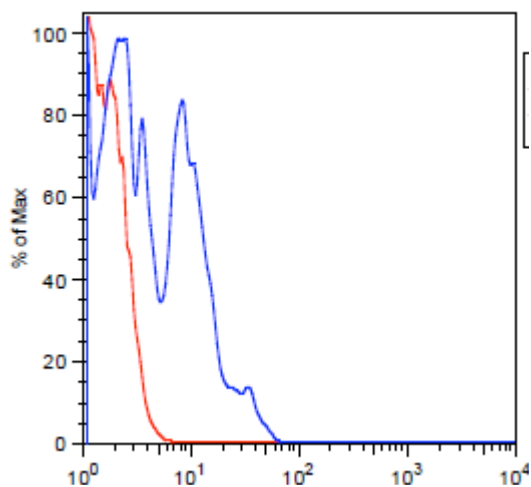
b)   Compound 2
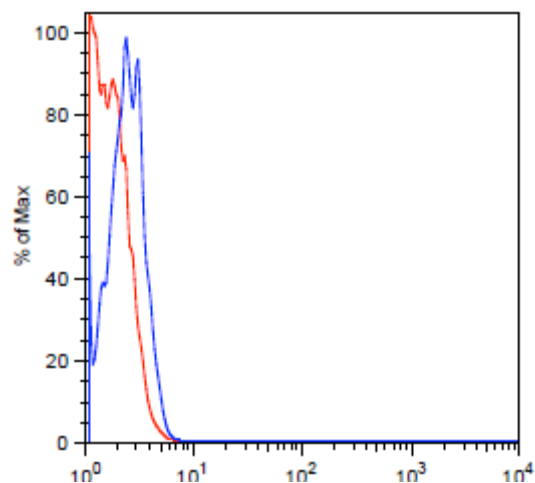
c)   Compound 5

d)   Compound 7

e)   Compound 9

f)   Compound 10

g)   Compound 11

h)   Compound 13

150
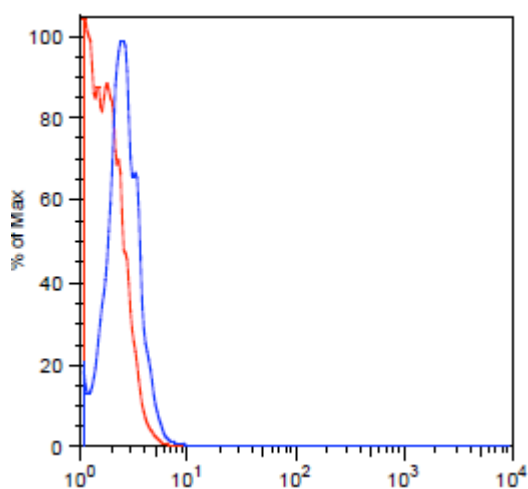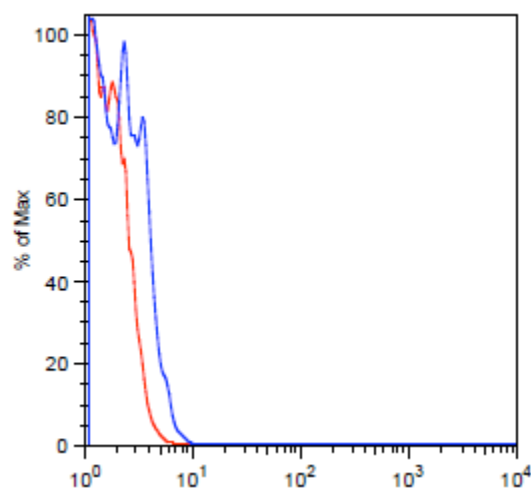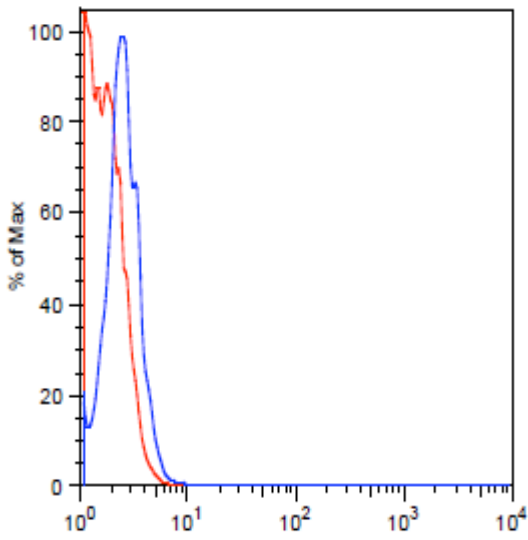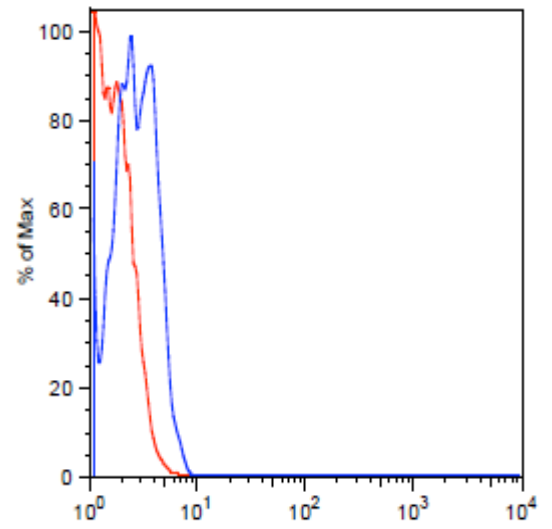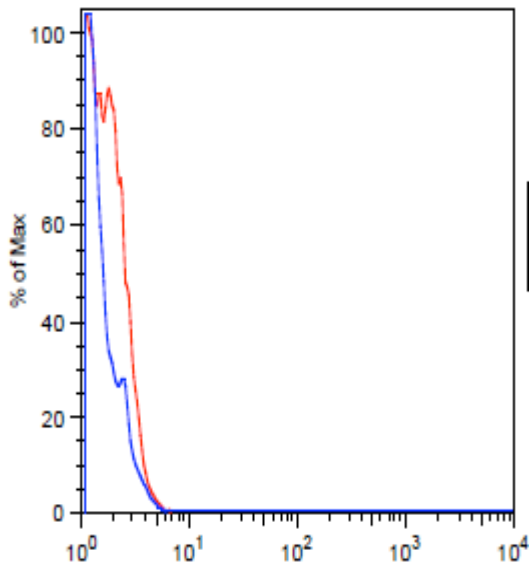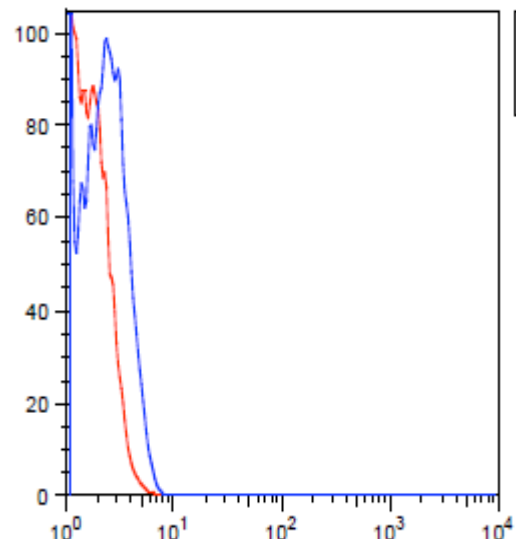
i) Compound 14
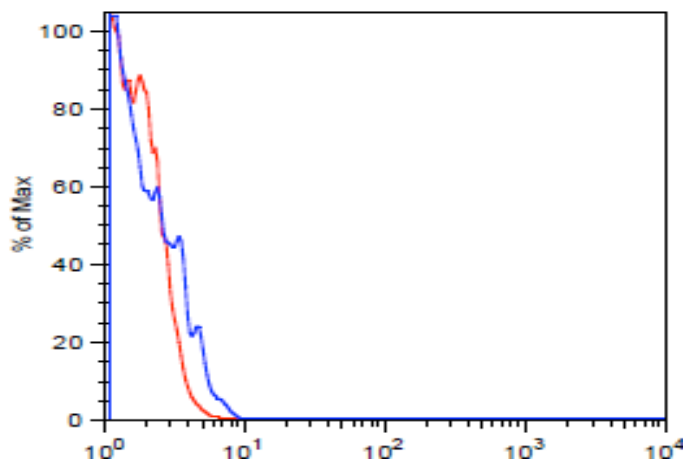
F. Comparative analysis of gene expression via qRT-PCR analysis in Jurkat cells

We followed up our FACS studies on p21 expression in Jurkat cells with quantitative real-time polymerase chain reaction (qRT-PCR). Reverse-transcription polymerase chain reaction (RT-PCR) assays are considered the most common method for characterizing and confirming gene expression patterns, and also for comparing the levels of mRNA in different sample populations (44). Quantitative real-time PCR is often used to further validate RT-PCR protocols through the use of a standardized primer and internal competitor template sets for each target gene (44). Therefore, following a 24h treatment with 10 µM concentrations of both SAHA and compound 2 in Jurkat cells, we conducted RT-PCR and qRT-PCR using methods that are detailed in Section J

of the Materials and Methods chapter (45-47). Assay was performed in triplicate and we compared our p21 data to published reports for our experimental control, SAHA (33). Standard deviation values are reported in the Appendix, section 36.

We evaluated the relative gene expression levels of HDAC2, p21 and the vitamin D receptor (VDR). Clinical studies have shown a correlation between low levels of vitamin D in patients with lymphomas and increased mortality thus prompting our interest in evaluating tropolone-mediated VDR expression (48). Our results are highlighted in table 7 and in Figure 2.

Table 7: Elucidation of relative expression of specific genes after a 24h treatment with 10 µM HDACi in Jurkat cells			
Treatment	**Relative Gene Expression**		
	HDAC2	p21	VDR
Control	1.00	1.00	1.00
Compound 2	0.86	0.95	0.58
SAHA	1.10	328.23	82.54

Figure 3: Elucidation of relative expression of specific genes after a 24h treatment of compound 2 in Jurkat cells
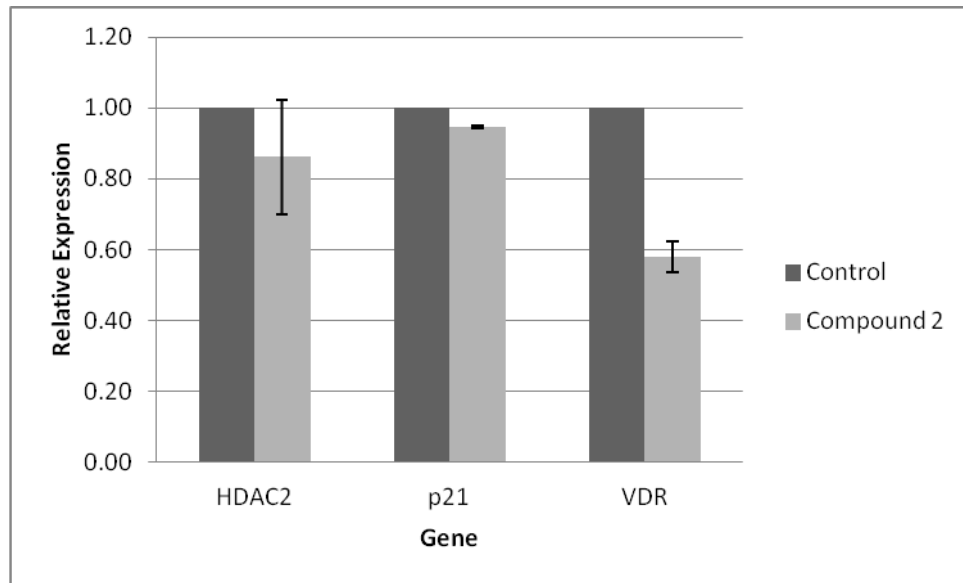
Similar to our flow cytometric data, we found that compound 2 induced gene expression levels of p21 around the same threshold as the untreated control. Even though HDAC2 expression was also around the same range as the untreated control, there was down-regulation of VDR gene expression levels by compound 2. Alternatively, SAHA significantly overexpressed p21 and VDR gene levels but HDAC2 levels were about the same when compared to either compound 2 or the untreated control. Our data suggests that p21 activation may not be a mechanism for tropolone-mediated growth inhibition; furthermore, overexpression of VDR and HDAC2 may not be involved in the mechanisms of action of tropolones. It may be plausible that the inability of the tropolones to

153

inhibit HDAC1 may hinder p21 activation since it has been reported that SAHA treatment in multiple myeloma cells resulted in a marked decrease in HDAC1 expression and a significant overexpression of p21 (20, 21, 28). Moreover, gene knockdown studies in human malignant melanoma cells have shown that p21 is not required for the induction of cell cycle arrest by hinokitiol, compound 10 (34). Furthermore, our preliminary assessment of gene expression highly suggests that there is a distinct need for comprehensive gene studies via microarray analysis in normal and mutant Jurkat and/or HuT-78 cells or even in animal models in order to more distinctly appraise genes that are altered as a result of tropolone treatment (49). Based on our enzyme inhibition data (Chapter 3), mutant hematological cells may either be deficient of or overexpressed with HDAC2 or HDAC8 thus serving as further proof of concept for our claim on the isoform-selective nature of HDAC inhibition by the tropolones.

G. Conclusions

Elucidation of specific gene expression is critical in understanding the molecular mechanisms of tropolones as HDACi. Selective binding of HDACs may involve pathways where p53 mediate repression of transcription. Furthermore, overexpression of CDKIs such as $p21^{CIP1/WAF1}$ is well demonstrated as one of the molecular mechanisms for anti-cancer effects of HDACi. Our results indicate that tropolone-mediated growth inhibition may involve a p53-independent pathway in Jurkat cells. Furthermore, preliminary evaluation of the overexpression of CDKIs

154

that play active roles at early to mid-stage G1 (p15^{INK4B}), as well as broad-spectrum CDKIs (p21$^{CIP1/WAF1}$ and p27^{KIP1}) did not reveal any significant activation of these proteins at the assayed concentrations and timepoints in Jurkat and HuT-78 cells. However, compound 13 at a 50 µM concentration was able to activate a two-fold increase of p15 after a 24h treatment in HuT-78 cells. qRT-PCR analysis of p21 expression in Jurkat cells was also used to validate our flow cytometric data. Based on published studies, we hypothesize that the inability of the tropolones to overexpress p21 in may be due to lack of HDAC1 inhibition. These preliminary assessments highly suggest that there is a need for a more comprehensive analysis of tropolone-mediated gene expression in normal and mutant Jurkat or HuT-78 cells via microarray analysis in order to more precisely determine altered genes.

H. References

1. Currais, A., Hortobágyi, T., & Salvador, S. The neuronal cell cycle as a mechanism of pathogenesis in Alzheimer's disease. Aging (Albany NY) 2009; 1(4): 363–371.
2. Weinberg, R. The Biology of Cancer. New York, NY: Garland Science, Taylor & Francis Group, LLC., 2007.
3. Elmore, S. Apoptosis: A Review of Programmed Cell Death. Toxicol Pathol. 2007: 35 (4): 495-516.
4. Wang X.W., & Harris, C.C. p53 tumor-suppressor gene: clues to molecular carcinogenesis. J Cell Physiol. 1997;173 (2):247-55.
5. Davies, C., Hogarth, L.A., Dietrich, P.A., et. al. p53-independent epigenetic repression of the p21(WAF1) gene in T-cell acute lymphoblastic leukemia. J Biol Chem. 2011; 286(43): 37639–37650.
6. Ouaissi, M., & Ouaissi, A. Histone deacetylase enzymes as potential drug targets in cancer and parasitic diseases.J Biomed Biotechnol. 2006; 2006(2):13474.

7. Knutson, A.K., Welsh, J., Taylor, T., et.al. Comparative effects of histone deacetylase inhibitors on p53 target gene expression, cell cycle and apoptosis in MCF-7 breast cancer cells. Oncol Rep. 2012; 27(3):849-53.

8. Ouaissi, M., Giger, U., Sielezneff, I., et al. Rationale for possible targeting of histone deacetylase signaling in cancer diseases with a special reference to pancreatic cancer. J Biomed Biotechnol. 2011: 315939.

9. Bajbouj, K., Mawrin, C., Hartig, R., et.al. P53-dependent antiproliferative and pro-apoptotic effects of trichostatin A (TSA) in glioblastoma cells. J Neurooncol. 2012; 107(3):503-16.

10. Nieto-Rementería, N., Pérez-Yarza, G., Boyano, M.D., et. al. Bexarotene activates the p53/p73 pathway in human cutaneous T-cell lymphoma. Br J Dermatol. 2009; 160(3):519-26.

11. Ouaissi, M., Cabral, S., Tavares, J., et al. Histone deacetylase (HDAC) encoding gene expression in pancreatic cancer cell lines and cell sensitivity to HDAC inhibitors. Cancer Biol Ther. 2008; 7(4): 523-531.

12. Singh, B.N., Zhang, G., Hwa, Y.L., et. al. Nonhistone protein acetylation as cancer therapy targets. Expert Rev Anticancer Ther. 2010; 10(6): 935–954.

13. Dickinson, M., Johnstone, R.W., & Prince, H.M. Histone deacetylase inhibitors: potential targets responsible for their anti-cancer effect. Invest New Drugs. 2010; 28 Suppl 1:S3-20.

14. Xiong, Y., Hannon, G.J., & Zhang, H. p21 is a universal inhibitor of cyclin kinases. Nature. 1993; 366(6456):701-4.

15. Wozniak, M.B., Villuendas, R., Bischoff, J.R., et.al. Vorinostat interferes with the signaling transduction pathway of T-cell receptor and synergizes with phosphoinositide-3 kinase inhibitors in cutaneous T-cell lymphoma.

16. Schrump, D.S. Cytotoxicity Mediated by Histone Deacetylase Inhibitors in Cancer Cells: Mechanisms and Potential Clinical Implications. Clin. Cancer. Res 2009; 15: 3947-3957.

17. Han, J., Ahn, S., Park, S. et. al. Apicidin, a histone deacetylase inhibitor, inhibits proliferation of tumor cells via induction of p21WAF1/Cip1 and gelsolin. Cancer Res. 2000; 60 (21): 6068–6074.

18. Han, J.W., Ahn, S.H., Kim, Y.K., et. al. Activation of p21(WAF1/Cip1) transcription through Sp1 sites by histone deacetylase inhibitor apicidin: involvement of protein kinase C. J Biol Chem. 2001 ;276(45):42084-90.

19. Hrzenjak, A., Moinfar, F., Kremser, M.L., et al. Histone deacetylase inhibitor vorinostat suppresses the growth of uterine sarcomas in vitro and in vivo. Mol Cancer. 2010; 9: 49.

20. Gui, C-Y., Ngo, L., Xu, W.S., et. al. Histone deacetylase (HDAC) inhibitor activation of p21WAF1 involves changes in promoter-associated proteins, including HDAC1. Proc. Natl. Acad. Sci. USA 2004; 101:1241-1246.

21. Richon, V.M., Sandhoff, T.W., Rifkind, R.A., et. al. Histone deacetylase inhibitor selectively induces p21^{WAF1} expression and gene-associated histone acetylation.

Proc Natl Acad Sci U S A. 2000; 97(18): 10014–10019.

22. Vinodhkumar, R., Song, Y-S., & Devaki, T. Romidepsin (depsipeptide) induced cell cycle arrest, apoptosis and histone hyperacetylation in lung carcinoma cells (A549) are associated with increase in p21 and hypophosphorylated retinoblastoma proteins expression. Biomed Pharmacother. 2008; 62(2):85-93.

23. Marks, P., Rifkind, R.A., Richon, V.M., et. al. Histone deacetylases and cancer: causes and therapies. Nat Rev Cancer. 2001;1(3):194-202.

24. Noureen, N., H. Rashid, & Kalsoom, S. Identification of type-specific anticancer histone deacetylase inhibitors: road to success. Cancer Chemother Pharmacol. 2010; 66(4):625-33.

25. Paris, M., Porcelloni, M., Binaschi, M., et al. Histone deacetylase inhibitors: from bench to clinic. J Med Chem 2008; 51(6): 1505-29.

26. Zhou, Q., Dalgard, C.L., Wynder, C., et. al. Histone deacetylase inhibitors SAHA and sodium butyrate block G1-to-S cell cycle progression in neurosphere formation by adult subventricular cells. BMC Neurosci. 2011;12:50.

27. Blagosklonny, M., Robey, R., Sackett, D., et al. Histone deacetylase inhibitors all induce p21 but differentially cause tubulin acetylation, mitotic arrest and cytotoxicity. Mol. Cancer Ther. 2002; 1 (11): 937–941.

28. Marks, P.A. & Dokmanovic, M. Histone deacetylase inhibitors: discovery and development as anticancer agents. Expert Opin Investig Drugs 2005; 14(12): 1497-511.

29. Kim, N.H., Kim, S.N., & Kim, Y.K. Involvement of HDAC1 in E-cadherin expression in prostate cancer cells; its implication for cell motility and invasion. Biochem Biophys Res Commun. 2011; 404(4):915-21.

30. Cao, Z.A., Bass, K.E., Balasubramanian, S., et al. CRA-026440: a potent, broad-spectrum, hydroxamic histone deacetylase inhibitor with antiproliferative and antiangiogenic activity in vitro and in vivo. Mol Cancer Ther, 2006; 5(7): 1693-701.

31. Hagelkruys, A., Sawicka, A., Rennmayr, M., et.al. The biology of HDAC in cancer: the nuclear and epigenetic components. Handb Exp. Pharmacol. 2011; 206: 13-37.

32. Butler, L.M., Agus, D.B., Scher, H.I., et al. Suberoylanilide hydroxamic acid, an inhibitor of histone deacetylase, suppresses the growth of prostate cancer cells in vitro and in vivo. Cancer Res, 2000; 60(18): 5165-70.

33. Almenara J, Rosato R, & Grant S. Synergistic induction of mitochondrial damage and apoptosis in human leukemia cells by flavopiridol and the histone deacetylase inhibitor suberoylanilide hydroxamic acid (SAHA). Leukemia. 2002; 16(7):1331-43.

34. Liu, S., & Yamauchi, H. p27-Associated G1 arrest induced by hinokitiol in human malignant melanoma cells is mediated via down-regulation of pRb,

Skp2 ubiquitin ligase, and impairment of Cdk2 function. Cancer Lett 2009; 286(2): 240-9.

35. Morales, J.C., Ruiz-Magana, M.J., Carranza, D., et. al. HDAC inhibitors with different gene regulation activities depend on the mitochondrial pathway for the sensitization of leukemic T cells to TRAIL-induced apoptosis. Cancer Lett. 2010 ;297(1):91-100.

36. Verma, R., Rigatti, M.J., Belinsky, G.S., et. al. DNA damage response to the Mdm2 inhibitor nutlin-3. Biochem Pharmacol. 2010 ;79(4):565-74.

37. Yale School of Medicine. Introduction to Flow Cytometry: A Learning Guide. Retrieved from:
http://medicine.yale.edu/labmed/cellsorter/start/411_66019_Introduction.pdf

38. Herzenberg, L.A., Tung, J., Moore, W.A., et. al. Interpreting flow cytometry data: a guide for the perplexed. Nat Immunol. 2006; 7(7):681-5.

39. Qu, C.X., Wang, J.Z., Wan, W.H., et.al. Establishment of a flow cytometric assay for determination of human platelet glycoprotein VI based on a mouse polyclonal antibody. J Clin Lab Anal. 2006; 20(6):250-4.

40. Noonan, E.J., Place, R.F., Pookot, D., et al. miR-449a targets HDAC-1 and induces growth arrest in prostate cancer. Oncogene, 2009; 28(14): 1714-24.

41. Furumai, R., Matsuyama, A., Kobashi, N., et al. FK228 (depsipeptide) as a natural prodrug that inhibits class I histone deacetylases. Cancer Res, 2002; 62(17): 4916-21.

42. Vigushin, D.M., Ali, S., Pace, P.E., et al. Trichostatin A is a histone deacetylase inhibitor with potent antitumor activity against breast cancer in vivo. Clin Cancer Res, 2001; 7(4): 971-6.

43. Tong, X., Joshi, S., Rosenberg, D.W., et.al. Cyclooxygenase-2 regulation in colon cancer cells: modulation of RNA polymerase II elongation by histone deacetylase inhibitors. J Biol Chem. 2005; 280(16):15503-9.

44. Bustin, S.A. Quantification of mRNA using real-time reverse transcription PCR (RT-PCR): trends and problems. Journal of Molecular Endocrinology 2002; 29: 23–39.

45. Lee, J-H., Jeong, E-G., Choi, M-C., et.al. Inhibition of Histone Deacetylase 10 Induces Thioredoxin-Interaction Protein and Causes Accumulation of Reactive Oxygen Species in SNU-620 Human Gastric Cancer Cells, 2010; Mol. Cells 30: 107-112.

46. Spurling, C.C., Godman, C.A., Noonan, E.J., et. al. HDAC3 Overexpression and Colon Cancer Cell Proliferation and Differentiation, Mol. Carc. 2008; 43: 137-147.

47. Godman, C.A., Joshi, R., Tierney, B.R., et.al. HDAC3 impacts multiple oncogenic pathways in colon cancer cells with effects on Wnt and vitamin D signaling. Cancer Biol. & Ther. 2008; 7 (10): 1570-1580.

48. Miller, K. Vitamin D may boost lymphoma survival. Retrieved from http://www.webmd.com/cancer/non-hodgkins-lymphoma/news/20091207/vitamin-d-may-boost-lymhoma-survival

49. Khleif, S.N., & Curt, G.A. Animal Models in Developmental Therapeutics. In: Bast R.C. Jr., Kufe, D.W., Pollock, R.E., et al., editors. Holland-Frei Cancer Medicine. 5th edition. Hamilton (ON): B.C. Decker; 2000. Chapter 42. Retrieved from: http://www.ncbi.nlm.nih.gov/books/NBK20822/

Chapter 8

Investigation of the induction and mechanisms of cell death by apoptosis

A. Introduction

The process of apoptosis, otherwise known as programmed cell death, is an important component of several physiological processes including normal cell turnover that involves the genetically determined elimination of cells (1-3). Defects in the regulation of apoptosis are implicated in many diseases including neurodegenerative diseases, ischemic damage, autoimmune disorders and many types of cancer (2, 3). In the last decade, significant attention has been focused on the exploitation of apoptosis as a novel and promising strategy for cancer chemoprevention and chemotherapy (1-3). Structurally diverse HDAC inhibitors have been shown to induce apoptosis in several human malignant cells (4-60). The natural product, hinokitiol (compound 10), has also been shown to induce apoptosis in human prostate cancer cells (61). The induction of apoptosis is distinguished by specific morphological and biochemical events, including exposure of phosphatidylserine (PS) on the outer leaflet of the plasma membrane as well as the activation of cysteine aspartic acid-specific protease (caspases) (1-7, 62-65).

There are two major mechanisms of apoptosis that are highly complex and involve an energy-dependent cascade of molecular events (2, 3, 9-12).

These two pathways are the extrinsic or death receptor pathway and the intrinsic or mitochondrial pathway; both pathways are linked and influence each other (Figure 1). Recent evidence shows that there is an additional pathway that involves T-cell mediated cytotoxicity and perforin-granzyme dependent killing of the cell (2, 3). The extrinsic, intrinsic, and granzyme B pathways converge on the same terminal, or execution pathway that is initiated by the cleavage of caspase-3 resulting in significant apoptotic events such as DNA fragmentation (2).

Figure 1: Schematic representation of apoptotic events (2)
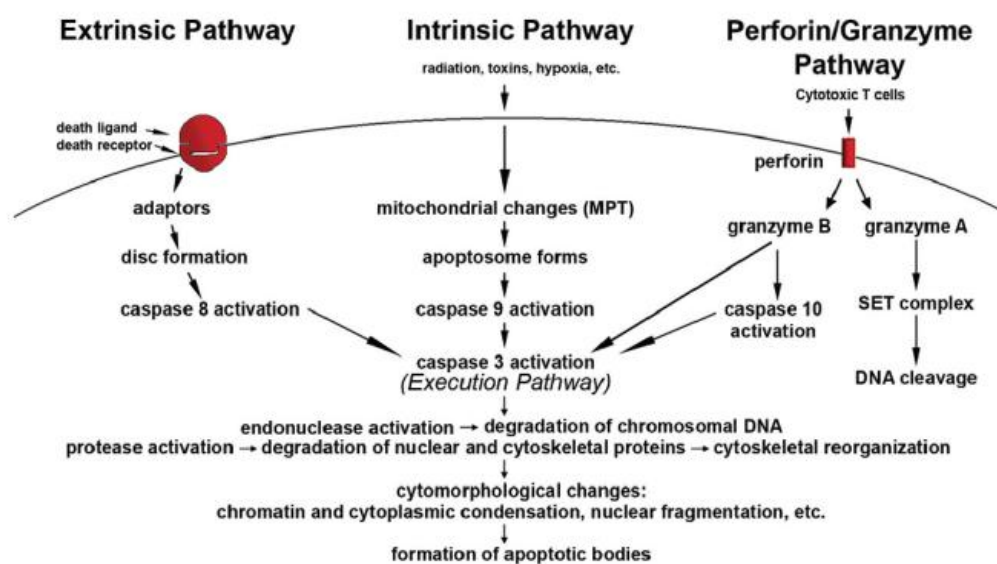
HDAC inhibition has been shown to upregulate the intrinsic apoptosis pathway via both the upregulation of proapoptotic proteins and downregulation

of anti-apoptotic proteins in the B-cell lymphoma 2 (Bcl-2) family (9-14, 16, 22, 24, 26- 28, 37, 40, 43, 49, 54, 57- 59). HDAC inhibition also induces elements of the extrinsic apoptotic pathway by increasing expression of death receptors, including Fas, tumor necrosis factor-α (TNF-α), and TNF-related apoptosis-inducing ligand (TRAIL) receptors (9, 14, 15, 17, 19, 22- 24, 26, 27, 49, 54, 57, 58). In fact, it has been reported that treatments with vorinostat results in upregulation of caspase-7 and caspase-9, key players in the intrinsic pathway of apoptosis, and downregulation of caspase-8, a key player in the extrinsic pathway (14, 37). Therefore, the purpose of this chapter is to investigate the ability of the tropolones to induce apoptosis and to explore the mechanisms of execution of apoptosis by the tropolones.

B. Elucidation of the induction of cell death by apoptosis

It is well established that cells lose their membrane phospholipids in the early stages of apoptosis and expose phosphatidylserine (PS) on the outer leaflet of the plasma membrane (2, 3, 5, 63-65). Conversely, an alternative to cell death by apoptosis is necrosis, which is a toxic process where cells passively follow an energy-independent mode of death resulting in interference with the energy supply of the cell as well as direct damage to cell membranes (1). Annexin V is a calcium-dependent phospholipid-binding protein with a high affinity for PS that is often used in conjugation with a fluorescein isothiocynanate (FITC) to label PS externalization (2, 60, 63-65). Given that AnnexinV complexed with FITC can

162

also label premature cell death by necrosis following the loss of membrane integrity, the simultaneous addition of propidium iodide that does not permeate cells with intact plasma cells allows for discrimination between intact cells and early apoptotic cells (60, 63, 65).

Based on cell line selective cytotoxicity data, the induction of cell death by apoptosis was evaluated by analyzing membrane phosphatidyl-serine (PS) exposure via flow cytometric analyses in Jurkat and HuT-78 cells because they were the two cell lines that are the most sensitive to inhibition by tropolones. Treated cells were analyzed for apoptosis with the aid of Annexin V and propidium iodide via flow cytometric analysis. Assays were performed at multiple time points and/or multiple concentrations when possible. We compared our results to published data on the induction of apoptosis by our experimental control, SAHA, lines when possible (59). Detailed methods for flow cytometric analysis are described in Section K of the Materials and Methods chapter. With the exception of the 24h time-point for the Jurkat cells, corresponding histograms for evaluation of specific gene expression are in sections 37 and 38 of the Appendix. With the aid of the FlowJo Workstation (Treestar Inc., USA), cells were identified as early apoptotic cells if they were Annexin V positive and PI negative; late apoptotic or necrotic cells were both Annexin V positive and PI positive whereas surviving cells were Annexin V negative and PI negative (5, 60, 63-65).

163

C. Initial assessment of the induction of apoptosis in Jurkat cells

Given our observations that an increase in the sub-diploid population of cells treated with tropolones, an index for apoptosis, was the most evident in Jurkat cells followed by the HuT-78 cells, our initial assessment of the induction of apoptosis was conducted in Jurkat cells. After a 20h treatment, 48.3% of SAHA-treated cells were undergoing early apoptosis compared to 25.6% in the untreated control. Both the alpha-substituted and the beta-substituted tropolones were able to induce an equivalent proportion of apoptosis in Jurkat cells (Table 1; Figure 2). For example, compound 2 and compound 7 with a phenyl at the alpha and beta positions respectively, induced early apoptosis in 34.6% and 35.8% of the Jurkat cells correspondingly. Similarly, compound 2 and compound 7 induced equivalent percentages of late stage apoptotic/necrotic cells (12.7% and 14.0% respectively).

Table 1: Analysis of the induction of apoptosis in Jurkat cells after a 20h treatment with 10 µM HDACi			
Treatment	% Intact cells	% Early Apoptotic cells	% Late Apoptotic/Necrotic cells
Control	63.4	**25.6**	11.0
SAHA	36.8	**48.3**	14.8
Compound 2	52.6	**34.6**	12.7
Compound 5	48.1	**36.8**	15.0
Compound 7	50.0	**35.8**	14.0
Compound 9	56.7	**30.6**	12.6
Compound 10	49.9	**35.0**	15.0
Compound 11	52.5	**31.4**	15.9
Compound 13	48.4	**35.8**	14.1

165

Figure 2: Analysis of the induction of apoptosis in Jurkat cells after a 20h incubation: y axis represents PI response whereas x axis represents Annexin V (AV) response. Quadrant 1 (bottom left) represents intact (live) cells (AV⁻, PI⁻); Quadrant 2 (bottom right) represents early apoptotic cells (AV⁺, PI⁻); Quadrant 3 (top right) represents late apoptotic/necrotic cells ((AV⁺, PI⁺).

a)   Control

b)   SAHA
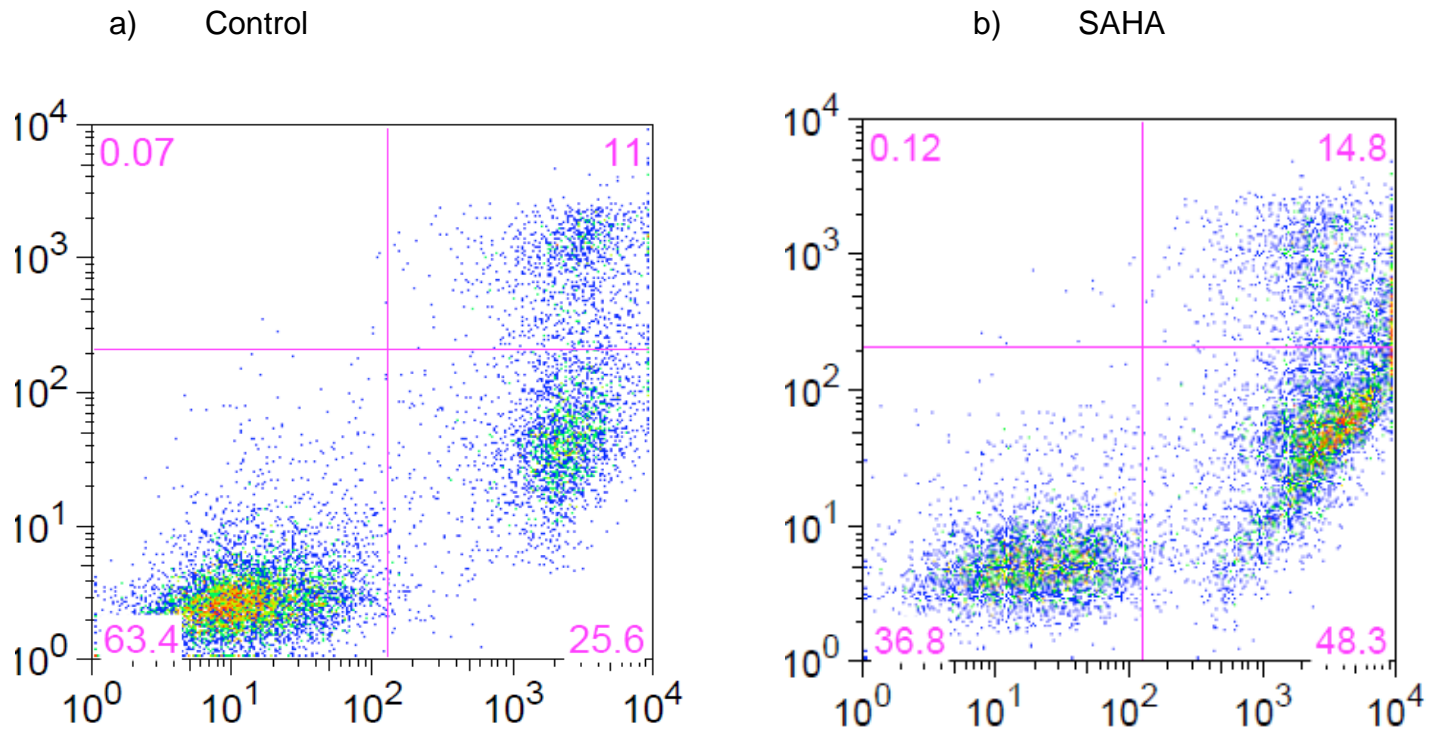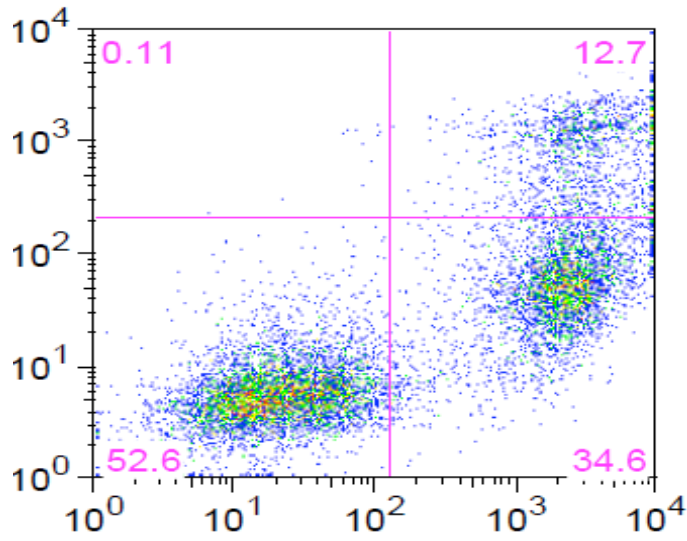
c) Compound 2
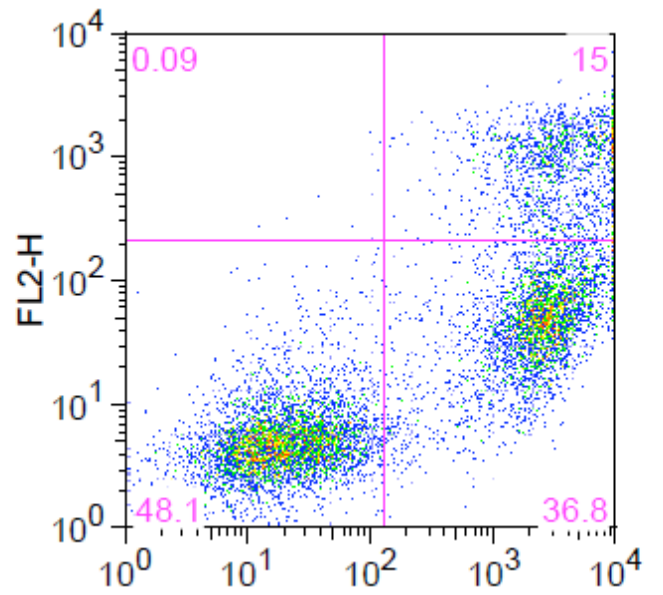
d) Compound 5
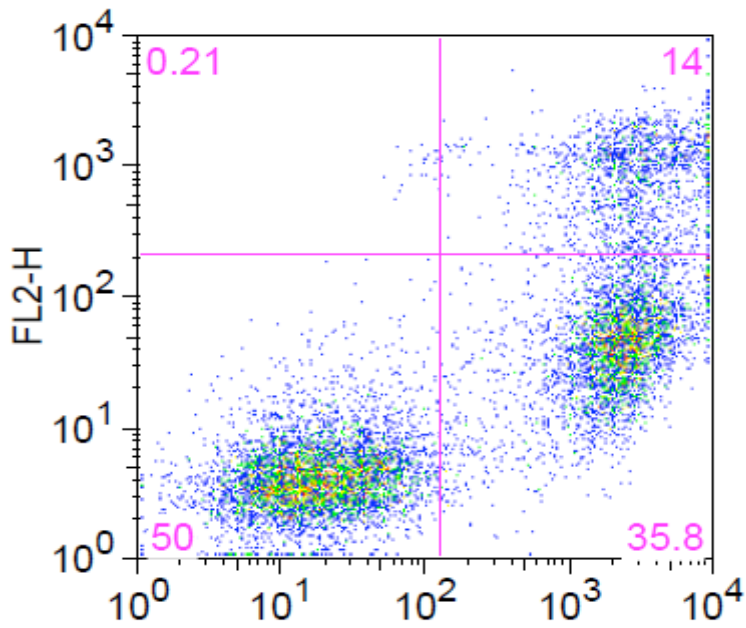
e) Compound 7
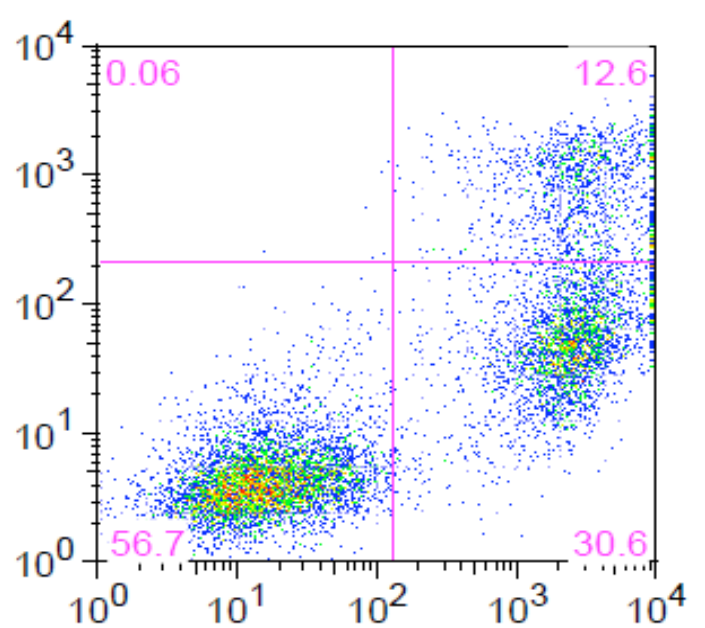
f) Compound 9
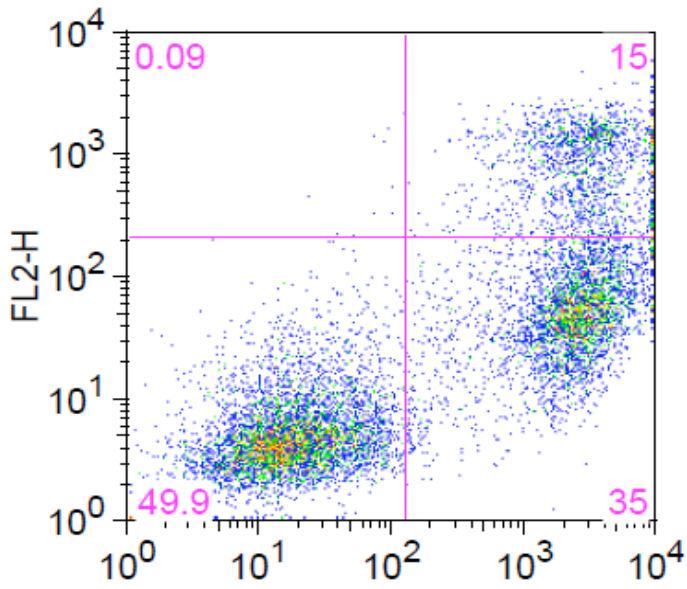
g)   Compound 10
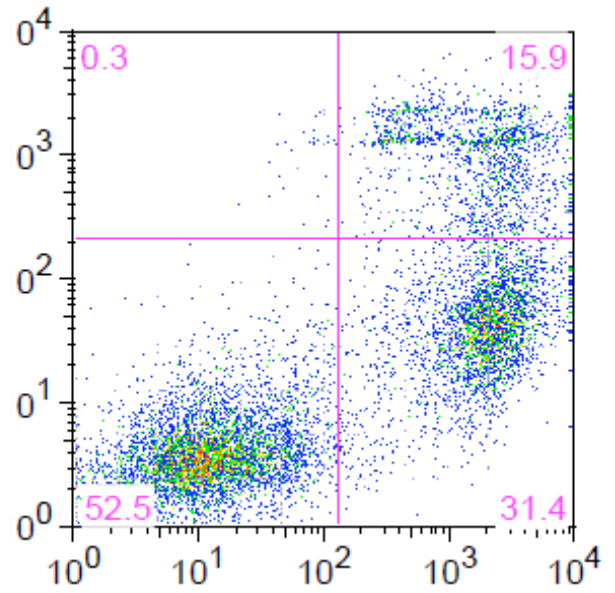
h)   Compound 11

i)   Compound 13
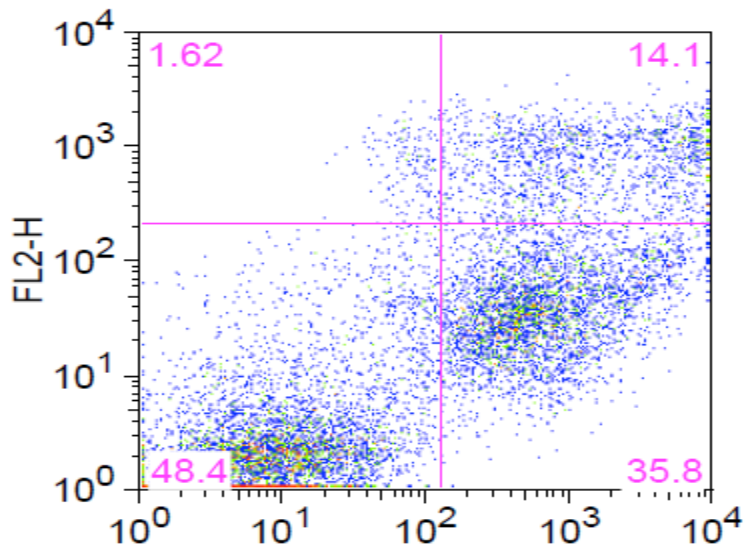
D. Time-dependent analysis of the induction of apoptosis in Jurkat cells

Following our 20h assessment of the induction of apoptosis in Jurkat cells, we evaluated multiple time-points to more accurately elucidate the ability of tropolones to induce apoptosis in a time-dependent manner. Based on cell line cytotoxicity and the 20h data on the induction of apoptosis, we chose compound 2 for comparative analysis (Table 2; Figure 3). Induction of early-stage apoptosis by both compound 2 and SAHA peaked at 24h even though SAHA activated a higher percentage of cells in early stage apoptosis than compound 2 (36.20% vs. 11.70%). However, after a 48h incubation, there were a significantly higher number of necrotic cells in the SAHA-treated cells (25.30%) than for those treated with compound 2 (3.51%).

Table 2: Elucidation of the induction of apoptosis in Jurkat cells after a 20h treatment with 10 µM HDACi

Treatment	6h		12h		24h		48h	
	% Apoptotic	% Necrotic	% Apoptotic	% Necrotic	% Apoptotic	% Necrotic	% Apoptotic	% Necrotic
Control	6.91	9.57	16.6	7.61	8.02	5.37	3.17	1.66
SAHA	4.35	9.29	22.50	8.49	36.20	1.94	4.63	25.3
2	5.00	8.21	11.50	8.32	11.70	2.07	9.63	3.51

This observation may be attributed to an accumulation of hyperacetylated histones that trigger different genes involved in the regulation of apoptosis and tumor growth in SAHA-treated cells when compared to compound 2 suggesting that the mechanisms of apoptosis by these two compounds may be executed by

169

different pathways (14, 22, 24, 26, 27, 44, 49, 54-58). Therefore, we will discuss

the mechanisms of apoptosis by SAHA and the tropolones subsequently.

Figure 3: Time-dependent analysis of the induction of apoptosis in Jurkat cells treated with 10 µM HDACi. Histograms indicate: a) % apoptotic cells; b) % necrotic cells

a)
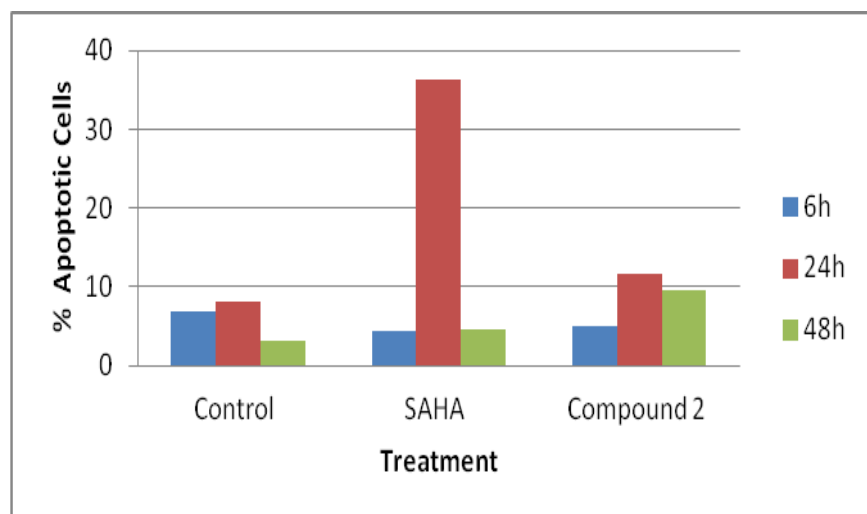
b)
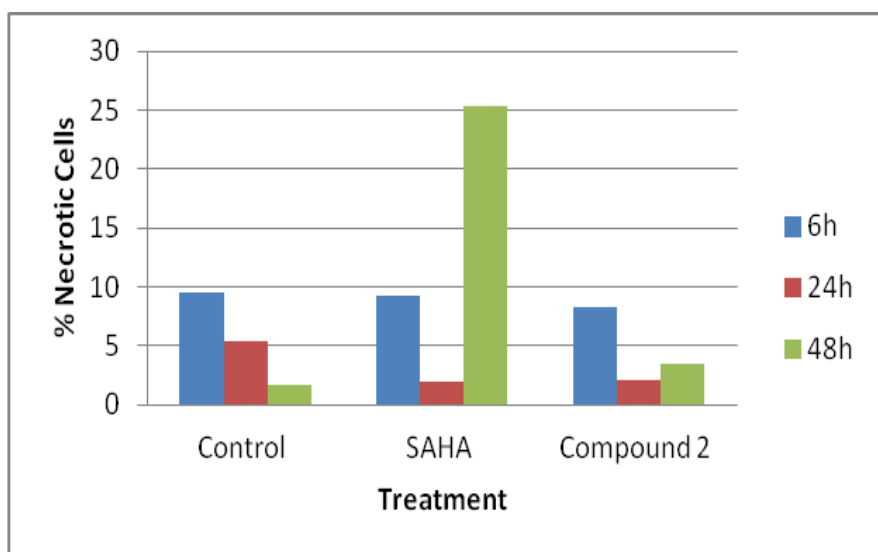
E. Elucidation of the induction of apoptosis in HuT-78 cells

Given that HuT-78 cells were also sensitive to tropolone-mediated growth inhibition, we evaluated the induction of apoptosis at two time-points, 12h and 20h. At the 12h time-point, there was very little apoptotic activity since the majority of the cells were still intact (Table 3). However, this observation is not surprising since an evaluation of a panel of cutaneous T-cell lymphoma (CTCL) cell lines showed that HuT-78 cells were the least sensitive to induction by apoptosis by HDACi including SAHA (14).

Table 3: Time-dependent analysis of the induction of apoptosis in HuT-78 cells treated with 10 µM HDACi				
	% Intact cells		% Early Apoptotic Cells	
Treatment	12h	20h	12h	20h
Control	96.10	91.30	3.46	6.12
SAHA	93.80	73.70	5.71	16.50
Compound 2	96.00	89.30	3.36	7.96
Compound 7	94.70	90.60	5.06	6.60
Compound 10	92.60	88.70	7.11	8.22
Compound 11	95.70	91.10	3.95	5.90

However, after a 20h incubation, SAHA was able to activate more than a 2-fold increase in the percentage of early apoptotic cells (16.5%) when compared to either the untreated control (6.12%) or compound 2 (7.96%). The

171

natural product, compound 10, induced the highest percentage of early apoptotic cells (8.22) among all tropolones; whereas the methylated tropolone, compound 11, resembled the untreated control thus lending support to our hypothesis about the availability of the alpha-hydroxyl ketone being essential for tropolone-mediated activity.

F. Investigation of the mechanisms of activation of the extrinsic apoptotic pathway in Jurkat cells

The extrinsic apoptotic pathway, also known as the receptor-activated apoptotic pathway and the death receptor pathway, is triggered by external cellular events and involves the activation of pro-apoptotic cell surface receptors (2, 3). The extrinsic apoptotic pathway functions through binding of death receptors such as Fas, TNF, or TRAIL to their corresponding ligands (2, 3, 9, 14). Activation of caspases often indicates an irreversible commitment towards cell death (2). There are ten major caspases (2, 66, 67) categorized into initiators (caspase-2, -8, -9, -10), effectors or executioners (caspase-3, -6, -7), and inflammatory caspases (caspase-1, -4, -5). In fact, interactions between death receptors and their corresponding ligands results in the release of caspase-8 and caspase-10, which in turn results in the activation of effector caspases (Figure 1; 2, 14, 66, 67). Moreover, HDACi such as SAHA alone and/or in combination with other anticancer agents have been shown to induce apoptosis in a caspase-8 dependent manner in several malignant cells (11, 12, 14, 16, 17, 37 58).

172

Therefore, we monitored the activation of caspase-8 by tropolones and SAHA after a 24h incubation in Jurkat cells with the aid of a fluorescent inhibitor of caspases (FLICA) reagent via flow cytometic analysis (66). Detailed experimental methods are in Section L of the Materials and Methods chapter.

We observed that SAHA activated over a 100-fold increase in caspase-8 activation in Jurkat cells when compared to either the untreated control or the tropolones (Table 4; Figure 5). Our data strengthens our earlier hypothesis that the mechanisms of apoptosis may involve different pathways since SAHA activated caspase-8 levels significantly higher than the untreated control whereas the tropolones, compound 2 and compound 7, activated caspase-8 at the same levels as the untreated control. This observation indicates that tropolones induce apoptosis in a caspase-8 independent manner, suggesting that the extrinsic apoptotic pathway may not be involved in the initiation of apoptosis by tropolones.

Table 4: Elucidation of Caspase 8 activation in Jurkat cells after a 24h treatment with 10 µM HDACi

Treatment	% Intact cells	% Caspase-8 responsive cells
Control	99.30	0.32
SAHA	62.60	35.90
Compound 2	98.90	0.43
Compound 7	99.40	0.40

Figure 5: Evaluation of Caspase 8 activation in Jurkat cells after a 24h treatment with 10 µM HDACi: y axis represents PI response whereas x axis represents caspase-8-carboxyfluorescein (FAM) response. Quadrant 1 (bottom left) represents intact (live) cells (FAM$^-$, PI$^-$); Quadrant 2 (bottom right) represents caspases-8 responsive cells (FAM$^+$, PI$^-$).

a) Control   b) SAHA

174
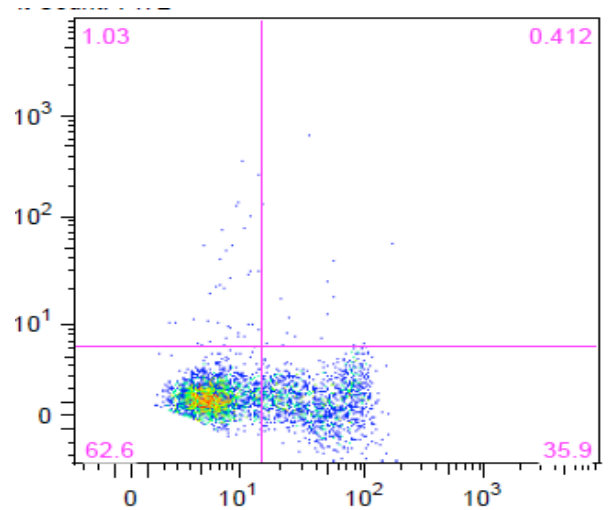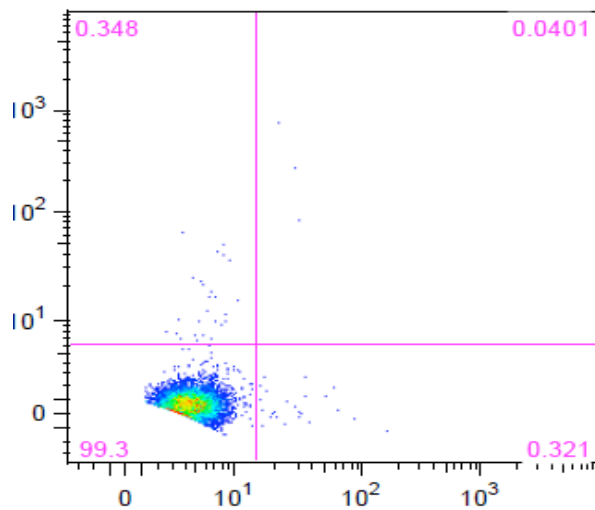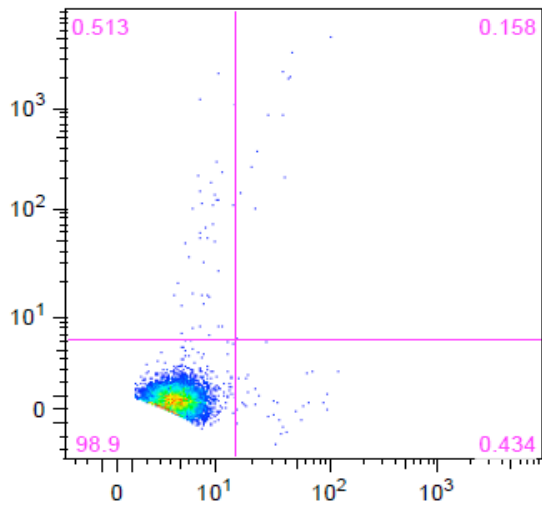
c)　　　Compound 2　　　　　　　　　　　　d)　　　Compound 7
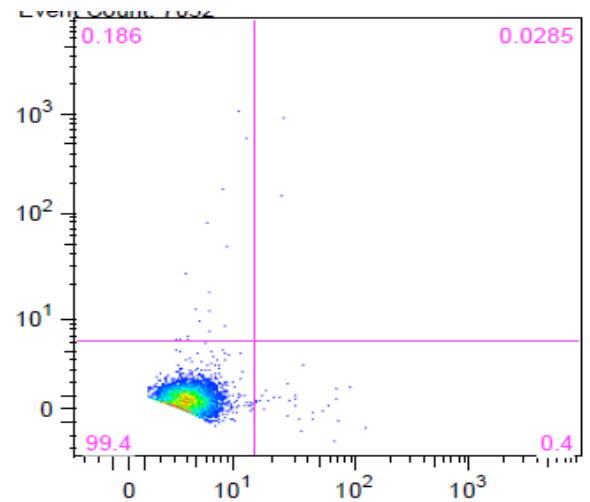
G. Investigation of the mechanisms of execution of the intrinsic apoptotic pathway in Jurkat cells

The intrinsic apoptotic pathway, also known as the stress-activated and the mitochondrial apoptotic pathway, is triggered by a diverse array of non-receptor-mediated stimuli that give rise to intracellular signals that act directly on targets within the cell (2, 3, 9, 14). The intrinsic apoptotic pathway, which is regulated by pro- and antiapoptotic proteins of the Bcl-family, are mitochondrial-initiated events that release proteins such as cytochrome c resulting in the activation of caspases (2, 3, 9, 14, 58, 62). Both the extrinsic and intrinsic pathways converge at the final pathway of apoptosis (2, 11, 12, 14, 58, 62, 66-68), the execution phase, as a result of activation of the execution caspases (caspase-3, -6, -7). Execution caspases activate cytoplasmic endonucleases

175

that degrade nuclear material as well as proteases that degrade the nuclear and cytoskeletal proteins (2, 3, 58, 62, 66-68).

Caspase-3, also known as CPP-32, Yama or Apopain, is an intracellular cysteine protease that exists as a proenzyme, becoming activated during the cascade of events associated with apoptosis (16, 25). Caspase-3 is considered to be the most important of the executioner caspases (2, 11, 12, 62, 66-68) and is activated by the other initiator caspases (caspase-8, -9, -10). Furthermore, direct activation of caspase-3 is critical for granzyme B-induced killing in the third apoptotic pathway, the perforin/granzyme pathway (2).

Based on the essential nature of caspase-3 in the execution of apoptosis, we conducted an investigation of caspase-3/7 activation in Jurkat cells. Our initial assessment of caspase-3/7 activation was conducted in Jurkat cells after a 12h treatment using a 96-well luminescent assay that correlates luminescence with caspase-3 activity (68-70). Detailed experimental methods are highlighted in Section M of the Materials and Methods chapter. Standard deviation values for all treatments are reported in the Appendix, Section 39.

After a 12h treatment, SAHA activated more than a 2-fold increase in caspase-3/7 activity when compared to the untreated control (Table 5; Figure 6). The tropolones were also able to activate an increase in caspase activity when compared to the untreated control albeit lower than SAHA-treated cells.

176

Table 5: Activation of caspase-3/7 after a 12h treatment with 10 μM HDACi	
Treatment	Caspase 3/7 Activity (Mean RLU) *RLU= relative luminescent units
Control	69,935
SAHA	157,988
Compound 2	97,513
Compound 7	110,650

Figure 6: Evaluation of Caspase-3/7 activation after a 12h treatment with 10 μM HDACi
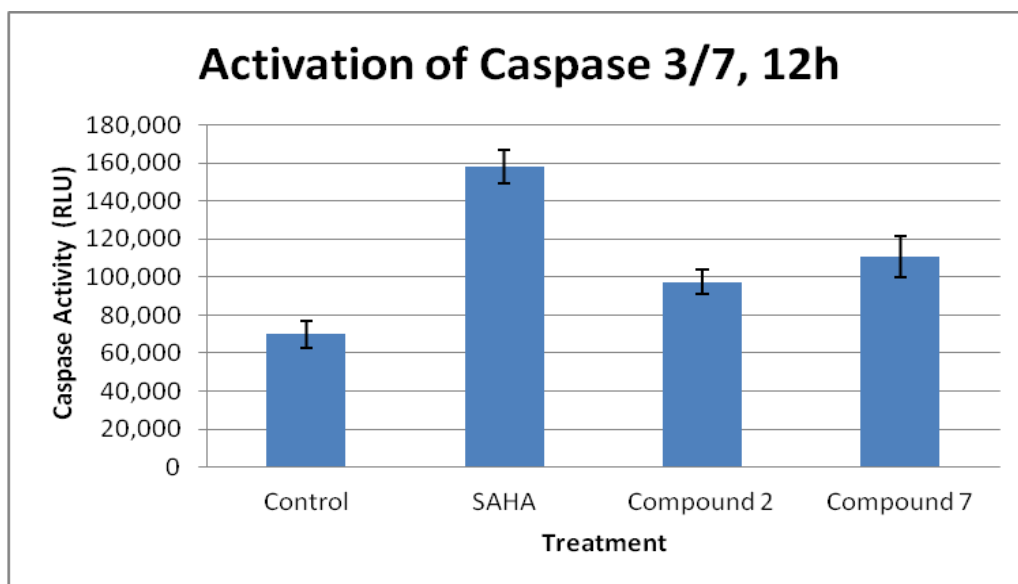
H. Time-dependent analysis of Caspase-3 activation in Jurkat cells

Given the promising data garnered from the 12h analysis, we conducted a comprehensive, time-point analyses of caspase-3 activation in Jurkat cells (Table 6; Figure 7). After a 6h treatment, compound 2 and compound 7 activated a higher proportion of caspase-3 activity than either the untreated control or SAHA. Caspase-3 activity dropped after 24h and increased again after a 48h treatment by the tropolones but at both time-points, tropolone-mediated caspase-3 activity was lower than the untreated control. On the other hand, caspase-3 activity increased in SAHA-treated cells after 24h and dropped after 48h but SAHA-mediated caspase-3 activity was lower than the untreated control for both time-points. However, our comprehensive analysis (Figure 7d) highly suggests that caspase-3/7 activation by both the tropolones and SAHA peak at 12h indicating that caspase-3 activation may be one of the mechanisms for the execution of apoptosis in Jurkat cells by both the tropolones and SAHA.

Table 6: Time-dependent analysis of caspases-3/7 activation in Jurkat cells			
	Caspase-3/7 Activity (Mean RLU)		
Treatment	6h	24h	48h
Control	59,417	136,627	109,510
SAHA	53,518	125,484	95,463
Compound 2	88,661	76,948	105,357
Compound 7	73,949	80,438	71,048

Figure 7: Time-dependent analysis of Caspase-3 activation in Jurkat cells

a) Activation of Caspase-3 after a 6h treatment in Jurkat cells

179
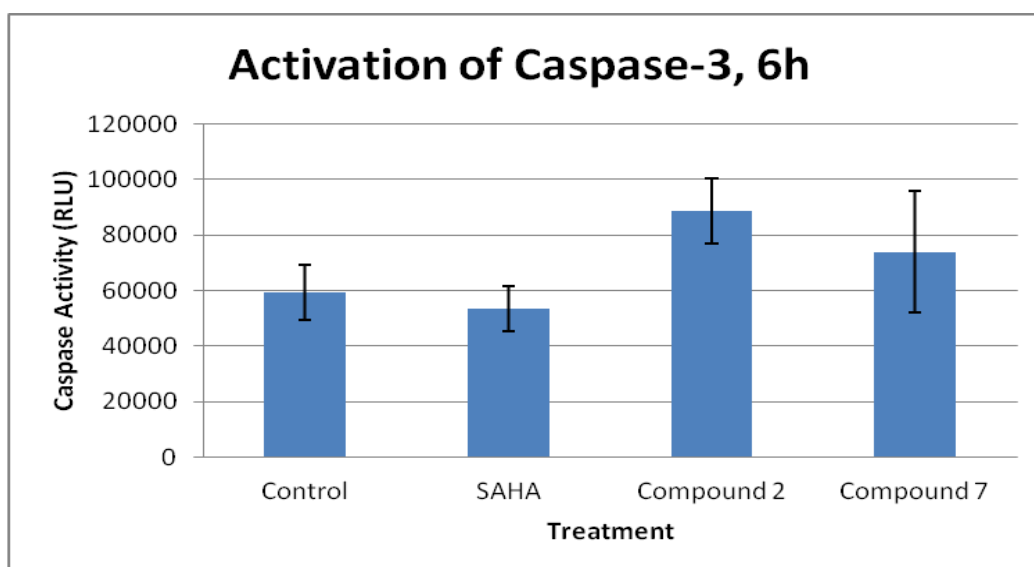
b)   Activation of Caspase-3 after a 24h treatment in Jurkat cells
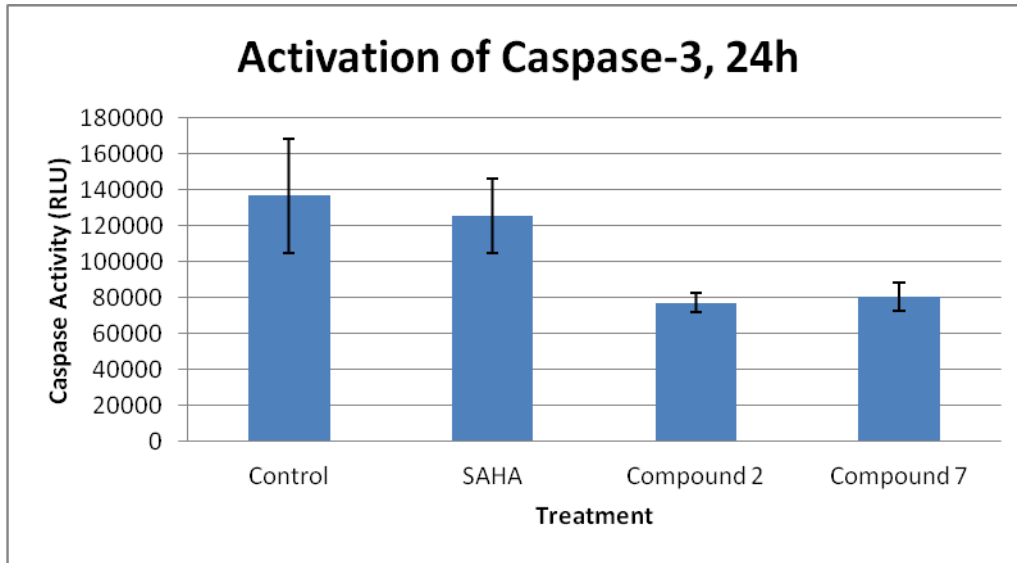
c)   Activation of Caspase-3 after a 48h treatment in Jurkat cells
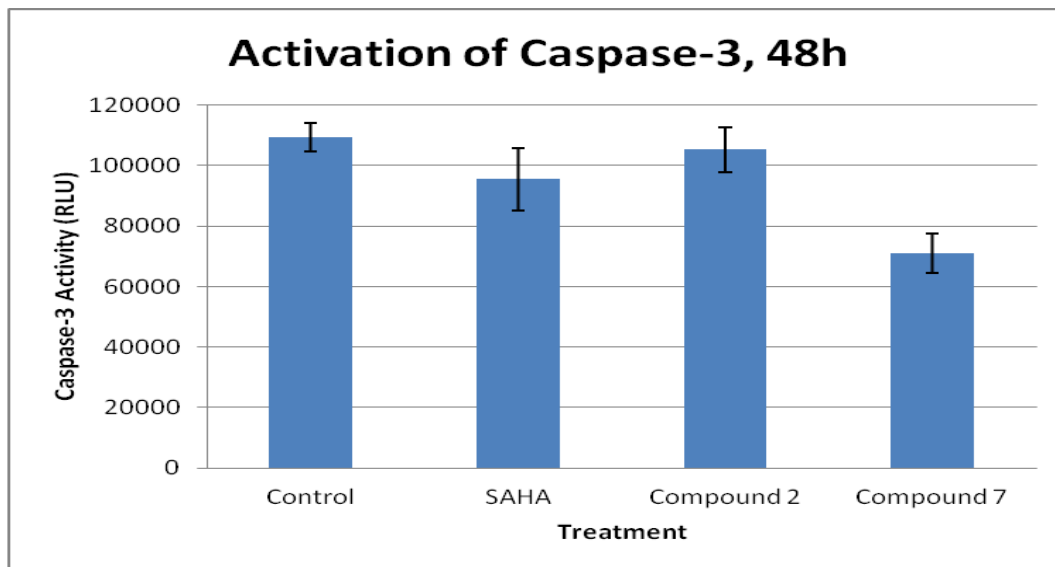
d)   Time-dependent analysis of Caspase-3 activation in Jurkat cells
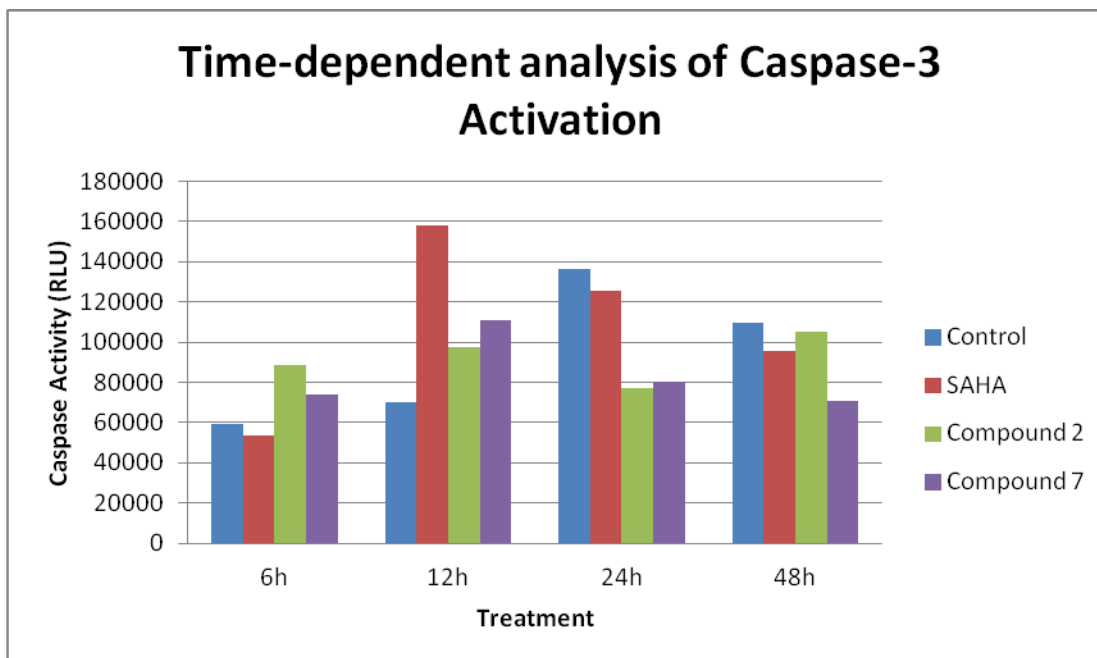
I. Evaluation of the ability of tropolones to enhance differentiation of perforin in Jurkat cells

Cytotoxic T lymphocytes (CTLs) and natural killer (NK) cells play a critical role in the immune system by recognizing and directly destroying virally infected tumorigenic cells (2, 3, 71-77). NK cells are critical to the innate immune system whereas CTLs play important roles in adaptive immunity (2, 3, 73). Both types of cells kill their cellular targets by either secreting membrane-disrupting proteins known as perforin and a family of structurally related serine proteases known as granzymes that work together to induce apoptosis of the target cell (2, 71-77); alternatively, a second pathway involves the engagement and aggregation of

181

target-cell death receptors such as Fas (2, 3, 71-77). Studies in gene-disrupted mice have shown that the perforin pathway is closely involved in defense against viral pathogens and tumorigenic cells (73). Furthermore, HDACi have been reported to modify the immune system via various effects on regulatory T cells and lysis of tumor targets by T cells and natural killer cells (11, 12, 75-77). Interestingly, lower numbers of CTLs has been correlated with less favorable prognosis in patients with mycosis fungoides (MF), the most common form of CTCL (72).

Therefore, we conducted a time-dependent analysis to evaluate the ability of the tropolones to differentiate perforin in Jurkat cells (Table 7; Figure 8). We used FACS analysis to monitor fluorescence intensities at multiple time points in Jurkat cells treated with 10 µM HDACi by sequentially incubating treated cells with primary antibodies for perforin followed by treatment with secondary antibodies conjugated with a fluorescein isothiocyanate (FITC; 58, 78-81). We determined values for geometric mean fluorescence intensities (GMFI), equivalent to the median cell population response, with the aid of the FlowJo Workstation. Detailed methods for experimental analysis are in Section G of the Materials and Methods chapter. Additional histograms are in the Appendix, section 40.

After 6h and 12h treatments, both SAHA and compound 2 enhanced differentiation of perforin in Jurkat cells around the threshold of the untreated

182

control; but differentiation of perforin peaked after 48h by both SAHA and compound 2 resulting in an approximate two-fold increase in the differentiation of perforin. We hypothesize that the differentiation of perforin by the tropolones may lead to the cascade of events that we observed in our time-dependent analysis in Jurkat cells. Hence, our observations suggest that tropolones may be able to execute cell death by apoptosis via the perforin/granzyme pathway.

Moreover, HDAC inhibitors such as valproic acid have been shown to improve sensitivity of Jurkat and humanhepatoma cells to NK cell-mediated killing (75, 76). Furthermore, studies in genetically identical murine tumor models of mammary, renal, prostate, and colorectal carcinomas have shown robust and prolonged eradication of solid tumors using SAHA combined with immune-stimulating antibodies, CD8(+) CTL that used perforin as the key immune effector molecule (77). These observations combined with our data for perforin differentiation suggest promising therapeutic applications and warrant further investigation of tropolones in combination with immune-activating antibodies for treatment of both solid tumors and hematological malignancies.

Table 7: Time-dependent analysis of the differentiation of perforin in Jurkat cells treated with 10 µM HDACi			
Treatment	**Perforin/Granzyme, GMFI** GMFI = geometric mean fluorescence intensities		
	6h	**24h**	**48h**
Control	1.28	1.57	3.15
SAHA	1.52	2.32	6.29
Compound 2	1.39	1.40	6.15

Figure 8: Time-dependent analysis of the differentiation of perforin in Jurkat cells. Note that histograms represent the untreated control superimposed with the HDACi treatment for comparative analysis.

a)   6h analysis of SAHA   b)   6h analysis of compound 2
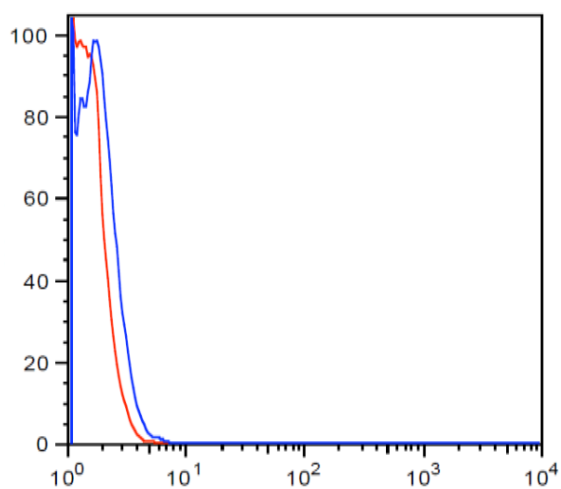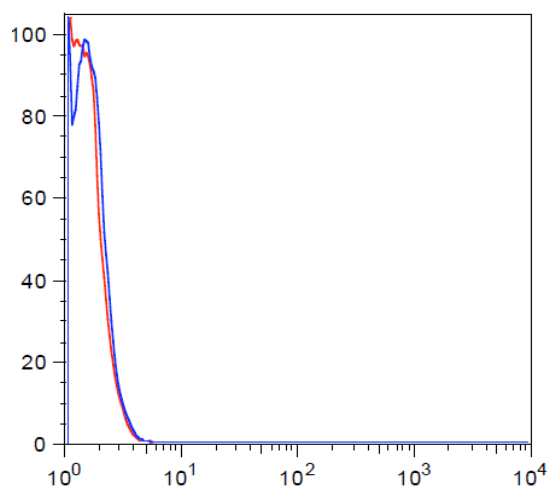
c)   24h analysis of SAHA
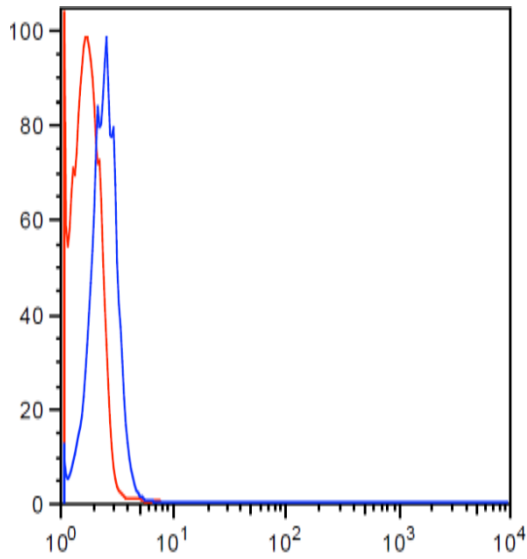
d)   24h analysis of compound 2
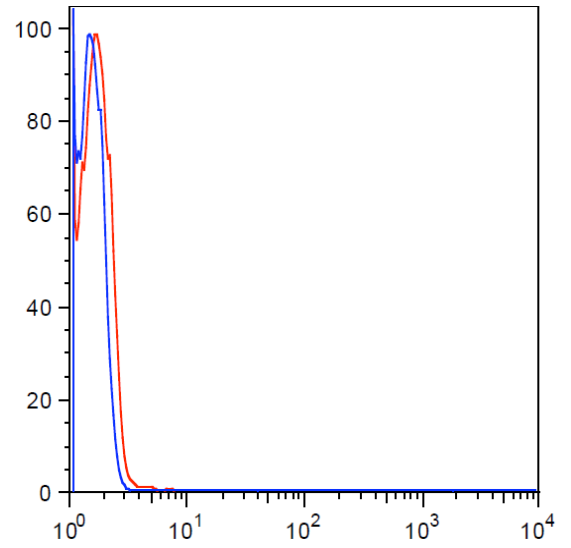
e)   48h analysis of SAHA
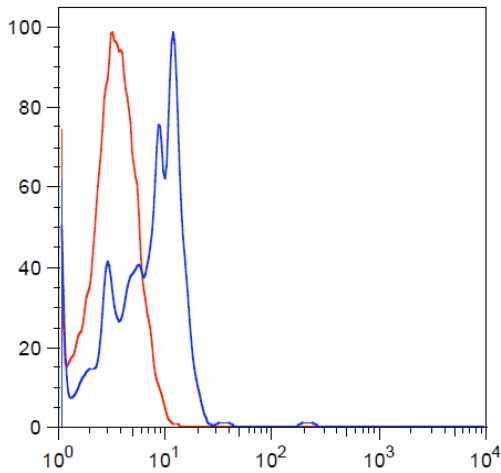
f)   48h analysis of compound 2
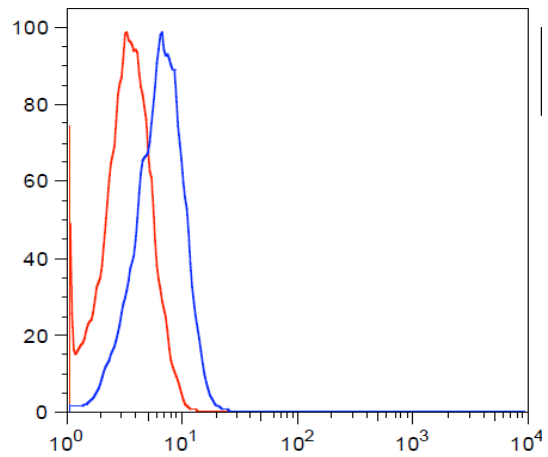
J. Preliminary studies on the synergistic effects of tropolones in breast cancer cells

It has been previously reported that co-treatment of breast cancer cell lines including MCF-7 cells with HDACi such as SAHA resulted in synergistic anti-tumor activity presumably with a depletion of both the estrogen receptor (ER) and progesterone receptor (PR) (82). In clinical studies, a combination treatment of vorinostat and tamoxifen resulted in a reduction in the resistance of tamoxifen in breast cancer patients (83). In both preclinical and clinical studies, histone acetylation and HDAC2 expression were used as biomarkers to monitor the efficacy of the combination treatment. Given these observations, we conducted a preliminary assessment of the co-treatment of 10 μM compound 2 with the anti-estrogen, tamoxifen, after 48h treatment in MCF-7 cells via FACS analysis (Table 8). 10 μM served as the experimental control and we compared our data to published reports on synergistic effects in MCF-7 cells by SAHA (82). Detailed experimental methods are in Section K of the Materials and Methods chapter.

As expected, combination of SAHA with tamoxifen resulted in some increase in the induction of apoptosis when compared to either the untreated control (30.30% vs. 3.12%), SAHA treatment alone (21.50%), or even tamoxifen treatment alone (4.24%); however, a combination of compound 2 with tamoxifen did not result in significant increase when compared to compound 2 alone (6.68%% vs. 3.15%). Our preliminary assessment of synergisitic effects in breast cancer cells warrants further investigation in multiple breast cancer cell

lines at multiple concentrations and time-points in addition to gene expression studies, gene knockdown studies and even cell cycle analyses in order to garner a more precise evaluation of the synergistic effects of tropolones in breast cancers.

Table 8: Elucidation of synergistic effects in MCF-7 cells after a 48h treatment period	
Treatment	**% Apoptotic cells**
Control	3.12
10 µM SAHA only	21.5
10 µM Compound 2 only	6.68
10 µM Tamoxifen only	4.24
10 µM SAHA + 10 µM Tamoxifen	30.3
10 µM Compound 2 + 10 µM Tamoxifen	3.15

Figure 9: Preliminary assessment of synergistic effects of 10 µM HDACi and 10 µM tamoxifen after a 48h treatment in MCF-7 cells. y axis represents PI response whereas x axis represents Annexin V (AV) response. Quadrant 1 (bottom left) represents intact (live) cells (AV⁻, PI⁻); Quadrant 2 (bottom right) represents early apoptotic cells (AV⁺, PI⁻); Quadrant 3 (top right) represents late apoptotic/necrotic cells ((AV⁺, PI⁺).

a)　Control
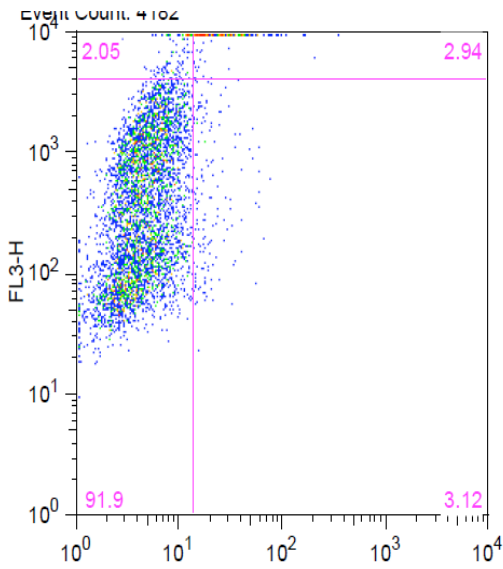
b)　SAHA only
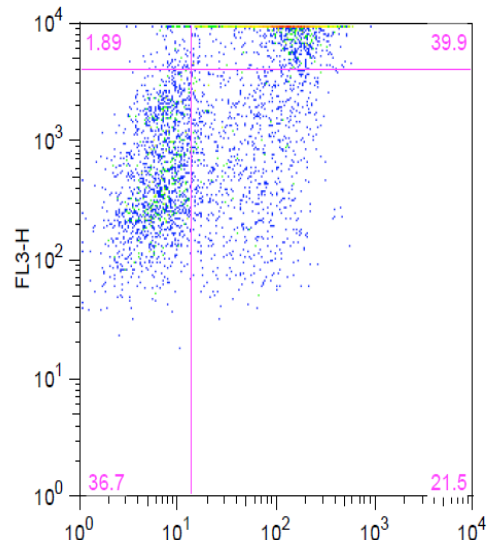
c)　Compound 2 only
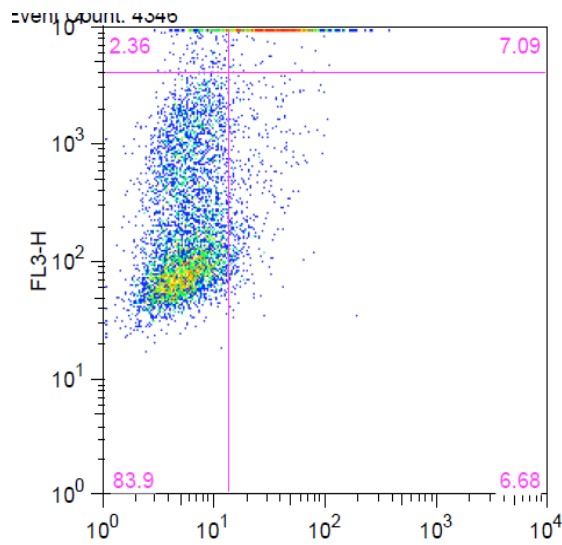
d)　Tamoxifen only
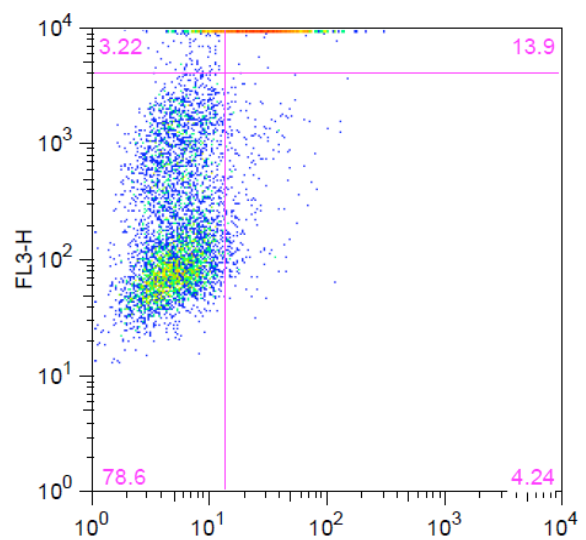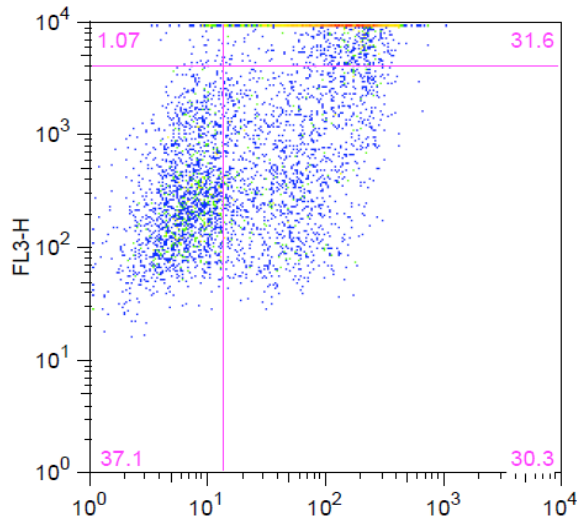
e)   Tamoxifen + SAHA   f)   Tamoxifen + Compound 2
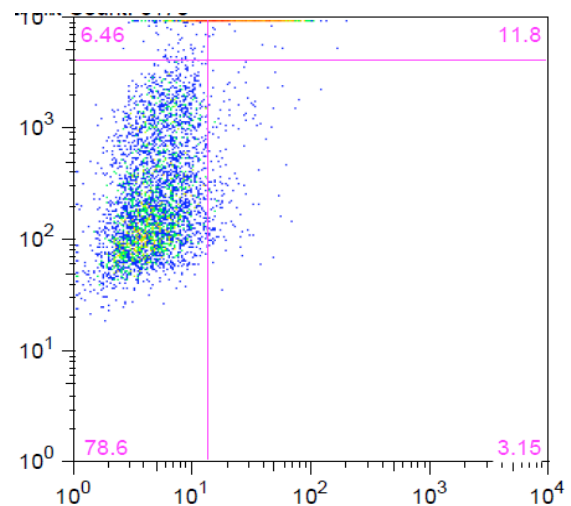
K. Conclusions

Apoptosis is a highly complex process that is implicated in many disease areas including cancers and neurological disorders. The induction of apoptosis is marked by specific biochemical events such as the exposure of phosphatidyl serine on the outer leaflet of the plasma membrane as well as the activation of caspases. There are three major mechanisms of apoptosis and these apoptotic pathways include: extrinsic (death receptor or receptor-activated), intrinsic (mitochondrial or stress-activated), and the granzyme/perforin pathway. HDACi, including SAHA, have been reported to alter both the intrinsic and extrinsic apoptotic pathways. Our comprehensive analysis of the induction of apoptosis shows that tropolones induce apoptosis in a time-dependent manner in both

189

Jurkat and HuT-78 cells. Our preliminary assessment of the synergistic effects of tropolones in MCF-7 cells indicates that a more comprehensive analysis in multiple breast cancer cell lines, at multiple concentrations, and an inclusion of gene expression studies will be required for a more precise analysis of synergistic effects. We also showed that tropolones initiate apoptosis in a caspase-8 independent manner but the activation of caspase-3 may be essential for the execution of apoptosis by tropolones. Finally, we discovered that tropolones are able to enhance differentiation of perforin in Jurkat cells in a time-dependent manner. Our observations suggest that tropolones may be able to execute cell death by apoptosis via the perforin/granzyme pathway and warrant further investigation particularly with regards to combining tropolones with immune-activating antibodies for robust and prolonged treatment of solid tumors and hematological malignancies.

L. References

1. Wu, X., Kassie, F., & Mersch-Sundermann, V. Induction of apoptosis in tumor cells by naturally occurring sulfur-containing compounds. Mutat Res. 2005;589(2):81-102.
2. Elmore, S. Apoptosis: A Review of Programmed Cell Death. Toxicol Pathol. 2007: 35 (4): 495-516.
3. Weinberg, R. The Biology of Cancer. New York, NY: Garland Science, Taylor & Francis Group, LLC., 2007.
4. Zhou, Q., Dalgard, C.L., Wynder, C., et.al., Histone deacetylase inhibitors SAHA and sodium butyrate block G1-to-S cell cycle progression in neurosphere formation by adult subventricular cells. BMC Neurosci. 2011; 12:50.
5. Ouaissi, M., Cabral, S., Tavares, J., et al. Histone deacetylase (HDAC) encoding gene expression in pancreatic cancer cell lines and cell sensitivity to HDAC inhibitors. Cancer Biol Ther. 2008; 7(4): 523-531.

6. Lobjois, V., Frongia, C., Jozan, S., et.al. Cell cycle and apoptotic effects of SAHA are regulated by the cellular microenvironment in HCT116 multicellular tumour spheroids. Eur J Cancer. 2009; 45(13):2402-11.

7. Knutson, A.K., Welsh, J., Taylor, T., et.al. Comparative effects of histone deacetylase inhibitors on p53 target gene expression, cell cycle and apoptosis in MCF-7 breast cancer cells. Oncol Rep. 2012; 27(3):849-53.

8. Ononye, S.N., van Heyst, M., Falcone, E., et.al. Toward isozyme selective histone deacetylase inhibitors as therapeutic agents for the treatment of cancer. Pharm. Patent Analyst 2012; 1 (2), 207-221.

9. Lemoine, M. & Younes, A. Histone deacetylase inhibitors in the treatment of lymphoma. Discov Med. 2010; 10 (54): 462-70

10. Ouaissi, M., Giger, U., Sielezneff, I., et al. Rationale for possible targeting of histone deacetylase signaling in cancer diseases with a special reference to pancreatic cancer. J Biomed Biotechnol. 2011: 315939.

11. Khan, O., & La Thangue, N.B. HDAC inhibitors in cancer biology: emerging mechanisms and clinical applications. Immunol Cell Biol. 2012; 90(1):85-94.

12. Khan, O., & La Thangue, N.B. Drug Insight: histone deactylase inhibitor-based therapies for cutaneous T-cell lymphomas. Nat Clin Pract Oncol. 2008;5 (12):714-26.

13. Hagelkruys, A., Sawicka, A., Rennmayr, M., et.al. The biology of HDAC in cancer: the nuclear and epigenetic components. Handb Exp. Pharmacol. 2011; 206: 13-37.

14. Wozniak, M.B., Villuendas, R., Bischoff, J.R., et.al. Vorinostat interferes with the signaling transduction pathway of T-cell receptor and synergizes with phosphoinositide-3 kinase inhibitors in cutaneous T-cell lymphoma.

15. Tang, Y.A., Wen, W.L., Chang, J.W., et. al. A novel histone deacetylase inhibitor exhibits antitumor activity via apoptosis induction, F-actin disruption and gene acetylation in lung cancer. PLoS One. 2010; 5(9):e12417.

16. Miller, C.P., Rudra, S., Keating, M.J., et. al. Caspase-8 dependent histone acetylation by a novel proteasome inhibitor, NPI-0052: a mechanism for synergy in leukemia cells. Blood. 2009; 113(18):4289-99.

17. Almenara J, Rosato R, & Grant S. Synergistic induction of mitochondrial damage and apoptosis in human leukemia cells by flavopiridol and the histone deacetylase inhibitor suberoylanilide hydroxamic acid (SAHA). Leukemia. 2002; 16(7):1331-43.

18. Huang, L., & Pardee, A. Suberoylanilide Hydroxamic Acid as a Potential Therapeutic Agent for Human Breast Cancer Treatment. Mol Med. 2000; 6 (10): 849-866.

19. Zhang, Q-L, Wang, L., Zhang, J.W., et.al. The proteasome inhibitor bortezomib interacts synergistically with the histone deacetylase inhibitor suberoylanilide hydroxamic acid to induce T-leukemia/lymphoma cells apoptosis. Leukemia 2009; 23 (8): 1507–1514.

20. LaBonte, M.J., Wilson, P.M., Fazzone, W., et.al. DNA microarray profiling of genes differentially regulated by the histone deacetylase inhibitors vorinostat and LBH589 in colon cancer cell lines. BMC Med Genomics 2009; 2:67

21. Ulrike, H., Rademacher, J., Lamottke, B., et.al. Synergistic interaction of the histone deacetylase inhibitor SAHA with the proteasome inhibitor bortezomib in cutaneous T cell lymphoma. Eur J Haematol 2009; 82 (6): 440–449.

22. Schrump, D.S. Cytotoxicity Mediated by Histone Deacetylase Inhibitors in Cancer Cells: Mechanisms and Potential Clinical Implications. Clin. Cancer. Res 2009; 15: 3947-3957.

23. Ruefli, A.A., Ausserlechner, M.J., Bernhard, D., et. al. The histone deacetylase inhibitor and chemotherapeutic agent suberoylanilide hydroxamic acid (SAHA) induces a cell-death pathway characterized by cleavage of Bid and production of reactive oxygen species. Proc Natl Acad Sci U S A. 2001; 98(19):10833-8.

24. Marks, P.A., & Dokmanovic, M. Histone deacetylase inhibitors: discovery and development as anticancer agents. Expert Opin Investig Drugs 2005; 14(12):1497-511.

25. Kong, Y., Jung, M., Wang, K., et. al. Histone deacetylase cytoplasmic trapping by a novel fluorescent HDAC inhibitor. Mol Cancer Ther. 2011;10 (9):1591-9.

26. Bolden, J.E., Peart, M.J., & Johnstone, R.W. Anticancer activities of histone deacetylase inhibitors. Nat Rev Drug Discov. 2006; 5(9):769-84.

27. Frew, A.J., Johnstone, R.W, & Bolden, J.E. Enhancing the apoptotic and therapeutic effects of HDAC inhibitors. Cancer Lett. 2009; 280(2):125-33.

28. Vigushin, D.M., Ali, S., Pace, P.E., et al. Trichostatin A is a histone deacetylase inhibitor with potent antitumor activity against breast cancer in vivo. Clin Cancer Res, 2001; 7(4): 971-6.

29. Huang, L., & Pardee, A.B. Suberoylanilide hydroxamic acid as a potential therapeutic agent for human breast cancer treatment. Mol Med. 2000; 6(10):849-66.

30. Walker, G.E., Wilson, E.M., Powell, D., et al., Butyrate, a histone deacetylase inhibitor, activates the human IGF binding protein-3 promoter in breast cancer cells: molecular mechanism involves an Sp1/Sp3 multiprotein complex. Endocrinology, 2001; 142(9): 3817-27.

31. Cao, Z.A., Bass, K.E., Balasubramanian, S., et al. CRA-026440: a potent, broad-spectrum, hydroxamic histone deacetylase inhibitor with antiproliferative and antiangiogenic activity in vitro and in vivo. Mol Cancer Ther, 2006; 5(7): 1693-701.

32. Thaler, F., Colombo, A., Mai, A., et al., Synthesis and biological evaluation of N-hydroxyphenylacrylamides and N-hydroxypyridin-2-ylacrylamides as novel histone deacetylase inhibitors. J Med Chem. 2010; 53(2): 822-39.

33. Vannini, A., Volpari, C., Filocamo, G., et al. Crystal structure of a eukaryotic zinc-dependent histone deacetylase, human HDAC8, complexed with a hydroxamic acid inhibitor. Proc Natl Acad Sci U S A 2004; 101(42): 15064-9.

34. Ontoria, J.M., Altamura, S., Di Marco, A., et al. Identification of novel, selective, and stable inhibitors of class II histone deacetylases. Validation studies of the inhibition of the enzymatic activity of HDAC4 by small molecules as a novel approach for cancer therapy. J Med Chem 2009; 52(21): 6782-9.

35. Na, Y.S., Jung, K.A., Kim, S.M., et. al. The histone deacetylase inhibitor PXD101 increases the efficacy of irinotecan in in vitro and in vivo colon cancer models. Cancer Chemother Pharmacol. 2011; 68 (2):389-98.

36. Attenni, B., Ontoria, B., Cruz, J.C., et al., Histone deacetylase inhibitors with a primary amide zinc binding group display antitumor activity in xenograft model. Bioorg Med Chem Lett, 2009; 19(11): 3081-4.

37. Portanova, P., Russo, T., Pellerito, O., et.al. The role of oxidative stress in apoptosis induced by the histone deacetylase inhibitor suberoylanilide hydroxamic acid in human colon adenocarcinoma HT-29 cells. Intl J Oncol. 2008; 33(2): 325-31.

38. Blagosklonny, M., Robey, R., Bates, S., et.al. Pretreatment with DNA-damaging agents permits selective killing of checkpoint-deficient cells by microtubule-active drugs. J. Clin. Invest. 2000; 105: 533–553

39. Clocchiatti A., Di Giorgio, E., Ingrao, S., et.al. Class IIa HDACs repressive activities on MEF2-depedent transcription are associated with poor prognosis of ER+ breast tumors. FASEB J. 2012 Nov 16. [Epub ahead of print]

40. Zafar, S.F., Nagaraju, G.P., & El-Raves, B. Developing histone deacetylase inhibitors in the therapeutic armamentarium of pancreatic adenocarcinoma. Expert Opin Ther Targets. 2012; 16(7):707-18.

41. Ouaissi, M., & Ouaissi, A. Histone deacetylase enzymes as potential drug targets in cancer and parasitic diseases. J Biomed Biotechnol 2006; 2006 (2): 13474.

42. Bajbouj, K., Mawrin, C., Hartig, R., et.al. P53-dependent antiproliferative and pro-apoptotic effects of trichostatin A (TSA) in glioblastoma cells. J Neurooncol. 2012; 107(3):503-16.

43. Vinodhkumar, R., Song, Y-S., & Devaki, T. Romidepsin (depsipeptide) induced cell cycle arrest, apoptosis and histone hyperacetylation in lung carcinoma cells (A549) are associated with increase in p21 and hypophosphorylated retinoblastoma proteins expression. Biomed Pharmacother. 2008; 62(2):85-93.

44. Weichert, W. HDAC expression and clinical prognosis in human malignancies. Cancer Letters. 2009; 280: 168-176.

45. Leoni, F., Zaliani, A., Bertolini, G., et.al. The antitumor histone deacetylase inhibitor suberoylanilide hydroxamic acid exhibits anitinflammatory properties

via suppression of cytokines. Proc Natl Acad Sci U S A 2012; 99 (5):2995-3000

46. Lai, M.J., Huang, H.L., Pan, S.L., et. al. Synthesis and biological evaluation of 1-arylsulfonyl-5-(N-hydroxyacrylamide)indoles as potent histone deacetylase inhibitors with antitumor activity in vivo. J Med Chem. 2012 26; 55(8):3777-91.

47. Krennhrubec, K., Marshall, B.L., Hedglin, M., et al., Design and evaluation of 'Linkerless' hydroxamic acids as selective HDAC8 inhibitors. Bioorg Med Chem Lett, 2007; 17(10): 2874-8.

48. Butler, L.M., Agus, D. B., Scher, H.I., et al. Suberoylanilide hydroxamic acid, an inhibitor of histone deacetylase, suppresses the growth of prostate cancer cells in vitro and in vivo. Cancer Res 2000; 60(18): 5165-70.

49. Dokmanovic, M., C. Clarke, & Marks, P.A. Histone deacetylase inhibitors: overview and perspectives. Mol Cancer Res 2007; 5(10): 981-9.

50. Estiu, G., West, N., Mazitschek, R., et al. On the inhibition of histone deacetylase 8. Bioorg Med Chem. 2010; 18 (11): 4103-10.

51. Furumai, R., Komatsu, Y., Nishino, N., et al., Potent histone deacetylase inhibitors built from trichostatin A and cyclic tetrapeptide antibiotics including trapoxin. Proc Natl Acad Sci U S A, 2001; 98(1): 87-92.

52. Garber, K. HDAC inhibitors overcome first hurdle. Nat Biotechnol 2007; 25(1): 17-9.

53. Hrzenjak, A., Moinfar, F., Kremser, M.L., et al. Histone deacetylase inhibitor vorinostat suppresses the growth of uterine sarcomas in vitro and in vivo. Mol Cancer. 2010; 9: 49.

54. Marks, P., Rifkind, R.A., Richon, V.M., et. al. Histone deacetylases and cancer: causes and therapies. Nat Rev Cancer. 2001;1(3):194-202.

55. Noureen, N., H. Rashid, & Kalsoom, S. Identification of type-specific anticancer histone deacetylase inhibitors: road to success. Cancer Chemother Pharmacol. 2010; 66(4):625-33.

56. Paris, M., Porcelloni, M., Binaschi, M., et al. Histone deacetylase inhibitors: from bench to clinic. J Med Chem 2008; 51(6): 1505-29.

57. Dickinson, M., Johnstone, R.W., & Prince, H.M. Histone deacetylase inhibitors: potential targets responsible for their anti-cancer effect. Invest New Drugs. 2010; 28 Suppl 1:S3-20.

58. Morales, J.C., Ruiz-Magana, M.J., Carranza, D., et. al. HDAC inhibitors with different gene regulation activities depend on the mitochondrial pathway for the sensitization of leukemic T cells to TRAIL-induced apoptosis. Cancer Lett. 2010; 29 7(1):91-100.

59. Shi, Z-J., Ouyang, D-Y., Zhu, J-S., et. al. Histone deacetylase inhibitor suberoylanilide hydroxamic acid exhibits anti-inflammatory activities through induction of mitochondrial damage and apoptosis in activated lymphocytes. Int Immunopharmacol. 2012; 12(4):580-7.

60. Spurling, C.C., Godman, C.A., Noonan, E.J., et. al. HDAC3 Overexpression and Colon Cancer Cell Proliferation and Differentiation, Mol. Carc. 2008; 43: 137-147.

61. Liu, S., & Yamauchi, H. Hinokitiol, a metal chelator derived from natural plants, suppresses cell growth and disrupts androgen receptor signaling in prostate carcinoma cell lines. Biochem Biophys Res Commun, 2006; 351(1): 26-32.

62. Liu, X., Zou, H., Slaughter, C., et.al. DFF, a Heterodimeric Protein That Functions Downstream of Caspase-3 to Trigger DNA Fragmentation during Apoptosis. Cell. 1997; 89 (2): 175–184.

63. Vermes, I., Haanen, H., Steffens-Nakken, H., et. al. A novel assay for apoptosis: Flow cytometry detection of phosphatidylserine expression on early apoptotic cells using fluorescein labeled annexin V. J Immunol Methods 1995; 184 (1):39-51.

64. Verhoven, B., Schlegel R.A., & Williamson, P. Mechanisms of phosphatidylserine exposure, a phagocyte recognition signal, on apoptotic T lymphocytes, J Experimental Med 1995;182 (5): 1597-601.

65. Nicoletti I., Migliorati, G., Pagliacci, M.C., et.al. A rapid and simple method for measuring thymocyte apoptosis by propidium iodide staining and flow cytometry. J. Immunol Methods 1991; 139:271-9.

66. Smolewski, P., Grabarek, J, Halicka, H.D., et. al. Assay of caspase activation in situ combined with probing plasma membrane integrity to detect three distinct stages of apoptosis. J Immunol Methods. 2002; 265(1-2):111-21.

67. Ekert, P.G., Silke, J., & Vaux, D.L. Caspase inhibitors. Cell Death Differ. 1999 ;6 (11):1081-6.

68. Porter, A.G., & Janicke, R.U. Emerging Roles of Caspase-3 in Apoptosis, Cell Death and Differentiation. Cell Death Differ. 1999; 6 (2): 99-104.

69. Liu, D., Li, C., Chen, Y., et. al. Nuclear import of proinflammatory transcription factors is required for massive liver apoptosis induced by bacterial lipopolysaccharide. J Biol Chem. 2004; 279(46):48434-42.

70. Ren, Y.G., Wagner, K.W., Knee, D.A., et. al. Differential regulation of the TRAIL death receptors DR4 and DR5 by the signal recognition particle. Mol Biol Cell. 2004; 15(11):5064-74.

71. Uellner, R., Zvelebil, M.J., Hopkins, J., et. al. Perforin is activated by a proteolytic cleavage during biosynthesis which reveals a phospholipid-binding C2 domain. EMBO J. 1997; 16 (24):7287-96.

72. Asadullah, K., Friedrich, M., & Döcke, W.D., et. al. Enhanced expression of T-cell activation and natural killer cell antigens indicates systemic anti-tumor response in early primary cutaneous T-cell lymphoma. J Invest Dermatol. 1997; 108(5):743-7.

73. Trapani, J.A., & Smyth, M.J. Functional significance of the perforin/granzyme cell death pathway. Nat Rev Immunol. 2002; 2 (10):735-47.

74. Barry, M., & Bleackley, R.C. Cytotoxic T lymphocytes: all roads lead to death. Nat Rev Immunol. 2002; 2(6):401-9.
75. Armeanu, S., Bitzer, M., Lauer, U.M., et. al. Natural killer cell-mediated lysis of hepatoma cells via specific induction of NKG2D ligands by the histone deacetylase inhibitor sodium valproate. Cancer Res.2005; 65 (14): 6321–6329.
76. Skov, S., Pedersen, M.T., Andresen, L., et. al. Cancer cells become susceptible to natural killer cell killing after exposure to histone deacetylases inhibitors due to glycogen synthase kinase-3-dependent expression of MHC class I-related chain A and B. Cancer Res. 2005; 65 (23):11136–11145.
77. Christiansen, A.J., West, A., Banks, K.M. et. al. Eradication of solid tumors using histone deacetylase inhibitors combined with immune-stimulating antibodies. Proc Natl Acad Sci U S A. 2011;108 (10):4141-6.
78. Verma, R., Rigatti, M.J., Belinsky, G.S., et. al. DNA damage response to the Mdm2 inhibitor nutlin-3. Biochem Pharmacol. 2010 ;79(4):565-74.
79. Yale School of Medicine. Introduction to Flow Cytometry: A Learning Guide. Retrieved from: http://medicine.yale.edu/labmed/cellsorter/start/411_66019_Introduction.pdf
80. Herzenberg, L.A., Tung, J., Moore, W.A., et. al. Interpreting flow cytometry data: a guide for the perplexed. Nat Immunol. 2006; 7(7):681-5.
81. Qu, C.X., Wang, J.Z., Wan, W.H., et.al. Establishment of a flow cytometric assay for determination of human platelet glycoprotein VI based on a mouse polyclonal antibody. J Clin Lab Anal. 2006; 20(6):250-4.
82. Bicaku, E., Marchion, D.C., Schmitt, M.L., et.al. Selective inhibition of histone deacetylase 2 silences progesterone receptor-mediated signaling. Cancer Res 2008; 68: 1513-1519.
83. Munster, P.N., Thurn, K.T., Thomas, S., et.al. A phase II study of the histone deacetylases inhibitor vorinostat combined with tamoxifen for the treatment of patients with hormone therapy-resistance breast cancer. Br J Cancer 2011; 104: 1828-1835.

196

Chapter 9

Characterizing other natural product derivatives as anticancer agents: viridin

analogs

A. Introduction

Collaborations between the Wright and Anderson laboratories have led
to the development of tropolones as well as furanosteroidal natural product
derivatives as potential therapeutic agents for the treatment of infectious
diseases, cancer and neurodegenerative diseases (1, 2). The furanosteroidal
natural products (Figure 1), wortmannin and viridin, are potent antifungal
metabolites isolated from *Penicillium wortmannii* and *Gliocladium virens*
respectively (1, 3-5). We have recently reported our efforts to characterize
these viridin analogs as inhibitors of phosphoinositide 3-kinase (PI3K)
enzymes (1). Our interest in these viridin analogs as PI3K inhibitors stems
from several studies that indicate that small molecules capable of inhibiting
PI3K signaling show promising applications in a diverse number of
therapeutic areas including autoimmune disorders, cardiovascular diseases
and cancer (1, 3-11).

Both wortmannin and viridin are potent, irreversible, pan-PI3K inhibitors
with IC_{50} values of 2-10 nM (1). However, wortmannin has significant stability,
solubility and toxicity issues that limit its therapeutic uses (1, 3-5). Therefore,
the purpose of this chapter is to discuss the biological activities of viridin

analogs that were synthesized by the Wright laboratories with the goal of improving PI3K enzyme selectivity as well as antiproliferative activities in multiple cell lines.

a)   b)
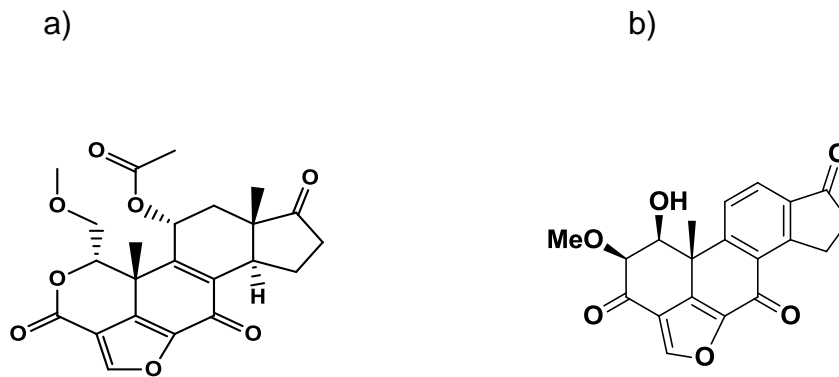
Figure 1: Structures of a) wortmannin and b) viridin

B. Biological and clinical significance of the PI3K signaling pathway

Cancer is a complex disease and there are multiple pathways that play important roles in carcinogenesis and mutagenesis (12). Since the discovery of the tyrosine kinase inhibitor Gleevec in 2001, there has been growing interest in protein and lipid kinases for the treatment of cancer and many other diseases (13-17). The PI3K signaling pathway is presumably the most commonly altered in human cancers (10, 18, 19). PI3Ks are a ubiquitously expressed family of enzymes that through the generation of phospholipids

serve as secondary messengers by modulating the levels of phosphotidylinasitol (PIs) in cells (1, 5, 10, 12, 17-20). PI3Ks influence many cellular functions including cell signaling, cell growth, cell-cycle progression, cell survival, motility, cell development and differentiation (7, 12, 17-20).

PI3Ks catalyze the phosphorylation of phosphoinositides from ATP to 3'-OH of the inositol ring for three different substrates: phosphotidylinasitol (PI), phosphatidyl inositol 4 phosphate (PI4P), and phosphatidyl inositol 4, 5-bisphosphate (PI(4, 5)P$_2$). Based on substrate specificity, PI3Ks are classified into three groups: I, II, III. (1, 5, 5, 19, 20). Class I PI3Ks are the most studied and consist of heterodimeric proteins with a smaller 85 kDa regulatory domain and a larger 110 kDa catalytic subunit (10). Class I PI3Ks occur in four isoforms subdivided into Class 1a (p110α, p110β, & p110σ) and Ib (p110γ). Studies in gene-targeted mice have shown that class 1A PI3Ks, particularly p110α, are important for vascular development & angiogenesis (7-9). The constitutive activation of PI3K signaling usually seen in many cancers is presumably as a result of the simultaneous promotion of proliferation and inhibition of cell death (6). However, the cross inhibition that is often observed with protein kinases has also made it very difficult to develop selective PI3K inhibitors (1, 5, 8, 10, 11). Yet, many natural products and corresponding derivatives are currently being explored for the development of more effective lipid and protein kinase inhibitors that selectively target these kinases while maintaining therapeutic efficiency (1, 3, 5, 8-11, 17, 21-27).

C. Evaluation of biological activity

Key enzyme kinetic parameters values for the class I PI3K enzyme, p110α and the PI substrate were obtained via a luminescent assay that correlates kinase activity to luminescence. Detailed experimental methods are reported in Section N of the Materials and Methods Chapter. Assay data were analyzed via non-linear regression analysis (GraphPad Prism Software, Inc., CA; 28). Best fit values are highlighted in Table 1 and Figure 1. Standard error values are reported in the Appendix, Section 41.

	K_M (µM)	V_{max} (µM)	k_{cat} (s^{-1})	k_{cat} /K_M (M^{-1} s^{-1})
Table 1: Elucidation of key enzyme parameters for the class I PI3K enzyme, p110α and the PI substrate				
p110α	9.64 ± 1.93	3453.00 ± 90.94	5.96	617.875.10
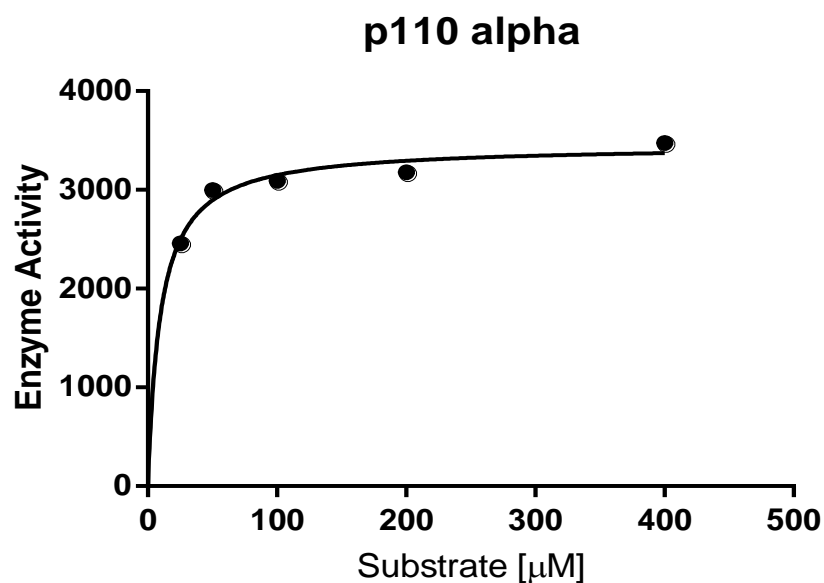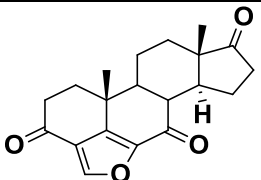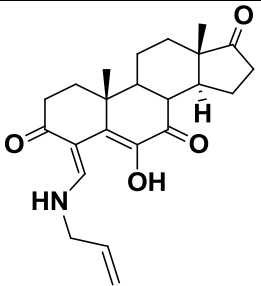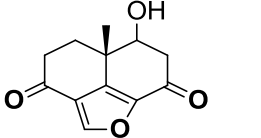
p110 alpha

Figure 2: Non-linear regression analysis of p110-alpha activity.

We recently reported our evaluation of PI3K-alpha inhibition IC_{50} values for the three viridin analogs (compounds 1a, 2a, & 3a) using a luminescent assay that correlates kinase activity to luminescence (Table 2; 1). Detailed experimental methods are reported in Section O of the Materials and Methods Chapter. We converted IC_{50} values to K_i values, using methods described by Cheng and Prusoff (29). We also evaluated the antiproliferative effects in three cell lines: HCT116 colon cancer cell line, U87 glioblastoma cell line, and MCF-7 breast cancer cell line (Table 2; 1). All three viridin analogs exhibited submicromolar inhibition of PI3K-α even though the IC_{50} values obtained were not as low as that of wortmannin (IC_{50} = 11.9 nM).

201

Table 2: Elucidation of biological activity for viridin analogs[1].						
Compound	Structure	IC_{50}, p110α/p85α (nM)	K_i (nM)	GI_{50} (µM)		
		PI substrate		HCT116	U87	MCF-7
1a		338.9	284.1	>100	>100	22.9
2a		270.5	226.8	>100	>100	37.7
3a		177.5	148.8	>100	>100	>100
Wortmannin		11.9	9.99	>100	>100	>100

None of the compounds were able to inhibit the growth of the colon cancer cell line, HCT116; however, compound 1a and 2a inhibited growth of the MCF-7 breast cancer cell line with GI_{50} values of 22.9 µM and 37.7 µM respectively. Interestingly, a higher potency for PI3K-α inhibition resulted in reduced growth inhibition of the MCF-7 cells since compound 1a and 2a had higher IC_{50} values

202

for the PI3K-α relative to compound 3a and wortmannin respectively. Hence, our results are promising and show potential for further development of viridin analogs as targeted therapies for the treatment of cancer.

D. Conclusions and future directions

Natural products and corresponding derivatives have found diverse applications in the treatment of neurodegenerative diseases as well as in the treatment of various microbial diseases and cancer. Since the discovery of Gleevec in 2001, there has been a growing interest in the development of other kinase inhibitors for the treatment of many cancers. Small molecule inhibitors of the PI3K pathway show promise as anticancer agents but cross-inhibition that is often observed with protein kinases has also made it very difficult to develop selective PI3K inhibitors. Our viridin analogs are highly promising PI3K inhibitors that exhibit submicromolar inhibition of the class I PI3K enzyme, p110α. Unlike wortmannin, two of our analogs, 1a and 2a, also inhibited the growth of the MCF-7 breast cancer cell line. Future investigations will also explore the synthesis of structurally diverse viridin analogs as well as the inhibition of other PI3K isoforms and multiple cell lines for the evaluation of isozyme selectivity and cancer cell line selective cytotoxicity respectively by our current library.

E. Acknowledgments

We would like to thank Dr. Kishore Viswanathan for synthesis of the viridin analogs. We would also like to thank Dr. M. Kyle Hadden for the cytotoxicity data on MCF-7 cells.

F. References

1. Viswanathan, K., Ononye, S.N., Cooper, H.D., et. al. Viridin analogs derived from steroidal building blocks. Bioorg. Med. Chem. Lett. 2012; 22(22):6919-22.
2. Oblak, E.Z., Bolstad, E.S., Ononye, S.N., et.al. The Furan Route to Tropolones: Probing the anti-proliferative effects of β-thujaplicin analogs. J. Org. Biomol. Chem. 2012; 10(43):8597-604.
3. Wipf, P., & Halter, R.J. Chemistry and biology of Wortmannin. Org Biomol Chem. 2005; 3(11):2053-61.
4. Anderson, E.A., Alexanian, E.J., & Sorensen, E.J. Synthesis of the furanosteroidal antibiotic viridin. Angew Chem Int Ed Engl. 2004; 43(15):1998-2001.
5. Sundstrom, T.J., Anderson, A.C., & Wright, D.L. Inhibitors of phosphoinositide-3-kinase: a structure-based approach to understanding potency and selectivity. Org. Biomol. Chem. 2009; 7: 840–850
6. Vanhaesebroeck, B., Leevers, S.J., Ahmadi, K., et. al. Synthesis and function of 3-phosphorylated inositol lipids. Annu Rev Biochem 2001; 70(7): 535-602.
7. Sliva, D. Signaling pathways responsible for cancer cell invasion as targets for cancer therapy. Curr Cancer Drug Targets 2004; 4(4): 327-36.
8. Zask, A., Verheijen, J.C., & Richard, D.J. Recent advances in the discovery of small-molecule ATP competitive mTOR inhibitors: a patent review. Expert Opin. Ther. Patents 2011; 21(7): 1109-1127.
9. Arteaga,C.L. Clinical Development of Phosphatidylinositol-3 Kinase Pathway Inhibitors. Curr Top Microbiol Immunol. 2010; 347: 189-208.
10. Zask, A. Recent advances in the discovery of small-molecule ATP competitive mTOR inhibitors: a patent review. Expert Opin. Ther. Patents 2011; 21(7): 1109-1127.
11. Zhang, F., Zhang, T., Jiang, T., et.al. Wortmannin potentiates roscovitine-induced growth inhibition in human solid tumor cells by repressing PI3K/Akt pathway. Cancer Letters 2009; 28: 232–239.
12. Weinberg, R. The Biology of Cancer. New York, NY: Garland Science, Taylor & Francis Group, LLC., 2007.

13. U.S. Food and Drug Administration. Gleevec (Imatinib Mesylate). Retrieved from http://www.fda.gov/drugs/drugsafety/postmarketdrugsafetyinformationforpatientsandproviders/ucm110502.htm
14. National Cancer Institute. FDA Approves Important New Leukemia Drug. Retrieved from http://www.cancer.gov/newscenter/newsfromnci/2001/gleevecpressrelease
15. U.S. Food and Drug Administration. FDA approves Gleevec for expanded use in patients with rare gastrointestinal cancer. Retrieved from http://www.fda.gov/NewsEvents/Newsroom/PressAnnouncements/ucm289760.htm
16. U.S. Food and Drug Administration. FDA approves Gleevec for children with acute lymphoblastic leukemia. Retrieved from http://www.fda.gov/NewsEvents/Newsroom/PressAnnouncements/ucm336868.htm
17. Willems, L., Tamburini, J., Chapuis, N., et. al. PI3K and mTOR signaling pathways in cancer: new data on targeted therapies. Curr Oncol Rep. 2012; 14(2):129-38.
18. Rameh, L.E., & Cantley, L.C. The role of phosphoinositide 3-kinase lipid products in cell function. J Biol Chem. 1999; 274(13): 8347-50.
19. Okkenhaug, K. & Vanhaesebroeck, B. PI3K in lymphocyte development, differentiation and activation. Nat Rev Immunol. 2003; 3(4): 317-30.
20. Cain, R.J., Vanhaesebroeck, B., & Ridley, A.J. The PI3K p110 alpha isoform regulates endothelial adherens junctions via Pyk2 and Racl. J. Cell Biol. 2010; 188 (6): 863–876.
21. Liu, J., Hu, Y., & Waller, D. L. Natural products as kinase inhibitors. Nat Prod Rep. 2012;29(3):392-403.
22. Harvey, A.L. Natural products in drug discovery. Drug Discov Today. 2008 : 13(19-20):894-901.
23. Cutler, S.J., & Cutler, H. G. Biologically active natural products: pharmaceuticals. CRC Press L.L.C., 2000.
24. Newman, D.J., & Cragg, G.M. Natural products as sources of new drugs over the last 25 years. J Nat Prod 2007; 70 (3): 461-477.
25. Baker, D.D., Chu, M., Oza, U., et. al. The value of natural products to future pharmaceutical discovery. Nat Prod Rep. 2007; 24(6):1225-44.
26. Martson, A. Natural products as a source of protein kinase activators and inhibitors. Curr Top Med Chem. 2011;11(11):1333-9.
27. García-Echeverría, C. Protein and lipid kinase inhibitors as targeted anticancer agents of the Ras/Raf/MEK and PI3K/PKB pathways. Purinergic Signal. 2009; 5(1): 117–125.
28. Williams, J. W., & Morrison, J. F. The kinetics of reversible tight-binding inhibition. Methods Enzymol. 1979; 63, 437-467.

205

29. Cheng, Y., & Prusoff, W.H. Relationship between the inhibition constant (Ki) and the concentration of inhibitor which causes 50 per cent inhibition (IC$_{50}$) of an enzymatic reaction. Biochem Pharmacol. 1973; 22(23): 3099-108.

Chapter 10

Comprehensive Analysis and Future Directions

A. Research summary and emerging directions

Cancer is the second leading cause of death in the United States and a major cause of death worldwide (1-5). The development of natural product derivatives for the treatment of cancer and many other diseases has been a trend in medicinal chemistry for over 25 years (6-19). Given that the PI3K signaling pathway is presumably the most commonly altered in human cancers (20-22), a biological analysis was performed on three furanosteroidal natural product derivatives synthesized by the Wright laboratory in order to evaluate enzyme inhibition and cytotoxicity in cultured human cancer cell lines. Evaluation of the three viridin analogs as PI3K inhibitors showed great promise particularly given submicromolar inhibition of a class I PI3K, p110α (23) . Unlike the well known, pan-PI3K inhibitor, wortmannin, two of the viridin analogs, 1a and 2a, also inhibited the growth of the MCF-7 breast cancer cell line (23). Future investigations will explore the synthesis of structurally diverse viridin analogs as well as the inhibition of other PI3K isoforms and multiple cell lines for the evaluation of isozyme selectivity and cancer cell line selective cytotoxicity respectively by our current library.

Alternatively, inhibitors that target major enzymes involved in epigenetic alterations, particularly HDACs, are also growing more popular in

cancer research because of the ability of these inhibitors to reversibly induce terminal differentiation of transformed cells presumably as a result of chromatin modulation (24-60). To date, two HDACi, Zolinza (vorinostat; SAHA) and Istodax (romidepsin) have been approved by the FDA for the treatment of cutaneous T-cell lymphoma (CTCL). Through an in-house collaborative effort, derivatives of hinokitiol (β-thujaplicin), a troplone-derived natural product are being developed by the Wright and Anderson laboratories as HDAC inhibitors (HDACi). Thujaplicins are a family of small tropolone-derived natural products that are associated with a wide range of biological effects (62-66).There are fourteen compounds currently in the tropolone library and the studies presented in this dissertation are the the first reported comprehensive analysis of tropolones as HDAC inhibitors.

Functional and biochemical studies were employed in this dissertation research to elucidate the mechanisms of action of fourteen tropolones as HDACi. Experimental data indicate that tropolones selectively target HDAC2 and HDAC8 in a competitive manner and at nanomolar potency. Mode of binding studies for compound 2 in HDAC8 suggest that tropolones inhibit HDACs in a competitive manner. Moreover, efforts are currently in place by the Anderson laboratory to gain further structural insights on HDAC8 binding by solving the three-dimensional crystal structure of the ACA-HDAC8 protein bound to a tropolone using preliminary methods for expression and purification described in this dissertation.

Furthermore, the tropolones show greater potency for HDAC2 inhibition relative to HDAC8. For example, compound 9 exhibits greater than 500-fold selectivity towards HDAC2 relative to HDAC8. This observation is highly promising and shows that it is possible to develop these tropolones as HDAC2-selective inhibitors particularly given that there are no reported HDAC2-selective inhibitors in pre-clinical and clinical development because of high degree of similarity in class I HDACs especially HDAC-1, -2, and -3 (33). Besides, it is well established that HDACi have multiple therapeutic purposes and have found success in the treatment of cancer, neurological disorders and neurodegenerative diseases (24-60).

Moreover, the natural product, hinokitiol (compound 10), has been shown to possess *in vitro* neuroprotective activity in HT22 cells, a neuronal cell line derived from mouse hippocampus that lack glutamate receptors (62). It is believed that the presence of the tropolone scaffold results in compounds with high potency against oxidative stress-induced cell death of HT22 cells that is typically implicated in Alzheimer's disease and many neurodegenerative disorders (62). Concurrently, HDAC2 inhibition has been shown to facilitate learning and memory in wild-type mice as well as in mouse models of neurodegeneration (26, 60). Our studies may have shown that the reported neuroprotective effects of hinokitiol may be as a result of HDAC2 inhibition but we cannot rule out the fact that other HDAC family members and nonhistone substrates may also be modulated by treatment with the

tropolones (62). Nevertheless, our preliminary assessments indicate that it is possible to explore the use of tropolones in the treatment of neurodegenerative diseases.

Tropolones also display cancer cell line selective cytotoxicity as evidenced by preferential inhibition to the two hematological cell lines, Jurkat and HuT-78. It can be deduced that selective HDAC inhibition may result in reduced toxicity profiles (25, 32-37, 41, 43-46, 49, 55, 57, 58, 67, 68) as further evidenced by biochemical data that shows that with the exception of compound 7, none of the tropolones exerted significant inhibition of the normal dermal fibroblasts unlike the pan-HDACi, SAHA. Tropolones also arrested the subdiploid phase of the cell cycle, usually viewed as an apoptotic index, in Jurkat and HuT-78 cells in a time-dependent manner. Furthermore, preliminary assessment of the extrinsic apoptotic pathway via caspase-8 activation by the tropolones did not show significant overexpression of caspase-8 in Jurkat cells when compared to the untreated control. However, the tropolones were shown to induce apoptosis via the intrinsic pathway of caspase-3/7 activation in Jurkat cells in a time-dependent manner

In a similar manner to SAHA, compound 2 was able to activate the differentiation of perforin in a time-dependent manner in Jurkat cells suggesting that tropolones may be able to execute cell death by apoptosis via the perforin/granzyme pathway (69-73). Moreover, HDAC inhibitors such as

210

valproic acid have been shown to improve sensitivity of Jurkat and humanhepatoma cells to natural killer (NK) cell-mediated killing (73, 74). Furthermore, studies in genetically identical murine tumor models of mammary, renal, prostate, and colorectal carcinomas have shown robust and prolonged eradication of solid tumors using SAHA combined with immune-stimulating antibodies, CD8(+) cytolytic T lymphocytes (CTL) that used perforin as the key immune effector molecule (75). These studies combined with the data on perforin differentiation by compound 2 suggest promising therapeutic applications and warrant further investigation of tropolones in combination with immune-activating antibodies for treatment of both solid tumors and hematological malignancies.

Histone acetylation is considered to be the most studied posttranslational modification (24, 51, 76); in addition to histones, HDACs modulate over 1700 nonhistone substrates including the structural protein, tubulin (77). Hyperacetylation of key lysine residues on histone H4 (H4K12) were observed in Jurkat cells and to a lesser extent in HuT-78 cells as a result of tropolone treatment (78). Interestingly, tropolone treatments in Jurkat and HuT-78 cells did not result in significant modulation of lysine residues on acetylated alpha-tubulins (Ac-α-tub-Lys40) typically indicative of HDAC6 inhibition (28, 68, 79-82). However, selective inhibition of class I HDAC enzymes, particularly HDAC8, is also associated with weak tubulin modulation (67); conversely, pan-HDACi and HDAC6-selective HDACi show

211

significant tubulin modulation as a result of HDAC6 hyperacetylation (28, 68). Hence, this observation supports our biochemical data that shows very poor inhibition of HDAC6 by the tropolones and further strengthens our claim on the isoform-selective nature of HDAC inhibition by the tropolones.

B. Distinct need for further evaluation of gene expression and analysis of drug-like properties

Elucidation of specific gene expression in both Jurkat and HuT-78 cells did not reveal any significant overexpression of the tumor-suppressor gene, p53, or CDKIs such as p15, p21 and p27. It may be possible that the inability of the tropolones to inhibit HDAC1 may hinder p21 activation since it has been reported that SAHA treatment in multiple myeloma cells resulted in a marked decrease in HDAC1 expression and a significant overexpression of p21 (83, 84). However, a more comprehensive analysis of tropolone-mediated gene expression via microarray analysis in normal and mutant Jurkat and/or HuT-78 cells as possibly in animal models will be required for a more precise evaluation of genes that are altered as a result of tropolone treatment (85). Moreover, gene expression analysis in mutant hematological cells that are deficient of or overexpressed with HDAC2 or HDAC8 may serve as further proof of concept for our claim on the isoform-selective nature of HDAC inhibition by the tropolones.

212

Elucidation of drug-like properties is an integral constituent of any drug discovery project (86). Preliminary assessment of toxicity in adult human dermal fibroblasts (hDF) indicates that selective HDAC inhibition by the tropolones may result in reduced toxicity profiles as evidenced by the fact that with the exception of compound 7, none of the tropolones showed significant inhibition of hDF unlike the pan HDAC inhibitor, SAHA (GI_{50} = 18.95 μM). However, despite the high potencies displayed against HDAC2 and HDAC8 in enzyme inhibition studies, the activities of tropolones within cell lines and possibly in future *in vivo* studies may be hindered by poor physicochemical properties such as permeability and chemical stability issues (86). Hence, current knowledge on the mechanisms of action of tropolones as HDACi will be strengthened by a better knowledge on the biochemical properties of the tropolones, particularly metabolism, as well as *in* vitro, and possibly *in* vivo, studies on pharmacokinetics and toxicity.

C. Proposed modification of the tropolone scaffold

Efforts are currently in place to develop a second generation library of tropolones using methods described in this dissertation that will potentially maintain isoform selectivity in HDAC inhibition while exerting a more robust therapeutic application particularly for the treatment of solid tumors and hematological malignancies. The proposed scaffold for second-generation tropolones (Figure 1) will now include a linker domain (the alkyl chain) that is

213

presumed to mimic the natural HDAC substrate and occupy the active site channel thus allowing for exploration for isozyme selectivity (24, 87).
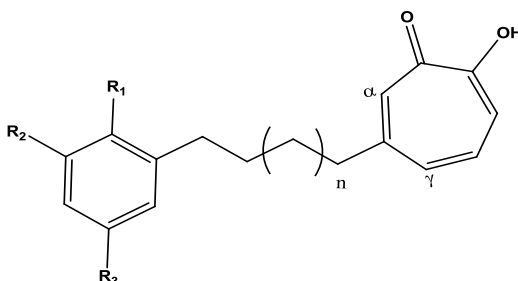
Figure 1: Proposed scaffold for 2nd generation tropolones

R groups will either be hydrogen atoms, alkyl groups, or aryl groups. The same substitutions will also be evaluated in the alpha and possibly gamma positions in order to elucidate SAR. Moreover, virtually all HDACi currently in clinical development for the treatment of cancer share this common pharmacophore pattern consisting of: a metal binding domain which complexes zinc; a linker domain and a surface domain or cap group, which makes contact with the rim of the catalytic pocket (24, 33, 87). Accordingly, the tropolone ring with the alpha-hydroxyl ketone will serve as the metal-binding domain, the alkyl chain will serve as the linker domain and the secondary aryl moiety will serve as the cap group. It is expected that modification of the tropolone scaffold may also lead to improvements in

214

pharmacokinetic properties that may improve *in vitro* potency & possibly *in vivo* efficacy (58).

D. Conclusions

Given the high incidence of cancer worldwide and growing interest in research on epigenetic alterations, a comprehensive investigation on the mechanisms of action of tropolones as HDACi was conducted via biochemical and functional studies. As a result of this dissertation research, several techniques that are relatively new to the Anderson laboratory have been developed for biochemical and functional analysis of HDAC inhibition by the tropolone library: 1) Evaluation of HDAC enzymatic activity and inhibition, 2) Investigation of antiproliferative effects via cytotoxicity assays and cell cycle analyses, 3) Elucidation of the induction and mechanisms of cell death by apoptosis, 4) Assessment of specific gene expression. The incorporation of these methods in present studies have improved understanding on the mechanisms of action of tropolones as isoform-selective HDACi and will also guide development of future tropolone libraries.

E. Final Acknowledgments

The research presented in this dissertation has truly been a multidisciplinary effort and I would like to thank the following individuals for their contribution. **Past and present members of the Anderson laboratory:** Dr. Kathleen Frey and Dr. Janet Paulsen for their assistance with HDAC8

215

F. References

1. Weinberg, R. The Biology of Cancer. New York, NY: Garland Science, Taylor & Francis Group, LLC., 2007.
2. The American Cancer Society. Cancer Facts and Figures 2013. Retrieved from http://www.cancer.org/acs/groups/content/@epidemiologysurveilance/documents/document/acspc-036845.pdf
3. The American Cancer Society. Global Cancer Facts and Figures, 2nd Edition. Retrieved from http://www.cancer.org/acs/groups/content/@epidemiologysurveilance/documents/document/acspc-027766.pdf
4. World Health Organization. Cancer Key Facts. Retrieved from http://www.who.int/mediacentre/factsheets/fs297/en/index.html
5. National Institutes of Health, Cancer. Retrieved from http://www.ncbi.nlm.nih.gov/pubmedhealth/PMH0002267/

6. Harvey, A.L. Natural products in drug discovery. Drug Discov Today. 2008 : 13(19-20):894-901.
7. Cutler, S.J., & Cutler, H. G. Biologically active natural products: pharmaceuticals. CRC Press L.L.C., 2000.
8. Newman, D.J., & Cragg, G.M. Natural products as sources of new drugs over the last 25 years. J Nat Prod 2007; 70 (3): 461-477.
9. Russo, P., Frustaci, A., Fini, M., et. al. Multitarget drugs of plants origin acting on Alzheimer's disease. Curr Med Chem. 2013 Feb 14. [Epub ahead of print]
10. Baker, D.D., Chu, M., Oza, U., et. al. The value of natural products to future pharmaceutical discovery. Nat Prod Rep. 2007; 24(6):1225-44.
11. Liu, J., Hu, Y., & Waller, D. L. Natural products as kinase inhibitors. Nat Prod Rep. 2012;29(3):392-403.
12. Harvey, A.L. Natural products in drug discovery. Drug Discov Today. 2008 : 13(19-20):894-901.
13. Cutler, S.J., & Cutler, H. G. Biologically active natural products: pharmaceuticals. CRC Press L.L.C., 2000.
14. Newman, D.J., & Cragg, G.M. Natural products as sources of new drugs over the last 25 years. J Nat Prod 2007; 70 (3): 461-477.
15. Baker, D.D., Chu, M., Oza, U., et. al. The value of natural products to future pharmaceutical discovery. Nat Prod Rep. 2007; 24(6):1225-44.
16. Martson, A. Natural products as a source of protein kinase activators and inhibitors. Curr Top Med Chem. 2011;11(11):1333-9.
17. García-Echeverría, C. Protein and lipid kinase inhibitors as targeted anticancer agents of the Ras/Raf/MEK and PI3K/PKB pathways. Purinergic Signal. 2009; 5(1): 117–125.
18. Seidel, C., Schnekenburger, M., Dicato, M., et.al. Histone deacetylases modulators provided by Mother Nature. Genes Nutr 2012; 7:357-367.
19. Licciardi, P.V., Kwa, F.A., Ververis, K., et. al. Influence of natural and synthetic histone deacetylase inhibitors on chromatin. Antioxid Redox Signal. 2012; 17(2):340-54.
20. Rameh, L.E., & Cantley, L.C. The role of phosphoinositide 3-kinase lipid products in cell function. J Biol Chem. 1999; 274(13): 8347-50.
21. Okkenhaug, K. & Vanhaesebroeck, B. PI3K in lymphocyte development, differentiation and activation. Nat Rev Immunol. 2003; 3(4): 317-30.
22. Zask, A., Verheijen, J.C., & Richard, D.J. Recent advances in the discovery of small-molecule ATP competitive mTOR inhibitors: a patent review. Expert Opin. Ther. Patents 2011; 21(7): 1109-1127.
23. Viswanathan, K., Ononye, S.N., Cooper, H.D., et. al. Viridin analogs derived from steroidal building blocks. Bioorg. Med. Chem. Lett. 2012; 22(22):6919-22.

24. de Ruijter, A.J., van Gennip, A.H., Caron, H.N. et al. Histone deacetylases (HDACs): characterization of the classical HDAC family. Biochem J, 2003. 370: 737-49.
25. Hu, E., Chen, Z., Fredrickson, T., et al. Identification of novel isoform-selective inhibitors within class I histone deacetylases. J Pharmacol Exp Ther 2003; 307 (2): 720-8.
26. Chuang, D., Leng, Y., Marinova, Z., et. al. Multiple roles of HDAC inhibition in neurodegenerative conditions. Trends Neurosci. 2009; 32(11):591-601.
27. Gore, S.D., Weng, L.J., Figg, W.D., et.al. Impact of prolonged infusions of the putative differentiating agent sodium phenylbutyrate on myelodysplastic syndromes and acute myeloid leukemia, Clin Cancer Res. 2002; 8(4):963-70.
28. Kaliszczak, M., Trousil, S., Aberg, O., et. al. A novel small molecule hydroxamate preferentially inhibits HDAC6 activity and tumour growth. Br J Cancer. 2013; 108 (2):342-50.
29. Hrebackova, J., Hrabeta, J., Eckschlager, T., et.al. Valproic acid in the complex therapy of malignant tumors. Curr Drug Targets. 2010; 11(30): 361-379.
30. Jeong, M.R., Hashimoto, R., Senatorov, V.V., et al. Valproic acid, a mood stabilizer and anticonvulsant, protects rat cerebral cortical neurons from spontaneous cell death: a role of histone deacetylase inhibition. FEBS Lett 2003; 542:74–78.
31. Ouaissi, M., & Ouaissi, A. Histone deacetylase enzymes as potential drug targets in cancer and parasitic diseases.J Biomed Biotechnol. 2006;2006(2):13474.
32. Marks, P.A. & Dokmanovic, M. Histone deacetylase inhibitors: discovery and development as anticancer agents. Expert Opin Investig Drugs 2005; 14(12): 1497-511.
33. Ononye, S.N., van Heyst, M., Falcone, E., et.al. Toward isozyme selective histone deacetylase inhibitors as therapeutic agents for the treatment of cancer. Pharm. Patent Analyst 2012; 1 (2), 207-221.
34. Lemoine, M., & Younes, A. Histone deacetylase inhibitors in the treatment of lymphoma. Discov Med. 2010; 10 (54): 462-70.
35. Ouaissi, M., Giger, U., Sielezneff, I., et al. Rationale for possible targeting of histone deacetylase signaling in cancer diseases with a special reference to pancreatic cancer. J Biomed Biotechnol. 2011: 315939.
36. Frew, A.J., Johnstone, R.W, & Bolden, J.E. Enhancing the apoptotic and therapeutic effects of HDAC inhibitors. Cancer Lett. 2009; 280(2):125-33.
37. Ontoria, J.M., Altamura, S., Di Marco, A., et al. Identification of novel, selective, and stable inhibitors of class II histone deacetylases. Validation studies of the inhibition of the enzymatic activity of HDAC4 by small

molecules as a novel approach for cancer therapy. J Med Chem 2009; 52(21): 6782-9.

38. Zafar, S.F., Nagaraju, G.P., & El-Raves, B. Developing histone deacetylase inhibitors in the therapeutic armamentarium of pancreatic adenocarcinoma. Expert Opin Ther Targets. 2012; 16(7):707-18.

39. Weichert, W. HDAC expression and clinical prognosis in human malignancies. Cancer Letters. 2009; 280: 168-176.

40. Krennhrubec, K., Marshall, B.L., Hedglin, M., et al., Design and evaluation of 'Linkerless' hydroxamic acids as selective HDAC8 inhibitors. Bioorg Med Chem Lett, 2007; 17(10): 2874-8.

41. Estiu, G., West, N., Mazitschek, R., et al. On the inhibition of histone deacetylase 8. Bioorg Med Chem. 2010; 18 (11): 4103-10.

42. Garber, K. HDAC inhibitors overcome first hurdle. Nat Biotechnol 2007; 25(1): 17-9.

43. Marks, P., Rifkind, R.A., Richon, V.M., et. al. Histone deacetylases and cancer: causes and therapies. Nat Rev Cancer. 2001;1(3):194-202.

44. Noureen, N., H. Rashid, & Kalsoom, S. Identification of type-specific anticancer histone deacetylase inhibitors: road to success. Cancer Chemother Pharmacol. 2010; 66(4):625-33.

45. Paris, M., Porcelloni, M., Binaschi, M., et al. Histone deacetylase inhibitors: from bench to clinic. J Med Chem 2008; 51(6): 1505-29.

46. Dickinson, M., Johnstone, R.W., & Prince, H.M. Histone deacetylase inhibitors: potential targets responsible for their anti-cancer effect. Invest New Drugs. 2010; 28 Suppl 1:S3-20.

47. Morales, J.C., Ruiz-Magana, M.J., Carranza, D., et. al. HDAC inhibitors with different gene regulation activities depend on the mitochondrial pathway for the sensitization of leukemic T cells to TRAIL-induced apoptosis. Cancer Lett. 2010 ;297(1):91-100.

48. Shi, Z-J., Ouyang, D-Y., Zhu, J-S., et. al. Histone deacetylase inhibitor suberoylanilide hydroxamic acid exhibits anti-inflammatory activities through induction of mitochondrial damage and apoptosis in activated lymphocytes. Int Immunopharmacol. 2012; 12(4):580-7.

49. Bicaku, E., Marchion, D.C., Schmitt, M.L., et.al. Selective inhibition of histone deacetylase 2 silences progesterone receptor-mediated signaling. Cancer Res 2008; 68: 1513-1519.

50. Munster, P.N., Thurn, K.T., Thomas, S., et.al. A phase II study of the histone deacetylases inhibitor vorinostat combined with tamoxifen for the treatment of patients with hormone therapy-resistance breast cancer. Br J Cancer 2011; 104: 1828-1835.

51. Khan, O., & La Thangue, N.B. HDAC inhibitors in cancer biology: emerging mechanisms and clinical applications. Immunol Cell Biol. 2012; 90(1):85-94.

52. Khan, O., & La Thangue, N.B. Drug Insight: histone deactylase inhibitor-based therapies for cutaneous T-cell lymphomas. Nat Clin Pract Oncol. 2008;5 (12):714-26.

53. Hagelkruys, A., Sawicka, A., Rennmayr, M., et.al. The biology of HDAC in cancer: the nuclear and epigenetic components. Handb Exp. Pharmacol. 2011; 206: 13-37.

54. Schrump, D.S. Cytotoxicity Mediated by Histone Deacetylase Inhibitors in Cancer Cells: Mechanisms and Potential Clinical Implications. Clin. Cancer. Res 2009; 15: 3947-3957.

55. Dokmanovic, M., C. Clarke, & Marks, P.A. Histone deacetylase inhibitors: overview and perspectives. Mol Cancer Res 2007; 5(10): 981-9.

56. Bolden, J.E., Peart, M.J., & Johnstone, R.W. Anticancer activities of histone deacetylase inhibitors. Nat Rev Drug Discov. 2006; 5(9):769-84.

57. Carafa, V., Miceli, M., Altucci, L., et. al. Histone deacetylase inhibitors: a patent review (2009 - 2011). Expert Opin Ther Pat. 2013 Jan;23(1):1-17.

58. Elaut, G., Rogiers, V., & Vanhaecke, T. The pharmaceutical potential of histone deacetylase inhibitors. Curr Pharm Des. 2007; 13(25):2584-620.

59. Dinarello, C.A., Fossati. G., & Mascagni, P. Histone deacetylase inhibitors for treating a spectrum of diseases not related to cancer. Mol Med. 2011; 17 (5-6):333-52.

60. Guan, J.S., Haggarty, S.J., Giacometti, E., et. al. HDAC2 negatively regulates memory formation and synaptic plasticity. Nature. 2009; 459 (7243):55-60.

61. Liu, S., & Yamauchi, H. Hinokitiol, a metal chelator derived from natural plants, suppresses cell growth and disrupts androgen receptor signaling in prostate carcinoma cell lines. Biochem Biophys Res Commun, 2006; 351(1): 26-32.

62. Koufaki, M., Theodorou, E., Alexi, X., et. al. Synthesis of tropolone derivatives and evaluation of their in vitro neuroprotective activity. Eur J Med Chem. 2010; 45(3):1107-12.

63. Liu, S., & Yamauchi, H. p27-Associated G1 arrest induced by hinokitiol in human malignant melanoma cells is mediated via down-regulation of pRb, Skp2 ubiquitin ligase, and impairment of Cdk2 function. Cancer Lett, 2009; 286(2): 240-9.

64. Matsumura, E., Morita, Y., Date, T., et al., Cytotoxicity of the hinokitiol-related compounds, gamma-thujaplicin and beta-dolabrin. Biol Pharm Bull, 2001; 24 (3): 299-302.

65. Morita, Y., Matsumura, E., Okabe, T., et al. Biological activity of alpha-thujaplicin, the minor component of Thujopsis dolabrata SIEB. et ZUCC. var. hondai MAKINO. Biol Pharm Bull, 2001; 24(6): 607-11.

66. Oblak, E.Z., Bolstad, E.S., Ononye, S.N., et.al. The Furan Route to Tropolones: Probing the anti-proliferative effects of β-thujaplicin analogs. J. Org. Biomol. Chem. 2012; 10(43):8597-604.

67. Balasubramanian, S., Ramos, J., Luo, W., et al. A novel histone deacetylase 8 (HDAC8)-specific inhibitor PCI-34051 induces apoptosis in T-cell lymphomas. Leukemia 2008; 22(5): 1026-34.
68. Jose, B., Okamura, S., Kato, T., et.al. Toward an HDAC6 inhibitor: synthesis and conformational analysis of cyclic hexapeptide hydroxamic acid designed from α-tubulin sequence. Bioorg Med Chem. 2004; 12(6):1351-6.
69. Uellner, R., Zvelebil, M.J., Hopkins, J., et. al. Perforin is activated by a proteolytic cleavage during biosynthesis which reveals a phospholipid-binding C2 domain. EMBO J. 1997; 16 (24):7287-96.
70. Asadullah, K., Friedrich, M., & Döcke, W.D., et. al. Enhanced expression of T-cell activation and natural killer cell antigens indicates systemic anti-tumor response in early primary cutaneous T-cell lymphoma. J Invest Dermatol. 1997; 108(5):743-7.
71. Trapani, J.A., & Smyth, M.J. Functional significance of the perforin/granzyme cell death pathway. Nat Rev Immunol. 2002; 2 (10):735-47.
72. Barry, M., & Bleackley, R.C. Cytotoxic T lymphocytes: all roads lead to death. Nat Rev Immunol. 2002; 2(6):401-9.
73. Armeanu, S., Bitzer, M., Lauer, U.M., et. al. Natural killer cell-mediated lysis of hepatoma cells via specific induction of NKG2D ligands by the histone deacetylase inhibitor sodium valproate. Cancer Res.2005; 65 (14): 6321–6329.
74. Skov, S., Pedersen, M.T., Andresen, L., et. al. Cancer cells become susceptible to natural killer cell killing after exposure to histone deacetylases inhibitors due to glycogen synthase kinase-3-dependent expression of MHC class I-related chain A and B. Cancer Res. 2005; 65 (23):11136–11145.
75. Christiansen, A.J., West, A., Banks, K.M. et. al. Eradication of solid tumors using histone deacetylase inhibitors combined with immune-stimulating antibodies. Proc Natl Acad Sci U S A. 2011;108 (10):4141-6.
76. Galdieri, L., Moon, J., & Vancura, A. Determination of histone acetylation status by chromatin immunoprecipitation. Methods Mol Biol. 2012; 809:255-65.
77. Bradner, J.E., West, N., Grachan, M.L., et.al. Chemical phylogenetics of histone deacetylases. Nat Chem Biol. 2010; 6(3):238-243.
78. Zhou, B.O., Wang, S.S., Zhang, Y., et. al. Histone H4 lysine 12 acetylation regulates telomeric heterochromatin plasticity in Saccharomyces cerevisiae. PLoS Genet. 2011; 13; 7(1):e1001272.
79. Yang, X.J., & Gregoire, S. Class II histone deacetylases: from sequence to function, regulation, and clinical implication. Mol Cell Biol 2005; 25(8): 2873-84.

80. Westermann, S., & Weber, K. Post-translational modifications regulate microtubule function. Nat Rev Mol Cell Biol. 2003; 4(12):938-47.
81. Liu, Y., Peng, L., Seto, E., et.al. Modulation of histone deacetylase 6 (HDAC6) nuclear import and tubulin deacetylase activity through acetylation. J Biol Chem. 2012; 287 (34):29168-74.
82. Yang, X.J., & Gregoire, S. Class II histone deacetylases: from sequence to function, regulation, and clinical implication. Mol Cell Biol 2005; 25(8): 2873-84.
83. Gui, C-Y., Ngo, L., Xu, W.S., et. al. Histone deacetylase (HDAC) inhibitor activation of p21WAF1 involves changes in promoter-associated proteins, including HDAC1. Proc. Natl. Acad. Sci. USA 2004; 101:1241-1246.
84. Richon, V.M., Sandhoff, T.W., Rifkind, R.A., et. al. Histone deacetylase inhibitor selectively induces p21^{WAF1} expression and gene-associated histone acetylation.
Proc Natl Acad Sci U S A. 2000; 97(18): 10014–10019.
85. Khleif, S.N., & Curt, G.A. Animal Models in Developmental Therapeutics. In: Bast R.C. Jr., Kufe, D.W., Pollock, R.E., et al., editors. Holland-Frei Cancer Medicine. 5th edition. Hamilton (ON): B.C. Decker; 2000. Chapter 42. Retrieved from: http://www.ncbi.nlm.nih.gov/books/NBK20822/
86. Kerns, E., & Di, L. Drug-like Properties: Concepts, Structure Design and Methods from ADME to Toxicity Optimization. UK: Academic Press, 2008.
87. Huangfu, D., Maehr, R., Guo, W., et.al. Induction of pluripotent stem cells by defined factors is greatly improved by small-molecule compounds. Nat Biotechnol. 2008; 26 (7):795-7.

222

Chapter 11

Materials and Methods

A. Expression and purification of HDAC8

HDAC8 expression and purification was performed essentially as described by in reference 1. Briefly, mid-log phase BL21 DE3 *E. coli* cells were induced with one millimolar isopropyl-1-thio-β-D-galactopyranoside (IPTG) (3h, 225 rpm, 37°C) in LB media. Harvested bacteria were resuspended in the lysis buffer, BugBuster 10X Protein Extraction Reagent (EMD4 Biosciences, USA), incubated with DNase I (5 units/mL) and clarified by centrifugation at 35,000 × g for 1 h. The supernatant was then loaded into a Ni-NTA resin column preequilibrated in the wash buffer (50 mM Tris•HCl, pH 8.0/3 mM MgCl$_2$/300 mM KCl/20 mM imidazole/5% glycerol/1 mM 2-mercaptoethanol/PMSF). HDAC8 was eluted with 250 mM imidazole, then dialyzed against the final buffer (50 mM Tris•HCl, pH 8.0/50 mM KCl /5% glycerol/10 μM ZnCl$_2$/1 mM DTT). The HDAC8 protein (ACA-HDAC8) was then loaded onto a G75 26/60 gel filtration column (GE Healthcare Life Sciences, USA), equilibrated in the gel filtration buffer (50 mM Tris•HCl pH 8.0/150 mM KCl/5% glycerol/1 mM DTT) and stored at -80$^{\text{o}}$C.

B. HDAC Activity Assays for the elucidation of enzyme kinetic parameters

K_M and V_{max} values for one class I HDAC enzyme (HDAC8), two class IIa HDAC enzymes (HDAC4, HDAC5) and one class IIb HDAC (HDAC6) were determined using commercially available human recombinant HDAC enzymes (BPS Bioscience, San Diego, CA) and fluorogenic HDAC assay kits (BPS Bioscience). Kinetic parameters for two class I HDAC enzymes (HDAC1, HDAC2) were obtained using human recombinant HDAC enzymes (BPS Bioscience) and a fluorogenic HDAC assay kit (Active Motif, Carlsbad CA). Both fluorogenic assays work by utilizing a short, patented, peptide substrate containing an acetylated lysine residue that upon deacetylation by a HDAC enzyme results in the production of a fluorescent product with an excitation wavelength of 360 nm and an emission wavelength of 460 nm. Assay was performed at substrate concentrations of 25-400 μM according to the manufacturer's protocol. Best-fit values for K_M and V_{max} were determined via non-linear regression analysis (GraphPad Software, Inc., CA) and compared to published HDAC enzyme kinetics data (2, 3). Values for k_{cat} and k_{cat}/K_M were determined from the K_M and V_{max} values obtained for each HDAC isozyme using methods described in references 2 and 4.

224

C. HDAC Inhibition Assays for the determination of IC_{50} and K_i values

HDAC inhibition assays measured the half maximal inhibitory concentration, IC_{50}, for tropolones for or one class I HDAC enzyme (HDAC8), two class IIa HDAC enzymes (HDAC4, HDAC5) and one class IIb HDAC (HDAC6) using commercially available human recombinant HDAC enzymes (BPS Bioscience, San Diego, CA) and fluorogenic HDAC assay kits (BPS Bioscience). IC_{50} values for two class I HDAC enzymes (HDAC1, HDAC2) were obtained using human recombinant HDAC enzymes (BPS Bioscience) and a fluorogenic HDAC assay kit (Active Motif, Carlsbad CA). Both fluorogenic assays work by utilizing a short, patented, peptide substrate containing an acetylated lysine residue that upon deacetylation by a HDAC enzyme results in the production of a fluorescent product with an excitation wavelength of 360 nm and an emission wavelength of 460 nm. Assay was performed in replicates essentially as described in the manufacturer's protocol. The potent hydroxamic acid HDACi, Trichostatin A (TSA), provided in the assay kit, served as a control for the assays. DMSO, at the same percentage as is present in the compounds, showed no significant inhibition of HDAC enzymes. Assay data were analyzed via non-linear regression (GraphPad Software, Inc., CA). Best-fit values for IC_{50} were determined via non-linear regression analysis (GraphPad Software, Inc., CA) and compared to published IC_{50} data (2, 3, 5). The IC_{50} of the tropolones were converted to the inhibition

225

constant, K_i, for each of the inhibitors using the K_M value in accordance to techniques previously described by Cheng and Prusoff (6).

D. Mode of binding studies in HDAC8

The mechanism of action of compound 2 in HDAC8 (BPS Bioscience) was determined using four concentrations of the fluorogenic class IIa HDAC substrate (BPS Bioscience; 10 µM, 20 µM, 40 µM and 80 µM) against four inhibitor concentrations (0.5 nM, 1 nM, 2 nM, 4 nM). Enzyme parameters were analyzed via non-linear regression analysis (GraphPad Prism); the mixed model inhibition module on the GraphPad Prism software was used to determine the best fit value for the K_i, the alpha value, and concurrently determine the mode of binding of compound 2 in HDAC8 (7, 8). The parameter, alpha, ($K_i^{'}/K_i$) is used to determine the degree to which binding of an inhibitor changes the affinity of the enzyme for the substrate (7, 8).

E. Cell culture

All ten human cell lines were obtained from the American Type Culture Collection (ATCC; Manassas, VA) and maintained in a humidified incubator ($37^{o}C$, 5% CO_2) using ATCC recommendations and pertinent methods required for culturing human solid tumor and hematological cells (9). With the exception of HuT-78 and MCF-10A, all cell lines were supplemented with 10% fetal bovine serum (FBS; Atlanta Biologicals, Lawrenceville, GA). BXPC-3 and Jurkat cells were cultured in RPMI 1640 (ATCC) supplemented with 1%

226

penicillin/streptomycin (PEN-STREP; Mediatech Inc., Manassas, VA) and 1% L-Glutamine (L-Glut; Mediatech Inc.). HuT-78 cells were cultured in IMDM (ATCC) supplemented with 20 % FBS, 1% PEN-STREP (Mediatech Inc.) and 1% L-Glut (Mediatech Inc.). HT-29 and HCT116 were cultured in McCoy's media (Life Technologies, Carlsbad CA) supplemented with 1% non-essential amino acids (NEAA; Mediatech Inc.) and 1 % PEN-STREP (Mediatech Inc.). MCF-7 cells were maintained in DMEM/F12 supplemented with 1% L-Glut and 1% PEN-STREP. MCF-10A cells were cultured with the MEGM kit (Lonza Biologics, Basel, Switzerland) supplemented with cholera toxins (Sigma Aldrich). MCF-10A cells were grown with the MEGM kit (Lonza, Switzerland) supplemented with 50 µg/mL cholera toxin (Sigma Aldrich, St. Louis, MO). U87 cells were cultured in MEM supplemented with 10% FBS. A549 were cultured in F-12 media supplemented with 10% FBS. Normal human adult dermal fibroblasts (hDF) were maintained in DMEM supplemented with 10% FBS. Vorinostat (SAHA), (Z)-4-hydroxytamoxifen, and wortmannin were obtained from Sigma Aldrich.

F. Cell viability assay

Confluent Jurkat and HuT-78 cells were seeded in triplicate at a density of 5 x10^4 cells/well in 96-well culture plates (Corning Inc., Corning, NY). MCF-7 and MCF-10A cell lines were seeded in triplicate at a density of 1 x 10^4 cells/well in 96-well culture plates (Corning Inc.). HCT116, HT-29, BXPC-3,

227

U87, A549, and hDF cells were seeded in triplicate at a density of 5×10^3 cells/well in 96-well culture plates (Corning Inc.). Cells were treated accordingly at varying concentrations (1 μM-100 μM) of a tropolone, a furanosteroid, SAHA or wortmannin. DMSO served as a vehicle control. After a 72h exposure, cytotoxicity was evaluated using the Cell Titer 96 Aqueous One kit (Promega, Madison, WI) according to the instructions of the manufacturer. Formazan content was determined by measuring the absorbance at 490 nm on an Infinite M200 microplate reader (Tecan Group Ltd., Switzerland). Assay data were analyzed via nonlinear regression analysis (GraphPad Software, Inc.) and best fit values for growth inhibition was compared to published data for the experimental controls (SAHA or wortmannin) when possible (10-17).

G. Analysis of histone and tubulin modification

Approximately 1×10^6 logarithmic-phase Jurkat and HuT-78 cells were treated with either a tropolone or SAHA for the applicable treatment period in 6-well culture plates (Corning Inc.). Control wells contained no HDACi. After pertinent exposure, cells were harvested using applicable methods described in reference 9. Harvested cells were chilled on ice for 10 min, washed with phosphate-buffered saline (PBS) and fixed with 4 % (w/v) paraformaldehyde (PFA) for 20 min. Fixed cells were resuspended in 5 % BSA/PBS and stored

228

overnight at 4°C. Cells were permeabilized with PBS plus 0.5 % (v/v) Triton-X-100, washed and blocked with 10 % normal goat serum.

Cells were then incubated with either H3K9Ac, H3K23Ac, H4K12Ac or Ac-α-Tub-K40 using primary antibodies purchased from Cell Signaling Technology (Beverly, MA) at a 1:100 dilution in 5 % BSA/PBS and a fluorescein isothiocyanate (FITC) conjugated secondary antibody (Millipore,Billerica, MA) at a 1:1000 dilution in 5 % BSA/PBS. Flow cytometric analysis has been shown to be a reliable method for evaluating epigenetic alterations including histone acetylation (18-20). Hence, following staining, cells were evaluated for fluorescence in-house at the at the UConn Flow Cytometry and Confocal Microscopy (FCCM) Facility using the Becton Dickinson (BD) FACSCalibur Flow Cytometer (San Jose, CA). Values for the geometric mean fluorescence intensities (GMFI), equivalent to the median cell population response, were obtained via analysis on the FlowJo Workstation (Treestar Inc., Ashland OR; 21-23).

H. Cell cycle Analyses

Approximately 1 x 10^6 logarithmic-phase HCT116, BXPC3, Jurkat and HuT-78 cells were treated with either a tropolone or SAHA for the relevant time period in 6-well culture plates (Corning Inc.). Control wells contained no HDACi. After pertinent exposure, cells were harvested using applicable methods described in reference 9. Harvested cells were washed with cold

phosphate-buffered saline (PBS). Cells were fixed with ice-cold 70 % ethanol, incubated at 4°C for several hours and incubated overnight at -20°C. Fixed cells were stained with 50 µg/mL of propidium iodide (Life Technologies) and 200 µg/mL of DNA-free RNAse A (Sigma Aldrich) and incubated in the dark for several minutes (24-26). Following staining, cells were analyzed for the distribution of DNA content in-house at the UConn FCCM Facility using the BD FACSCalibur Flow Cytometer. Percentages of cell populations in each cell cycle phase were calculated based on DNA content histograms with the aid of the FlowJo Workstation. Assay results were compared to published reports on cell cycle analysis for the experimental control, SAHA when possible (27-29).

I. Evaluation of specific gene expression

Approximately 1 x 10^6 logarithmic-phase Jurkat and/or HuT-78 cells were treated with either a tropolone or vorinostat for either 12h or 24h in 6-well culture plates (Corning Inc.). Control wells contained no HDACi. After pertinent exposure, cells were harvested using applicable methods described in reference 9. Harvested cells were chilled on ice for 10 min, washed with PBS and fixed with 4 % (w/v) paraformaldehyde (PFA) for 20 min. Fixed cells were resuspended in 5 % BSA/PBS and stored overnight at 4°C. Cells were permeabilized with PBS plus 0.5 % (v/v) Triton-X-100, washed and blocked with 10 % normal goat serum. Cells were then incubated with either perforin, p15, p21, p27, or p53 using primary antibodies purchased from Cell Signaling

Technology (Beverly, MA) at a 1:100 dilution in 5 % BSA/PBS and a FITC conjugated secondary antibody (Millipore,Billerica, MA) at a 1:1000 dilution in 5 % BSA/PBS. Following staining, cells were evaluated for fluorescence in-house at the UConn FCCM Facility using a BD FACSCalibur flow cytometer (21-23). Values for the geometric mean fluorescence intensities (GMFI), equivalent to the median cell population, were obtained via analysis on the FlowJo Workstation. Assay results were compared to published data when possible (30-32).

J. Reverse-transcription PCR and quantitative real-time PCR analysis

A quantitative real-time polymerase chain reaction (qRT-PCR) analysis was further used to validate p21 expression in Jurkat cells after a 24h treatment with compound 2 and SAHA (33-36). Briefly, 5 x10^6 treated Jurkat cells were harvested and washed with ice-cold PBS. RNA was isolated using the Trizol reagent (Life Technologies) according to the instructions of the manufacturer. Two micrograms of extracted RNA was subjected to reverse transcription using the Applied Biosystems High Capacity cDNA kit according to the manufacturer's instructions. Following the PCR reaction, Taqman gene expression systems (Applied Biosystems) for p21, HDAC2, vitamin D receptor (VDR) and beta-actin were prepared and added in triplicate to optical 96-well micro-titer plates (Applied Bioystems) containing one microliter of cDNA according to the instructions of the manufacturer. All cDNA samples were

231

synthesized in parallel and qRT-PCR was performed in triplicate on an Applied Biosystem's 7500 Fast Real-Time PCR system and software. Relative mRNA expression for p21, VDR and HDAC2 were normalized to β-actin levels.

K. Evaluation of induction of apoptosis

Approximately 1×10^6 logarithmic-phase Jurkat and HuT-78 cells were treated with either a tropolone or SAHA for the pertinent time period in 6-well culture plates (Corning Inc.). Approximately 5×10^5 MCF-7 cells were treated alone with either compound 2 or SAHA and/or in combination with (Z)-4-Hydroxytamoxifen, the active metabolite of the antiestrogen tamoxifen in 6-well culture plates (Corning Inc.) for 48h (37). Control wells contained no HDACi or 4-OH-tamoxifen. After exposure, cells were harvested using relevant technique for each cell line (9). Harvested cells were washed with cold PBS, and resuspended in Annexin-binding buffer [10 mM HEPES, 140 mM NaCl and 2.5 mM CaCl$_2$, pH 7.4]. Cells were stained with Annexin V conjugated with a fluorescein molecule (Life Technologies) according to the instructions of the manufacturer. Propidium iodide (PI; Life Technologies) was also added to the cell suspension as a dead cell indicator. Following staining, cells were analyzed for fluorescence in-house at the UConn FCCM Facility using a BD FACSCalibur flow cytometer (24, 33, 38, 39). Populations of cells were sorted with the aid of the FlowJo Workstation as follows: live cells [Annexin V (-), PI (-)]; early apoptotic cells [Annexin V (+), PI (-)]; late apoptotic/necrotic cells

232

[Annexin V (+), PI (+)]. Assay data were compared to published reports for the experimental control, SAHA when possible (37, 40).

L. Evaluation of Caspase-8 activation

Approximately 1 x10^6 logarithmic phase Jurkat cells were treated with either a tropolone or SAHA for 24h in 6-well culture plates (Corning Inc.). Untreated wells served as negative controls for the assay. Cells were harvested, washed with cold PBS and evaluated for caspase-8 activation via FACS analysis with the aid of a fluorescent inhibitor of caspases (FLICA) reagent (Vybrant FAM Caspase-8 assay kit, Life Technologies) according to the instructions of the manufacturer (41). Assay data were collected at the UConn FCCM using a FACSCalibur and data were analyzed on the FlowJo Workstation.

M. Caspase-3/7 Analysis

Approximately 2 x10^4 logarithmic phase Jurkat cells were treated in triplicate in 96-well culture plates with 10 μM of either tropolone or SAHA for the applicable time period. Untreated wells served as experimental controls for the assay. Following treatment, Caspase-3/7 activity was measured in Jurkat cells using the luminescent Caspase-Glo 3/7 assay (Promega) according to the manufacturer's instructions (42-44). The luminescent signal generated from the assay is correlated with caspase-3/7 activity and luminescence was measured using a Veritas Microplate reader (Promega).

233

N. PI3K enzyme activity assays

Key enzyme kinetic parameters (K_M, V_{max}, k_{cat}, k_{cat}/K_M) for the class Ia PI3K enzyme, p110α, was determined using a commercially available human recombinant enzyme (Sigma Aldrich) phosphatidyl inositol substrate (PI; Sigma Aldrich), and the luminescent ADP-Glo Kinase assay kit (Promega). Assay was performed in a black, flat bottom 96-well plate essentially as described by the manufacturer's protocol. Briefly, twenty five microliters of a reaction mixture containing 50 ng of PI3K enzyme, 25-400 μM of PI and 10 μM ATP (provided in the assay kit) was incubated for 1 hour at 37°C. The reaction mixture was cooled and incubated sequentially at room temperature with the ADP-Glo and Kinase Detection reagents in order to simultaneously convert ADP to ATP and allow the newly synthesized ATP to be measured using a luciferase/luciferin reaction. The luminescent signal generated from the assay is correlated with kinase activity and luminescence was measured using a Veritas Microplate reader (Promega). Assay data were subjected to non-linear regression analysis (GraphPad Software); k_{cat}/K_M values were calculated from best fit values for $K_{M\ and}\ V_{max}$ using methods described in reference 4.

O. PI3K enzyme inhibition assays

Enzyme inhibition assays were performed using a commercially available human recombinant Class I PI3K enzyme (p110α/p85α, Sigma Aldrich, St. Louis, MO), phosphatidyl inositol substrate (PI; Sigma Aldrich), and

the luminescent ADP-Glo Kinase assay kit (Promega, Fitchburg, WI). Wortmannin served as an experimental control. Assay was performed in replicates in a black, flat bottom 96-well plate essentially as described by the manufacturer's protocol. Briefly, twenty five microliters of a reaction mixture containing 0.5 nM to 25,000 nM concentrations of the compounds, 50 ng of PI3K enzyme, 50 μM of PI and 10 μM ATP (provided in the assay kit) was incubated for 1 hour at 37°C. The reaction mixture was cooled and incubated sequentially at room temperature with the ADP-Glo and Kinase Detection reagents in order to simultaneously convert ADP to ATP and allow the newly synthesized ATP to be measured using a luciferase/luciferin reaction. The luminescent signal generated from the assay is correlated with kinase activity and luminescence was measured using a Veritas Microplate reader (Promega). Assay data were subjected to non-linear regression analysis (GraphPad Software). Best fit values for IC_{50} values have been reported (16); IC_{50} values were also converted to K_i values using methods described in reference 6.

P. References

1. Vannini, A., Volpari, C., Filocamo, G., et al. Crystal structure of a eukaryotic zinc-dependent histone deacetylase, human HDAC8, complexed with a hydroxamic acid inhibitor. Proc Natl Acad Sci U S A 2004; 101(42): 15064-9.
2. Schultz, B.E., Misialek, S., Wu, J., et. al. Kinetics and comparative reactivity of human class I and class IIb histone deacetylases. Biochemistry 2004; 43(34):11083-91.

3. Bradner, J.E., West, N., Grachan, M.L., et.al. Chemical phylogenetics of histone deacetylases. Nat Chem Biol. 2010; 6(3):238-243.

4. Williams, J. W., and Morrison, J. F. The kinetics of reversible tight-binding inhibition, Methods Enzymol. 1979; 63, 437-467.

5. BPS Bioscience HDAC screening and profiling. Retrieved from http://bpsbioscience.com/images/pdf/HDAC_profiling_Sheet.pdf

6. Cheng, Y., & Prusoff, W.H. Relationship between the inhibition constant (Ki) and the concentration of inhibitor which causes 50 per cent inhibition (IC_{50}) of an enzymatic reaction. Biochem Pharmacol. 1973; 22(23): 3099-108.

7. Copeland, R.A., Enzymes: A Practical Introduction to Structure, Mechanism and Data Analysis. 2000, 2nd Edition, Wiley.

8. Strelow, J., Dewe, W., Iversen, P.W., et.al., Mechanism of Action assays for enzymes. Retrieved from http://www.ncbi.nlm.nih.gov/books/NBK92001/

9. Masters, J.R., & Stacey, G.N. Changing medium and passaging cell lines. Nat Protoc. 2007;2(9):2276-84.

10. Huang, L., & Pardee, A. Suberoylanilide Hydroxamic Acid as a Potential Therapeutic Agent for Human Breast Cancer Treatment. Mol Med. 2000; 6 (10): 849-866.

11. Zhang, Q-L, Wang, L., Zhang, J.W., et.al. The proteasome inhibitor bortezomib interacts synergistically with the histone deacetylase inhibitor suberoylanilide hydroxamic acid to induce T-leukemia/lymphoma cells apoptosis. Leukemia 2009; 23 (8): 1507–1514.

12. LaBonte, M.J., et.al. DNA microarray profiling of genes differentially regulated by the histone deacetylase inhibitors vorinostat and LBH589 in colon cancer cell lines. BMC Med Genomics 2009; 2:67

13. Ulrike, H., Rademacher, J., Lamottke, B., et.al. Synergistic interaction of the histone deacetylase inhibitor SAHA with the proteasome inhibitor bortezomib in cutaneous T cell lymphoma. Eur J Haematol 2009; 82 (6): 440–449.

14. Wozniak, M.B., Villuendas, R., Bischoff, J.R., et.al. Vorinostat interferes with the signaling transduction pathway of T-cell receptor and synergizes with phosphoinositide-3 kinase inhibitors in cutaneous T-cell lymphoma.

15. Oblak, E.Z., Bolstad, E.S., Ononye, S.N., et.al. The Furan Route to Tropolones: Probing the anti-proliferative effects of β-thujaplicin analogs. J. Org. Biomol. Chem. 2012; 10 (43):8597-604.

16. Viswanathan, K., Ononye, S.N., Cooper, H.D., et. al. Viridin analogs derived from steroidal building blocks. Bioorg. Med. Chem. Lett. 2012 Nov 15;22(22):6919-22.

17. Wipf, P., & Halter, R.J. Chemistry and biology of Wortmannin. Org Biomol Chem. 2005; 3(11):2053-61.

18. Ronzoni, S., Faretta, M., Ballarini, M.., et.al. New method to detect histone acetylation levels by flow cytometry. Cytometry Part A 2005; 66A (1): 52-61.
19. Obier, N., & Muller, A.M. Chromatin flow cytometry identifies changes in epigenetic cell states. Cells Tissues Organs. 2010; 191(3):167-74.
20. Verma, R., Rigatti, M.J., Belinsky, G.S., et. al. DNA damage response to the Mdm2 inhibitor nutlin-3. Biochem Pharmacol. 2010 ;79(4):565-74.
21. Yale School of Medicine. Introduction to Flow Cytometry: A Learning Guide. Retrieved from http://medicine.yale.edu/labmed/cellsorter/start/411_66019_Introduction.pdf
22. Herzenberg, L.A., Tung, J., Moore, W.A., et. al. Interpreting flow cytometry data: a guide for the perplexed. Nat Immunol. 2006; 7(7):681-5.
23. Qu, C.X., Wang, J.Z., Wan, W.H., et.al. Establishment of a flow cytometric assay for determination of human platelet glycoprotein VI based on a mouse polyclonal antibody. J Clin Lab Anal. 2006; 20(6):250-4.
24. Ouaissi, M., Cabral, S., Tavares, J., et al. Histone deacetylase (HDAC) encoding gene expression in pancreatic cancer cell lines and cell sensitivity to HDAC inhibitors. Cancer Biol Ther. 2008; 7(4): 523-531.
25. Gong, J., Traganos, F., & Darzynkiewicz, Z. A Selective Procedure for DNA extraction from Apoptotic Cells Applicable for Gel Electrophoresis and Flow Cytometry. Anal Biochem. 1994; 218: 314-319.
26. Nicoletti I., Migliorati, G., Pagliacci, M.C., et.al. A rapid and simple method for measuring thymocyte apoptosis by propidium iodide staining and flow cytometry. J. Immunol Methods 1991; 139:271-279.
27. Zhu, P., Huber, E., Kiefer, F., et. al. Specific and redundant functions of histone deacetylases in regulation of cell cycle and apoptosis. Cell Cycle. 2004; 3(10):1240–1242
28. Zhou, Q., Dalgard, C.L., Wynder, C., et.al., Histone deacetylase inhibitors SAHA and sodium butyrate block G1-to-S cell cycle progression in neurosphere formation by adult subventricular cells. BMC Neurosci. 2011; 12:50.
29. Lobjois, V., Frongia, C., Jozan, S., et.al. Cell cycle and apoptotic effects of SAHA are regulated by the cellular microenvironment in HCT116 multicellular tumour spheroids. Eur J Cancer. 2009; 45(13):2402-11.
30. Wozniak, M.B., Villuendas, R., Bischoff, J.R., et.al. Vorinostat interferes with the signaling transduction pathway of T-cell receptor and synergizes with phosphoinositide-3 kinase inhibitors in cutaneous T-cell lymphoma.
31. Gui, C-Y., Ngo, L., Xu, W.S., et. al. Histone deacetylase (HDAC) inhibitor activation of p21WAF1 involves changes in promoter-associated proteins, including HDAC1. Proc. Natl. Acad. Sci. USA 2004; 101:1241-1246.
32. Almenara J, Rosato R, & Grant S. Synergistic induction of mitochondrial damage and apoptosis in human leukemia cells by flavopiridol and the

histone deacetylase inhibitor suberoylanilide hydroxamic acid (SAHA). Leukemia. 2002; 16(7):1331-43.

33. Spurling, C.C., Godman, C.A., Noonan, E.J., et. al. HDAC3 Overexpression and Colon Cancer Cell Proliferation and Differentiation, Mol. Carc. 2008; 43: 137-147.

34. Godman, C.A., Joshi, R., Tierney, B.R., et.al. HDAC3 impacts multiple oncogenic pathways in colon cancer cells with effects on Wnt and vitamin D signaling. Cancer Biol. & Ther. 2008; 7 (10): 1570-1580.

35. Ashihara, E. RNA Interference for Cancer Therapies. Gan To Kagaku Ryoho. 2010; 37(11):2033-41.

36. Bustin, S.A. Quantification of mRNA using real-time reverse transcription PCR (RT-PCR): trends and problems. Journal of Molecular Endocrinology 2002; 29: 23–39.

37. Bicaku, E., Marchion, D.C., Schmitt, M.L., et.al. Selective inhibition of histone deacetylase 2 silences progesterone receptor-mediated signaling. Cancer Res 2008; 68: 1513-1519.

38. Vermes, I., Haanen, H., Steffens-Nakken, H., et. al. A novel assay for apoptosis: Flow cytometry detection of phosphatidylserine expression on early apoptotic cells using fluorescein labeled annexin V. J Immunol Methods 1995; 184 (1):39-51.

39. Verhoven, B., Schlegel R.A., & Williamson, P. Mechanisms of phosphatidylserine exposure, a phagocyte recognition signal, on apoptotic T lymphocytes, J Experimental Med 1995;182 (5): 1597-601.

40. Shi, Z-J., Ouyang, D-Y., Zhu, J-S., et. al. Histone deacetylase inhibitor suberoylanilide hydroxamic acid exhibits anti-inflammatory activities through induction of mitochondrial damage and apoptosis in activated lymphocytes. Int Immunopharmacol. 2012; 12(4):580-7.

41. Smolewski, P., Grabarek, J, Halicka, H.D., et. al. Assay of caspase activation in situ combined with probing plasma membrane integrity to detect three distinct stages of apoptosis. J Immunol Methods. 2002; 265(1-2):111-21.

42. Liu, D., Li, C., Chen, Y., et. al. Nuclear import of proinflammatory transcription factors is required for massive liver apoptosis induced by bacterial lipopolysaccharide. J Biol Chem. 2004; 279(46):48434-42.

43. Ren, Y.G., Wagner, K.W., Knee, D.A., et. al. Differential regulation of the TRAIL death receptors DR4 and DR5 by the signal recognition particle. Mol Biol Cell. 2004; 15(11):5064-74.

44. Kaliszczak, M., Trousil, S., Aberg, O., et. al. A novel small molecule hydroxamate preferentially inhibits HDAC6 activity and tumour growth. Br J Cancer. 2013; 108 (2):342-50.

Appendix

	Class I HDAC			Class IIa HDAC		Class IIb HDAC
Kinetic Parameter	HDAC1	HDAC2	HDAC8	HDAC4	HDAC5	HDAC6
K_M (μM)	7.97	7.07	6.61	17.35	72.88	4.91
V_{max} (μM)	33.94	35.56	184.5	1130.00	242.4	340.60

1. Standard error values for elucidation of K_M and V_{max} values (Chapter 3, Table 2)

2. Graphs for Enzyme Kinetics (Chapter 3)

HDAC1 Kinetics

239

HDAC2 Kinetics
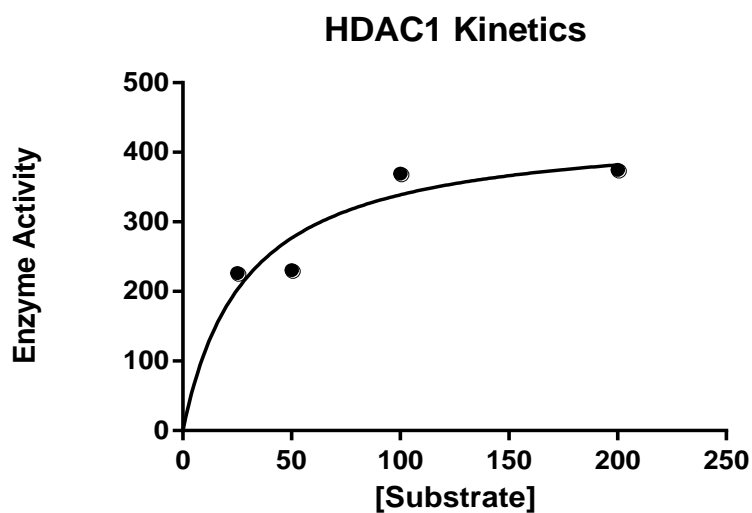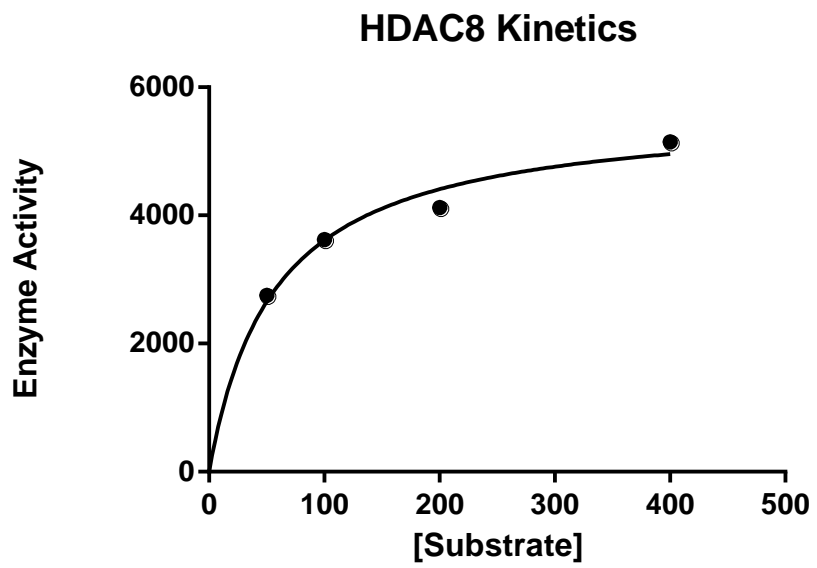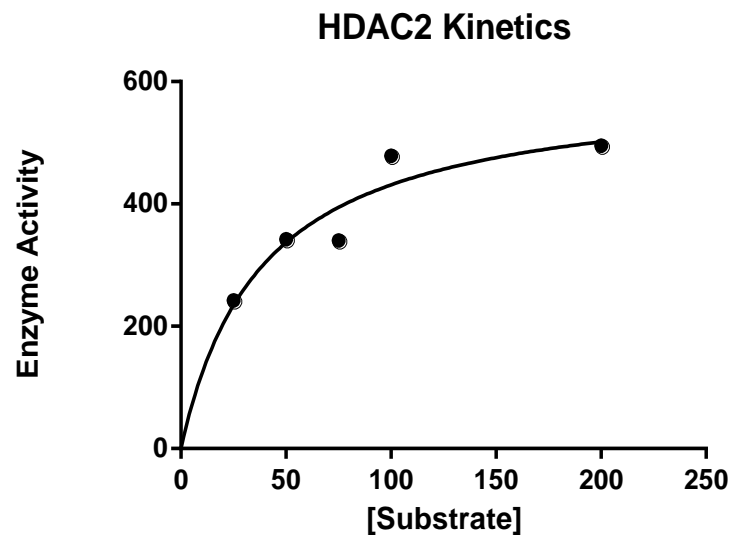
HDAC8 Kinetics

HDAC4 Kinetics
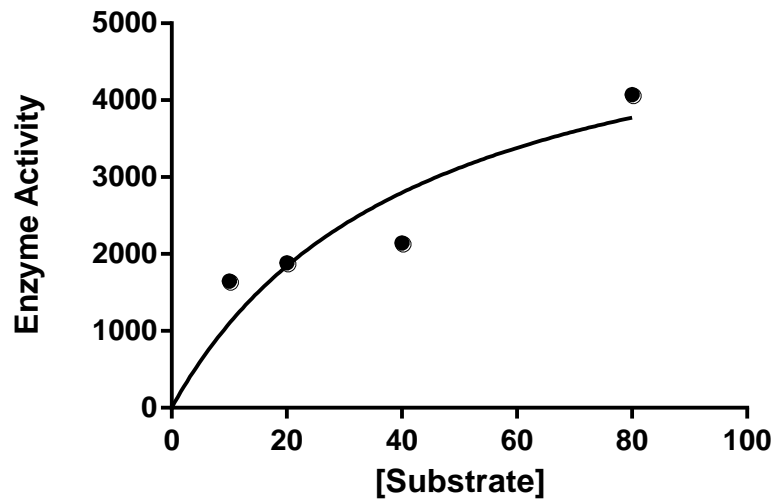
HDAC5 Kinetics

HDAC6 Kinetics
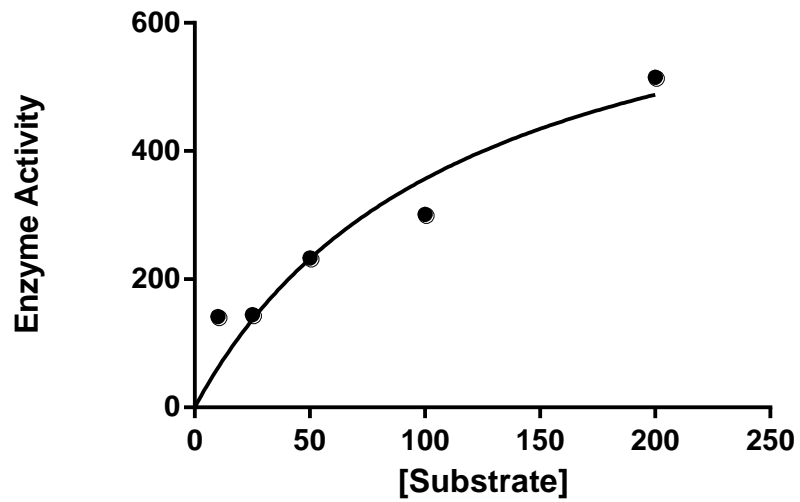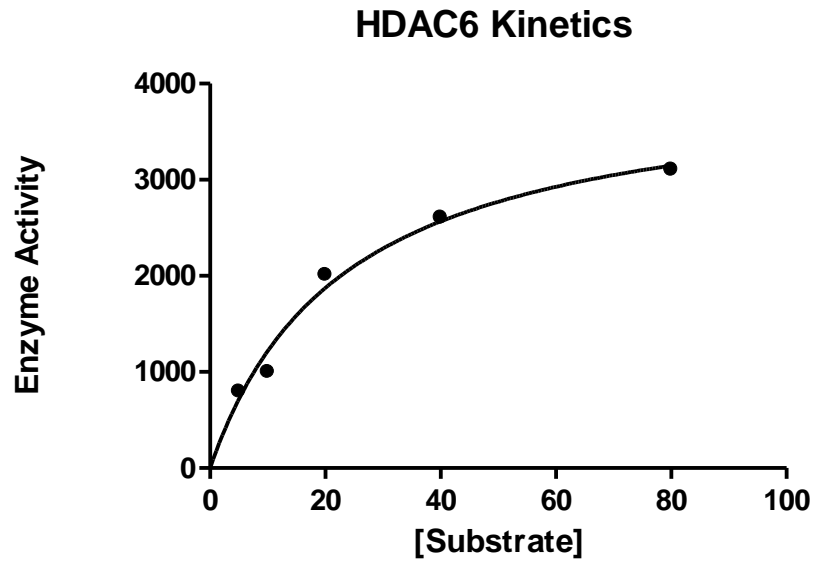
3. Standard error values for HDAC2 inhibition (Chapter 3, Figure 5a & 5b)	
Single time-point analysis	Comprehensive analysis
1.40	1.57

4. Standard error values for IC_{50} analysis of HDAC2 and HDAC8 (Chapter 3, Table 3)		
Compound	**HDAC2**	**HDAC8**
TSA	1.40	1.58
1	1.41	2.78
2	1.65	3.24
3	1.66	2.27
4	2.07	3.03
5	2.75	2.74
6	2.03	3.27
7	1.60	4.11
8	1.58	2.34
9	1.53	3.91
10	1.39	2.81
11	1.73	2.96
12	1.38	3.41
13	1.68	2.40
14	2.17	2.26

243

5. Standard error values for elucidation of calculated K_i and Alpha values for Compound 2 (Chapter 3, Figure 6)	
K_i	**Alpha**
0.52	6.46

6. Standard error values for determination of GI_{50} values for solid tumor cell lines (Chapter 4, Table 1)							
Compound	**HCT116**	**HT-29**	**BXPC-3**	**A549**	**U87**	**MCF-7**	**MCF-10A**
SAHA	1.19	1.18	1.19	1.49	1.27	1.28	1.20
1	1.24	1.00	1.75	1.00	1.66	1.24	1.23
2	1.16	1.46	1.32	1.47	1.44	1.24	1.16
3	1.25	1.42	1.27	1.62	1.00	1.78	1.21
4	1.26	1.26	1.20	1.30	1.65	1.49	1.19
5	1.22	1.22	1.39	1.44	1.00	1.48	1.13
6	1.19	1.19	1.36	1.45	1.69	1.17	1.27
7	1.21	1.41	1.29	1.40	1.27	1.38	1.37
8	1.28	1.28	1.42	1.62	1.00	1.51	1.13
9	1.34	1.34	1.67	3.03	1.00	1.00	1.22
10	1.19	1.15	1.27	1.36	1.00	1.46	1.40
11	2.23	1.51	1.00	1.00	2.06	1.00	1.19
12	1.19	1.40	1.39	1.23	2.54	2.27	1.19
13	1.16	1.31	1.52	1.29	1.78	1.16	1.29
14	1.29	1.29	1.60	1.30	1.91	1.45	1.20

244

7. Standard error values for determination of GI_{50} values for Jurkat, HuT-78 and hDF cells (Chapter 4, Table 2).			
Compound	**Jurkat**	**HuT-78**	**hDF**
SAHA	1.35	1.16	1.35
1	1.21	1.22	5.07
2	1.25	1.17	1.38
3	1.39	1.23	1.22
4	1.48	1.26	3.91
5	1.35	1.25	1.00
6	1.23	1.16	1.58
7	1.44	1.20	1.32
8	1.46	1.31	1.00
9	1.21	1.29	1.63
10	1.34	1.19	1.00
11	7.63	1.38	1.00
12	1.42	1.19	1.76
13	1.86	1.24	1.37
14	1.40	1.18	1.69

8. Modulation of histone H4 antibodies in Jurkat cells after a 12h treatment with HDACi (Chapter 5. Table 1). Note that histograms for the HDACi treatments represent the untreated control (red) superimposed with the HDACi treatment (blue) for comparative analysis.

a) Experimental/compensation controls [unlabeled cells (red); 2° antibody (green); untreated control (blue)].
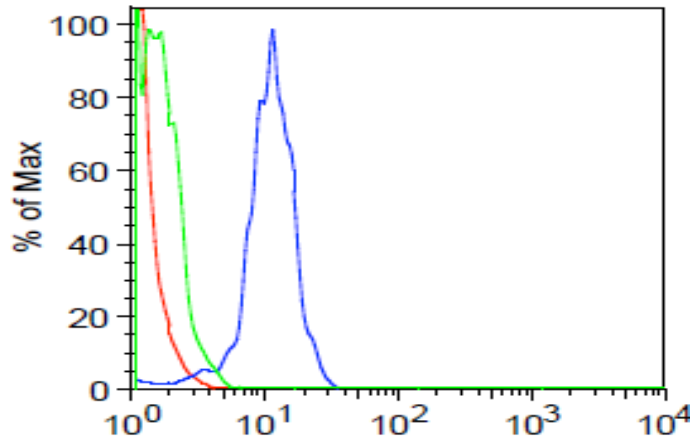

b)   SAHA treatment
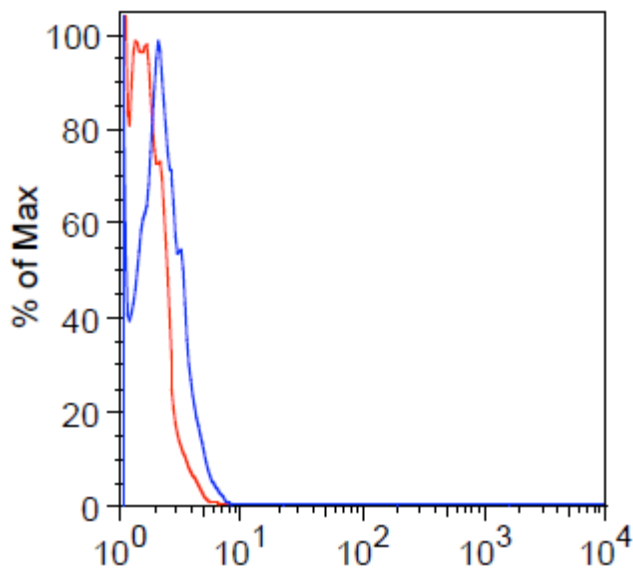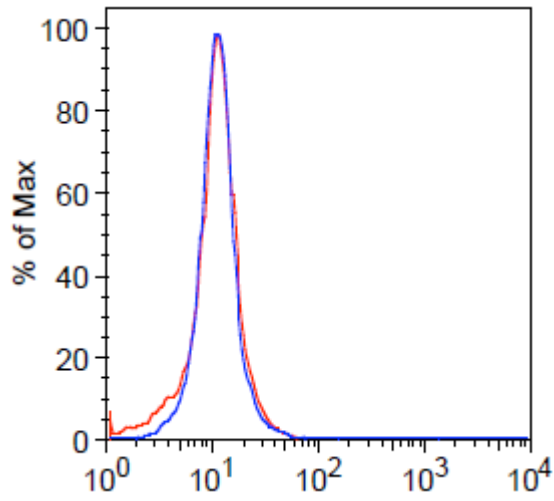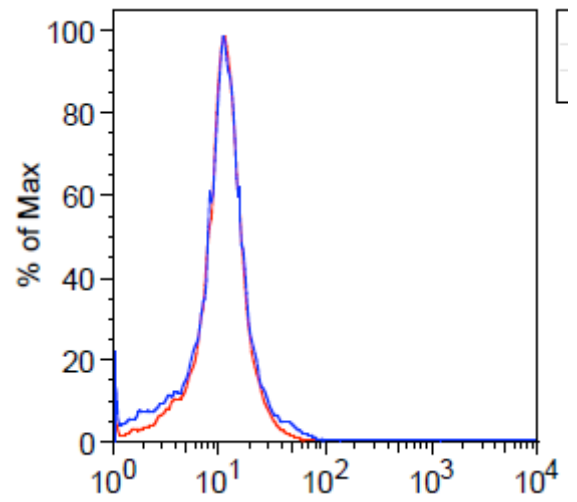
c)   Compound 2
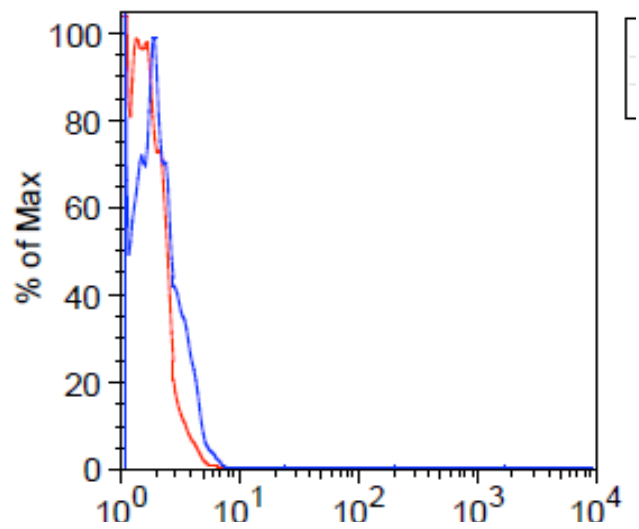
d)   Compound 5
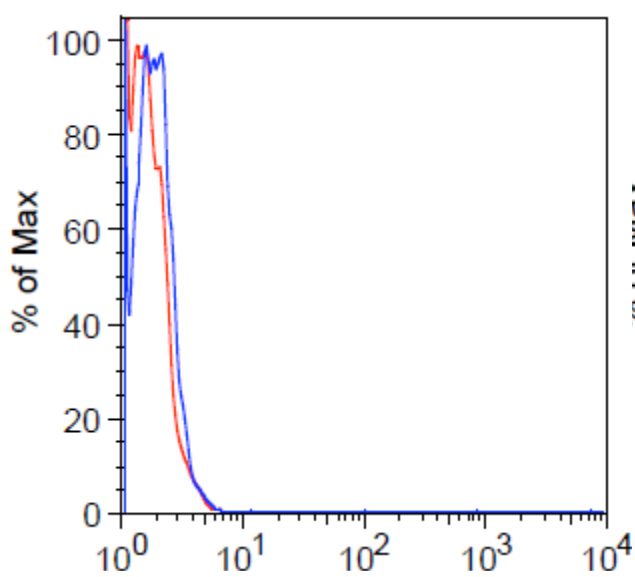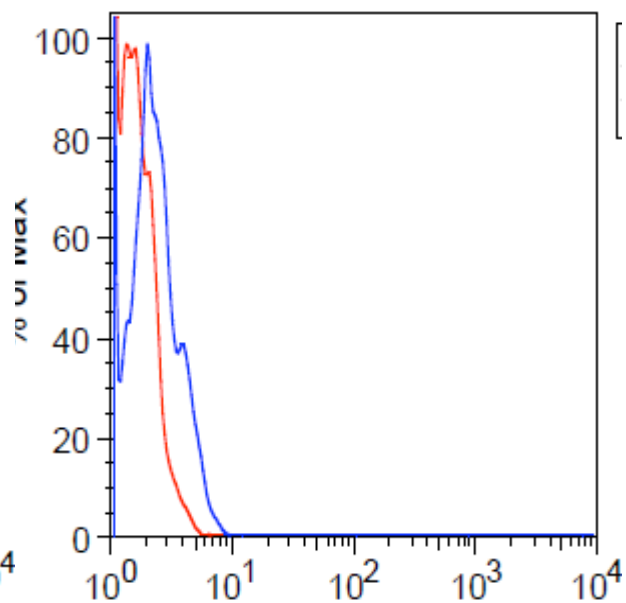
e)   Compound 7
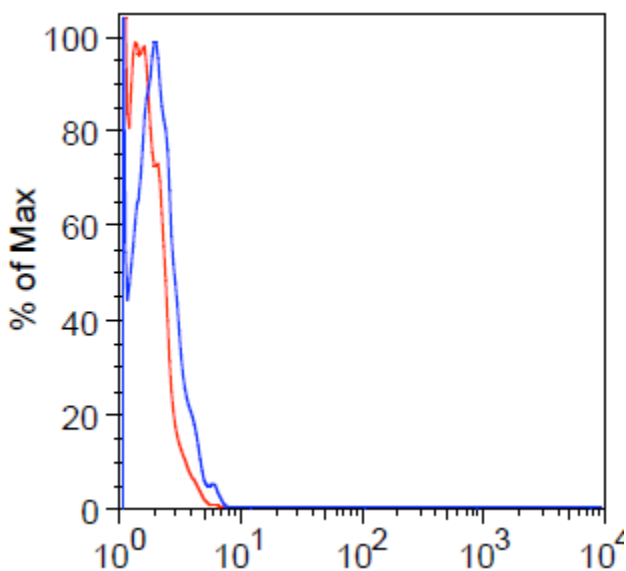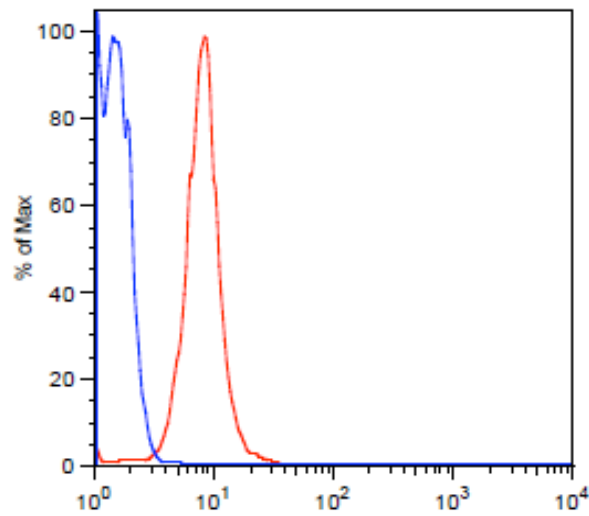
f)   Compound 9
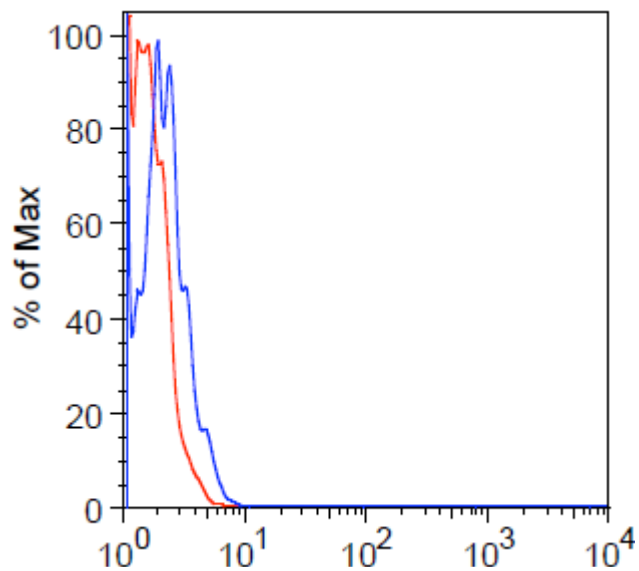
g)   Compound 10
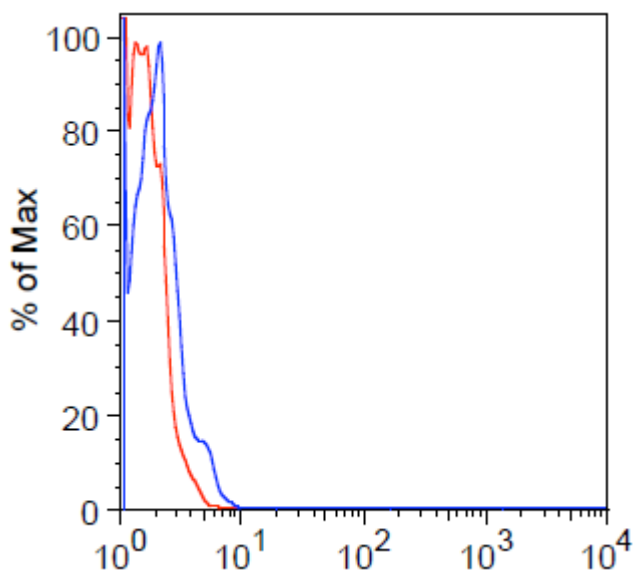
h)   Compound 11

i)   Compound 12
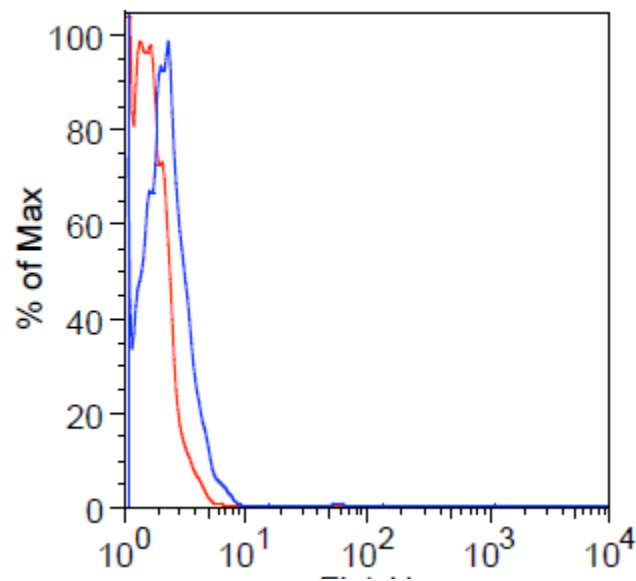
k)   Compound 14
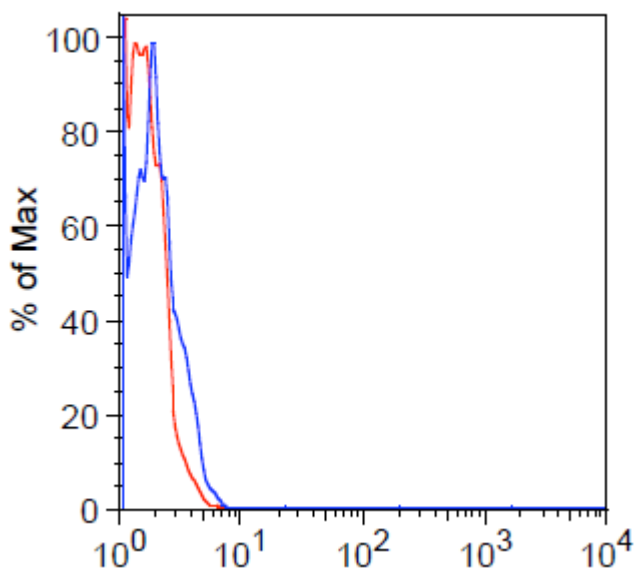
9. Comparative analysis of unlabeled cells (green), secondary (2°) antibody treatment only (blue) and the untreated control (primary (1°) + 2° antibody; red) for evaluation of H4K12Ac modulation in Jurkat cells treated with 10 µM HDACi for 12h (Chapter 5, Table 2).
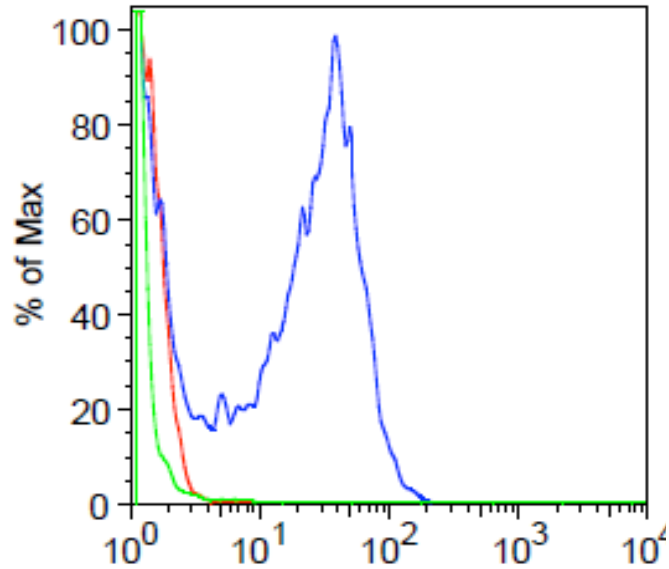
Modulation of histone H4K12Ac antibodies in Jurkat cells after a 4h treatment with HDACi (Chapter 5). **Note:** Untreated control for pertinent HDACi treatments represented in red and HDACi represented in blue on the corresponding histograms.

a) Experimental/compensation controls [unlabeled cells (green); 2° antibody (blue); untreated control (red)].

249

b)   10 µM SAHA

c)   25 µM Compound 2

d)   25 µM Compound 5

e)   25 µM Compound 7

250
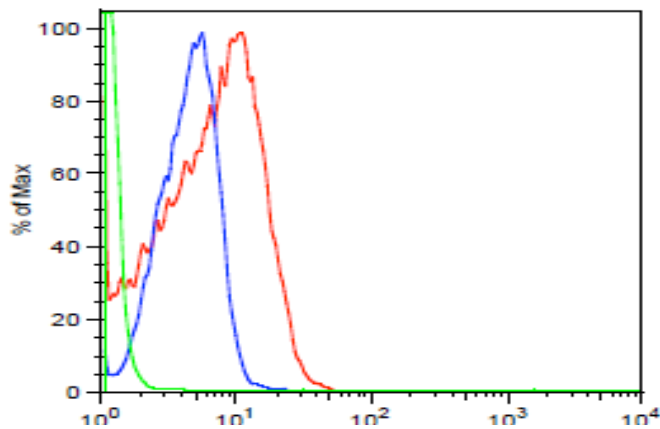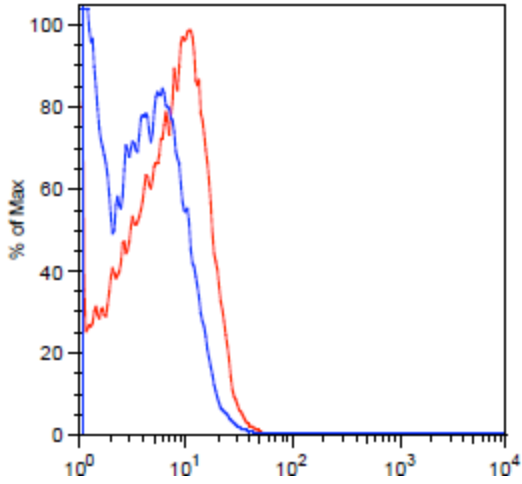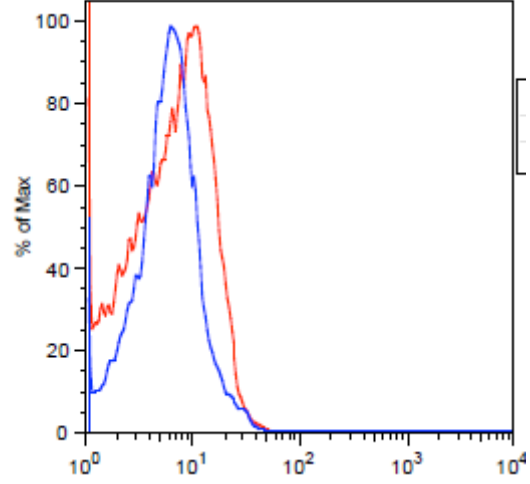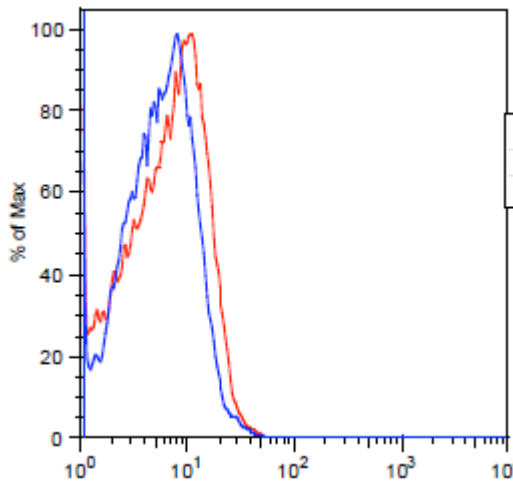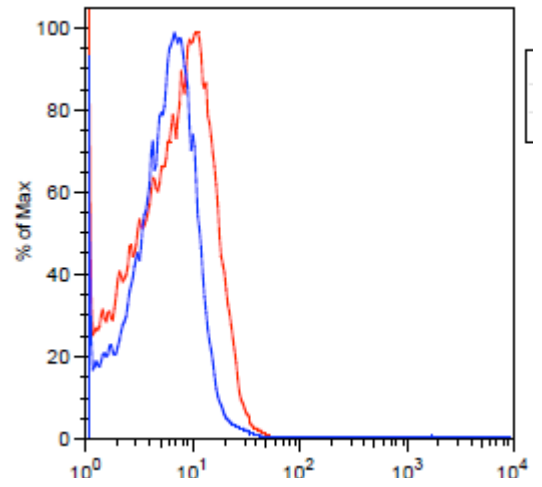
f)   25 µM Compound 9
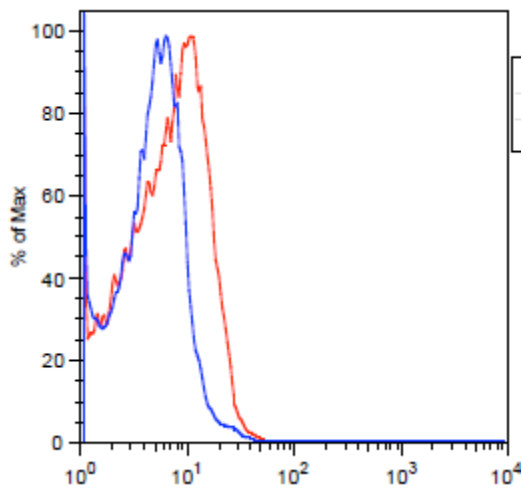
g)   25 µM Compound 10
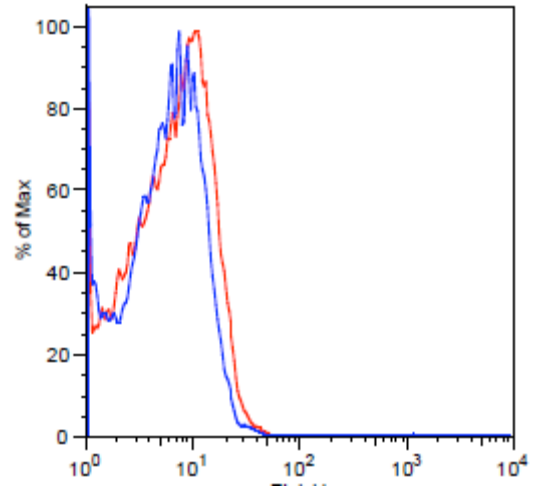
h)   25 µM Compound 11
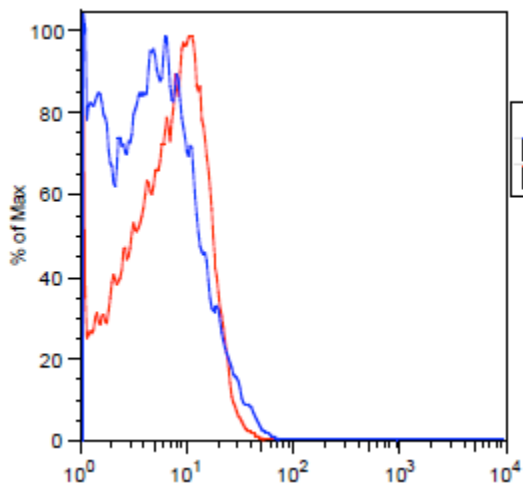
i)   25 µM Compound 13
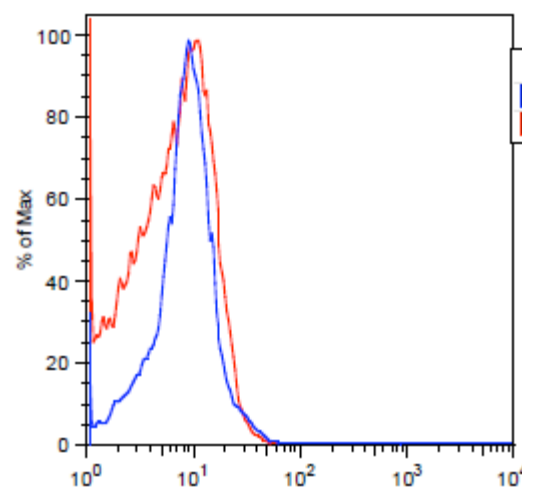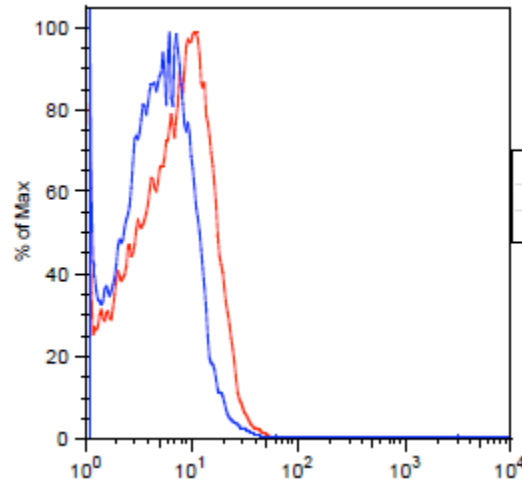
10. Modulation of histone H4K12Ac antibodies in Jurkat cells after a 12h treatment with 25 µM tropolones (Chapter 5, Table 3). **Note:** Untreated control for pertinent tropolone treatments represented in red and HDACi represented in blue on the corresponding histograms.

a) Experimental/compensation controls [unlabeled cells (red); 2° antibody (blue); untreated control (green)].
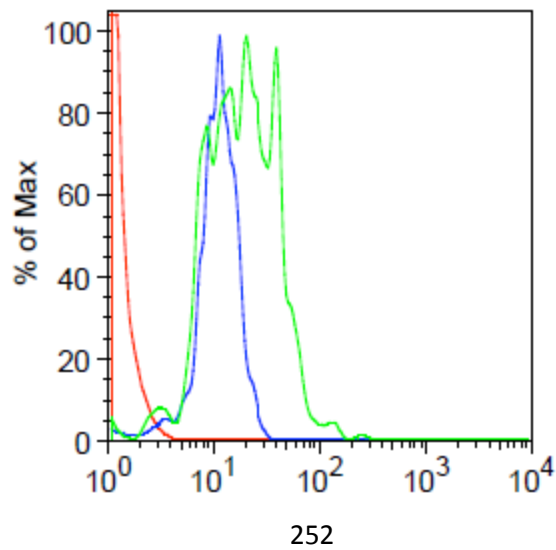
252

b)   SAHA
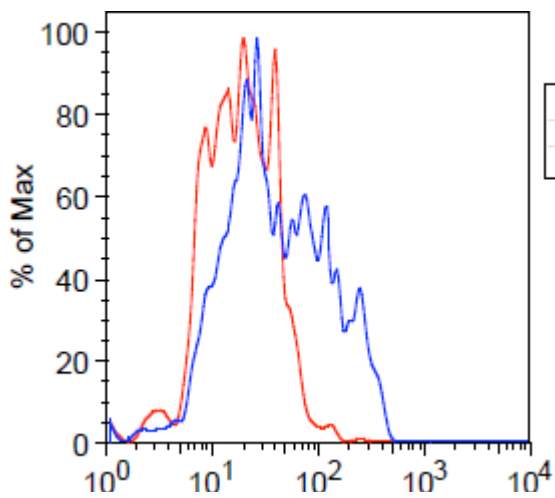
c)   Compound 2

d)   Compound 5

e)   Compound 7

253
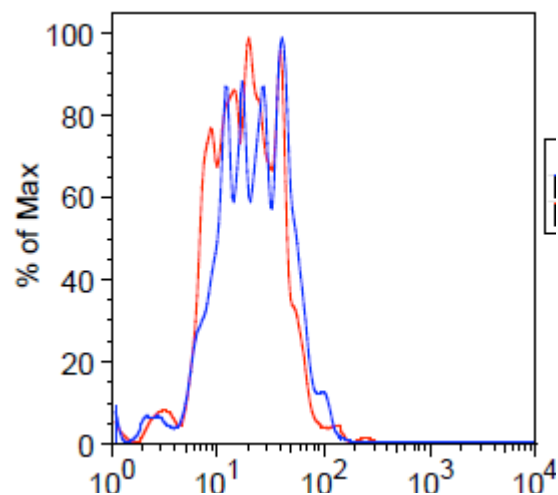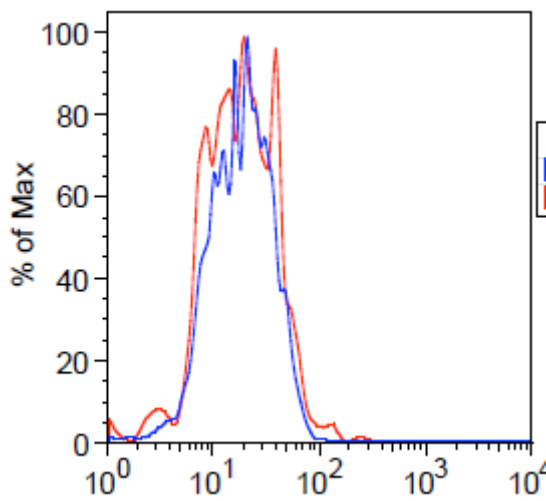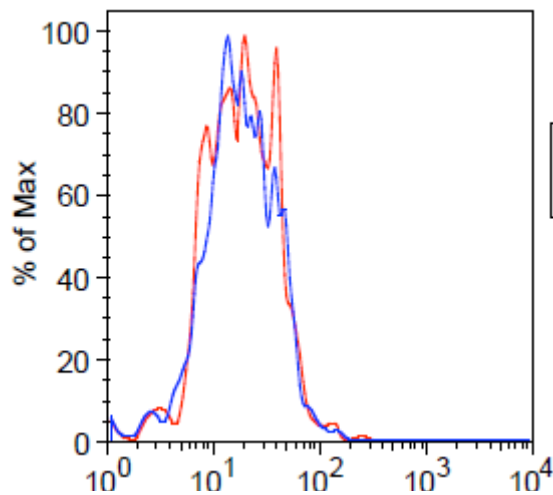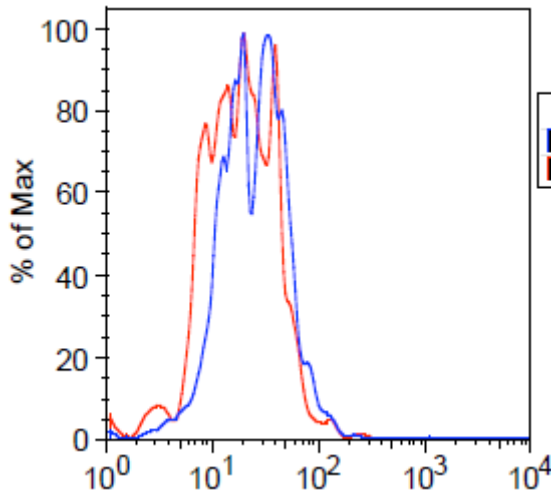
f) Compound 9
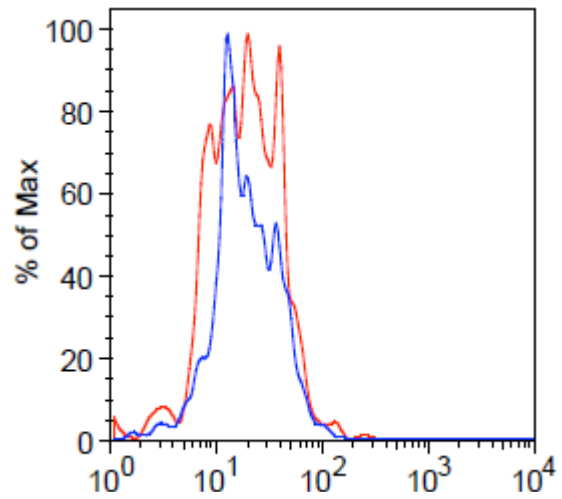
g) Compound 10
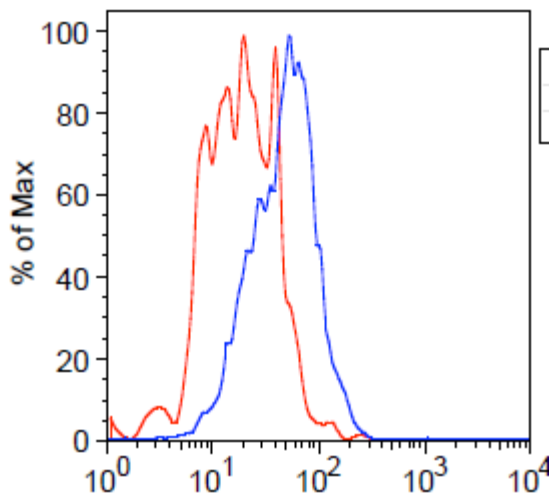
h) Compound 11
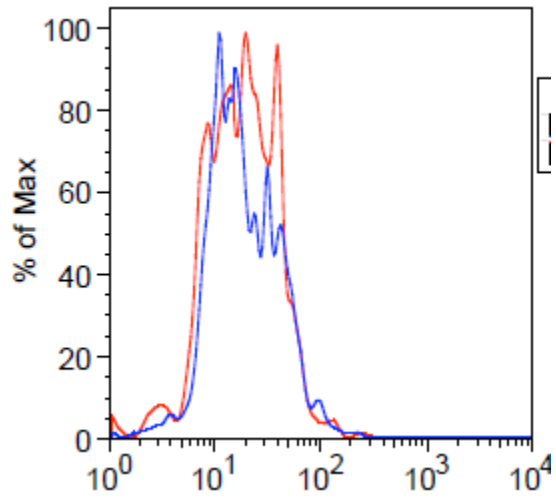
i) Compound 13

j)   Compound 14
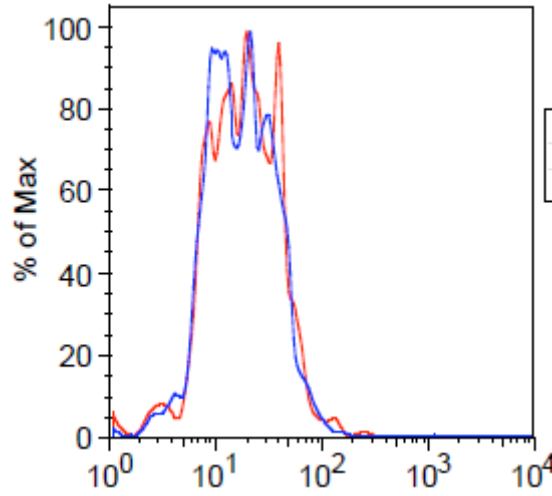
11. Modulation of histone H3K9Ac antibodies in Jurkat cells after a 12h
    treatment with 10 µM HDACi (Chapter 5, Table 4). **Note:** Untreated control
    for pertinent HDACi treatments represented in red and HDACi represented
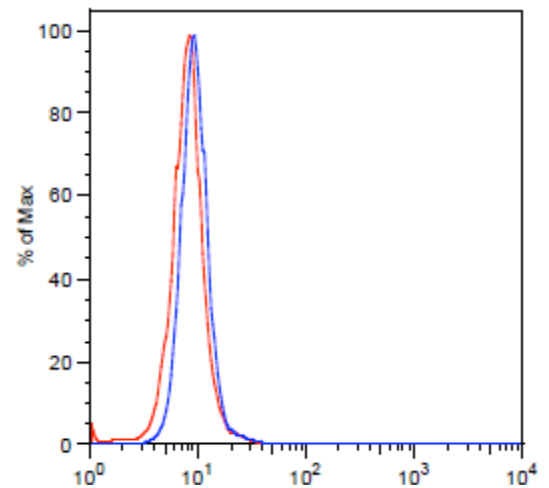   in blue on the corresponding histograms.

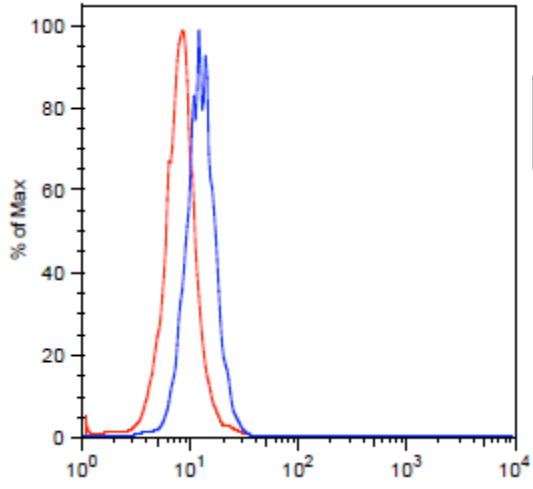a) Experimental/compensation controls [2° antibody (blue); untreated control
   (red)].

255

b)   SAHA

c)   Compound 2

d)   Compound 5

e)   Compound 7

256
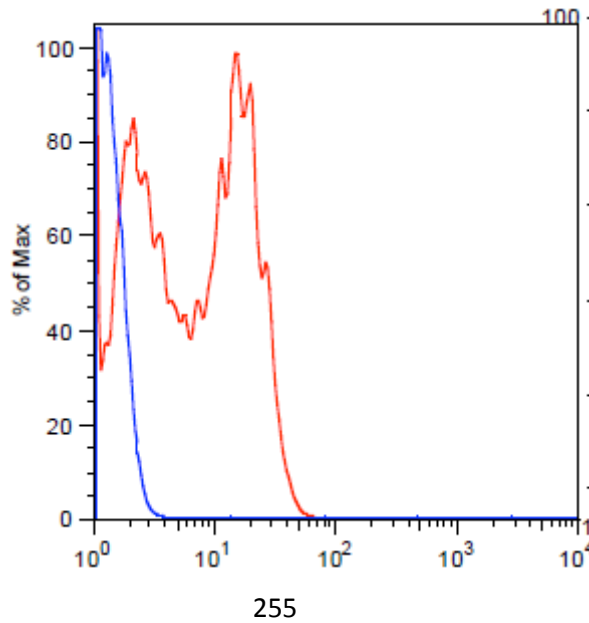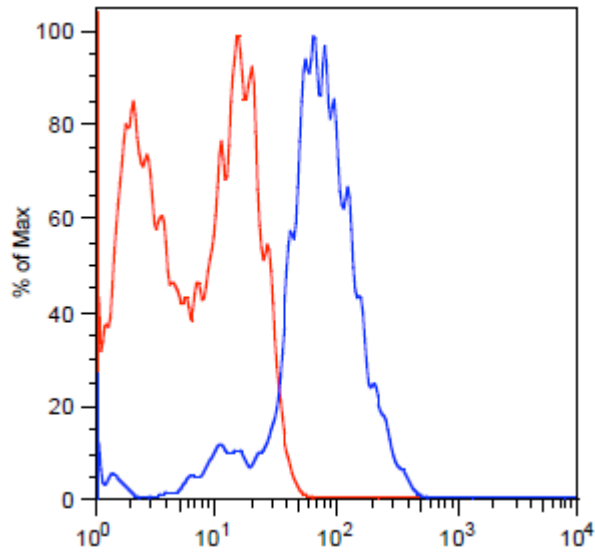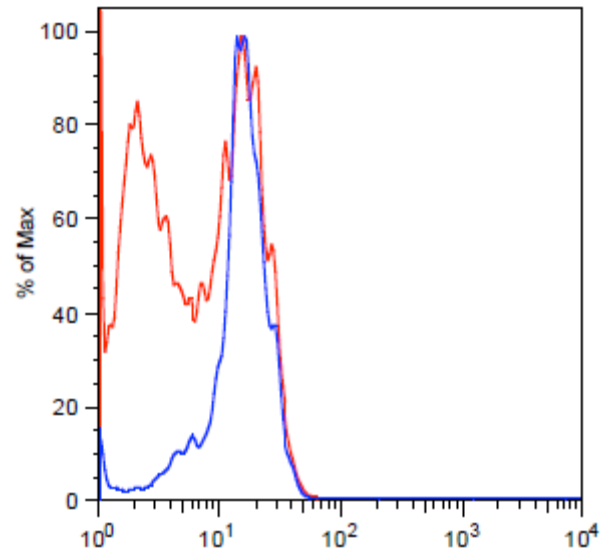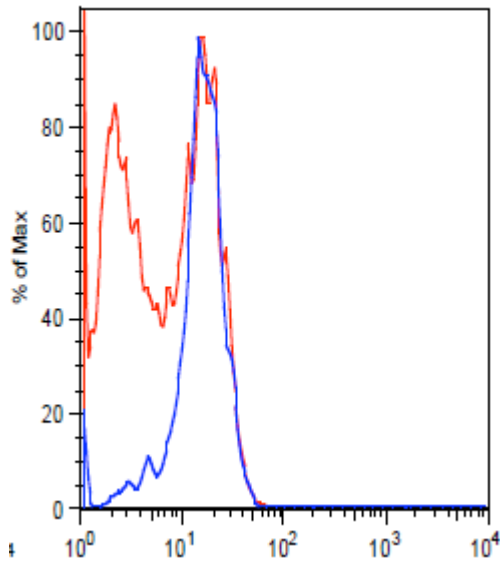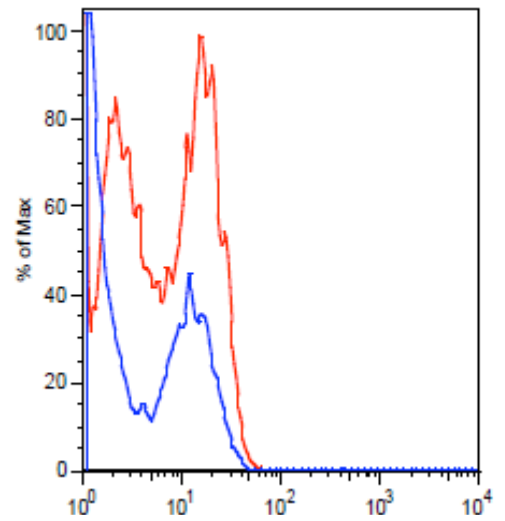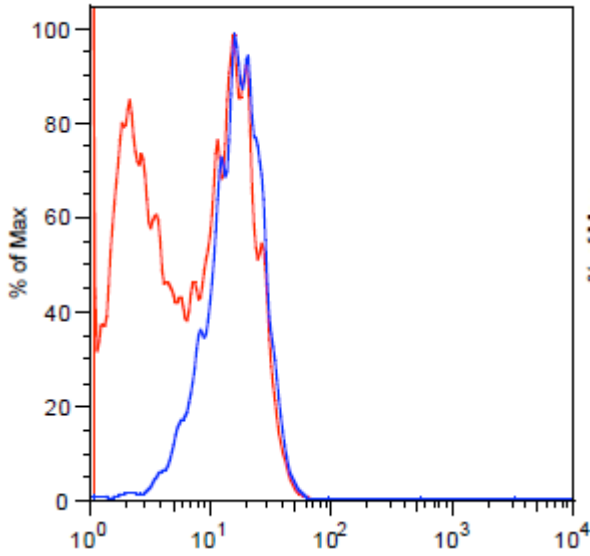
f)   Compound 9
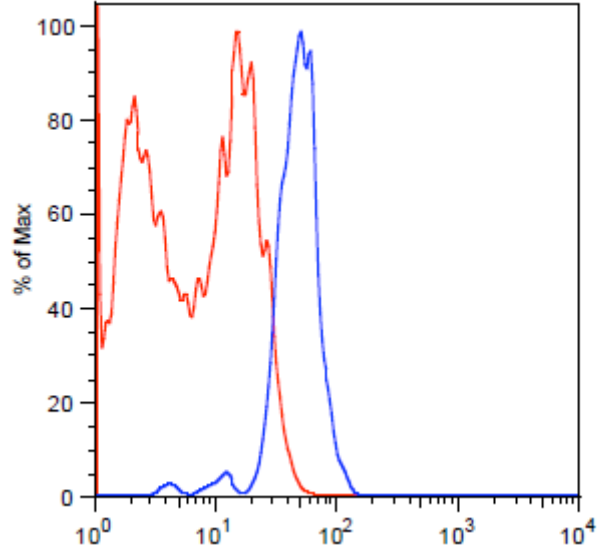
g)   Compound 10
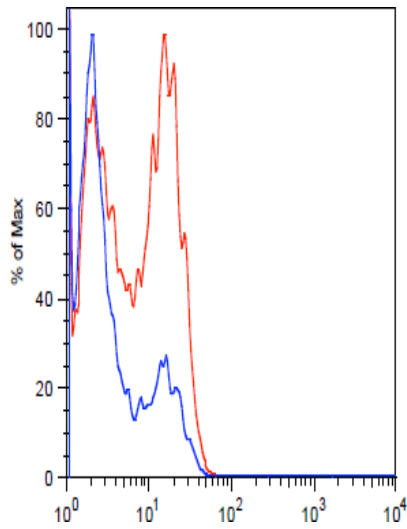
h)   Compound 11
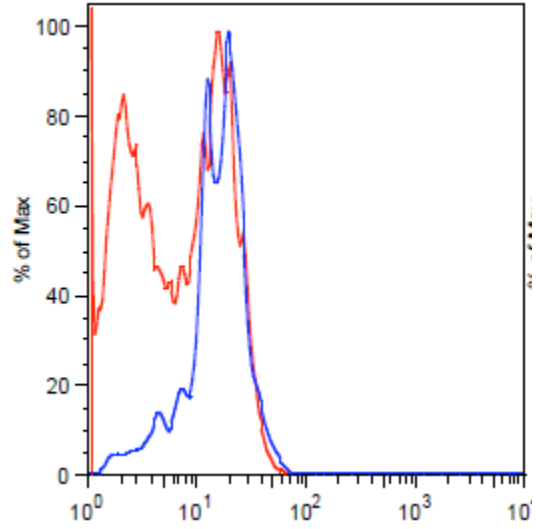
i)   Compound 13

j)   Compound 14
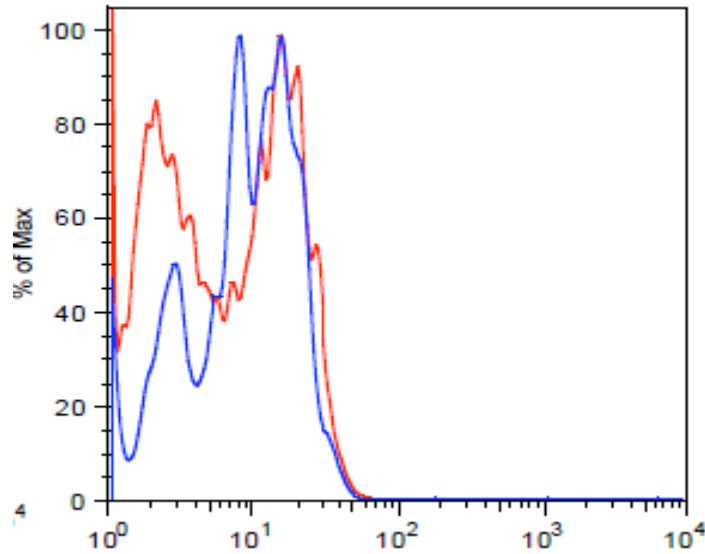
12. Modulation of histone H3K23Ac antibodies in Jurkat cells after a 12h treatment with 10 µM HDACi (Chapter 5, Table 5). **Note:** Untreated control for pertinent HDACi treatments represented in red and HDACi represented in blue on the corresponding histograms.
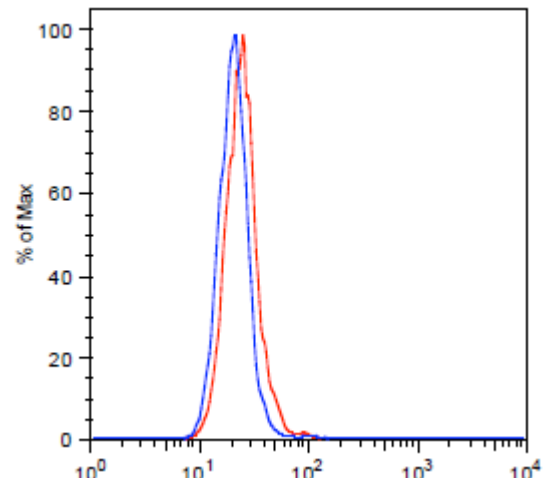
a)   Experimental/compensation controls [unlabeled cells (green); 2° antibody (blue); untreated control (red)].

258

b)   SAHA

c)   Compound 2

d)   Compound 5

e)   Compound 7

259
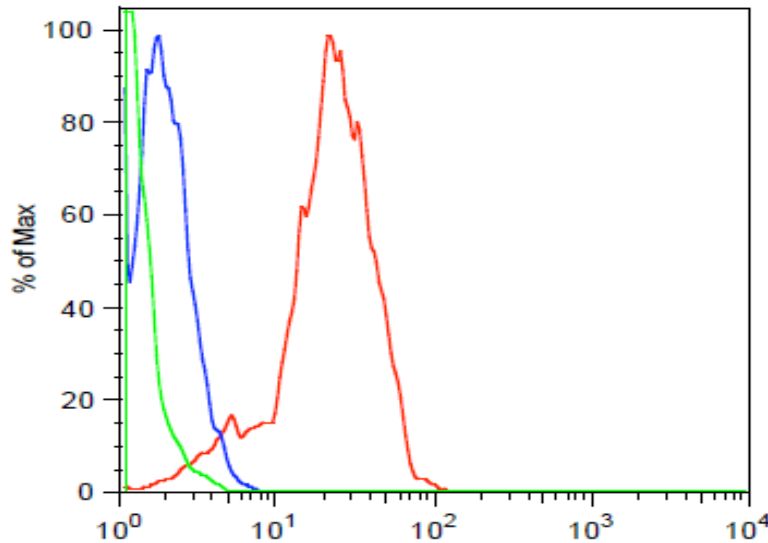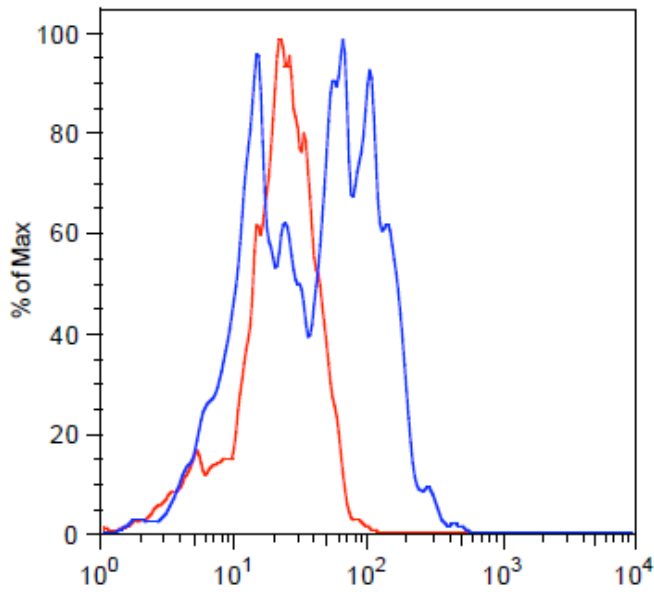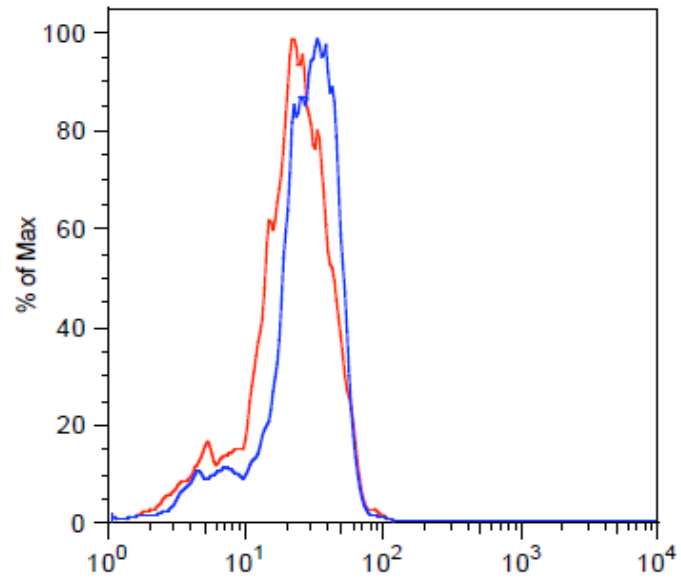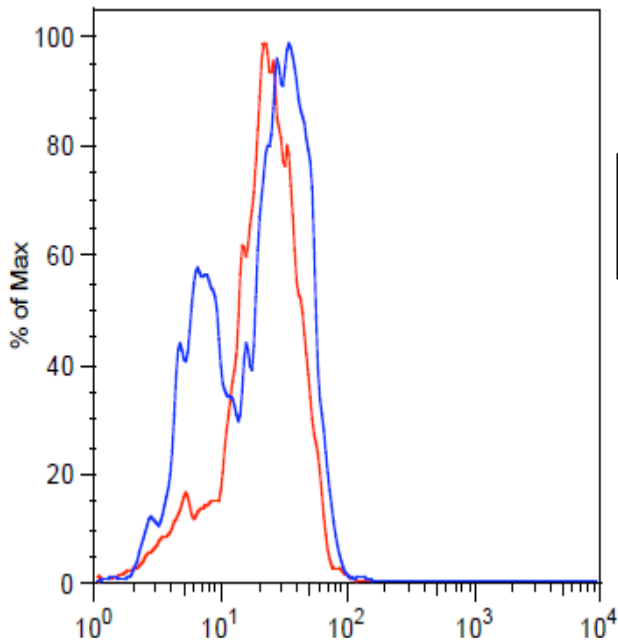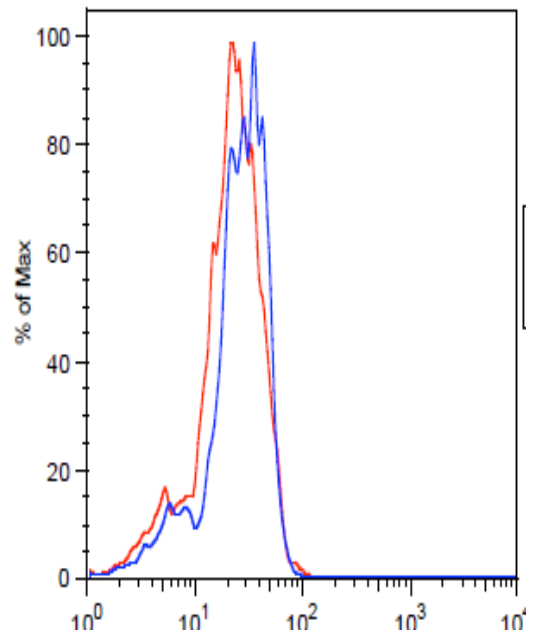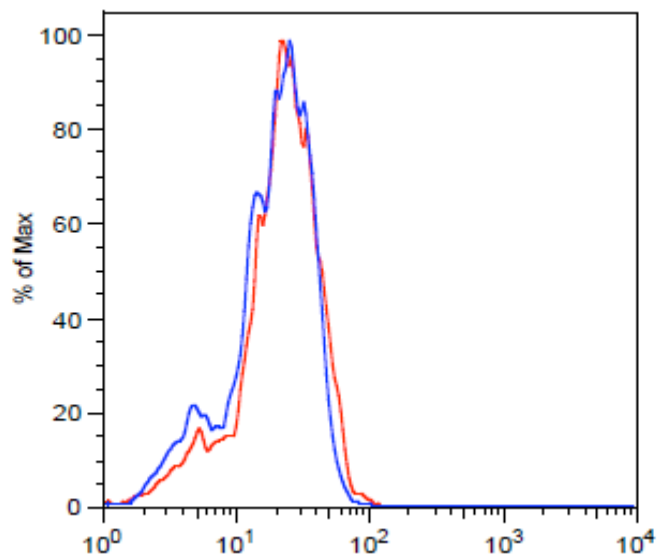
f)   Compound 10
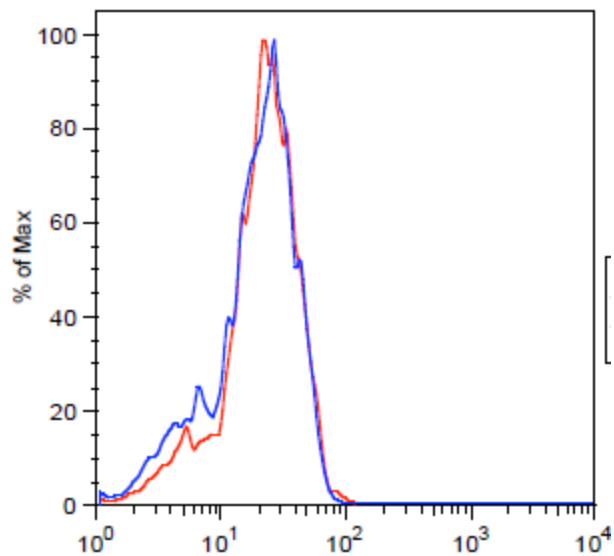
g)   Compound 11
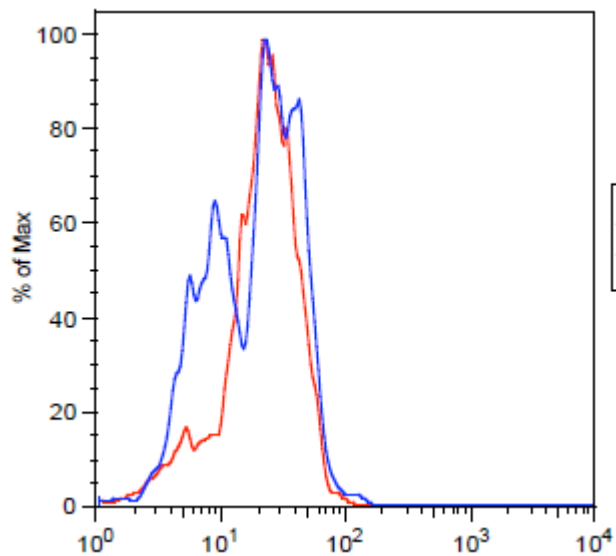
h)   Compound 13

i)   Compound 14

13. Modulation of histone H4K12Ac antibodies in HuT-78 cells after a 12h treatment with 10 µM HDACi (Chapter 5, Table 6). **Note:** Untreated control for pertinent HDACi treatments represented in red and HDACi represented in blue on the corresponding histograms.

a) Experimental/compensation controls [unlabeled cells (red); 2° antibody (blue); untreated control (green)].
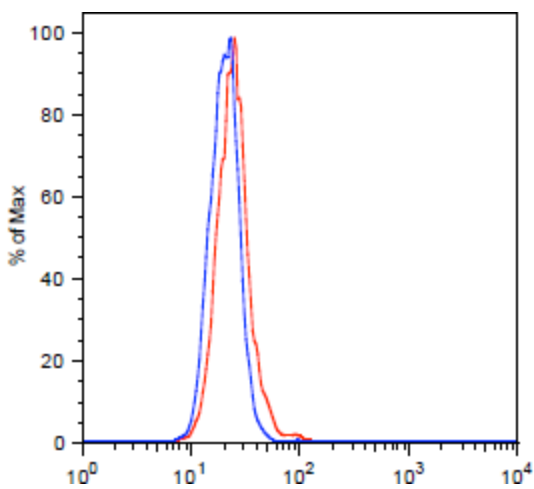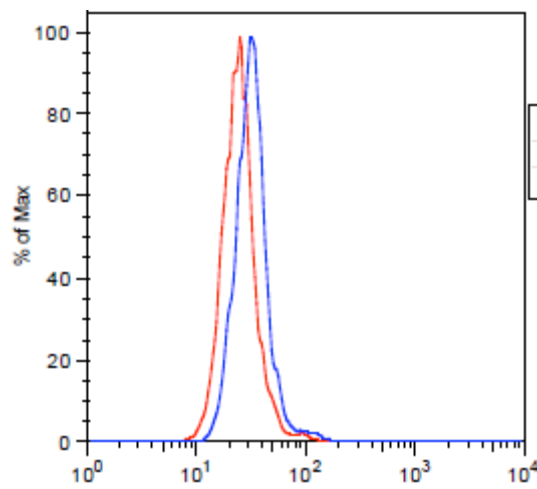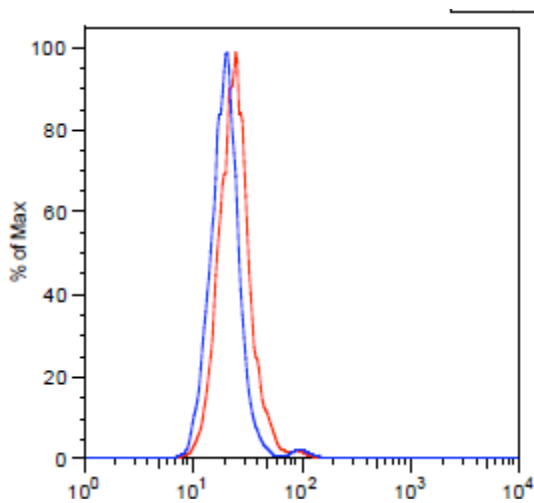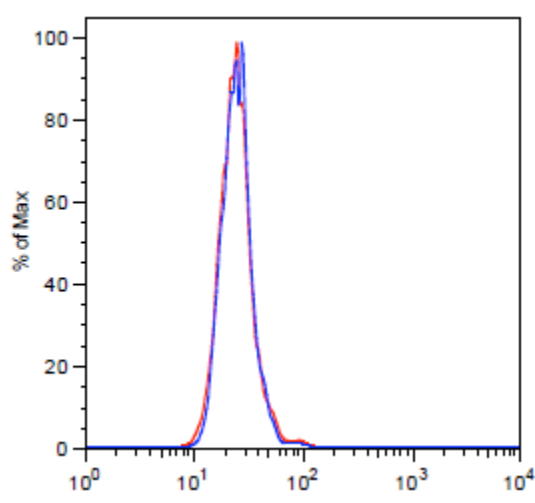

b) SAHA

c) Compound 2

261

d) Compound 5

e) Compound 7

f) Compound 9

g) Compound 10

262

h)   Compound 11

i)   Compound 13

j)   Compound 14

263
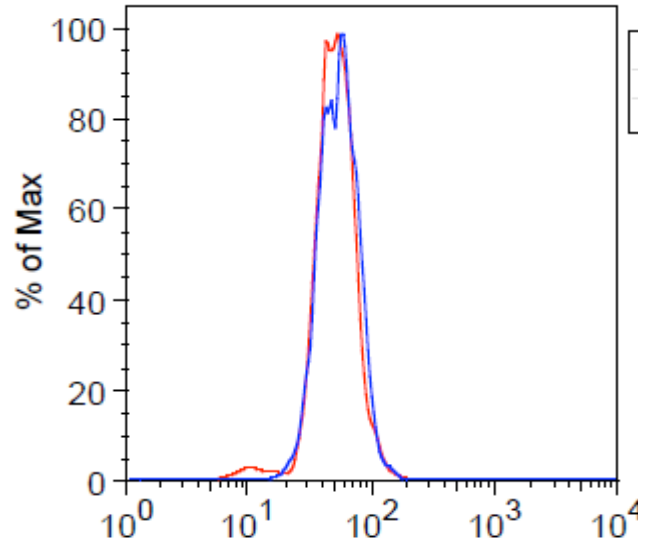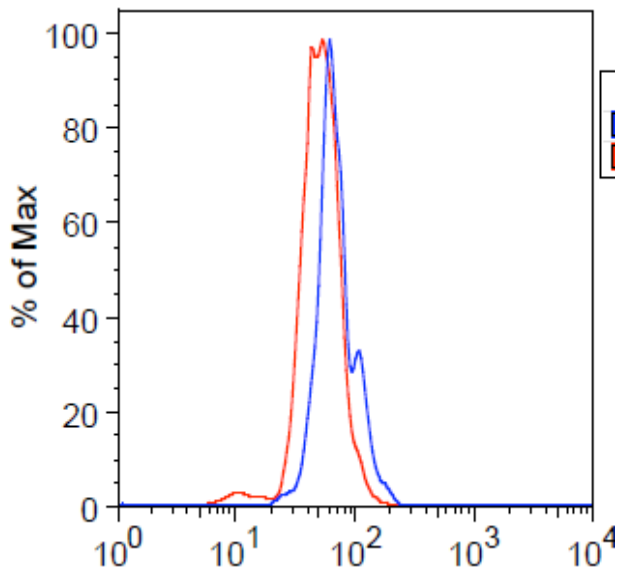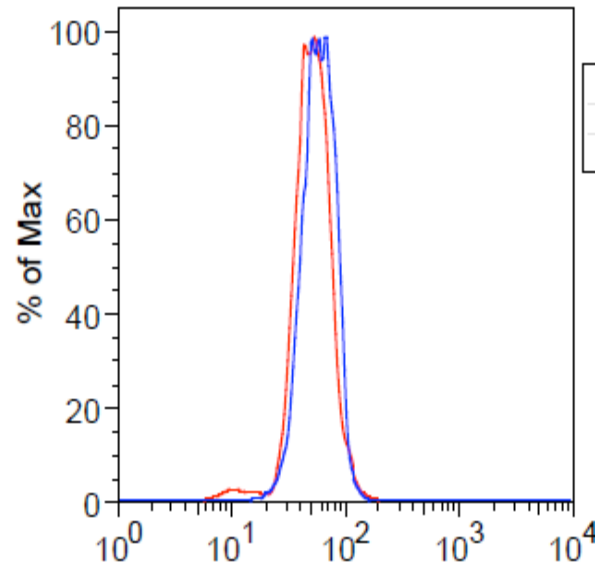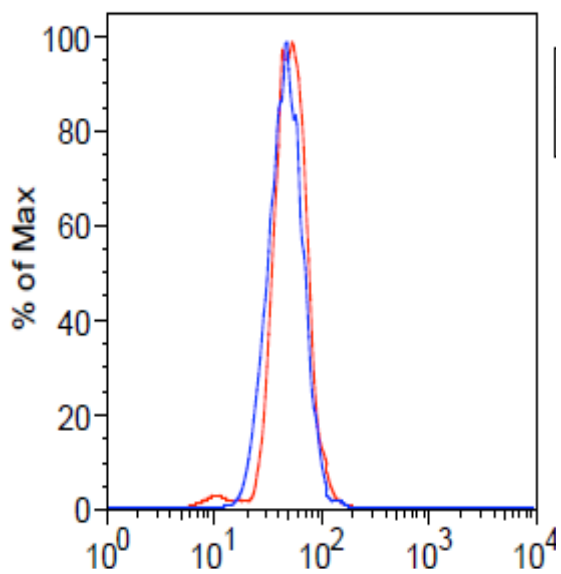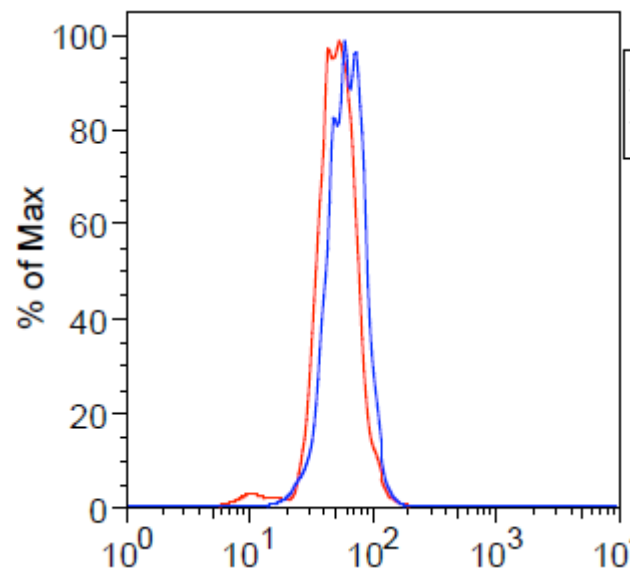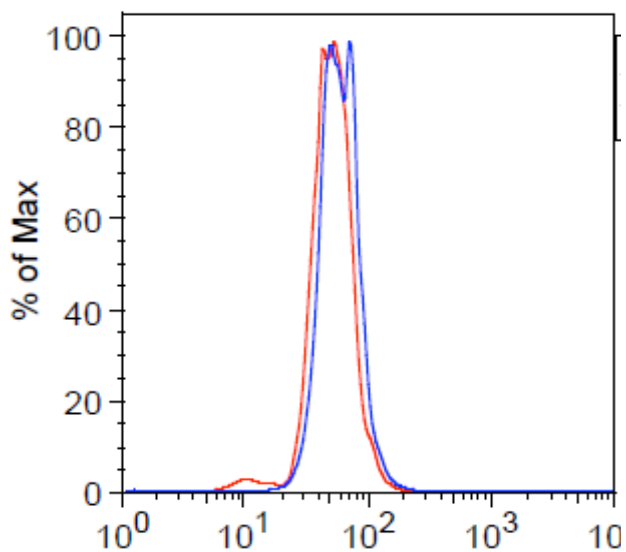
14. Modulation of histone H3K9Ac antibodies in HuT-78 cells after a 12h treatment with 10 μM HDACi (Chapter 5, Table 6). **Note:** Untreated control for pertinent HDACi treatments represented in red and HDACi represented in blue on the corresponding histograms.

a) Experimental/compensation controls [unlabeled cells (green); 2° antibody (blue); untreated control (red)].

b) SAHA

c) Compound 2

264

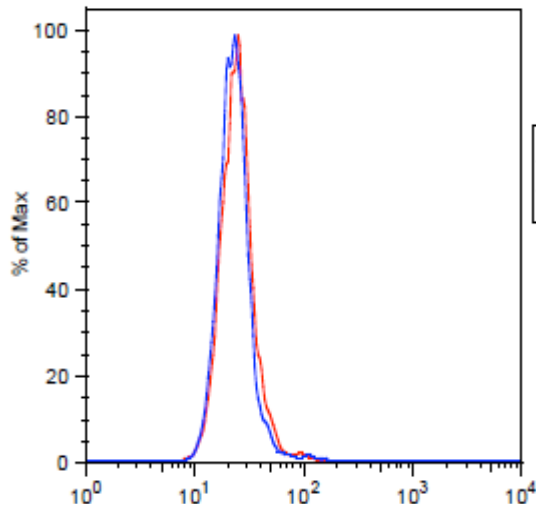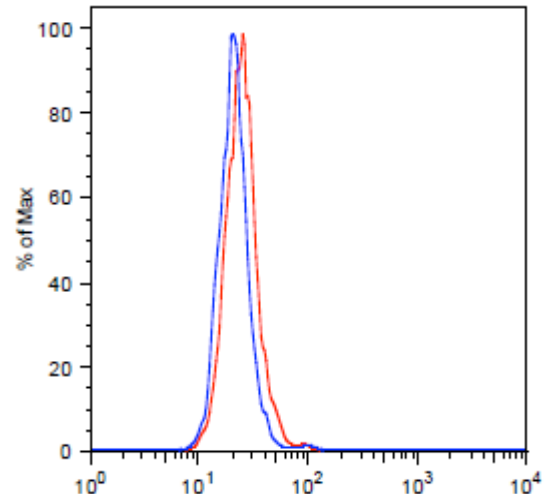d)   Compound 5

e)   Compound 7
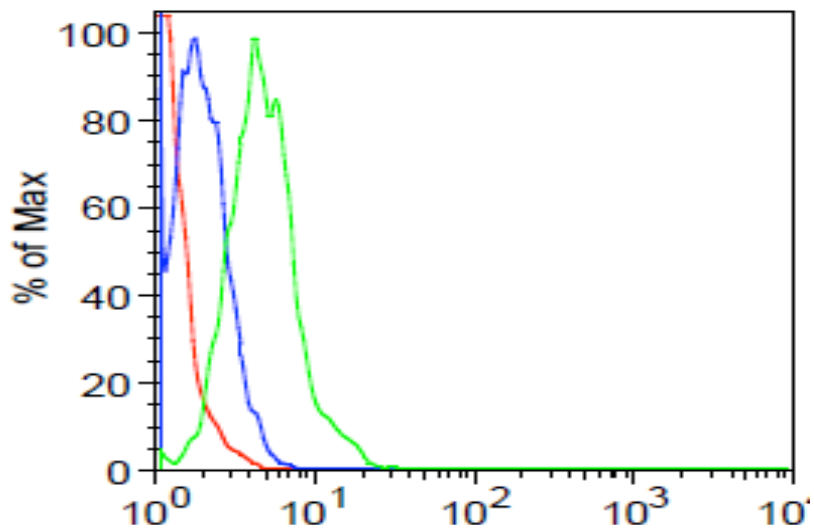
f)   Compound 9

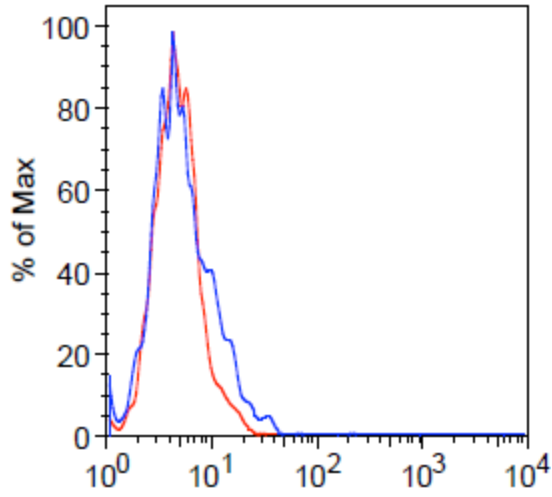g)   Compound 10

h)   Compound 11

i)   Compound 13

j)   Compound 14

266

15. Modulation of histone H3K23Ac antibodies in HuT-78 cells after a 24h treatment with 10 µM HDACi (Chapter 5, Table 7). **Note:** Untreated control for pertinent HDACi treatments represented in red and HDACi represented in blue on the corresponding histograms.

a) Experimental/compensation controls [unlabeled cells (green); 2° antibody (blue); untreated control (red)].
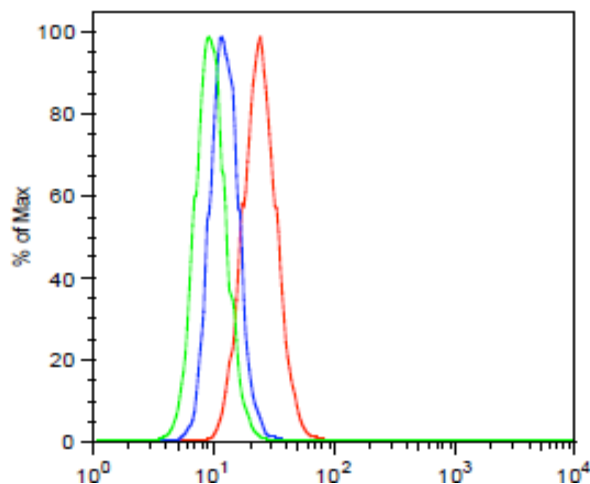
b) SAHA   c) Compound 2
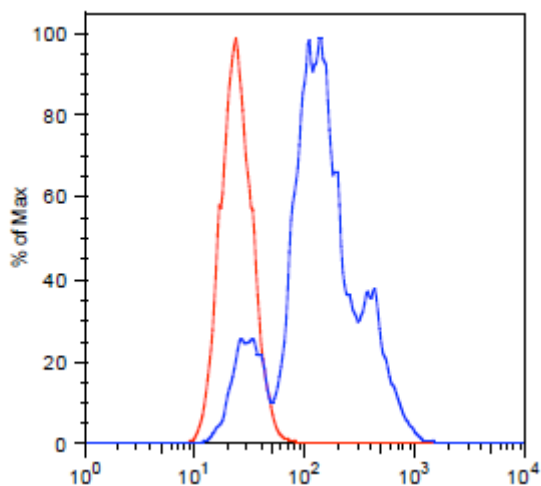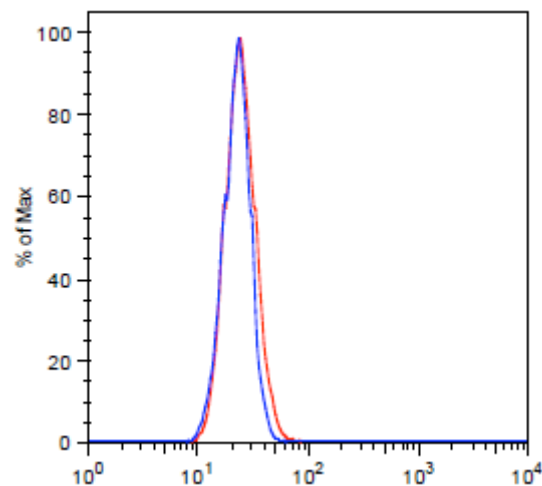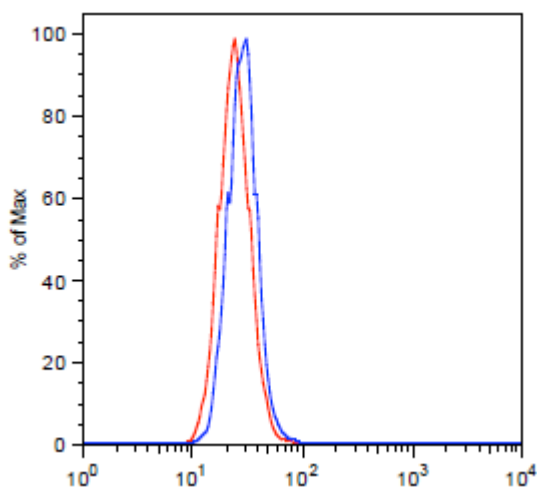
d)   Compound 3

e)   Compound 7
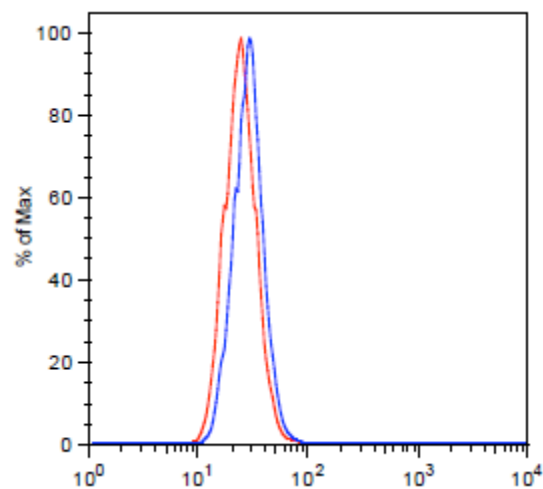
f)   Compound 10
 11

g)   Compound

268
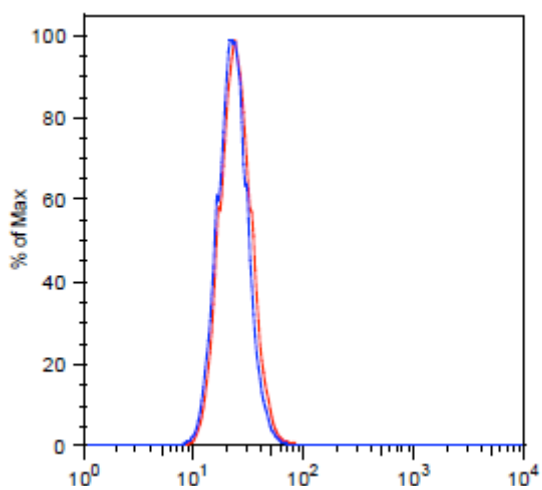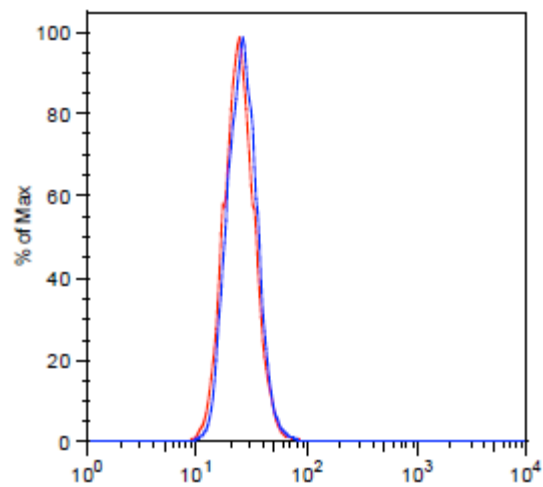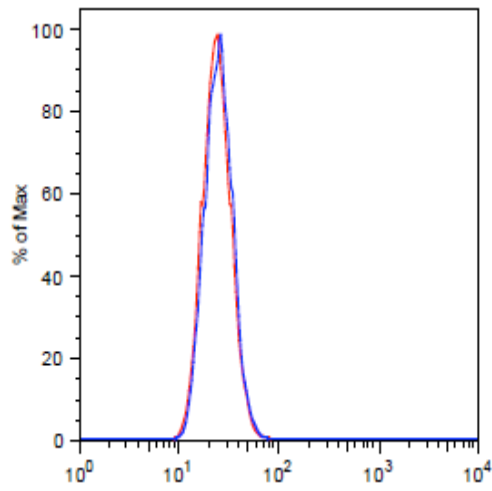
h)   Compound 12   i)   Compound 13
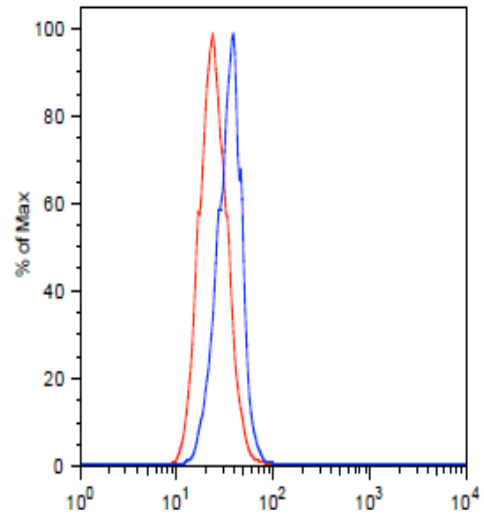
j)   Compound 14
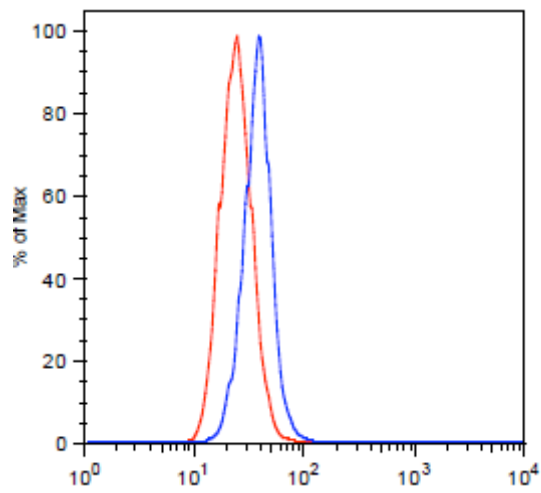
16. Modulation of tubulin (Ac-α-tub-K40) antibodies in Jurkat cells after a 12h treatment with 10 µM HDACi (Chapter 5, Table 8). **Note:** Untreated control for pertinent HDACi treatments represented in red and HDACi represented in blue on the corresponding histograms.

a)   Experimental/compensation controls [unlabeled cells (green); 2° antibody (blue); untreated control (red)].
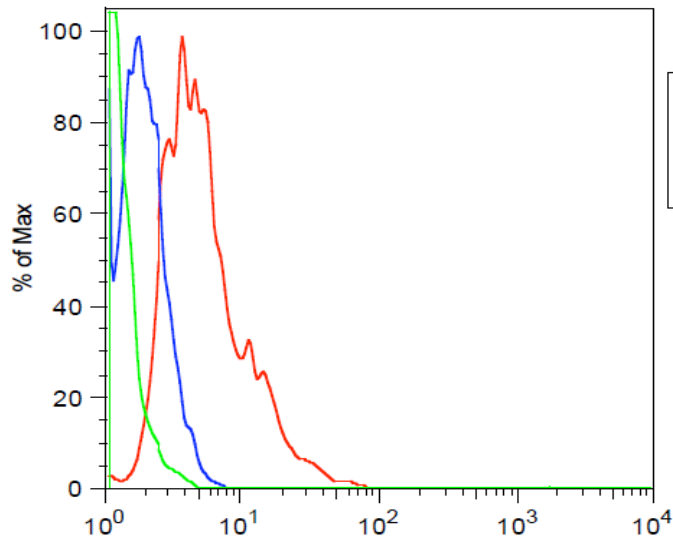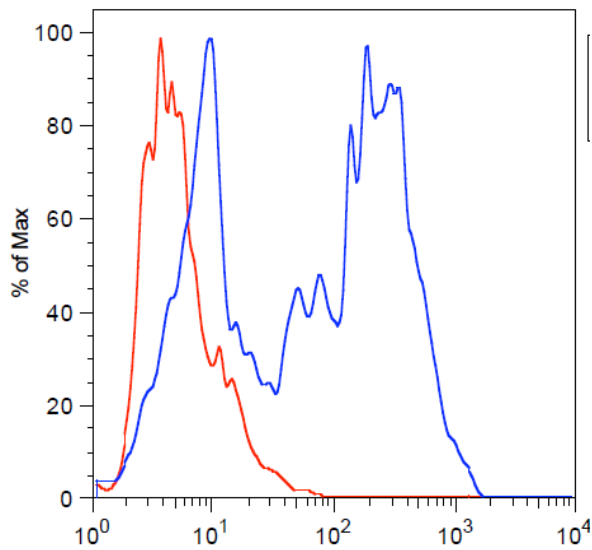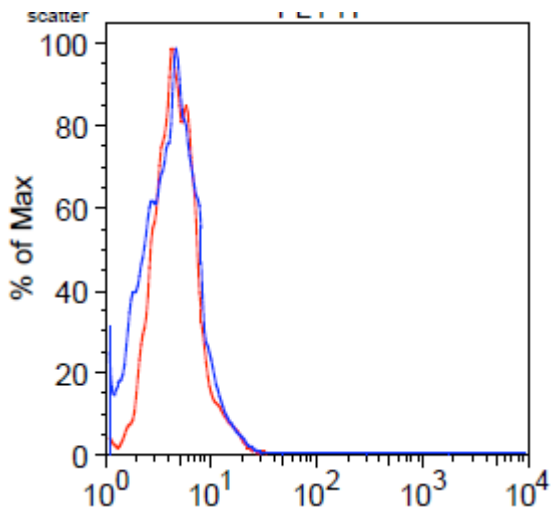

b)   SAHA   c)   Compound 2
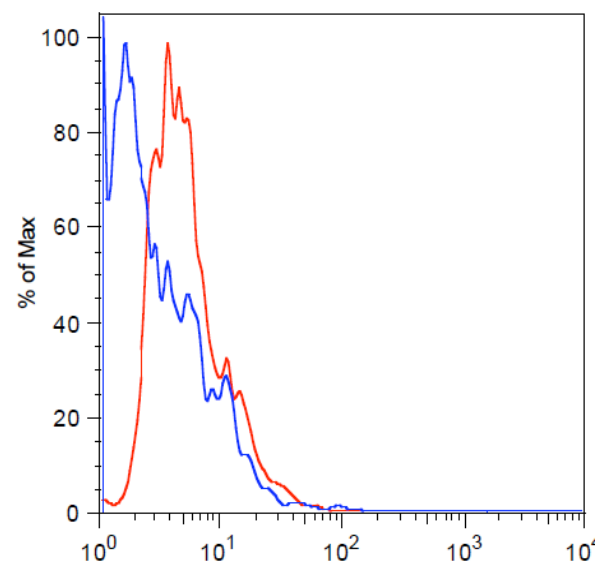

270

d)   Compound 5
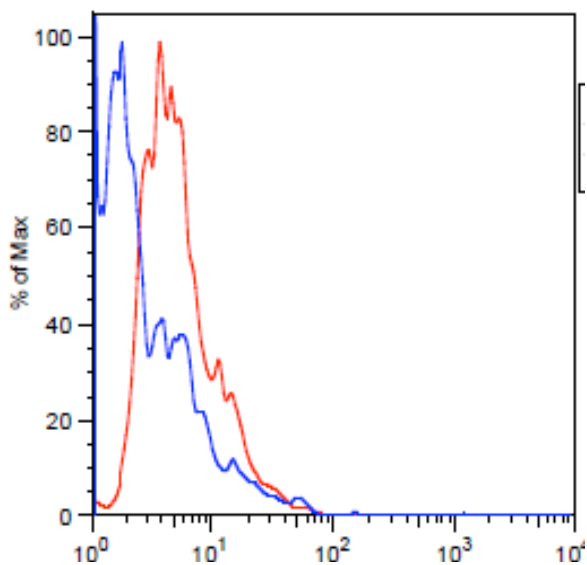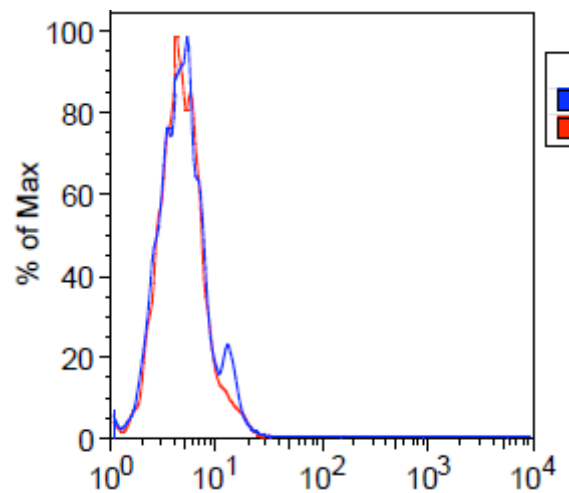
e)   Compound 7
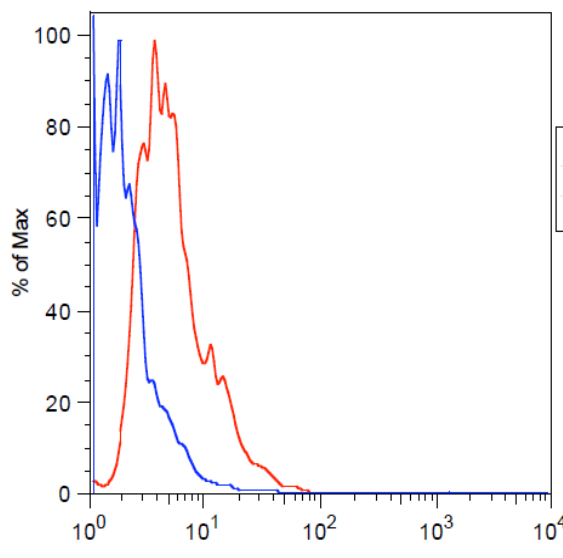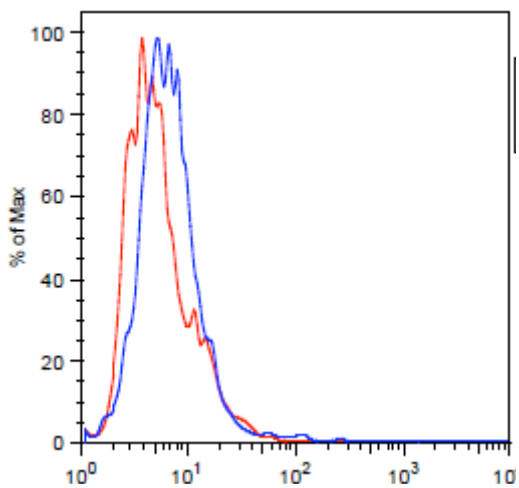
f)   Compound 9
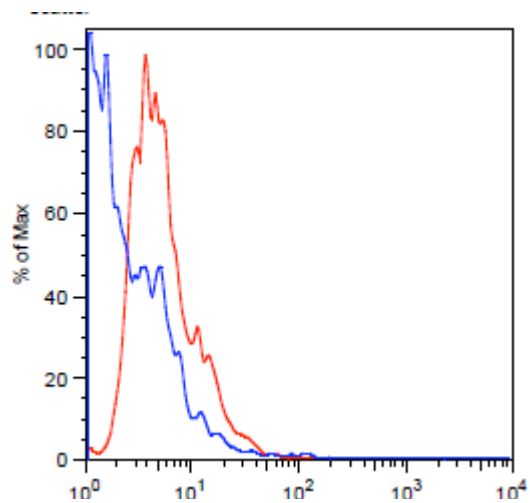
g)   Compound 10
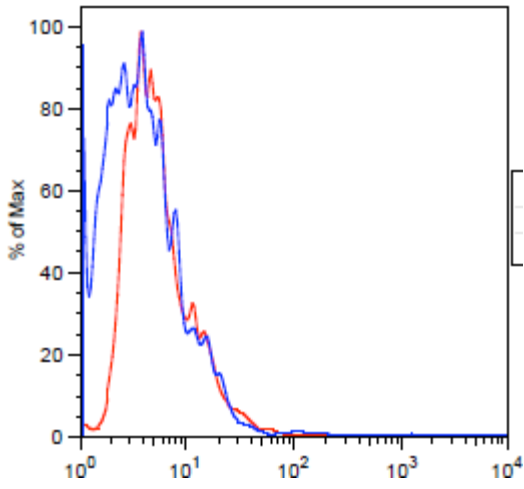
h)   Compound 11
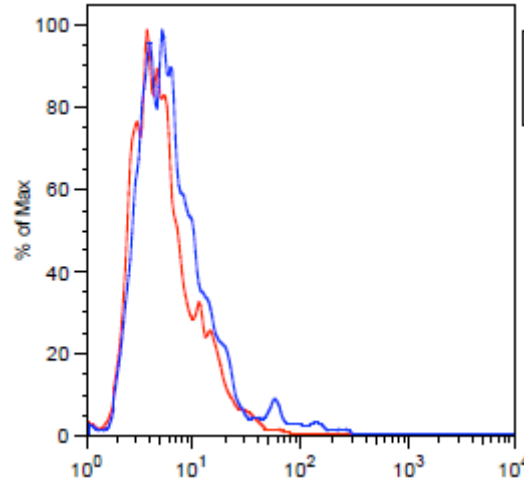
i)   Compound 13

j)   Compound 14
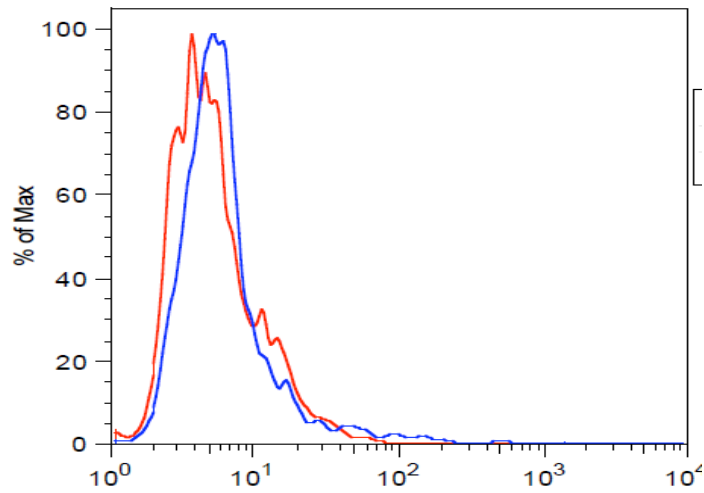
17. Modulation of tubulin (Ac-α-tub-K40) antibodies in HuT-78 cells after a 12h treatment with 10 µM HDACi (Chapter 5, Table 8). **Note:** Untreated control for pertinent HDACi treatments represented in red and HDACi represented in blue on the corresponding histograms.

a) Experimental/compensation controls [unlabeled cells (green); 2° antibody (blue); untreated control (red)].

b) SAHA

c) Compound 2

273
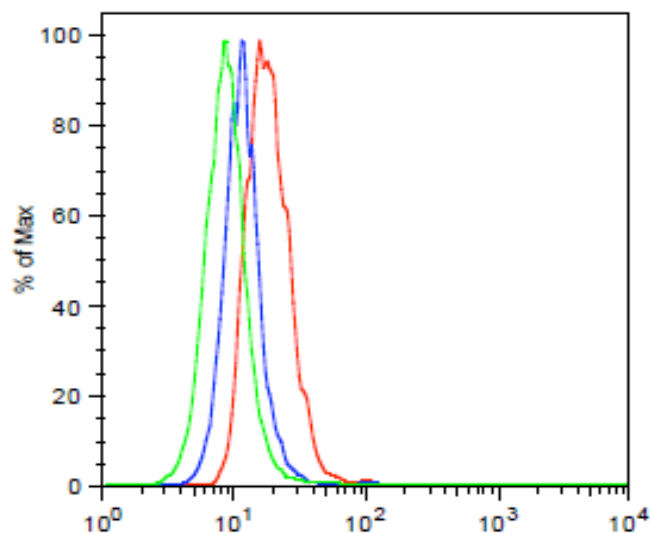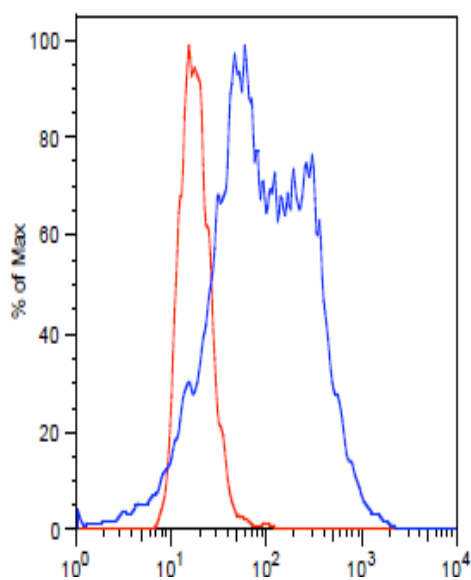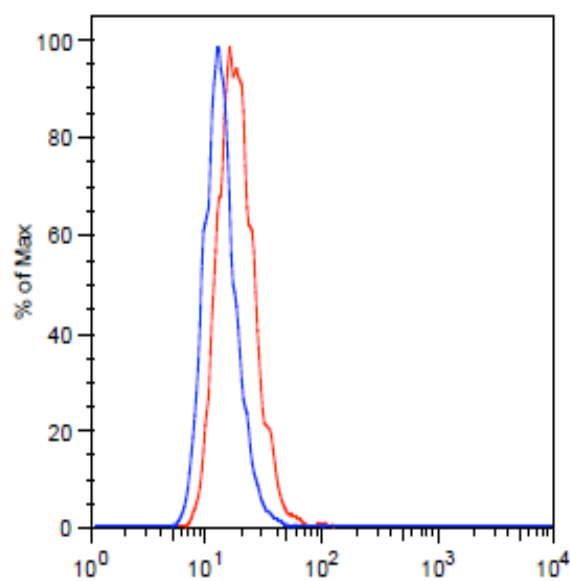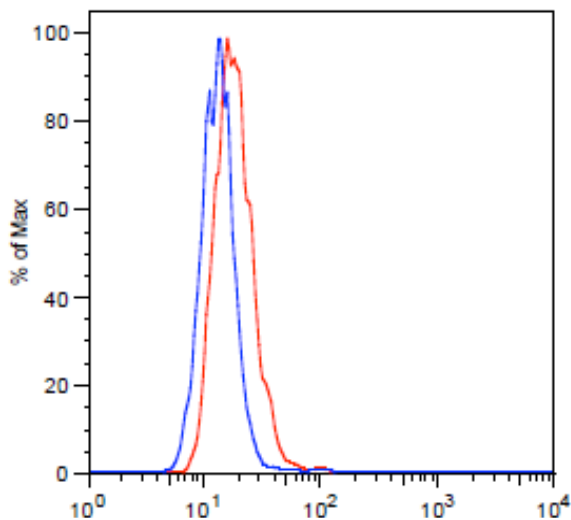
d)   Compound 7
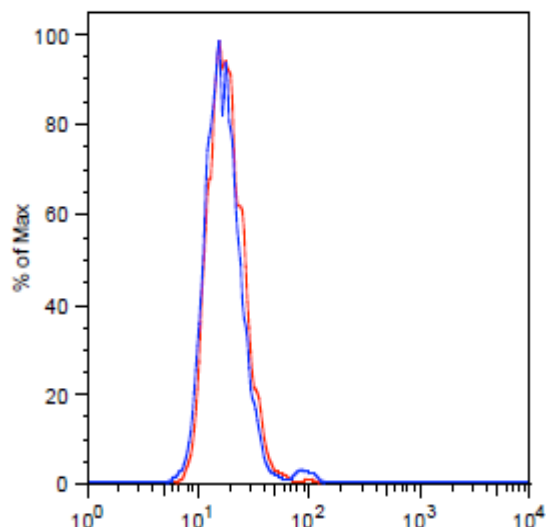
e)   Compound 9
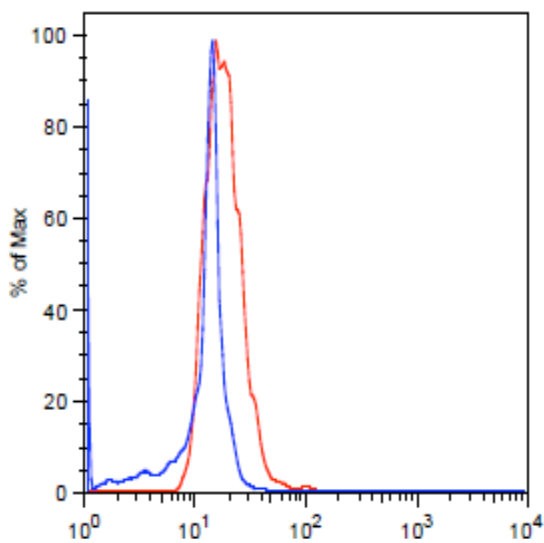
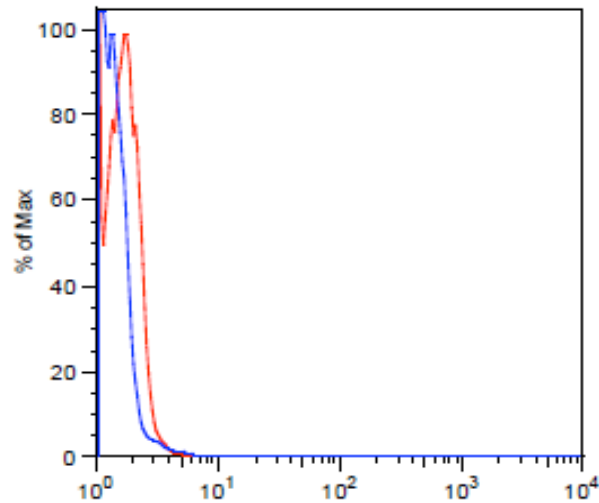f)   Compound 10
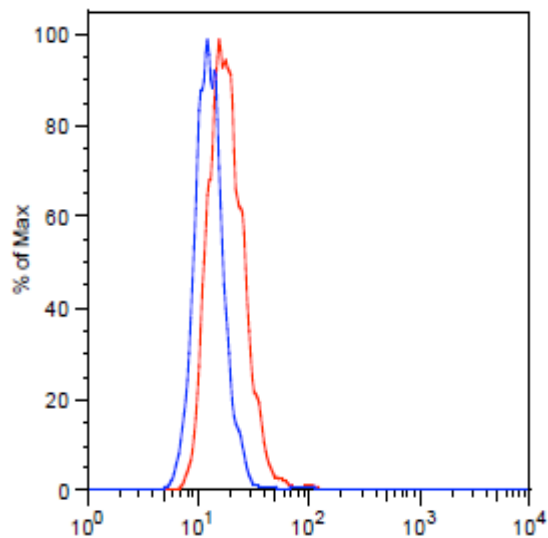
g)   Compound 11
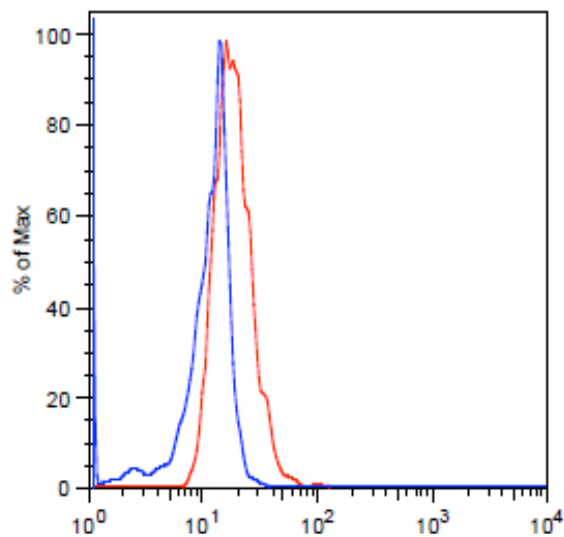
h)   Compound 13
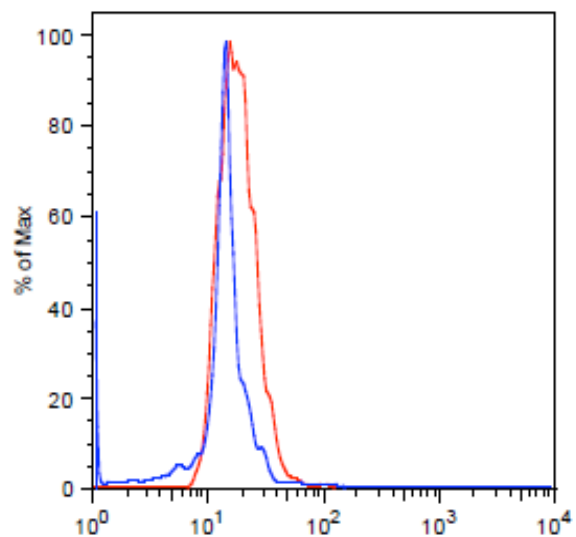
i)   Compound 14

18. Analysis of Cell Cycle Progression in HCT116 cells after a 24 treatment (Chapter 6, Table 1)

a.   Control
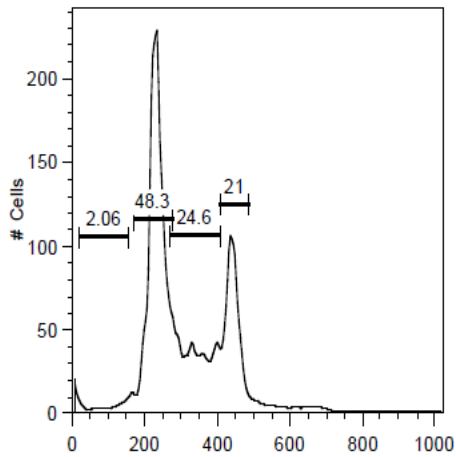
b.   10 µM SAHA
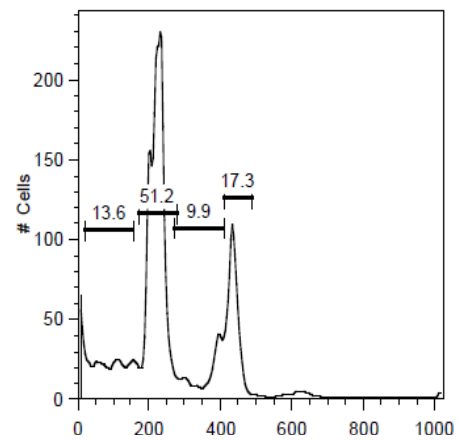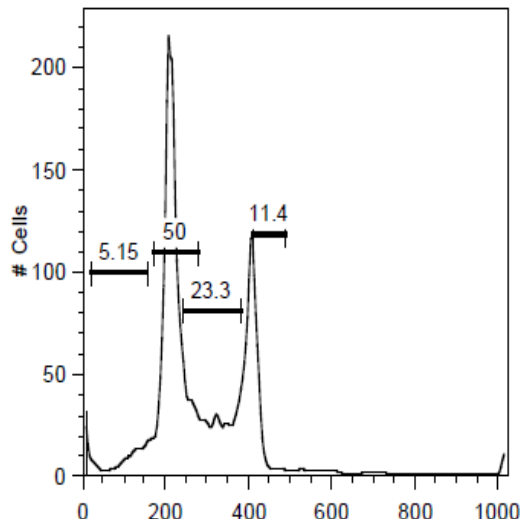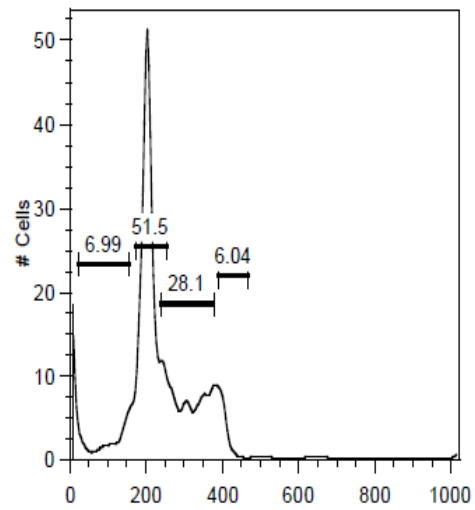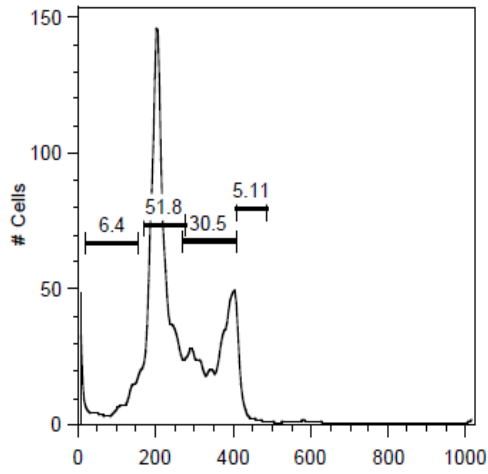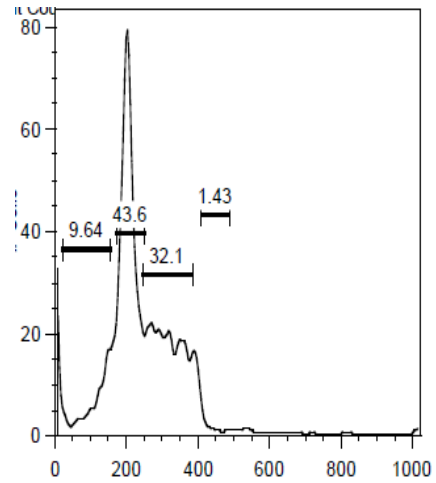
c.   10 µM Compound 2

d.   50 µM Compound 2

e.   10 µM Compound 3

f.   50 µM Compound 3

g.   10 µM Compound 7

h. 50 µM Compound 7

277

i.   10 µM Compound 12

j.   50 µM Compound 12

k.   10 µM Compound 13

l.   50 µM Compound 13

278
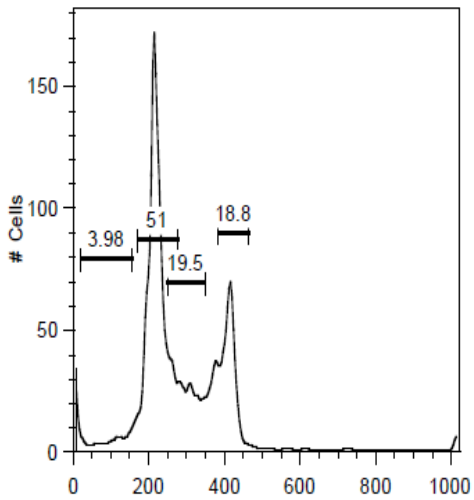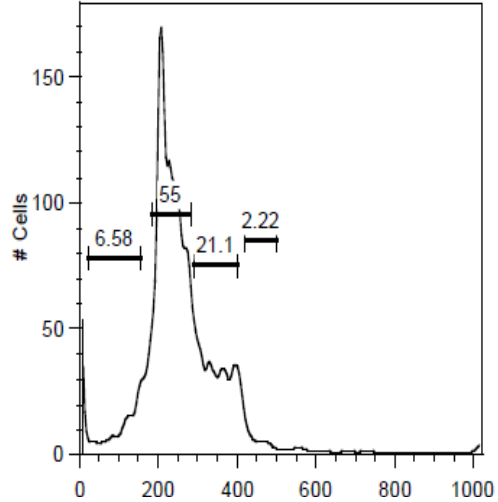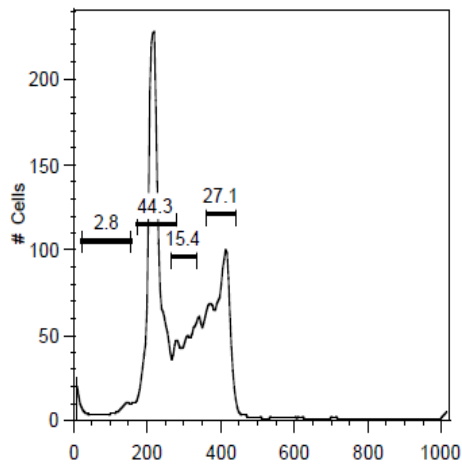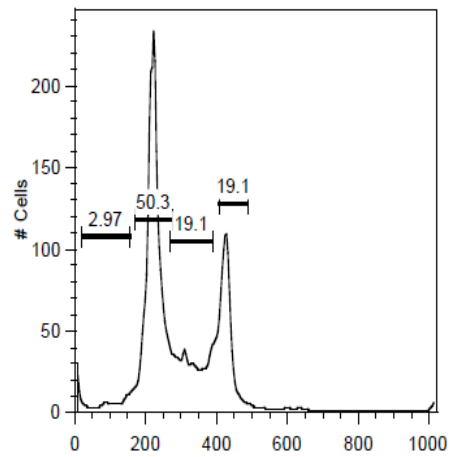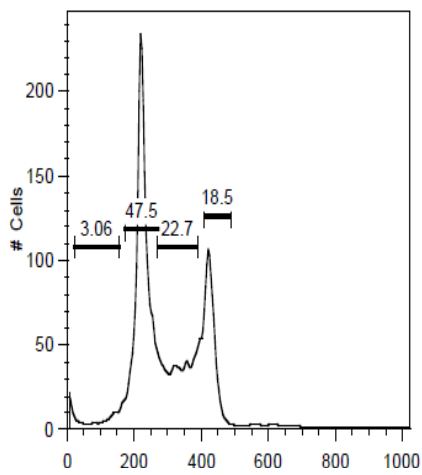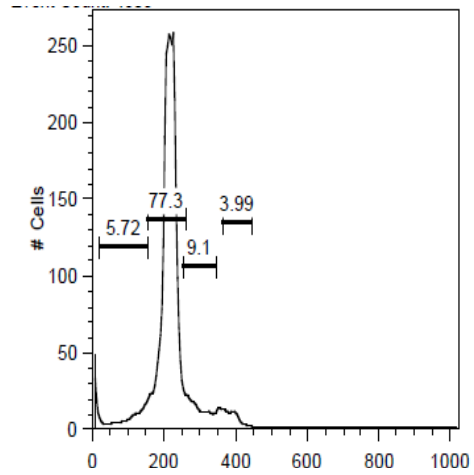
19. Analysis of Cell Cycle Progression in BXPC3 cells after a 12h treatment (Chapter 6, Table 2)

a. Control
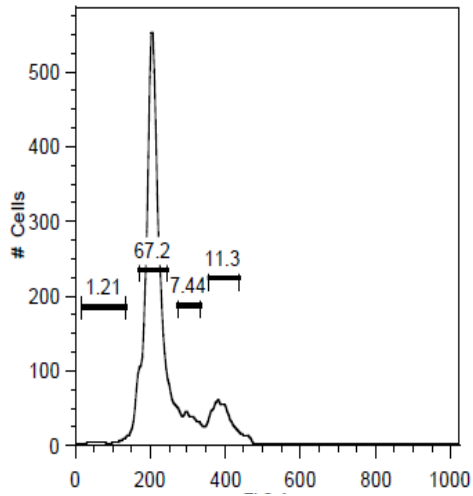
b. 10 µM SAHA
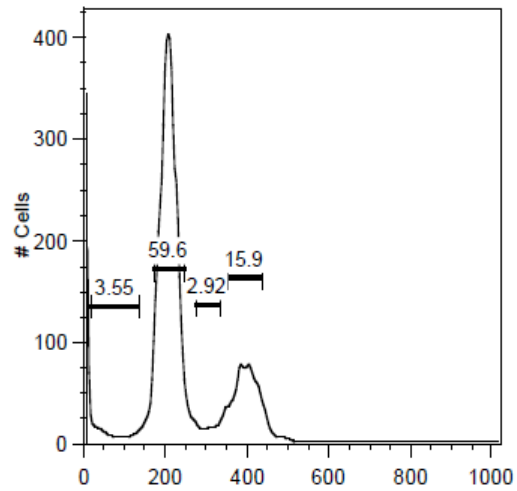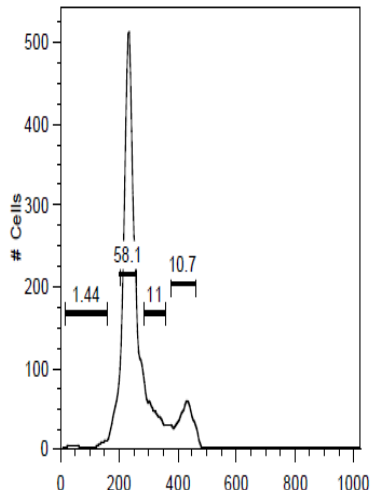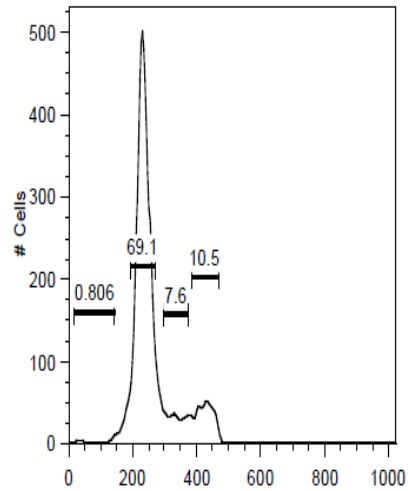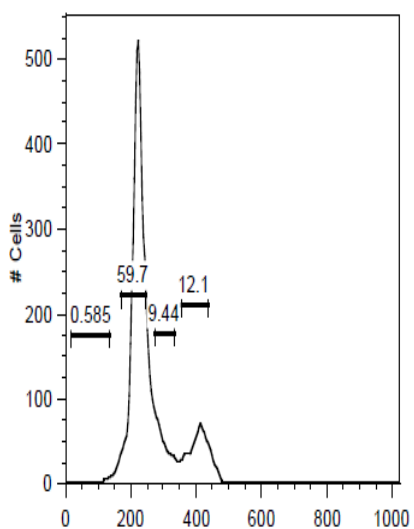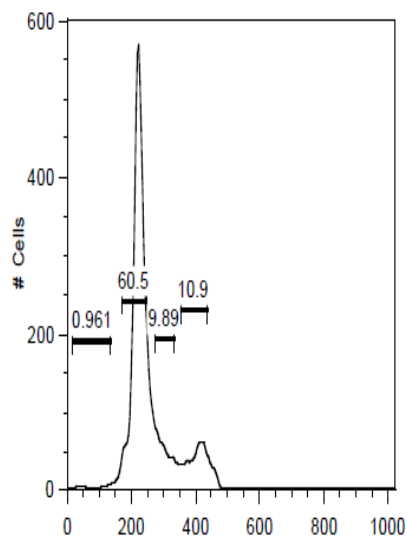
c. 10 µM Compound 2

d. 10 µM Compound 3

e.   10 µM Compound 5   f.   10 µM Compound 7

g.   10 µM Compound 9   h.   10 µM Compound 10

280
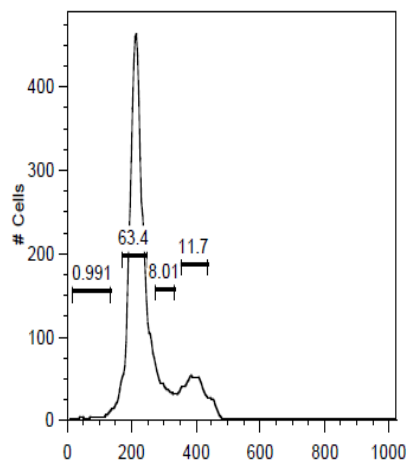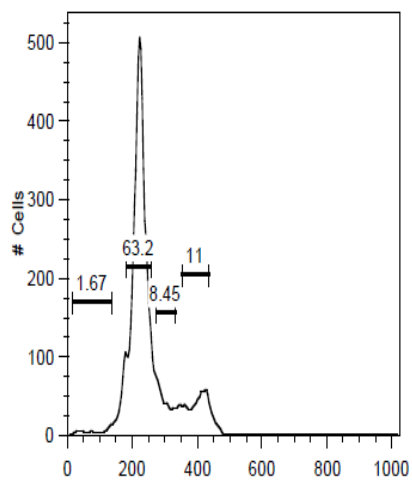
i.   10 µM Compound 11
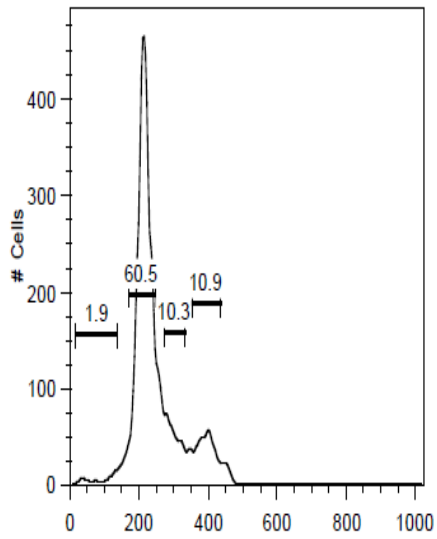
j.   10 µM Compound 12
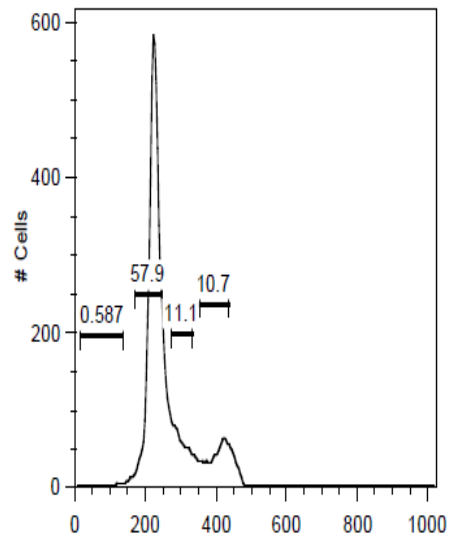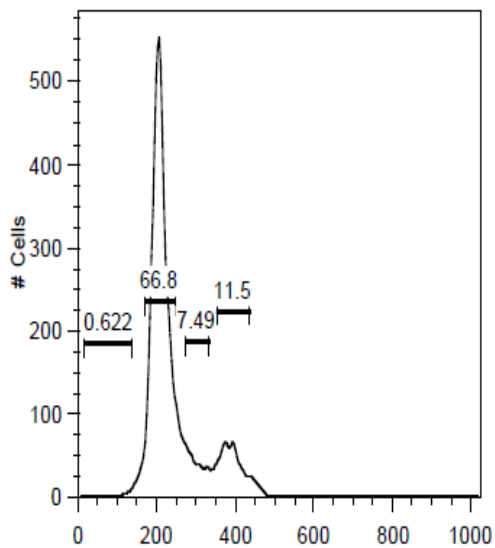
k.   10 µM Compound 13

l.   10 µM Compound 14
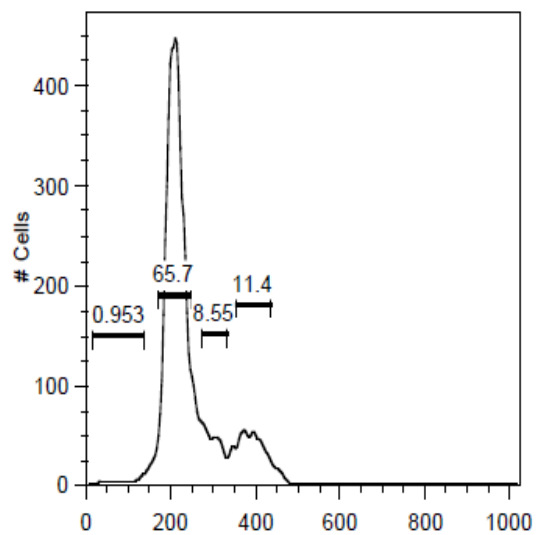
20. Time Dependent Analysis of Cell Cycle Progression in Jurkat Cells
(Chapter 6, Tables 4 & 5)

24h

Control

b.   10 µM SAHA
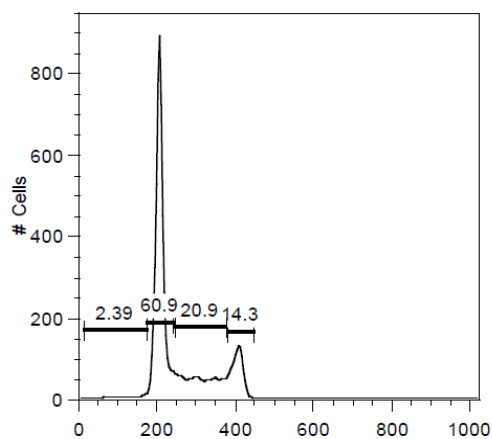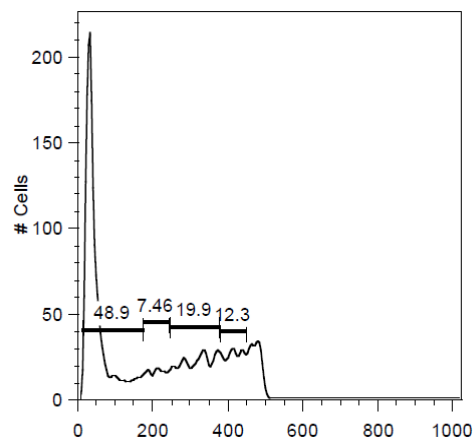
c.   10 µM Compound 2
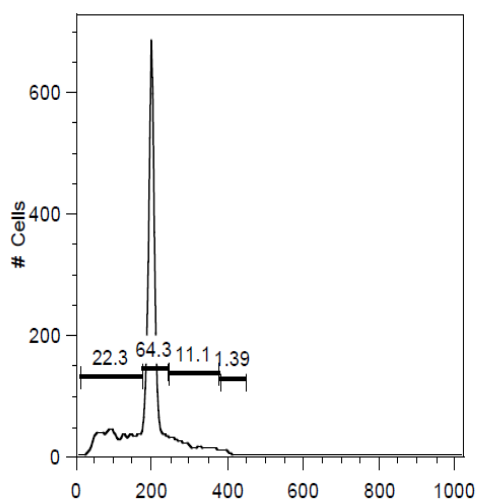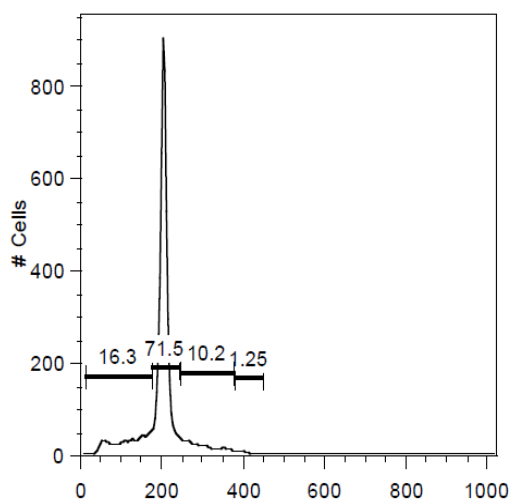
d.   10 µM Compound 7
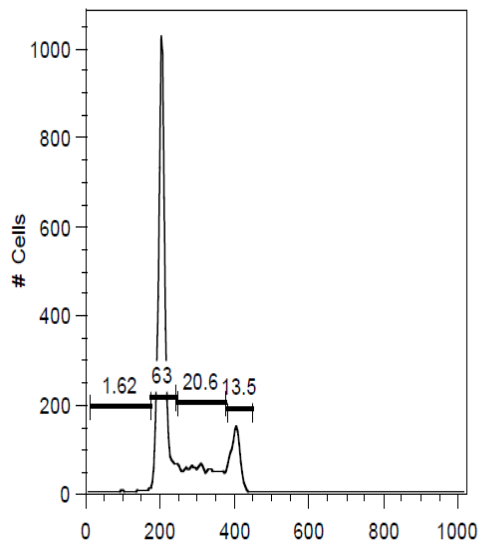
e. 10 µM Compound 11

f. 10 µM Compound 13

36h

g. Control

h. 10 µM SAHA
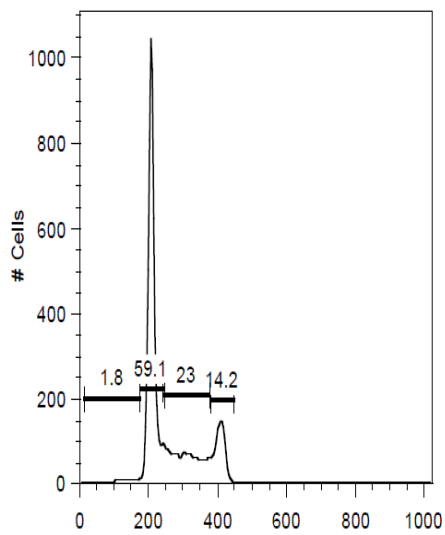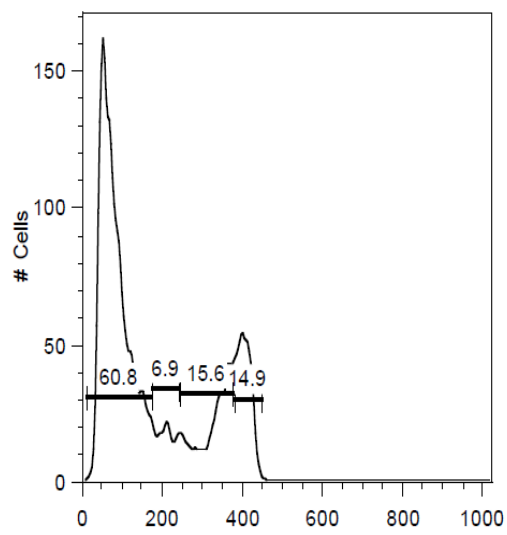
i.   10 μM Compound 2
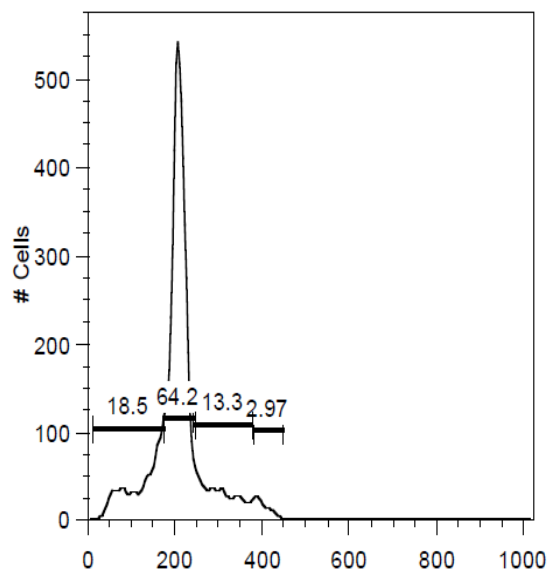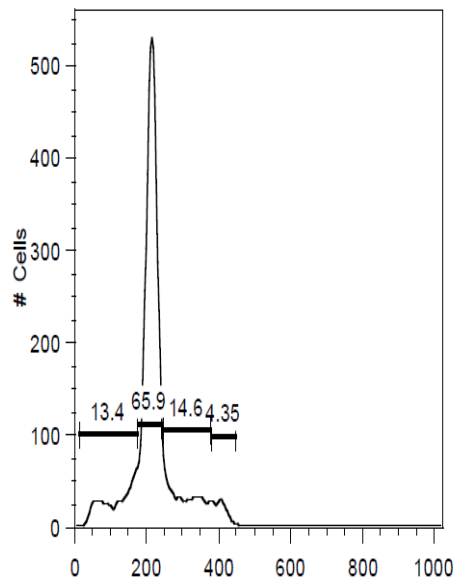
j.   10 μM Compound 7
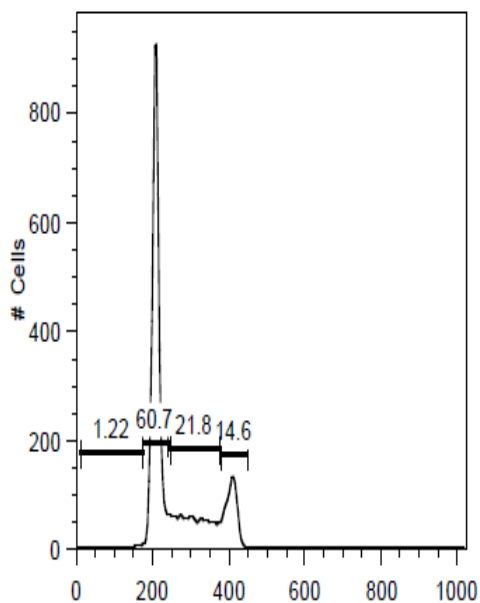
k.   10 μM Compound 11
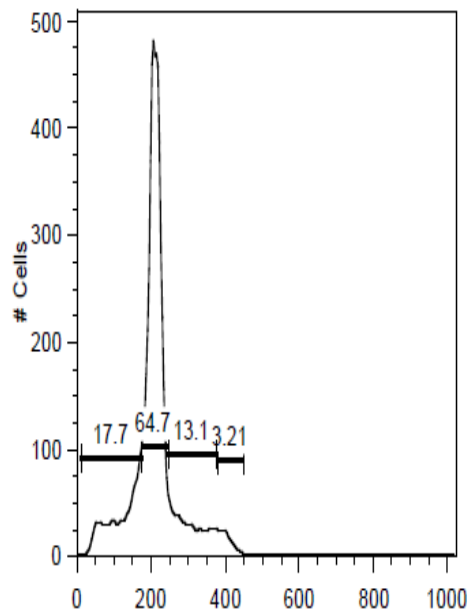
l.   10 μM Compound 13

21. Analysis of Cell Cycle Progression in Jurkat cells after a **24h** treatment with **25 µM** HDACi (Chapter 6, Table 6)

a.   Control
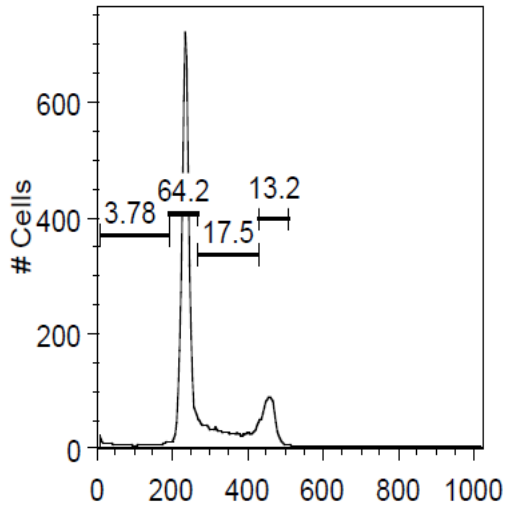
b.   25 µM Compound 2
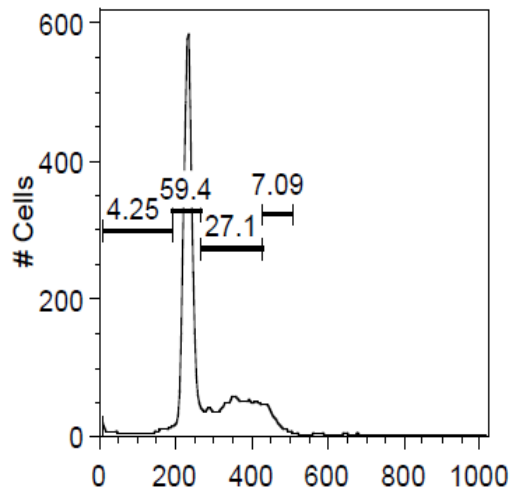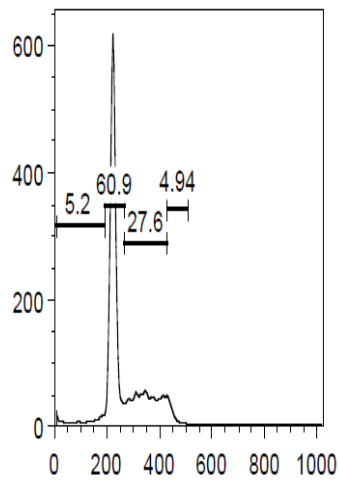
c.   25 µM Compound 5

d.   25 µM Compound 7

285
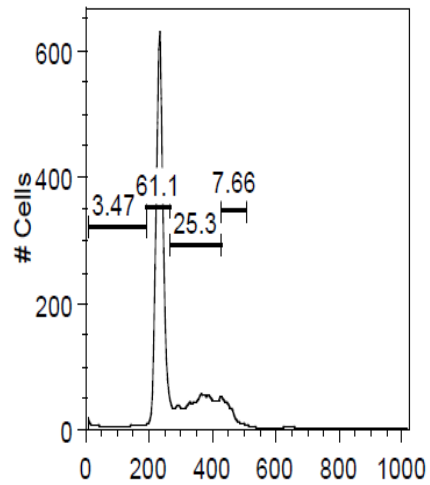
e.   25 µM Compound 9
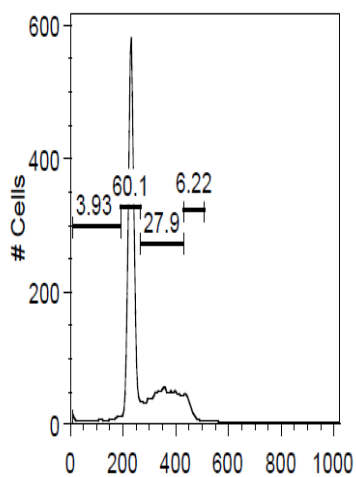
f.   25 µM Compound 10
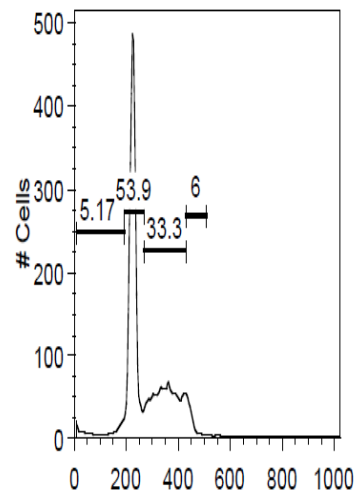
g.   25 µM Compound 11
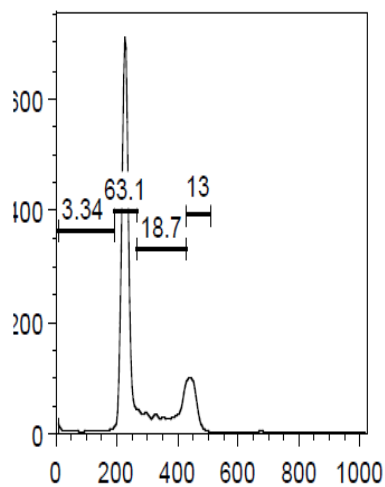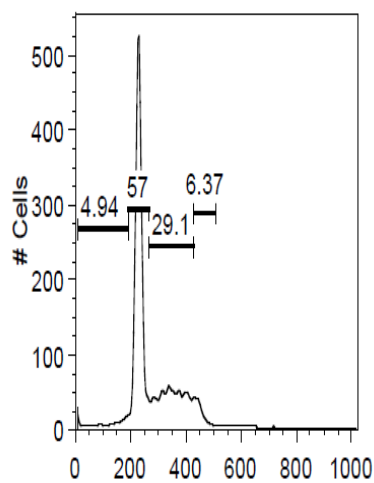
h.   25 µM Compound 13

i. 25 μM Compound 14
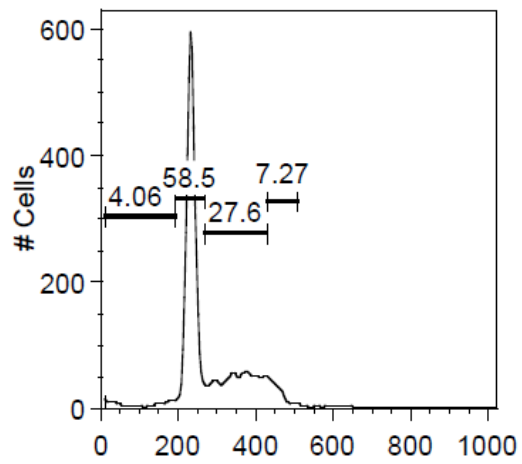
22. Time-dependent analysis of cell cycle progression in HuT-78 cells
(Chapter 6, Tables 7-9)

12h

a. Control

b. 5 μM SAHA

287
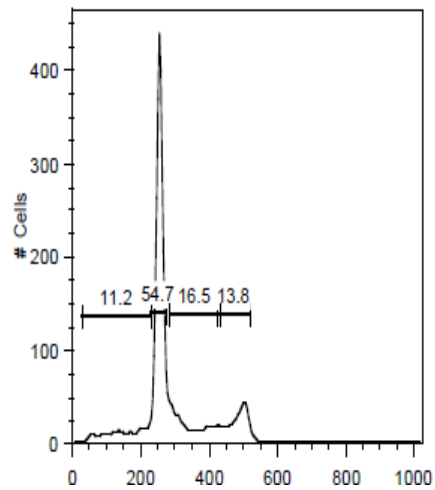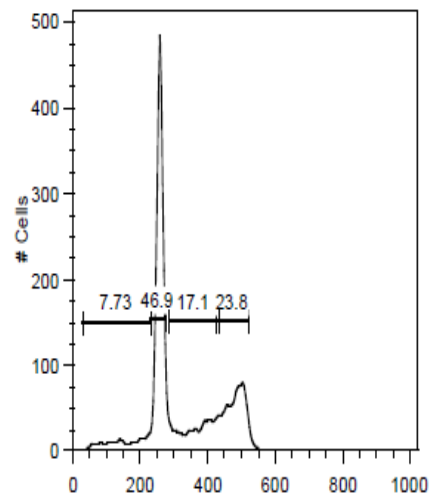
c.   10 µM Compound 2
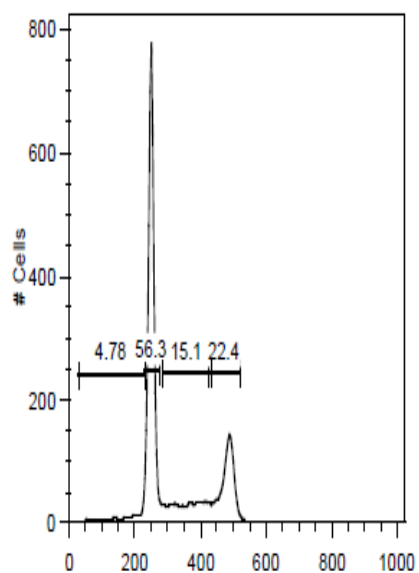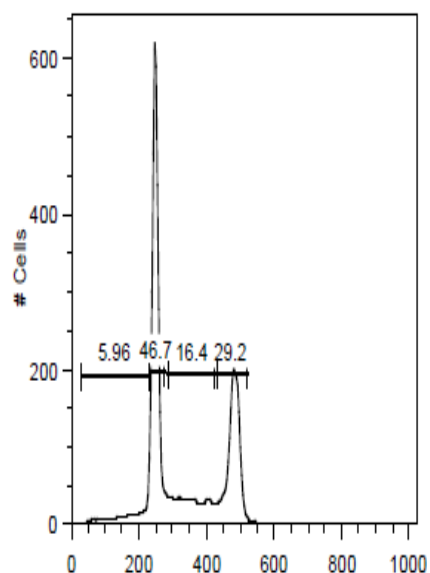
d.   10 µM Compound 7
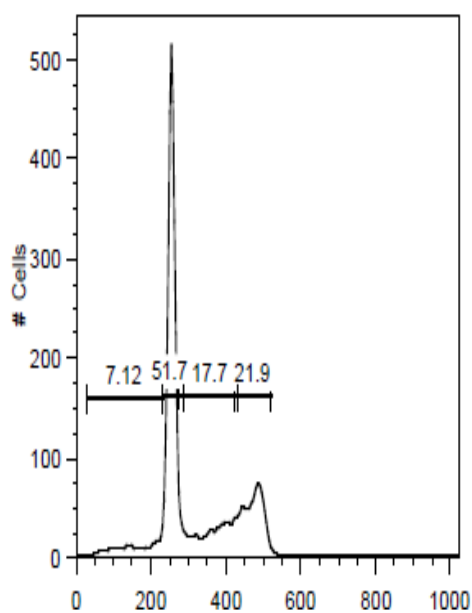
e.   10 µM Compound 11

f.   10 µM Compound 13

24h

g.   Control   h.   5 µM SAHA
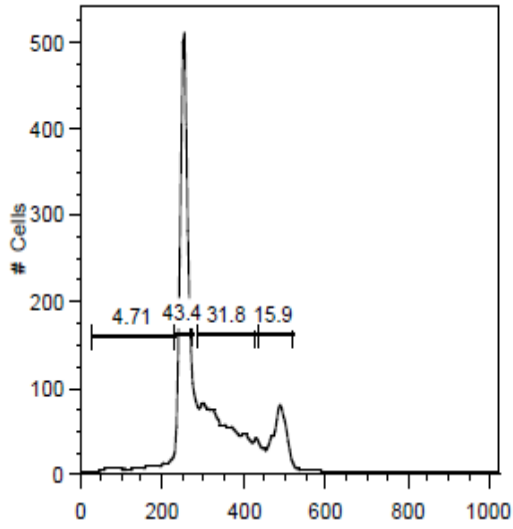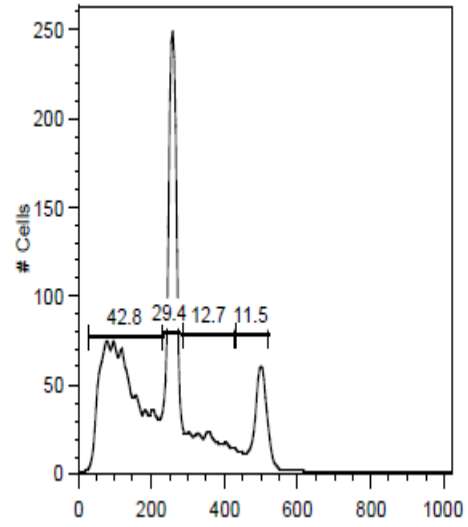
i.   10 µM Compound 2   j.   10 µM Compound 7
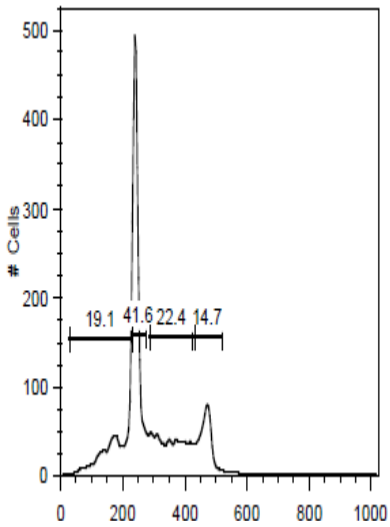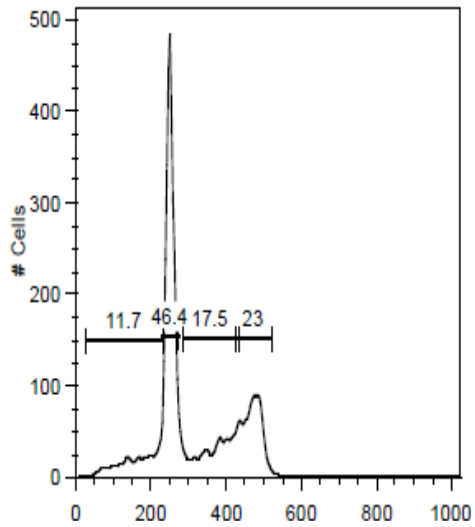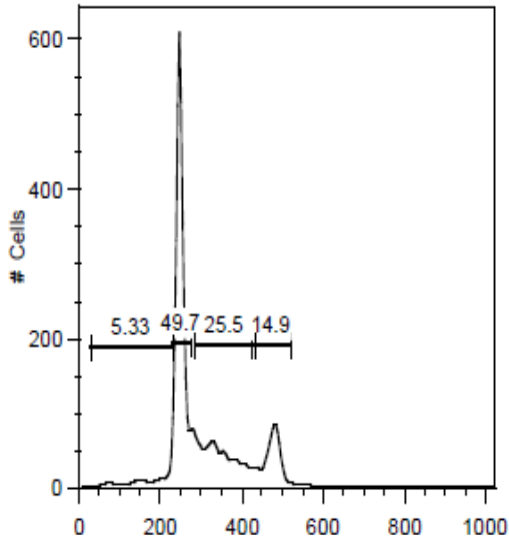
k.   10 μM Compound 11   l.   10 μM Compound 13

36h

m.   Control   n.   5 μM SAHA
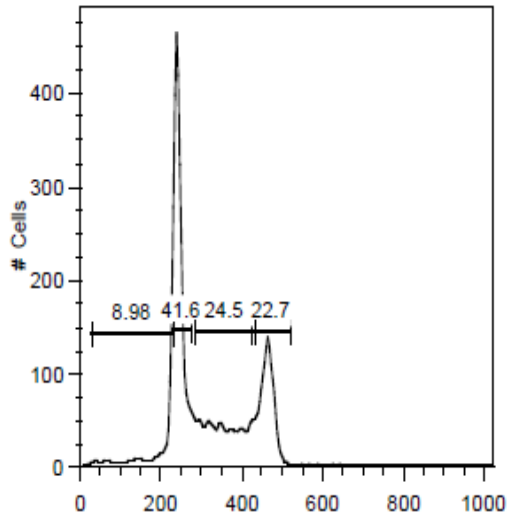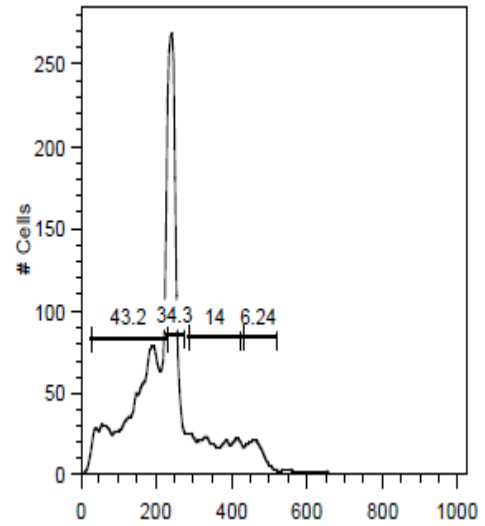
o.   10 µM Compound 2
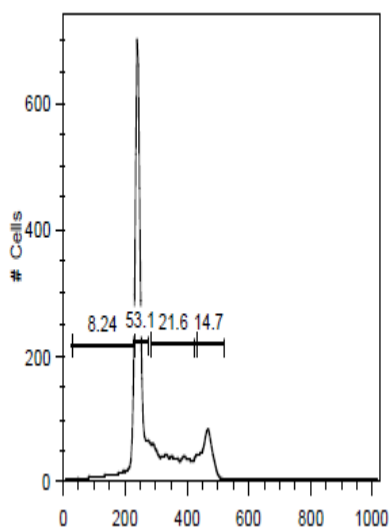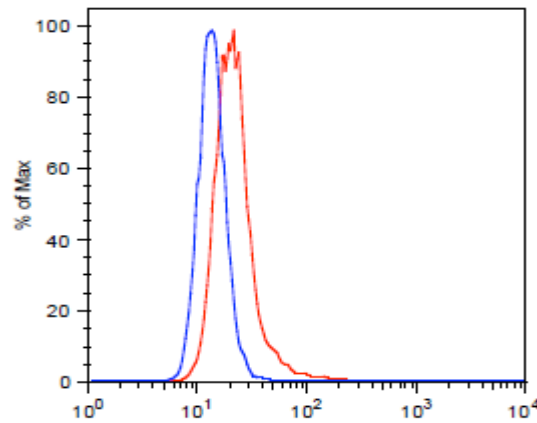

p.   10 µM Compound 7
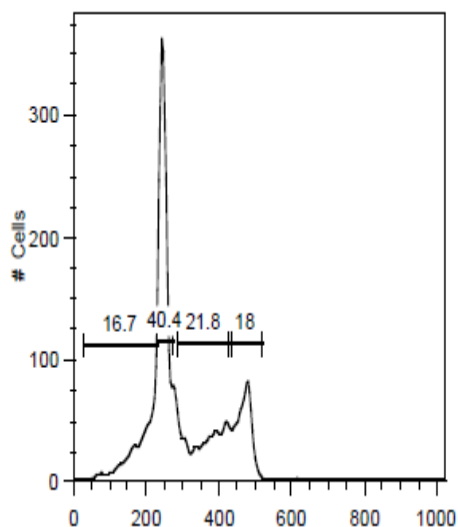
q.   10 µM Compound 11
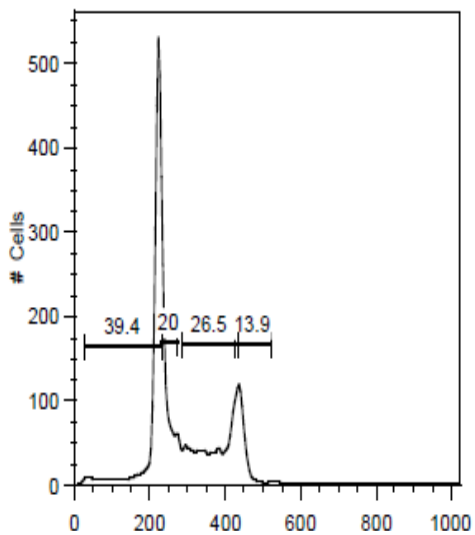
r.   10 µM Compound 13
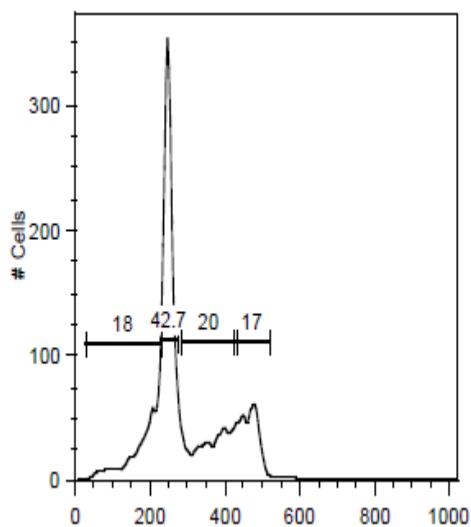
23. Evaluation of p53 expression in Jurkat cells after a 12h treatment with 10 µM HDACi (Chapter 7, Table 1). **Note:** Untreated control for pertinent HDACi treatments represented in red and HDACi represented in blue on the corresponding histograms.

a) Experimental/compensation controls [unlabeled cells (red); 2° antibody (blue); untreated control (green)].

b) SAHA

c) Compound 2

292
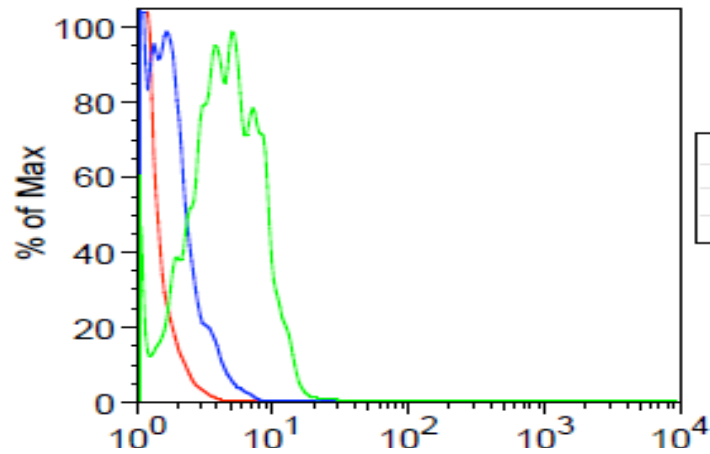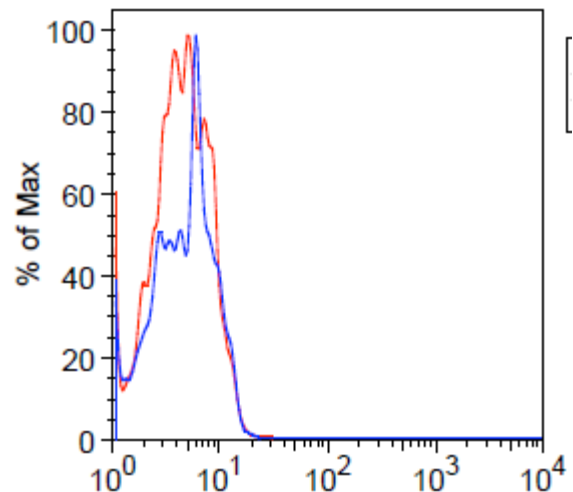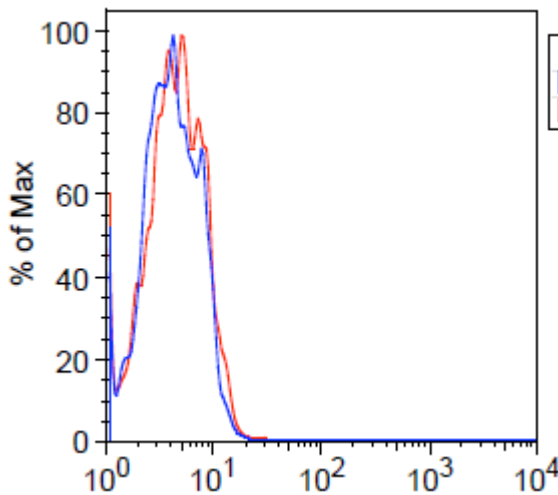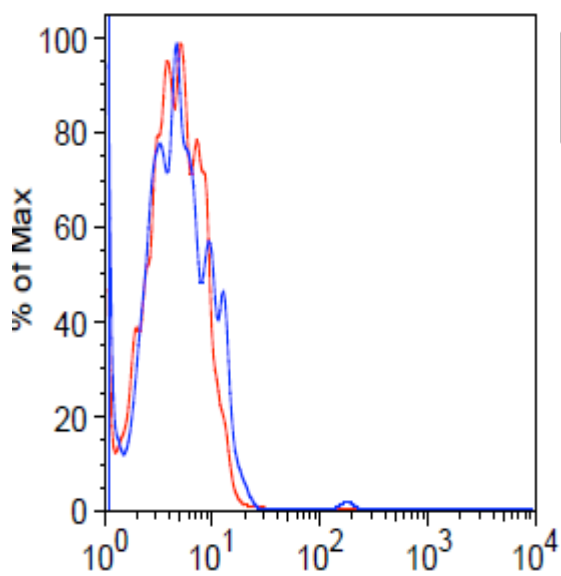
d)   Compound 5
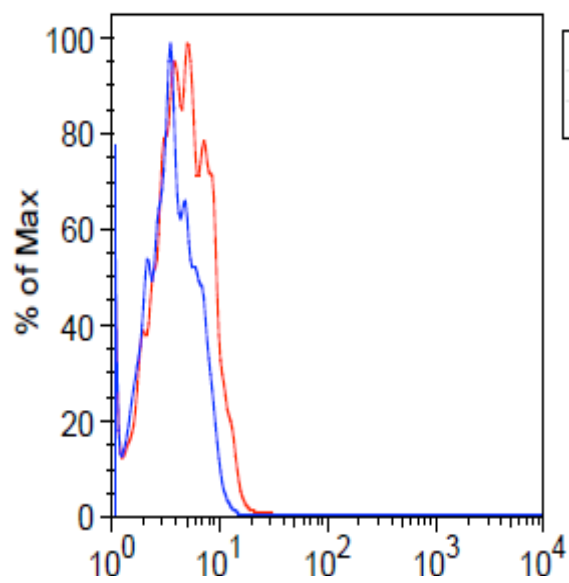
e)   Compound 7
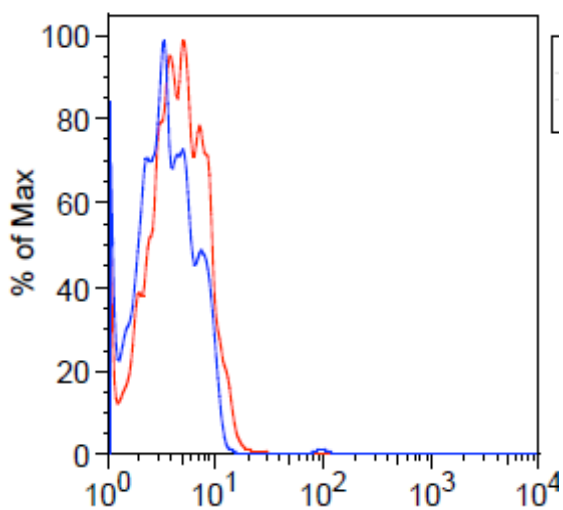
f)   Compound 9
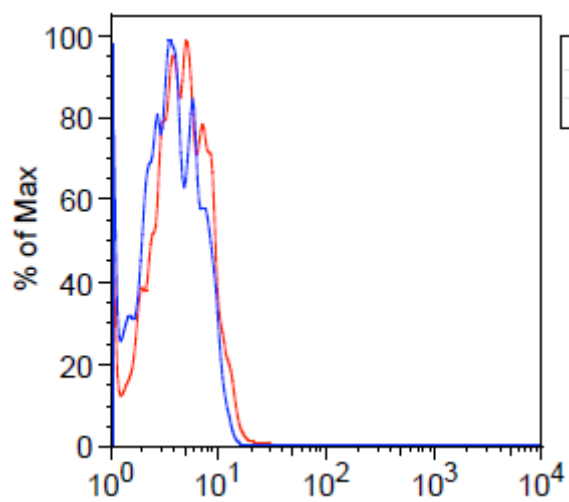
g)   Compound 10
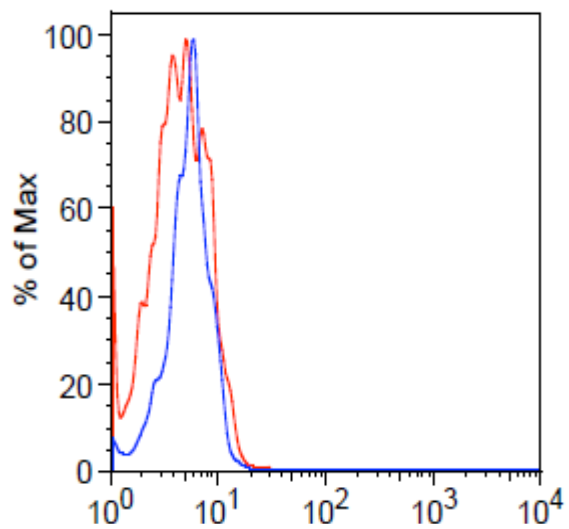
h)   Compound 11
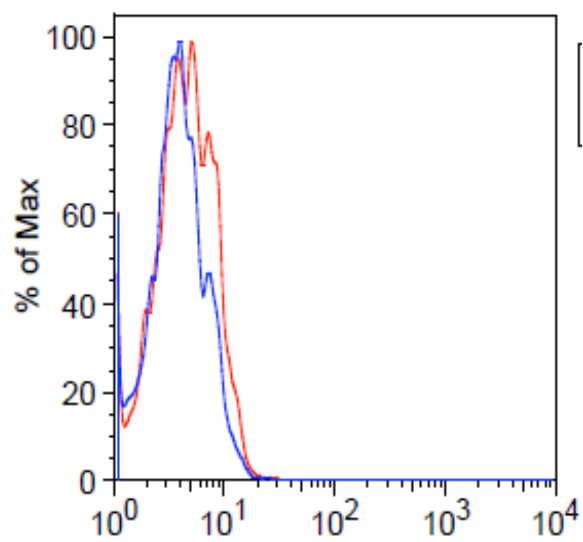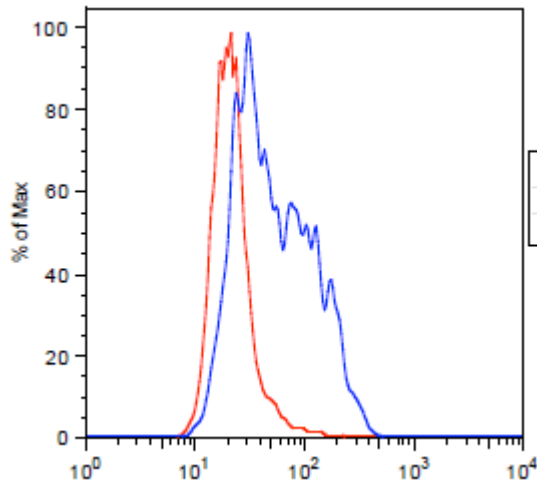
i)   Compound 13

j)   Compound 14

24. Evaluation of p15 expression in Jurkat cells after a **24h** treatment with **10 µM** HDACi (Chapter 7, Table 2). **Note:** Untreated control for pertinent HDACi treatments represented in red and HDACi represented in blue on the corresponding histograms.
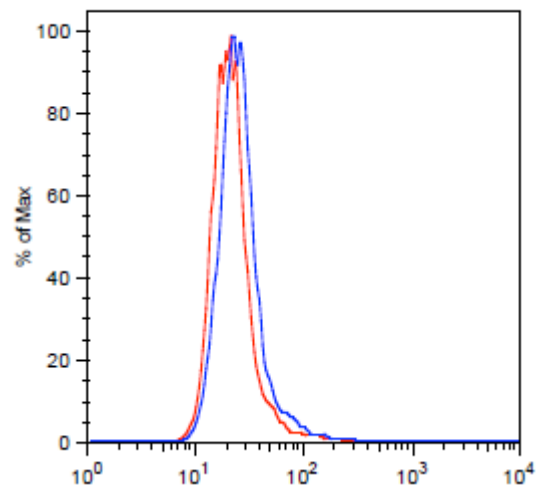
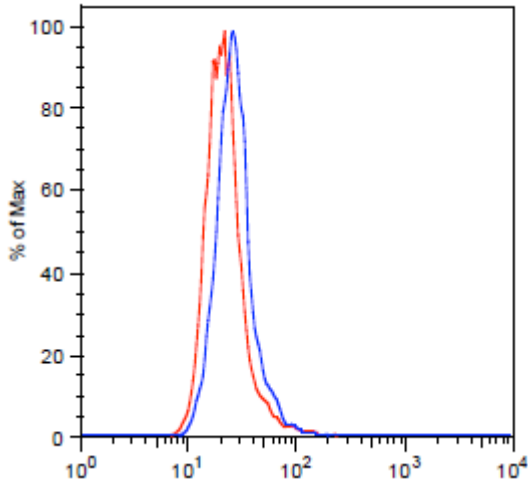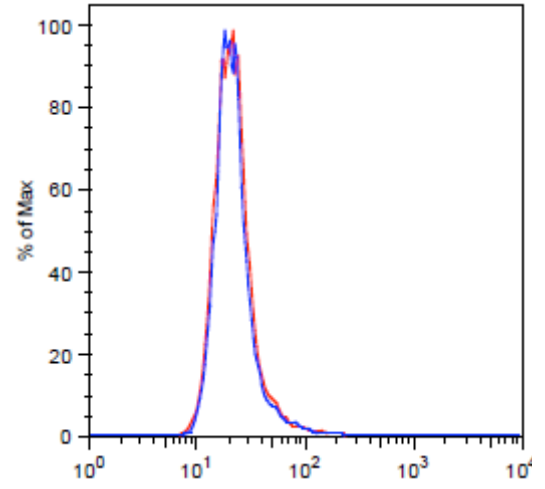a) Experimental/compensation controls [2° antibody (blue) and untreated control (red)].
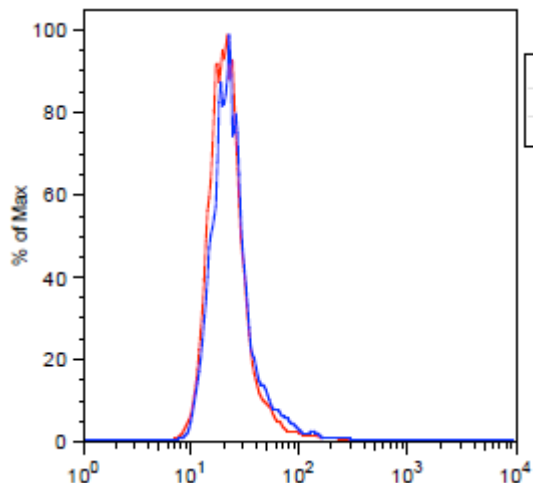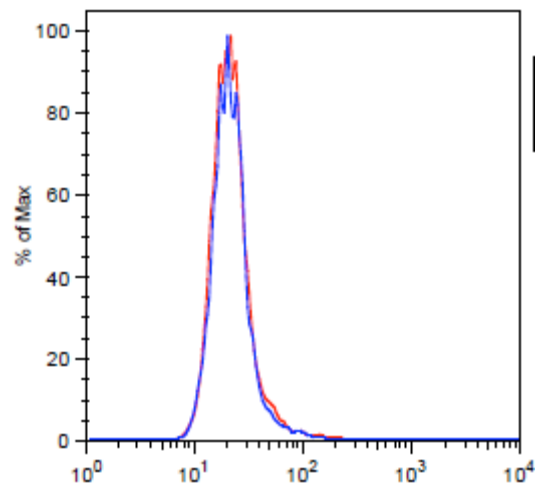

b) SAHA

c) Compound 2

d)   Compound 5

e)   Compound 7

f)   Compound 9

g)   Compound 10

296

h)   Compound 11

i)   Compound 13

j)   Compound 14

297
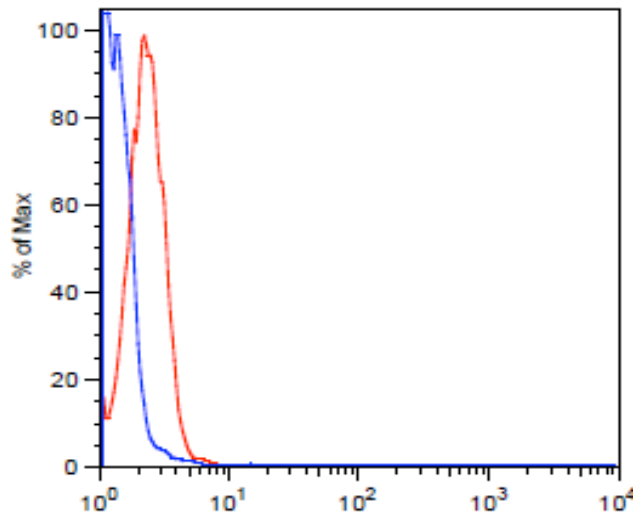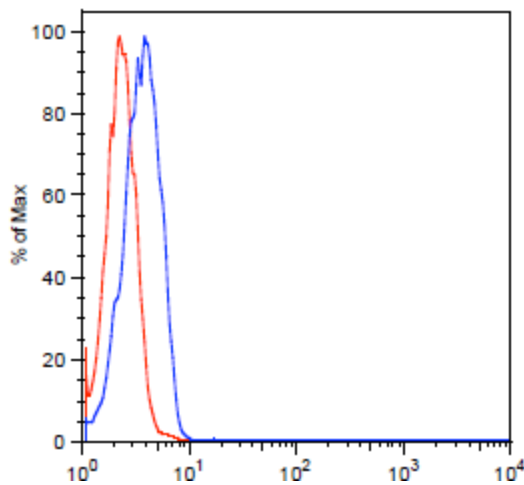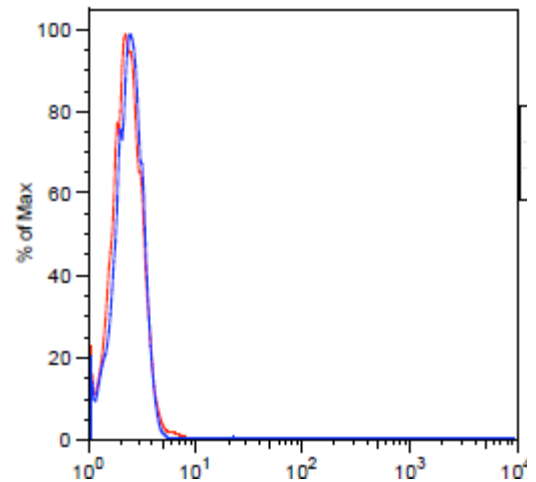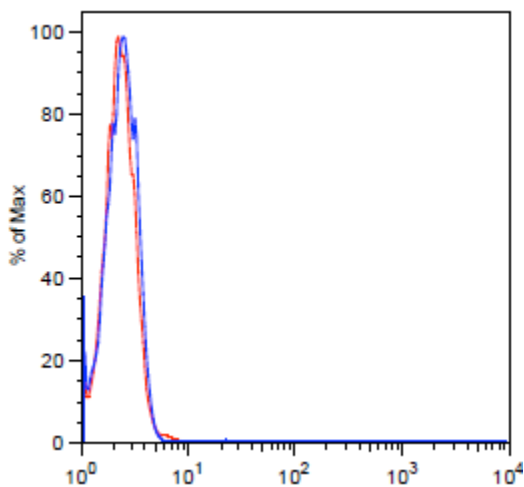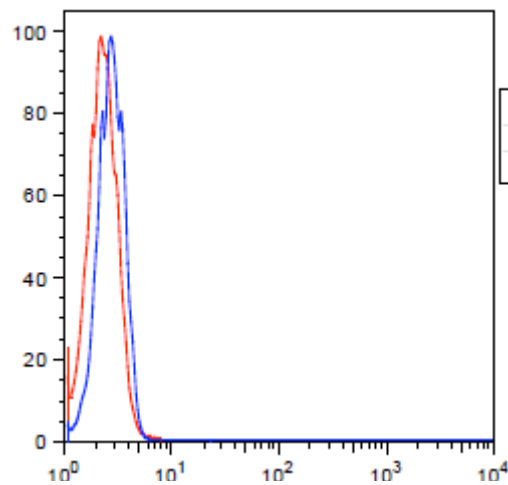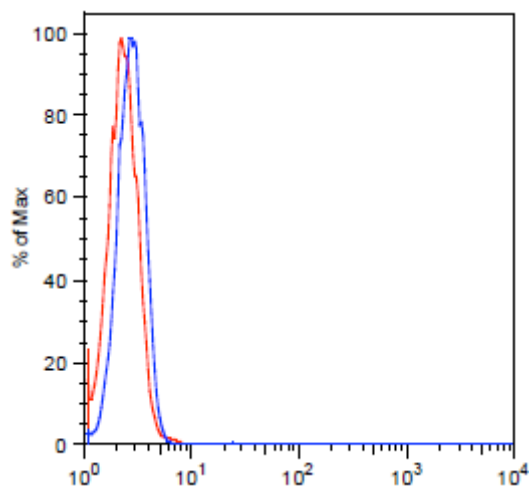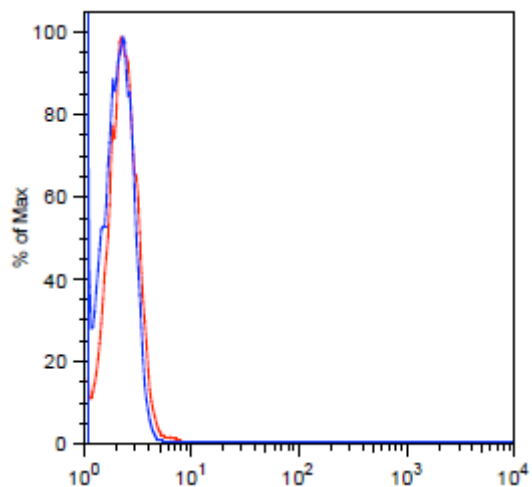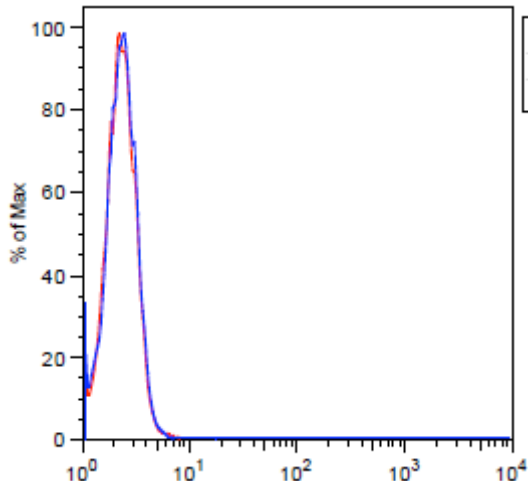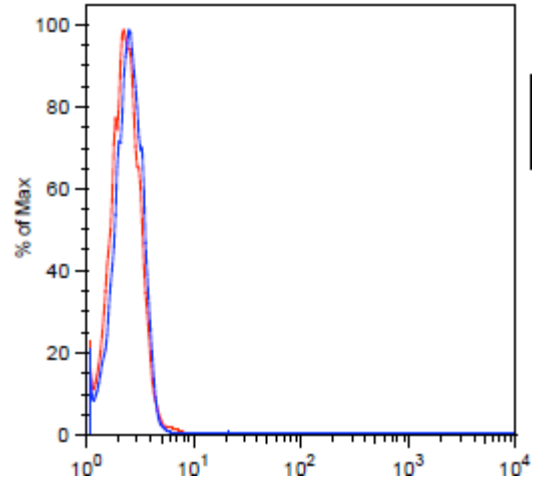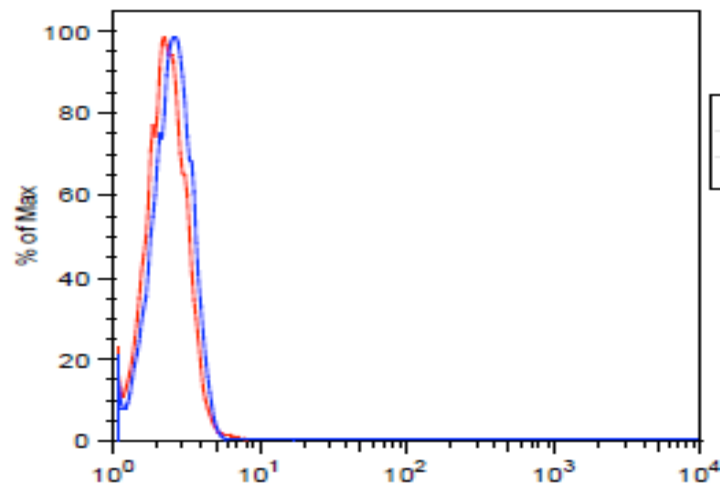
25. Evaluation of p15 expression in Jurkat cells after a **24h** treatment with **50 μM** HDACi (Chapter 7, Table 2). **Note:** Untreated control for pertinent HDACi treatments represented in red and HDACi represented in blue on the corresponding histograms.

a)   Experimental/compensation controls [2° antibody (blue) and untreated control (red)].

b)   Compound 2

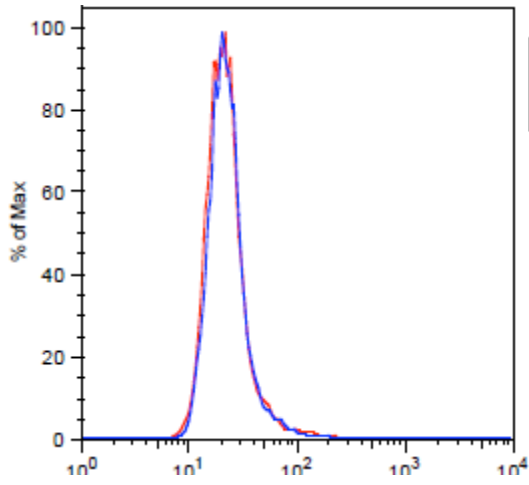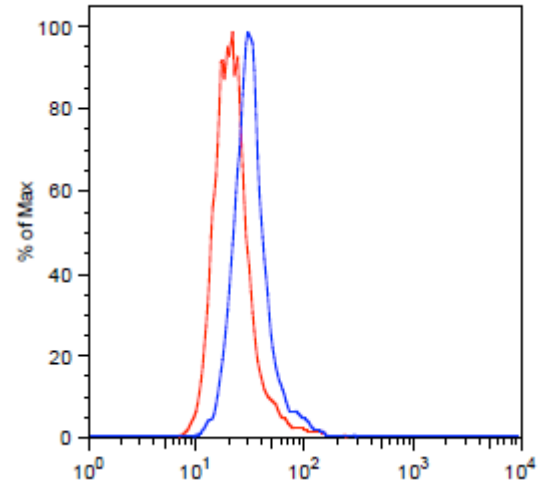c)   Compound 3

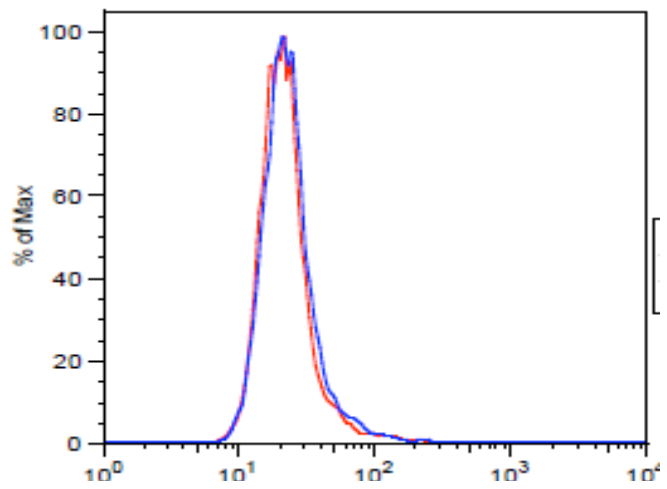d)   Compound 7

e)   Compound 10

f)   Compound 11

g)   Compound 12

h)   Compound 13

i)   Compound 14

26. Evaluation of p15 expression in HuT-78 cells after a 24h treatment with 10 µM HDACi (Chapter 7, Table 2). **Note:** Untreated control for pertinent HDACi treatments represented in red and HDACi represented in blue on the corresponding histograms.

a)   Experimental/compensation controls [2° antibody (blue) and untreated control (red)].

300
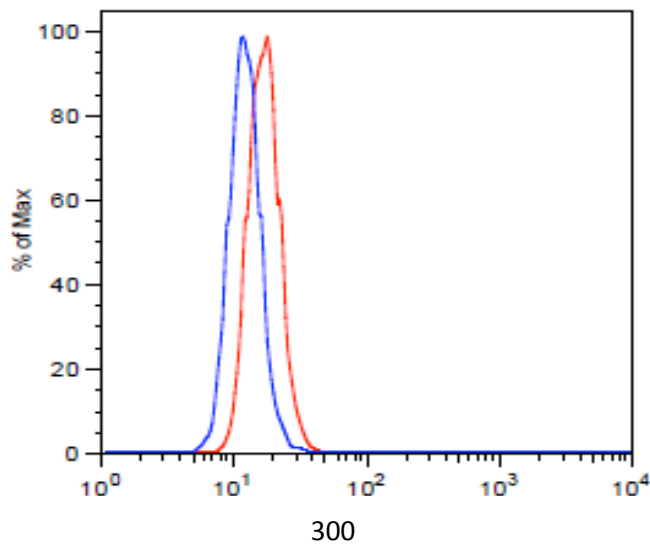
b)   SAHA
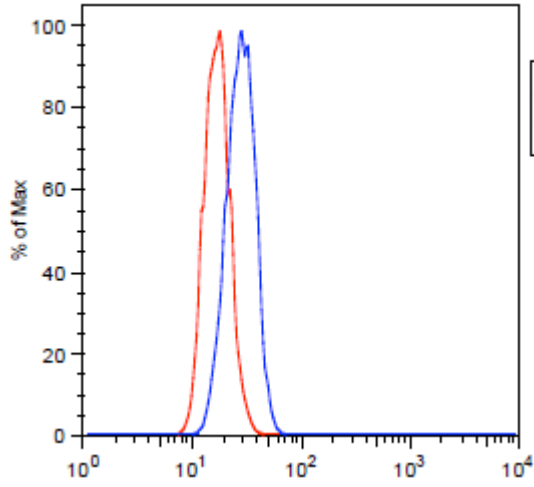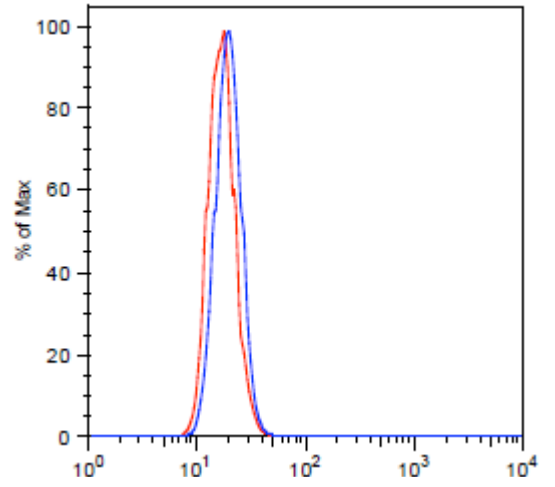
c)   Compound 2

d)   Compound 3

e)   Compound 5

301
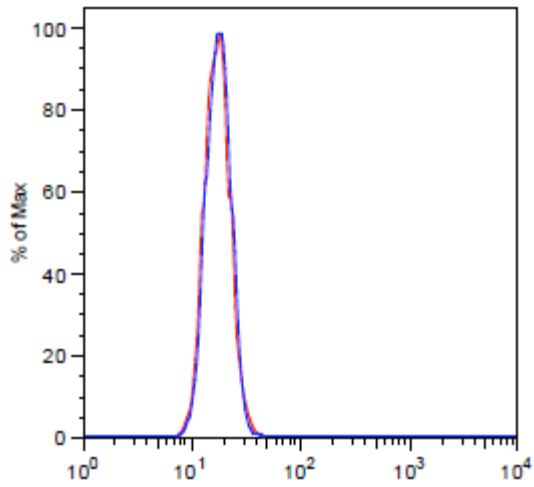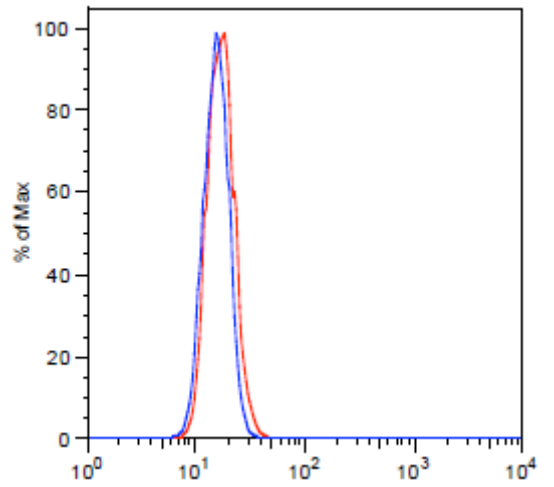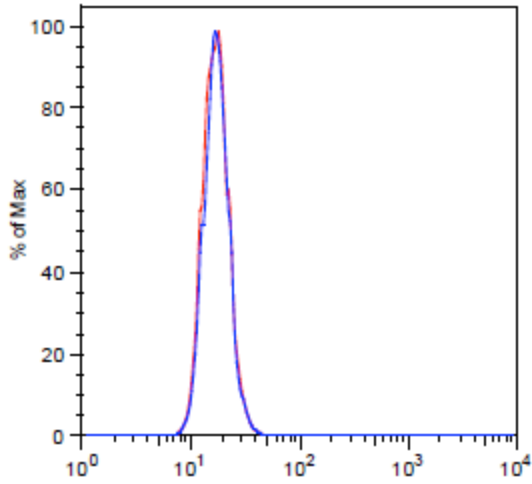
f)   Compound 7

g)   Compound 9
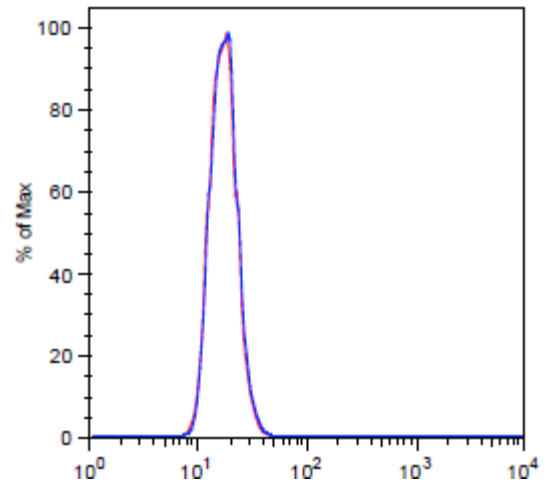
h)   Compound 10
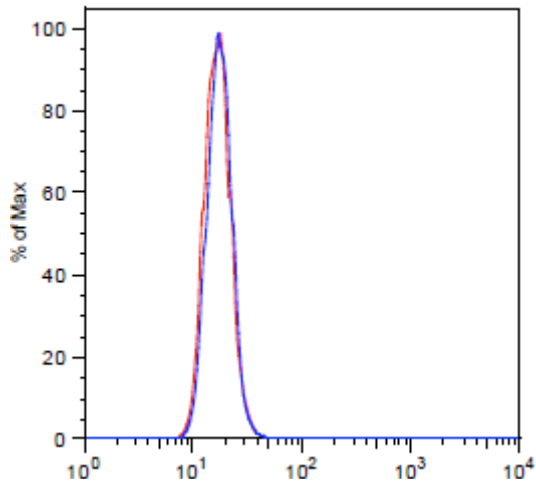
i)   Compound 12

302
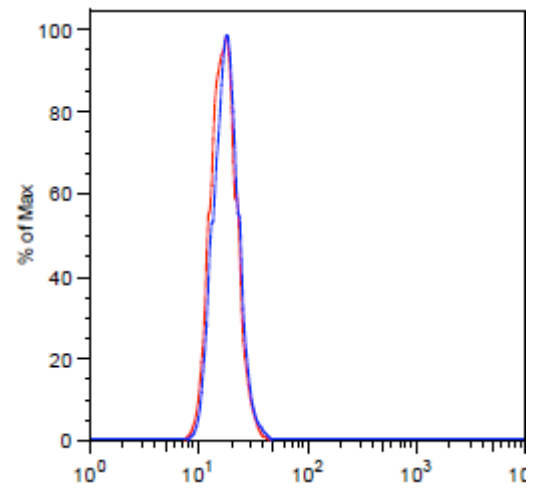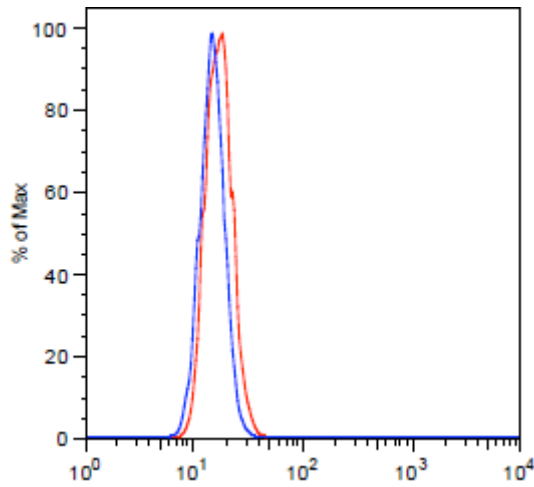
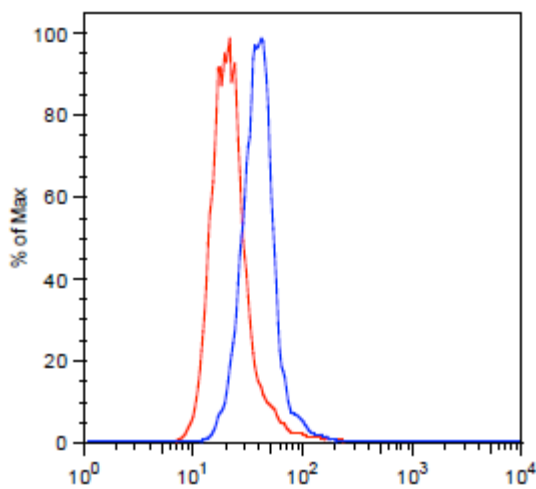j)   Compound 13   k)   Compound 14
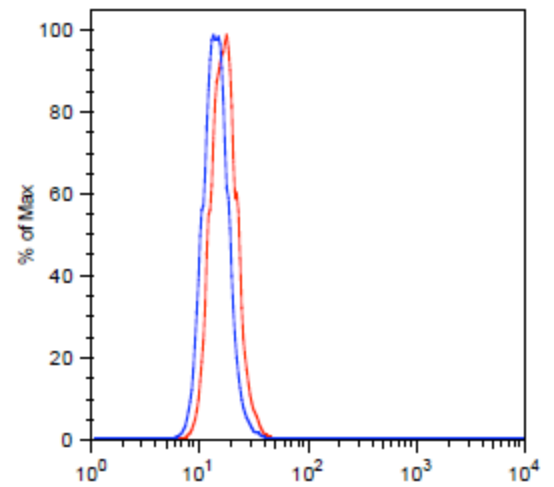
27. Evaluation of p15 expression in HuT-78 cells after a 24h treatment with **50** μM HDACi (Chapter 7, Table 2). **Note:** Untreated control for pertinent HDACi treatments represented in red and HDACi represented in blue on the corresponding histograms.

a)   Experimental/compensation controls [2° antibody (blue) and untreated control (red)].


303

b)   Compound 2

c)   Compound 3

d)   Compound 7

e)   Compound 10

304
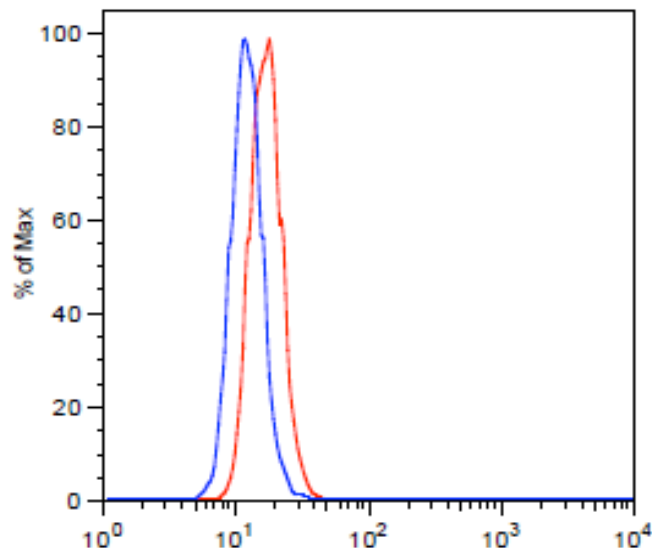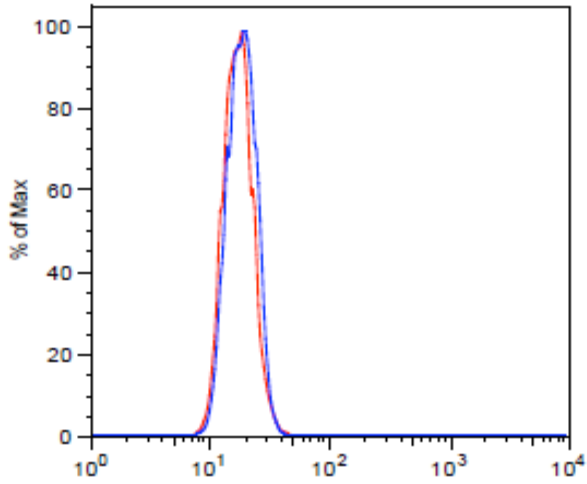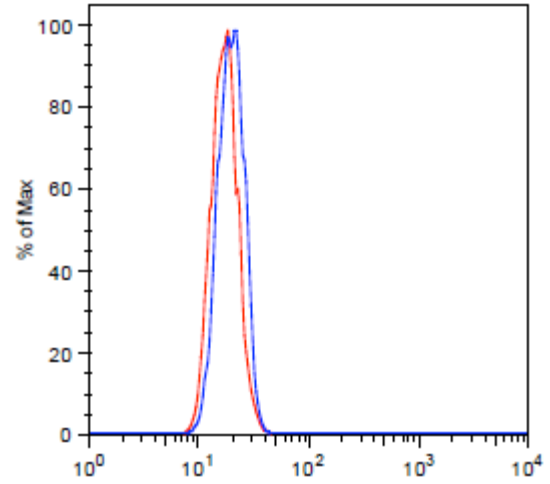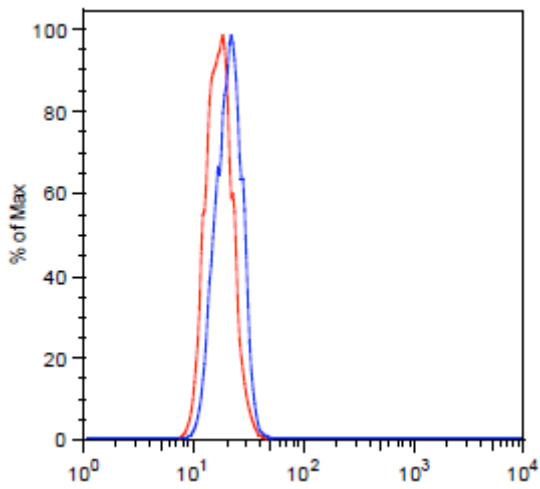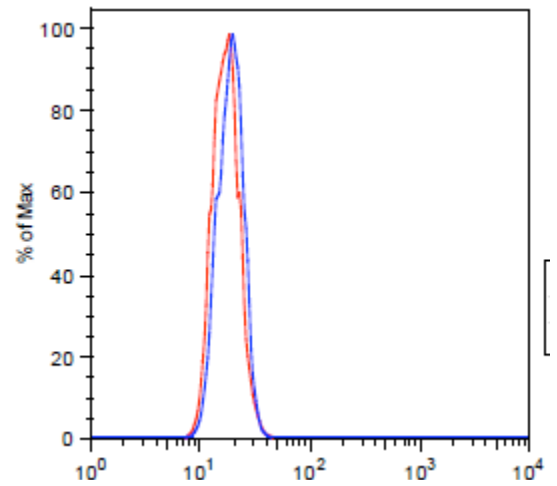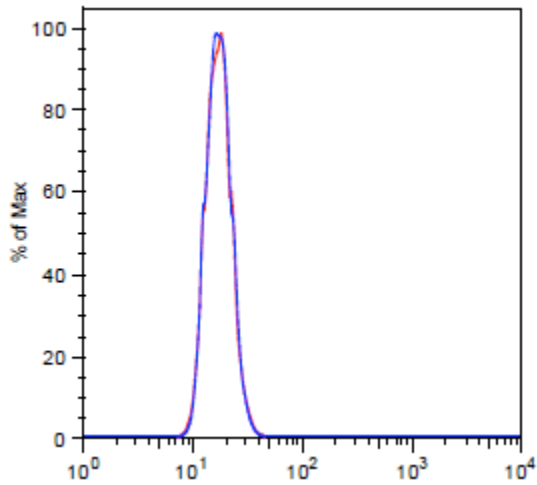
f)   Compound 11
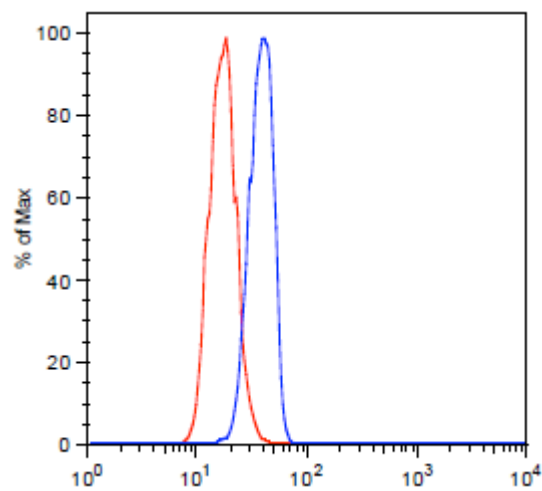
g)   Compound 12
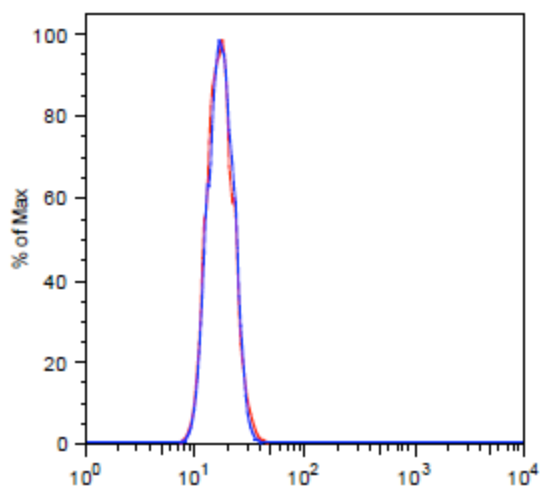
h)   Compound 13

i)   Compound 14
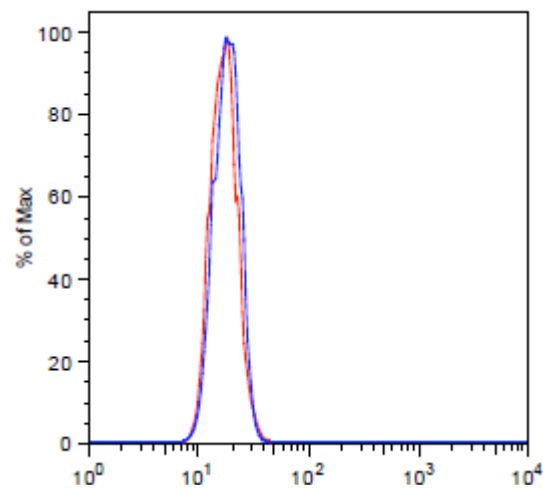
28. Evaluation of p27 expression in Jurkat cells after a **24h** treatment with HDACi (Chapter 7, Table 3). **Note:** Untreated control for pertinent HDACi treatments represented in red and HDACi represented in blue on the corresponding histograms.

a) Experimental/compensation controls [Unlabeled cells (red); 2° antibody (blue) and untreated control (green)].


b) SAHA

c) Compound 2

d)   Compound 5

e)   Compound 7

f)   Compound 9

g)   Compound 10

307
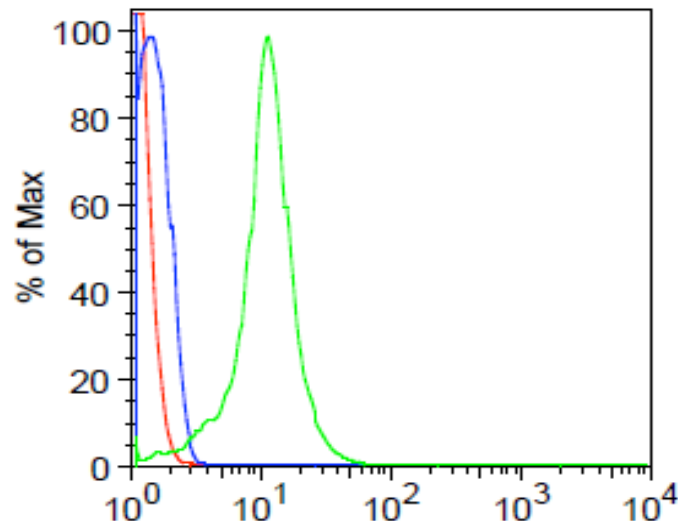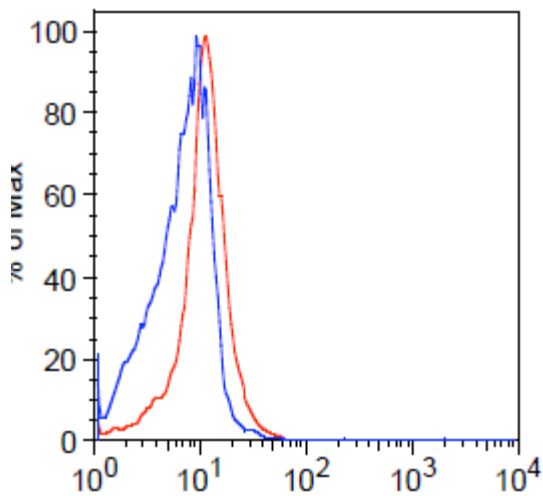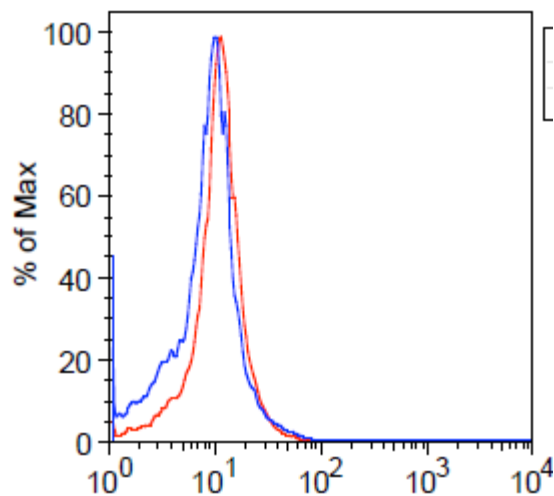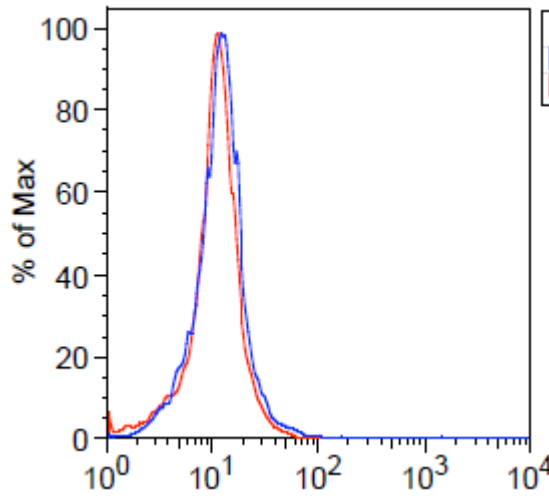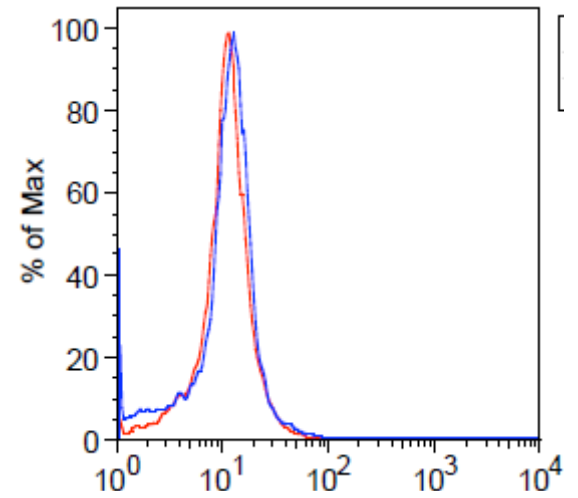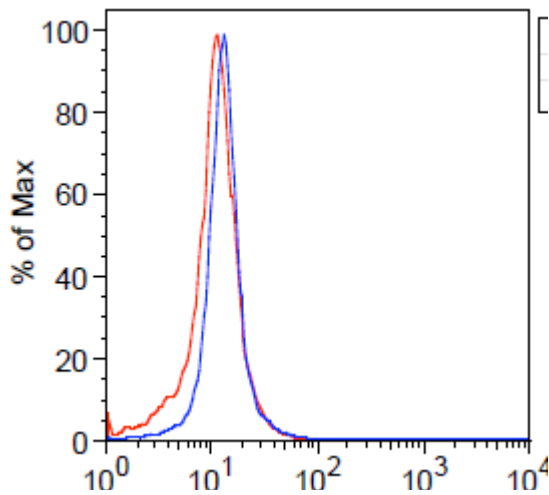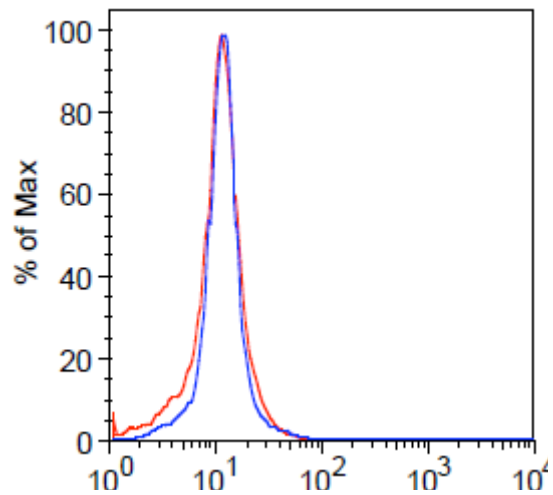
h)   Compound 11

i)   Compound 13

j)   Compound 14
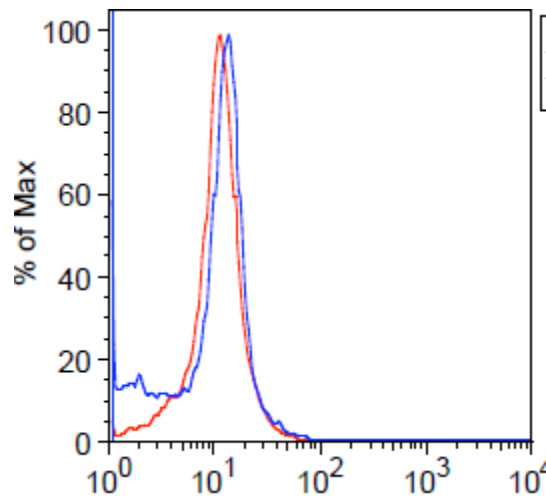
29. Evaluation of p27 expression in Jurkat cells after a **24h** treatment with HDACi (Chapter 7, Table 4). **Note:** Untreated control for pertinent HDACi treatments represented in red and HDACi represented in blue on the corresponding histograms.

a)   Experimental/compensation controls [2° antibody (blue) and untreated control (red)].

b)   10 µM SAHA   c)   10 µM Compound 2
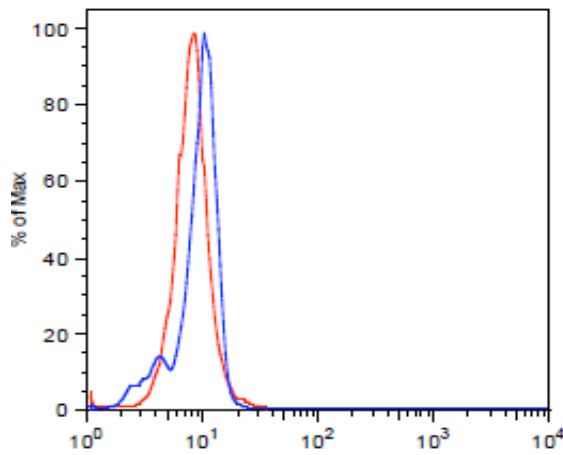
d)   50 µM Compound 2
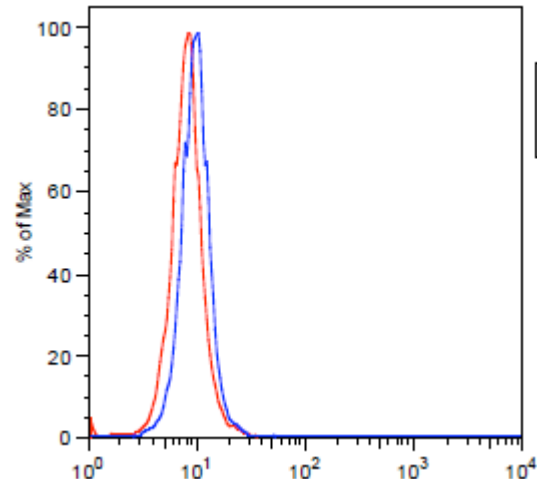
e)   10 µM Compound 7

e)   10 µM Compound 7
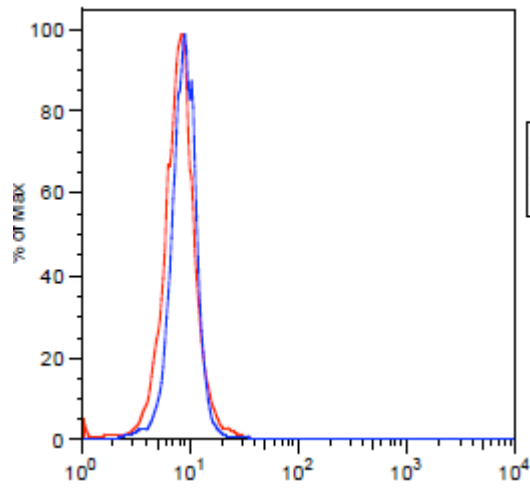
30. Evaluation of p27 expression in HuT-78 cells after a 12h treatment with 10 µM HDACi (Chapter 7, Table 4). **Note:** Untreated control for pertinent HDACi treatments represented in red and HDACi represented in blue on the corresponding histograms.

a)   Experimental/compensation controls [2° antibody (blue); untreated control (red)]

b)   Compound 2

c)   Compound 5

311
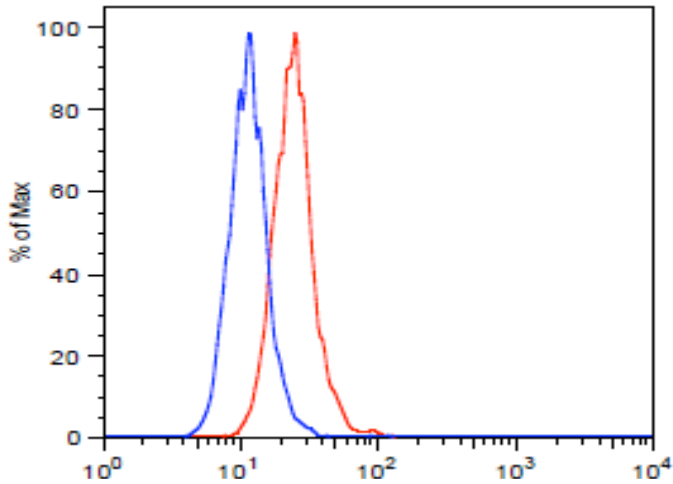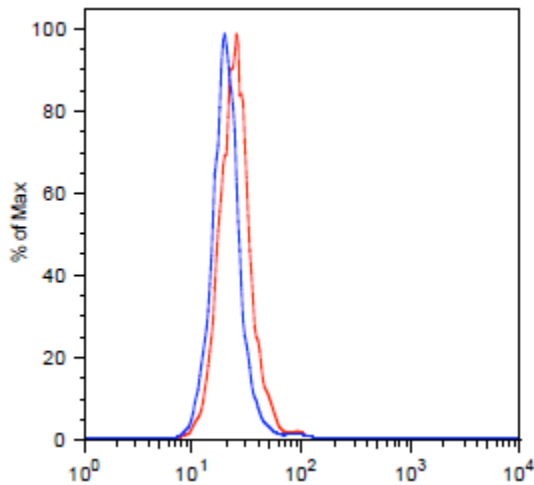
d)   Compound 7

e)   Compound 9

f)   Compound 10

g)   Compound 11

h)   Compound 13

i)   Compound 14

31. Evaluation of p21 expression in Jurkat cells after a 12h treatment with
    10 µM HDACi (Chapter 7, Table 5). **Note:** Untreated control for
    pertinent HDACi treatments represented in red and HDACi
    represented in blue on the corresponding histograms.

a)   Experimental/compensation controls [unlabeled cells (red); 2° antibody
       (blue); untreated control (green)].

313

b)   SAHA

c)   Compound 2

d)   Compound 5

e)   Compound 7

f)　　Compound 9

g)　　Compound 10

h)　　Compound 11

i)　　Compound 13

315
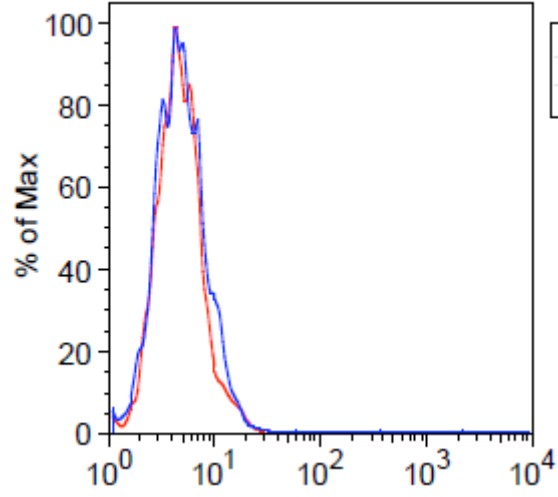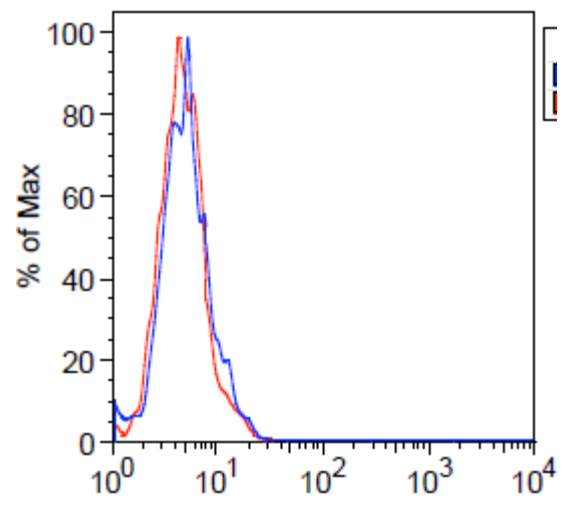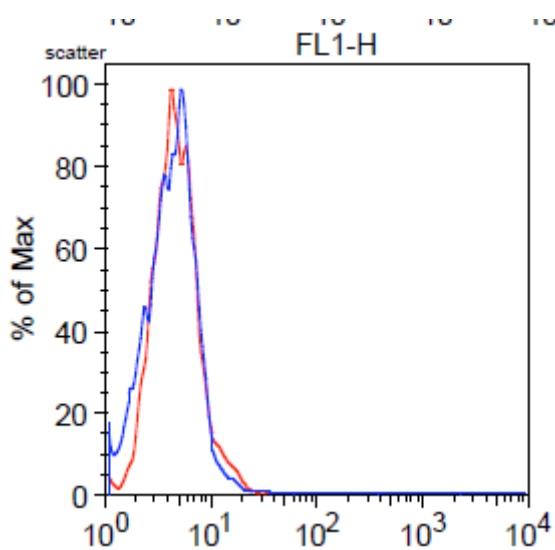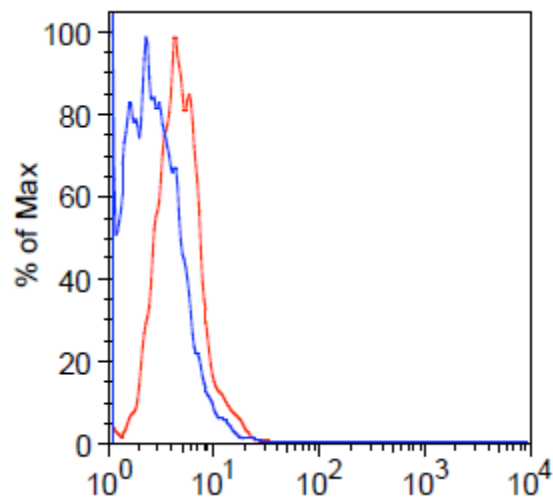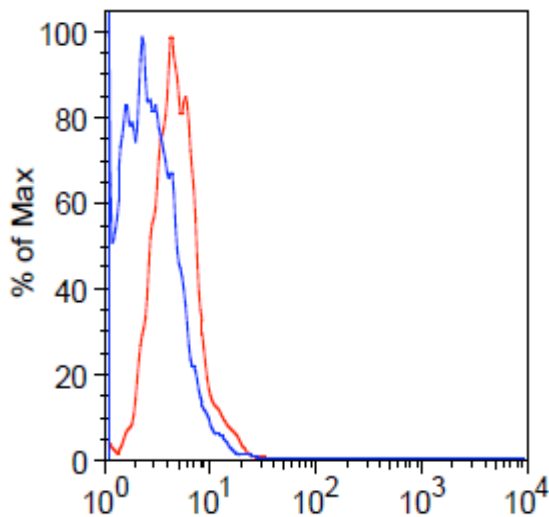
j)   Compound 14
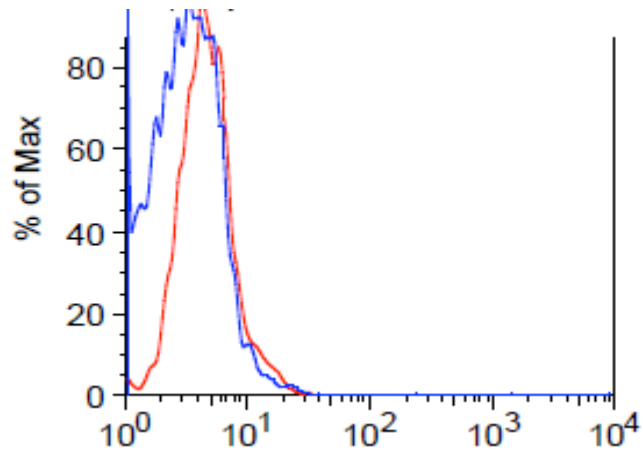
32. Comparative analysis of secondary (2°) antibody treatment only (blue) and the untreated control (primary (1°) + 2° antibody; red) for evaluation of p21 expression in Jurkat cells after a **24h** treatment with **10** µM HDACi (Chapter 7, Table 6).
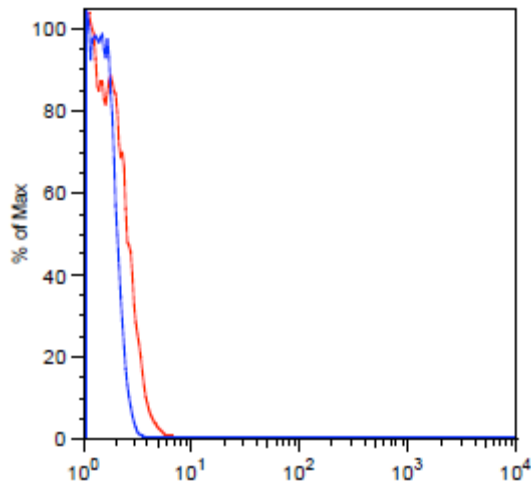
33. Evaluation of p21 expression in Jurkat cells after a **24h** treatment with **50** μM HDACi (Chapter 7, Table 6). **Note:** Untreated control for pertinent HDACi treatments represented in red and HDACi represented in blue on the corresponding histograms.

a)   Experimental/compensation controls [2° antibody (blue); untreated control (red)].
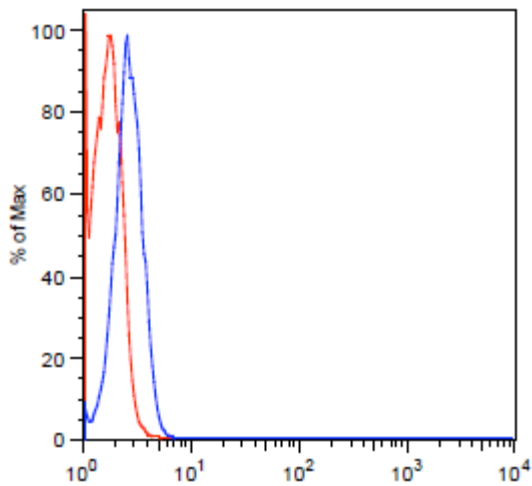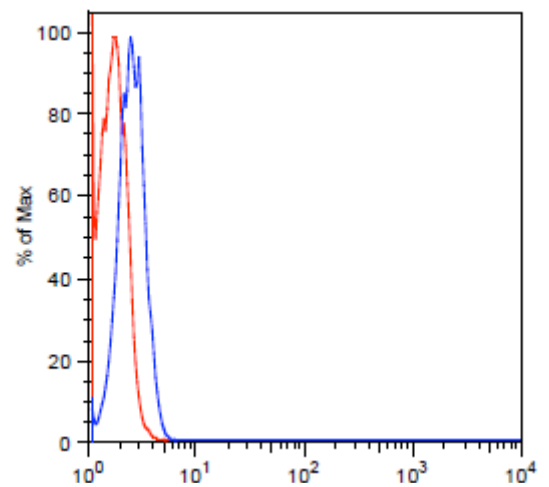
b)   Compound 2

c)   Compound 3

317

d)   Compound 7

e)   Compound 10

f)   Compound11

318

g)   Compound 12

h)   Compound 13

i)   Compound 14

319
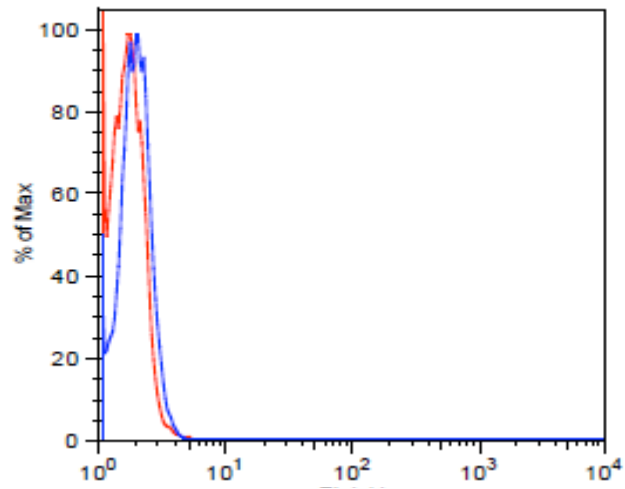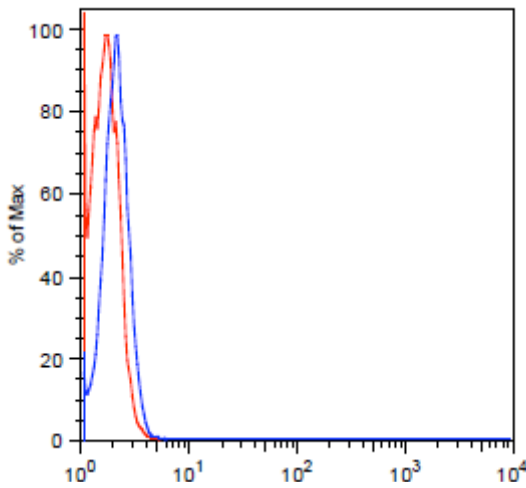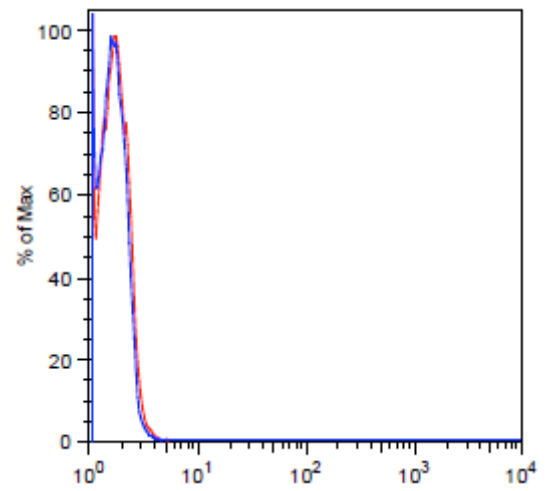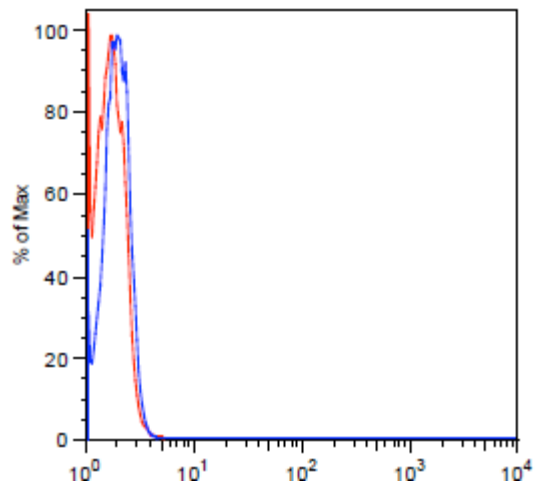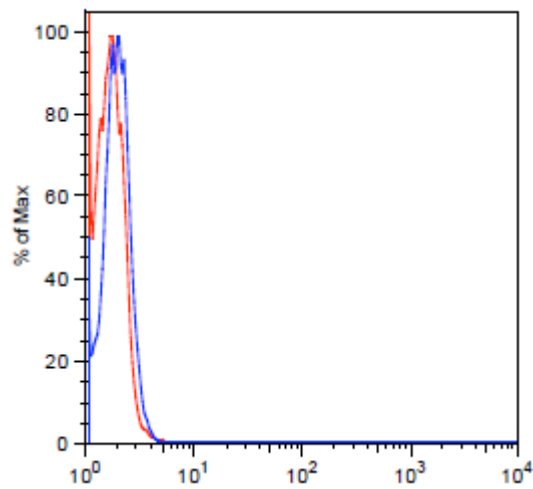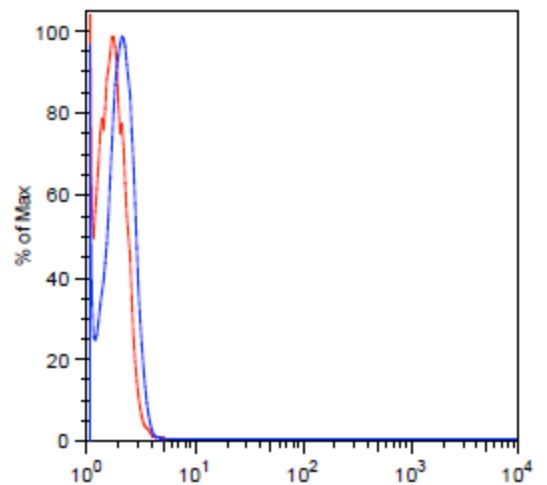
34. Evaluation of p21 expression in HuT-78 cells after a **24h** treatment with **10 µM** HDACi (Chapter 7, Table 6). **Note:** Untreated control for pertinent HDACi treatments represented in red and HDACi represented in blue on the corresponding histograms.

a) Experimental/compensation controls [2° antibody (blue) and untreated control (red)].

b) SAHA

c) Compound 2

320

d)   Compound 5   e)   Compound 7

f)   Compound 9   g)   Compound 10

h) Compound 11

i) Compound 13

j) Compound 14

35. Evaluation of p21 expression in HuT-78 cells after a **24h** treatment with **50 µM** HDACi (Chapter 7, Table 6). **Note:** Untreated control for pertinent HDACi treatments represented in red and HDACi represented in blue on the corresponding histograms.

a) Experimental/compensation controls [2° antibody (blue) and untreated control (red)].

b) Compound 2

c) Compound 3

323
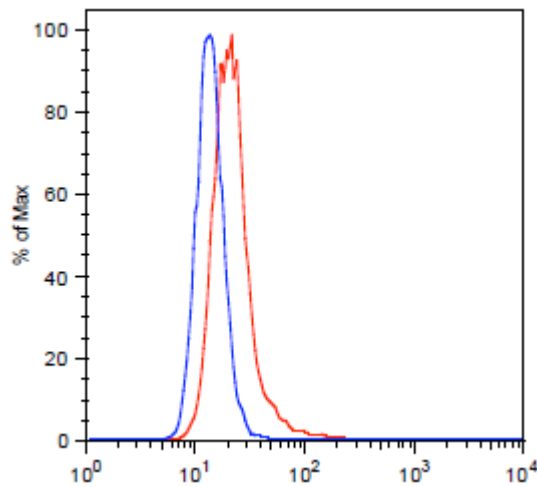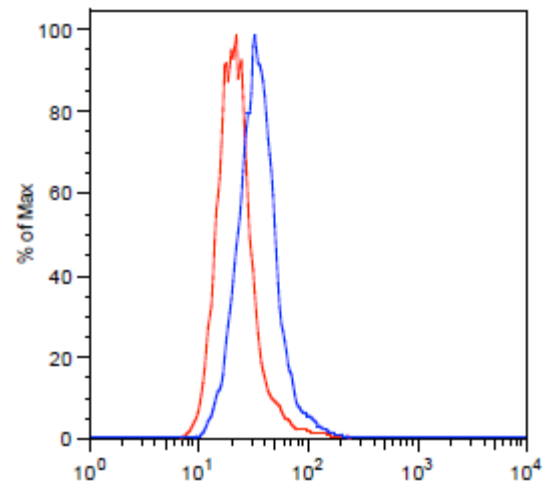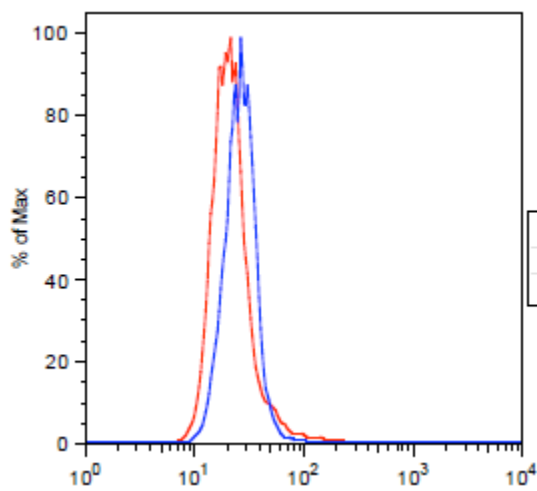
d) Compound 7
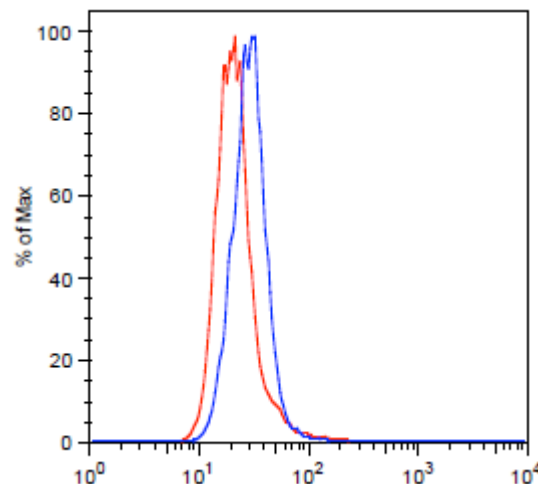
e) Compound 10
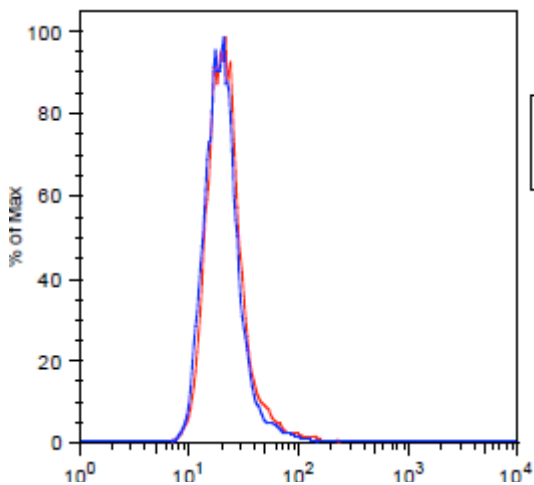
f) Compound 11
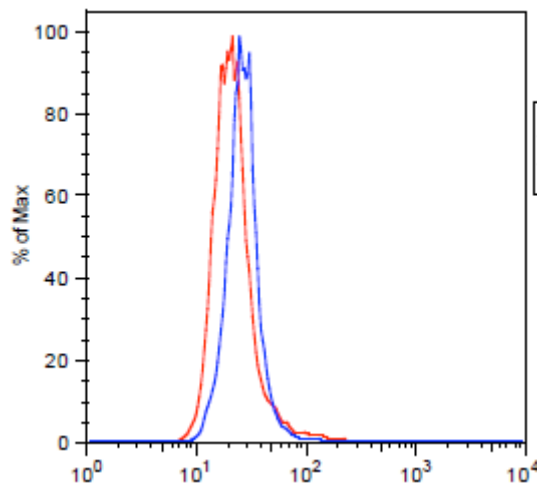
g) Compound 12
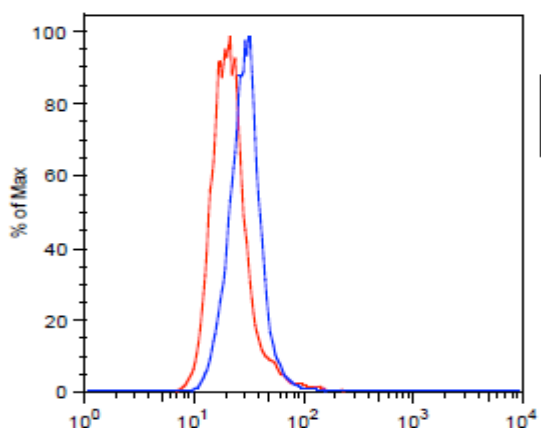
h)   Compound 13   i)   Compound 14
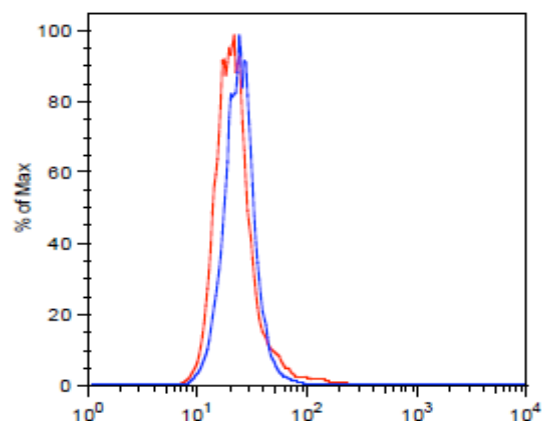
36. Elucidation of standard error values for gene expression analyses (Chapter 7, Table 7).			
	HDAC2	**p21**	**VDR**
Compound 2	0.16	0.01	0.04
SAHA	0.11	36.74	8.59

37. Time-dependent analysis of the induction of apoptosis in Jurkat cells (Chapter 8, Table 2): y axis represents PI response whereas x axis represents Annexin V (AV) response. Quadrant 1 (bottom left) represents intact (live) cells (AV⁻, PI⁻); Quadrant 2 (bottom right) represents early apoptotic cells (AV+, PI⁻); Quadrant 3 (top right) represents late apoptotic/necrotic cells ((AV⁺, PI⁺).

6h

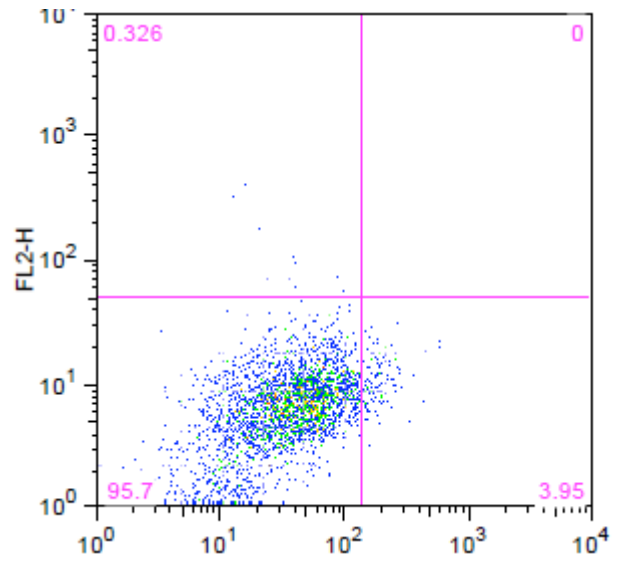a)   Control   b)   10 μM SAHA

c)   10 μM Compound 2

326

12h
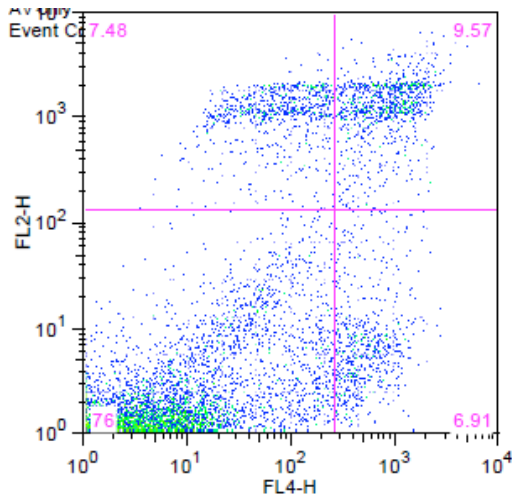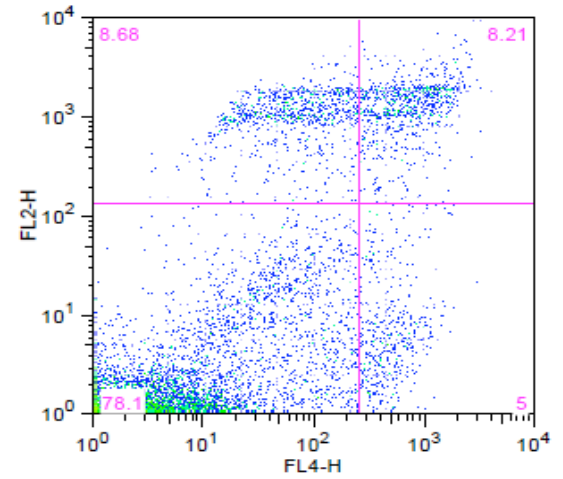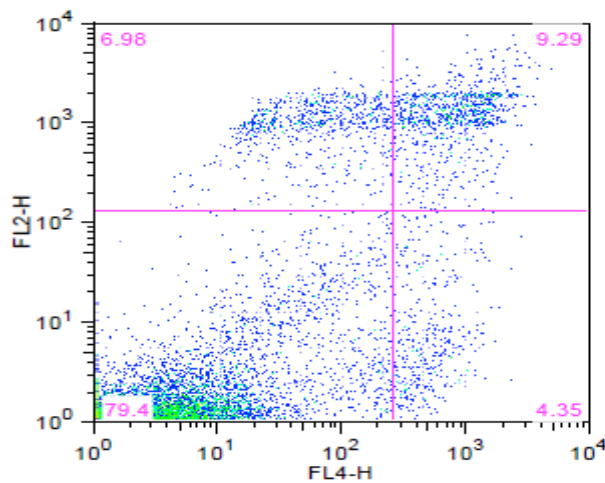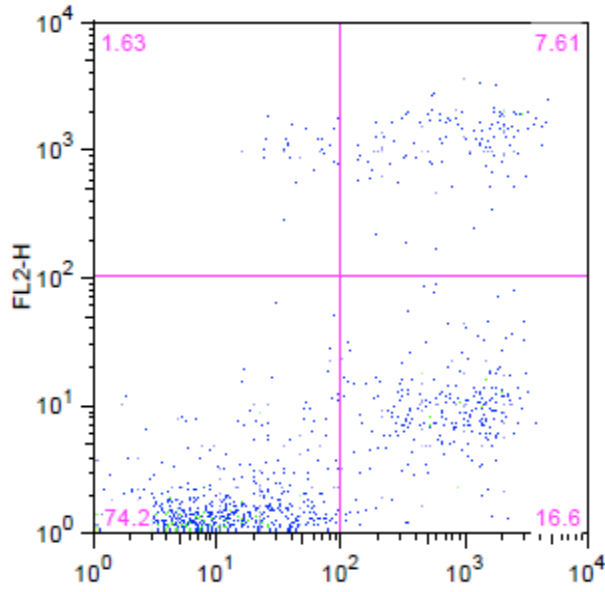
a)   Control   b)   10 µM SAHA
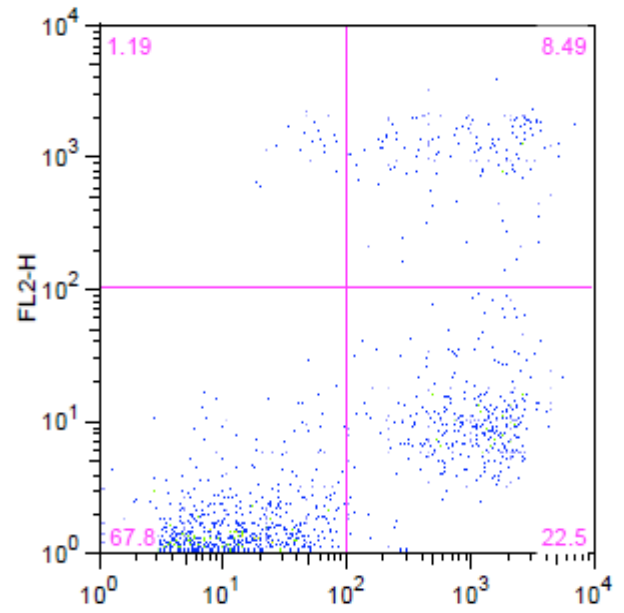
c)   10 µM Compound 2

24h

a)   Control

b)   10 µM SAHA
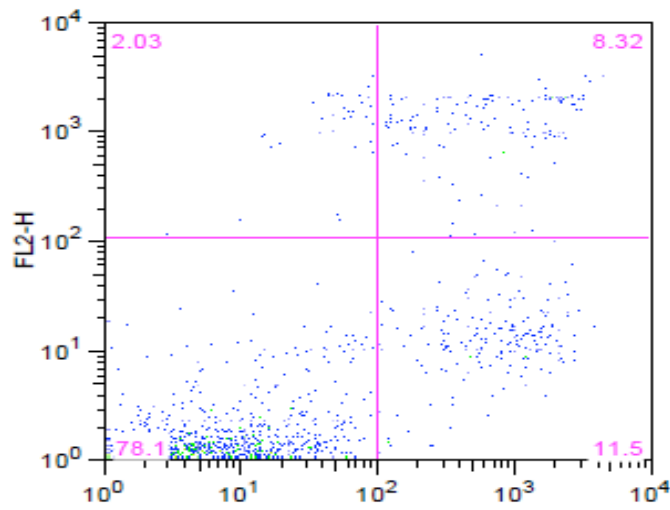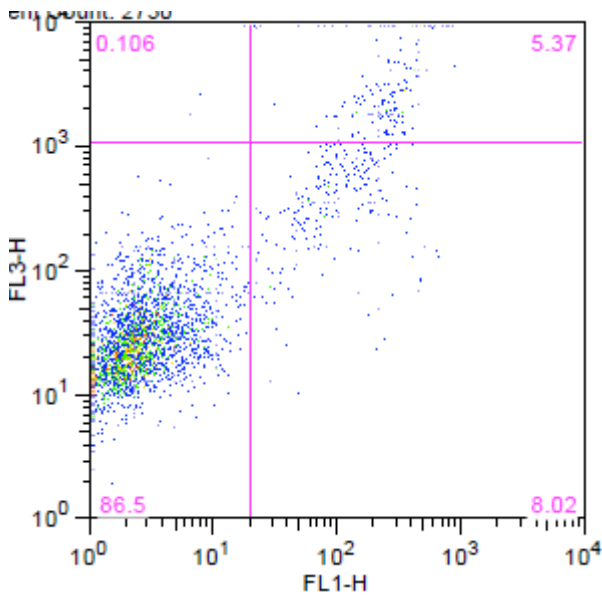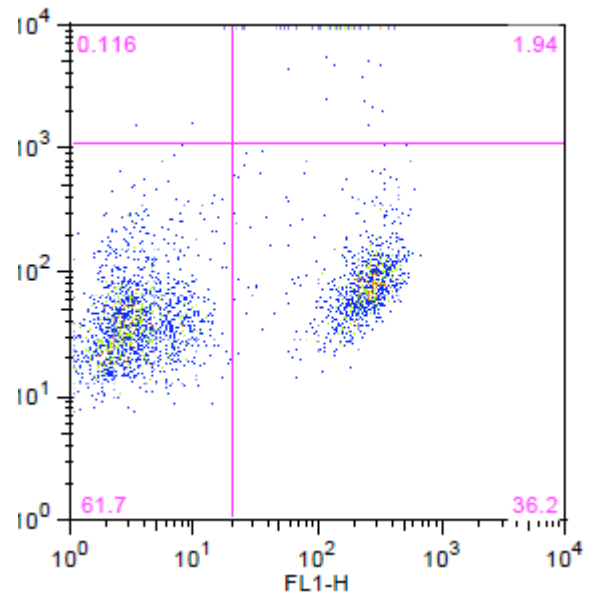
c)   10 µM Compound 2

48h

a)   Control

b)   10 µM SAHA

c)   10 µM Compound 2

329
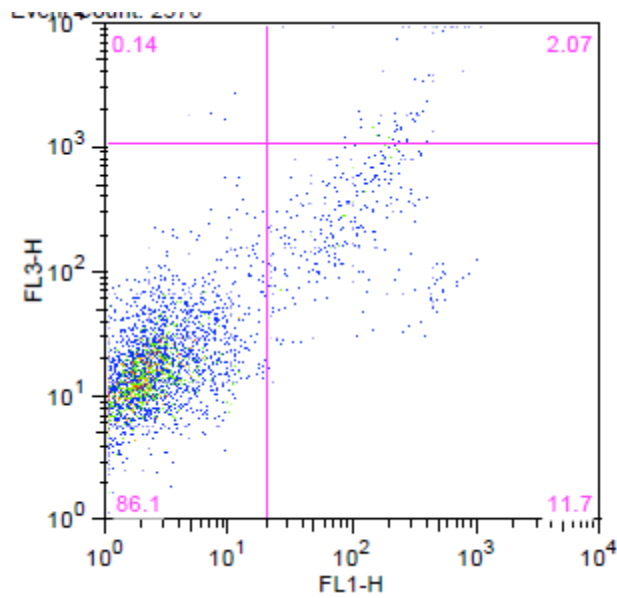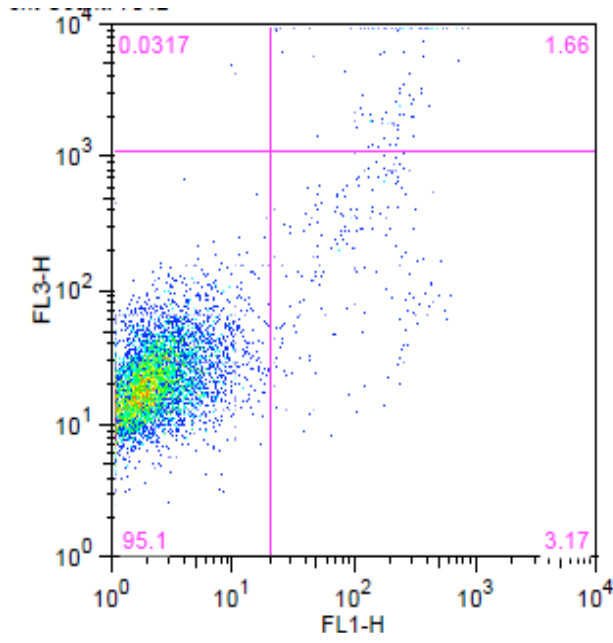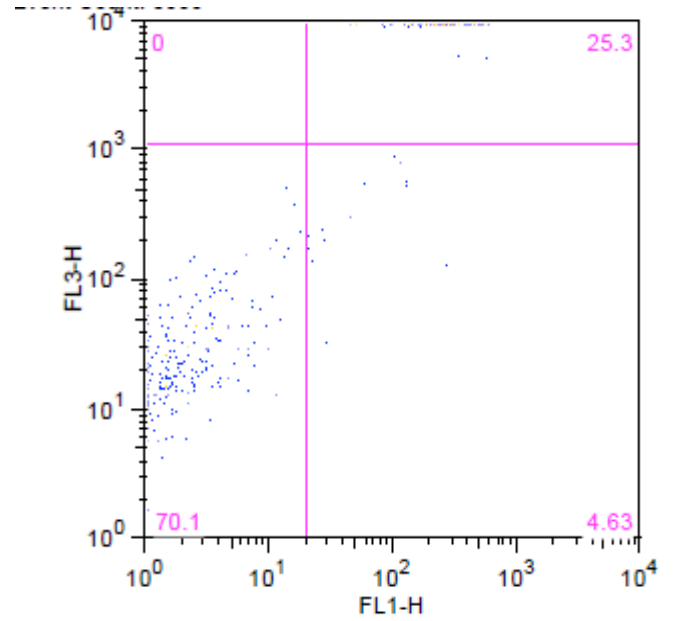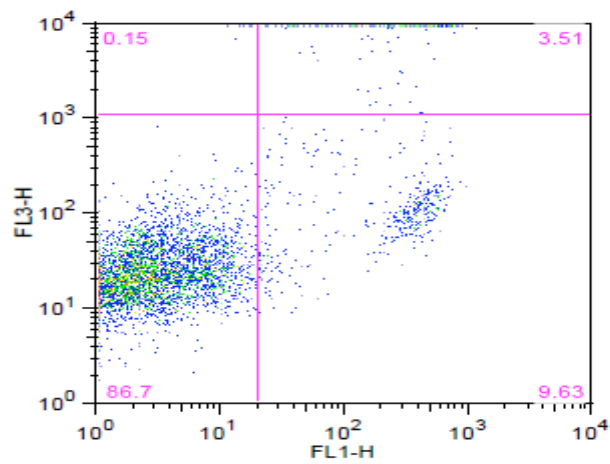
38. Time-dependent analysis of the induction of apoptosis in HuT-78 cells (Chapter 8, Table 3): y axis represents PI response whereas x axis represents Annexin V (AV) response. Quadrant 1 (bottom left) represents intact (live) cells (AV⁻, PI⁻); Quadrant 2 (bottom right) represents early apoptotic cells (AV+, PI⁻); Quadrant 3 (top right) represents late apoptotic/necrotic cells ((AV⁺, PI⁺).

12h

a) Control
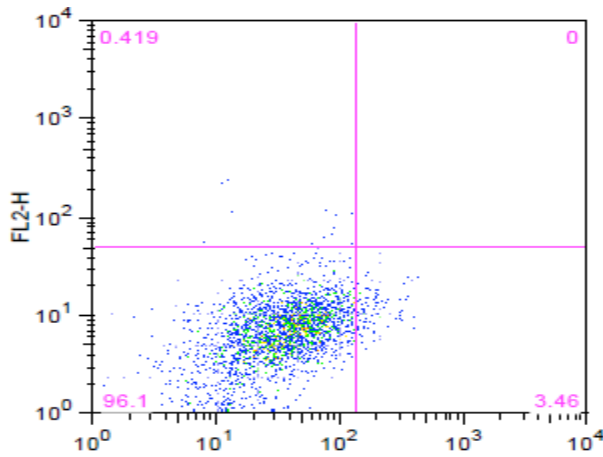
b) 10 µM SAHA
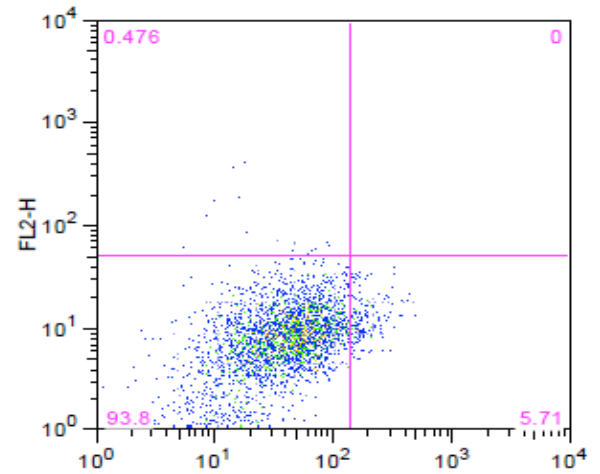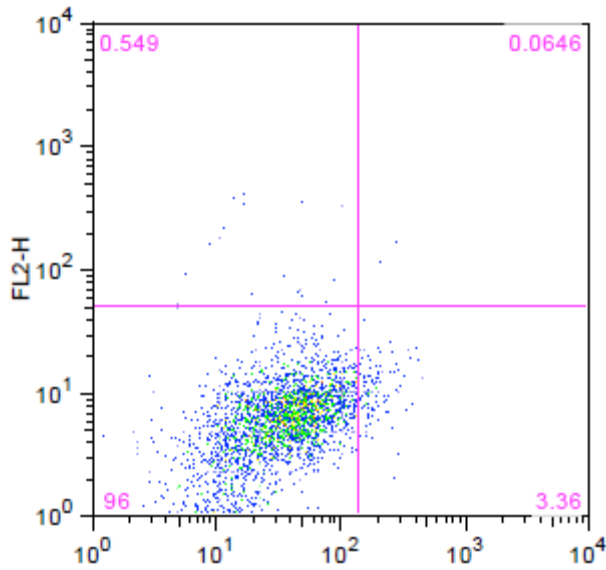
c) 10 µM Compound 2
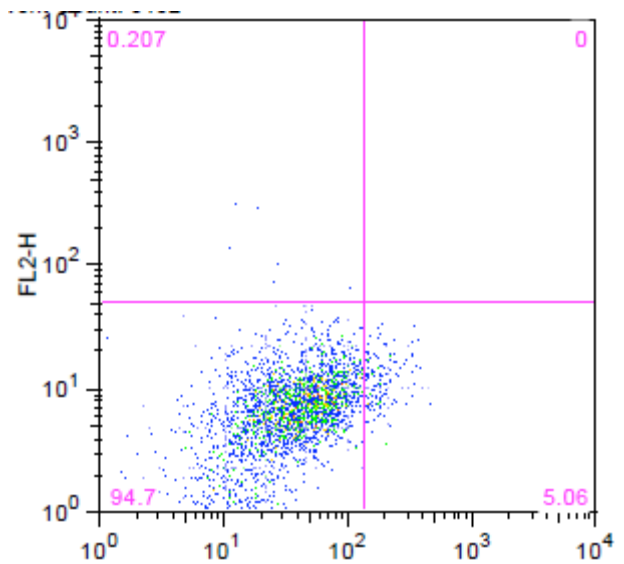
d) 10 µM Compound 7

e) Compound 10
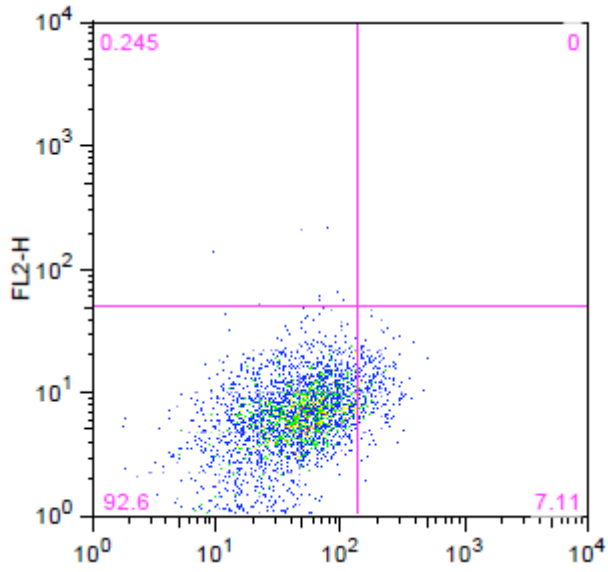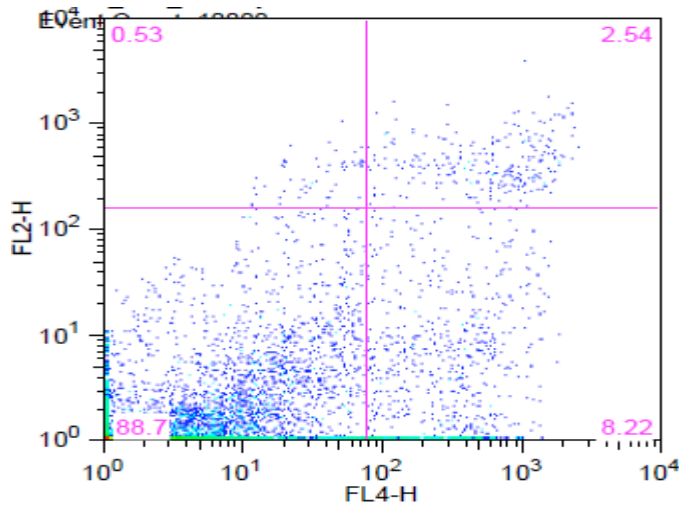
f) Compound 11

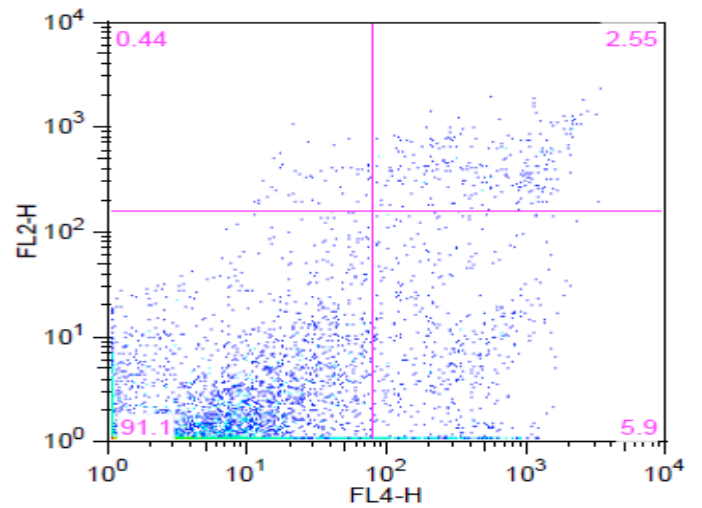**20h**

a) Control
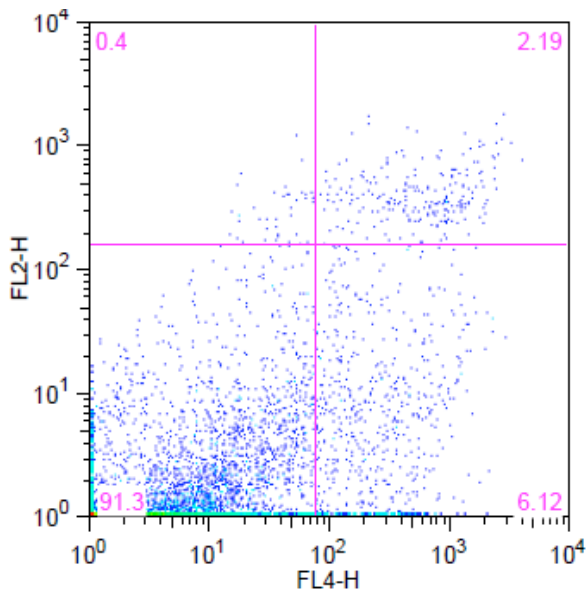
b) 10 µM SAHA
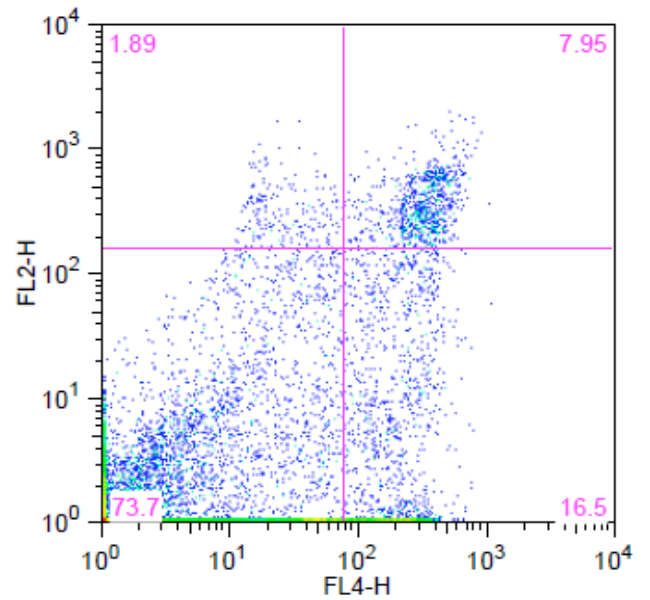
c) 10 µM Compound 2
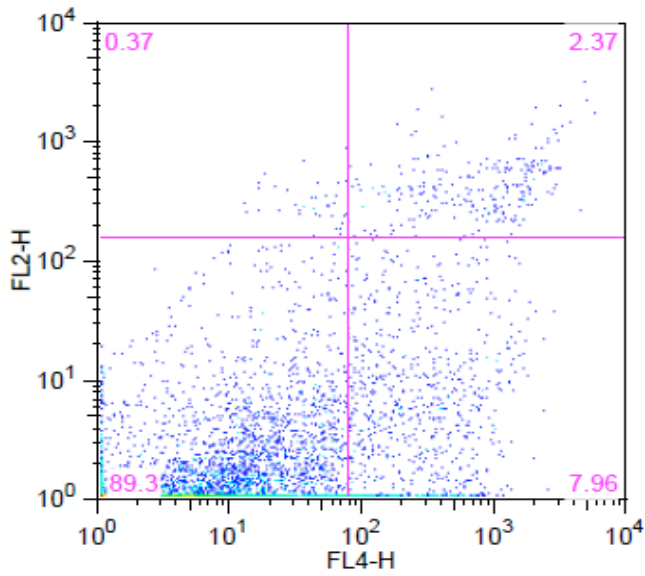
d) 10 µM Compound 7
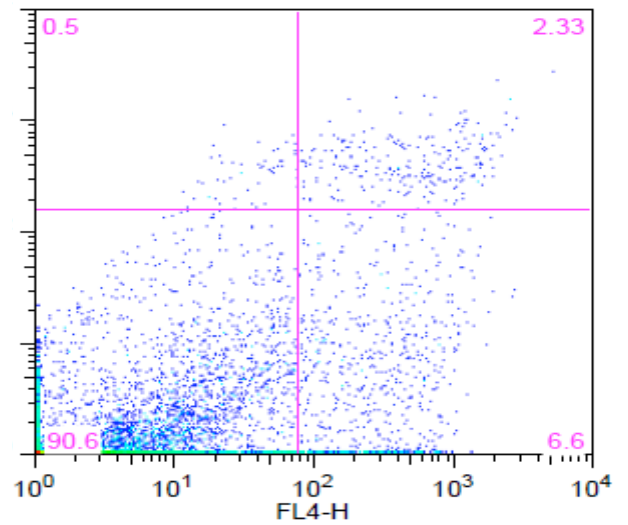
e) 10 µM Compound 10

f) 10 µM Compound 11

39. Standard deviation values for Caspase-3/7 analysis in Jurkat cells (Chapter 8, Tables 5 & 6)				
Treatment	6h	12h	24h	48h
Control	10002.74	7003.63	31846.96	4710.453
SAHA	7939.778	8869.66	20509.97	10357.53
Compound 2	11860.49	6312.14	5292.832	7390.019
Compound 7	21813.73	10670.77	8117.586	6650.594

333

40. Comparative analysis of unlabeled cells (green), secondary (2°) antibody treatment only (blue) and the untreated control (primary (1°) + 2° antibody; red) for evaluation of perforin differentiation in Jurkat cells (Chapter 8, Table 4).
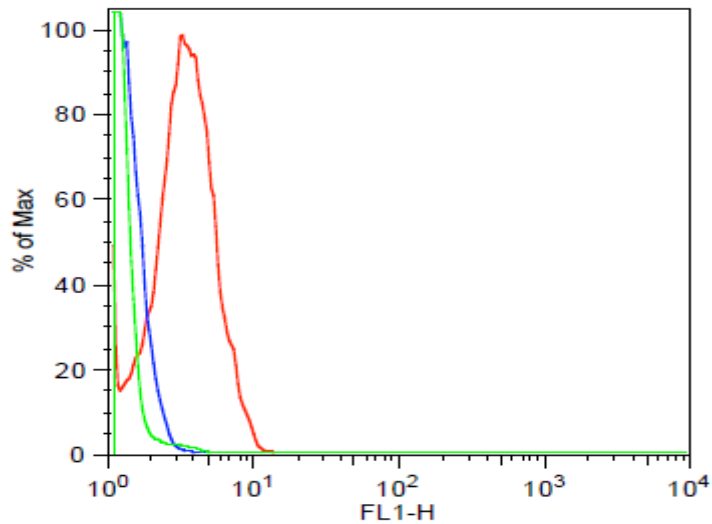
a)   6h analysis
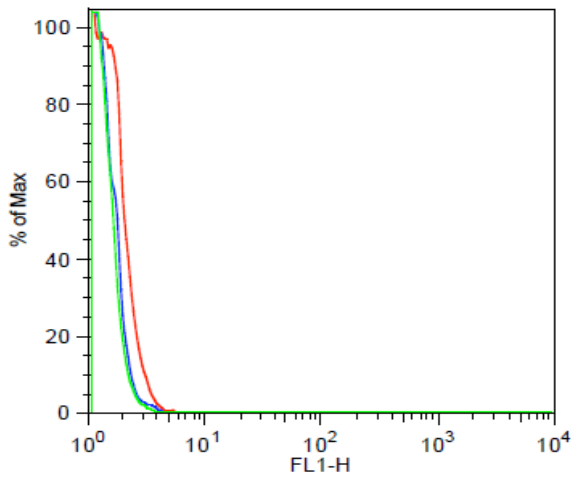
b)   24h analysis

c)   48h analysis

334
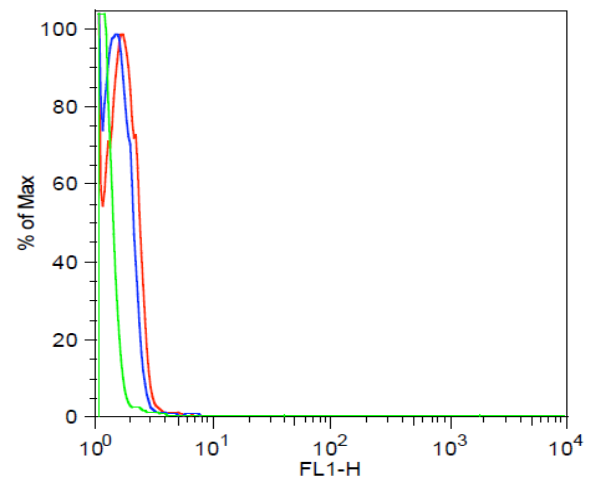
41. Standard error values for elucidation of key enzyme parameters for the class I PI3K enzyme, p110α and the PI substrate (Chapter 9, Table 1).		
	K_M (μM)	V_{max} (μM)
p110α	1.93	90.94